

# Isotopes and Chemical Principles



# Isotopes and Chemical Principles

Peter A. Rock, *Editor*

A symposium sponsored  
by the Division of  
Chemical Education, Inc.  
at the 167th Meeting  
of the American Chemical  
Society, Los Angeles,  
Calif., April 3, 1974

ACS SYMPOSIUM SERIES **11**

AMERICAN CHEMICAL SOCIETY  
WASHINGTON, D. C. 1975



Library of Congress CIP Data

Isotopes and chemical principles.  
(ACS symposium series; 11)

Includes bibliographical references and index.

1. Isotopes—Congresses. 2. Chemical reaction, Conditions and laws of—Congresses.

I. Rock, Peter A., 1939- ed. II. American Chemical Society. Division of Chemical Education. III. Series: American Chemical Society. ACS symposium series; 11.

QD466.I86                      541'.388                      75-2370  
ISBN 0-8412-0225-7                      ACSmc8 11 1-215

Copyright © 1975

American Chemical Society

All Rights Reserved

PRINTED IN THE UNITED STATES OF AMERICA

**American Chemical  
Society Library  
1155 16th St., N.W.  
Washington, D.C. 20036**

In Isotopes and Chemical Principles: 120-126:  
ACS Symposium Series; American Chemical Society: Washington, DC, 1975.

# ACS Symposium Series

**Robert F. Gould, *Series Editor***

## FOREWORD

The ACS SYMPOSIUM SERIES was founded in 1974 to provide a medium for publishing symposia quickly in book form. The format of the SERIES parallels that of its predecessor, ADVANCES IN CHEMISTRY SERIES, except that in order to save time the papers are not typeset but are reproduced as they are submitted by the authors in camera-ready form. As a further means of saving time, the papers are not edited or reviewed except by the symposium chairman, who becomes editor of the book. Papers published in the ACS SYMPOSIUM SERIES are original contributions not published elsewhere in whole or major part and include reports of research as well as reviews since symposia may embrace both types of presentation.

## PREFACE

This volume contains all of the papers presented at the symposium entitled Isotopes and Chemical Principles. The objective of the symposium was to present the major developments, both past and present, in the field of isotope effects in such a way as to make this material available to chemistry teachers who may wish to use isotope effects in their discussions of chemical principles.

The order of the papers in this volume is the same as that which was used at the symposium. The papers fall roughly into two groups. Papers 1-4 deal primarily with theoretical aspects whereas papers 5-9 deal primarily with experimental aspects. It is hoped that this symposium volume will serve to convey a fair measure of the utility and power of isotope effects in the continuing development of our understanding of chemical behavior and chemical principles. I would like to thank Bassam Z. Shakhashiri and Jerry A. Bell, the former chairpersons of the Program Committee of the Division of Chemical Education, for their help in bringing about this symposium.

PETER A. ROCK

University of California  
Davis, Calif.  
January 16, 1975





**To**  
**Marvin J. Stern**  
**and**  
**T. Ivan Taylor**



**Marvin J. Stern**  
(1935–1974)



**T. Ivan Taylor**  
(1909–1973)

## IN MEMORIUM

At the start of this symposium in Los Angeles, Jacob Bigeleisen expressed the deep feeling of sadness of the entire community of isotope scientists at the loss during the past year of two of our esteemed colleagues, Marvin J. Stern and T. Ivan Taylor. This is an attempt to express in a more permanent way our appreciation to them and our sense of loss.

### Marvin J. Stern

Marvin J. Stern was born in New York, N. Y., June 1, 1935 and was 38 yrs old at the time of his death on January 29, 1974. During his all-too-brief career he served on the faculties of Rutgers University, Columbia University, and Yeshiva University. From 1961 to 1969 he was affiliated with the Chemistry Department at Brookhaven National Laboratory as research associate, visiting associate chemist, and research collaborator. During a sabbatical leave from Yeshiva University in 1971–1972 he was a Chaim Weizmann Memorial Fellow at the Weizmann Institute of Science, Rehovot, Israel and a John Simon Guggenheim Memorial Fellow at the University of Kent, Canterbury, England.

He was actively involved in stable isotope studies for his entire scientific career, contributing over 30 publications during 1960–1974 on a variety of experimental and theoretical studies of both kinetic and equilibrium isotope effects. His experimental researches contributed greatly to the development of chemical exchange and distillation processes for concentrating the isotopes of nitrogen and oxygen and to the understanding of the relationship between inter- and intra-molecular forces in liquids and vapor pressure isotope effects. At Brookhaven National Laboratory, he participated in some of the first applications of high-speed digital computer calculations to the understanding of isotope effects. Most of his subsequent research career was devoted to such calculations. An initial theoretical study which related the vapor pressure isotope effects in ethylene to force fields in the condensed phase led into an extensive program in which computer calculations on "model molecules" were used to compare "exact" calculations of equilibrium and kinetic isotope effects with various approximation methods. The validity and the applicability

limits of a variety of approximation procedures were defined and new approaches were developed to help chemists working with large molecules. Calculations were carried out to study the temperature dependence of isotope effects, and the use of isotope effects in studying quantum mechanical tunnelling in chemical rate processes was investigated. Throughout these studies, Marvin Stern's unusual thoroughness and meticulous attention to detail were uniquely suited to the tasks. The breadth of his interests and of his impact on isotope chemistry can be best appreciated from the fact that five of the participants in this symposium have worked with him. His insights, his tenacity, his thoroughness, and his wit will not be soon forgotten by us.

### **T. Ivan Taylor**

T. Ivan Taylor was born in Farwest, Utah, September 11, 1909 and was 63 yrs old at the time of his death on July 27, 1973. He received his undergraduate and initial graduate education in Idaho, where he earned B.S. and M.S. degrees at the University of Idaho in Moscow. He continued his graduate education at Columbia University, where he received a Ph.D. degree in 1938. In recognition of his outstanding accomplishments, the University of Idaho conferred an Honorary Doctor of Science degree upon him in 1972. He served on the faculties of the University of Idaho, the University of Minnesota, the University of Iowa, and Columbia University. His most recent tenure at Columbia University extended over 28 yrs, from his appointment as an associate professor in 1945, through his promotion to professor in 1949, until his death this past year. During World War II, he served at the National Bureau of Standards in Washington, D.C., at Oak Ridge, Tenn., and in New York, N.Y. as a member of the research control group of the Manhattan District Atomic Energy Project. In addition to his teaching and research, he found time to serve on visiting and advisory committees for Brookhaven National Laboratory, the National Bureau of Standards, the National Academy of Sciences, and the American Chemical Society. He served a term as chairman of the New York Section of the American Chemical Society and several terms as councilor and as member of the Board of Directors of the New York Section of the American Chemical Society. He also served for many years as a consultant to the Carbide and Carbon Chemicals Corp. at Oak Ridge and as a research collaborator at Argonne National Laboratory and at Brookhaven National Laboratory.

Ivan Taylor was an early pioneer in studies of methods for separating stable isotopes and of their use for elucidating kinetics, mechanisms, and the catalysis of reactions. His initial research on isotope separation was in collaboration with Harold C. Urey. He went on to guide personally

the studies of numerous post-doctoral associates, as well as those of 22 successful Ph.D. candidates, 14 of whom wrote dissertations either on the separation of isotopes or their use.

He and his research group published more than 58 papers dealing with isotopes from 1937 to 1973. One of his major contributions to isotope science was the imaginative development of numerous chemical exchange processes for concentrating a variety of isotopes of the lighter elements. His group explored and developed countercurrent processes using exchanges between gas-liquid, gas-gas, and liquid-solid phases to enrich the rarer isotopes of hydrogen, lithium, carbon, nitrogen, oxygen, and potassium. The nitric acid-nitric oxide exchange process developed in his laboratory for the concentration of nitrogen-15 was the first system to produce this isotope at 99.8% purity. The process has been used during the past 20 yrs to produce laboratory-scale quantities of highly enriched nitrogen-15 and still remains the prime method for the commercial production of this useful isotope. Separation plants have been constructed and operated in the United States, United Kingdom, East Germany, Romania, the Soviet Union, and Israel. Innumerable scientific studies using  $^{15}\text{N}$  have been facilitated by Ivan Taylor's work.

Ivan Taylor was an unusually skilled and creative experimentalist. He never lost the joy of working in the laboratory with his own hands, and he never quite forgot his early days in research when "string and sealing wax" was the rule rather than the exception. In a time of rapidly expanding research costs and increasing dependence on expensive commercial instruments, he was almost fiercely determined to carry out experiments in the most simple and direct manner with equipment of his own design and often his own fabrication. His was a unique mold; we are all the poorer for his loss.

WILLIAM SPINDEL  
MAX WOLFSBERG

# Quantum Mechanical Foundations of Isotope Chemistry

JACOB BIGELEISEN

Department of Chemistry, University of Rochester, Rochester, N. Y. 14627

## Introduction

I shall open this symposium with a brief overview of the quantum and statistical mechanical foundations of isotope chemistry. A number of monographs already exist dealing with the principles and applications of isotope chemistry in chemical kinetics, geochemistry, isotope separation, and equilibrium processes. This symposium is directed, in part, toward establishing a bridge from the present habitat of isotope chemistry, graduate students and professional scientists, to the undergraduate classroom. For this purpose I find it convenient to develop the fundamental principles of isotope chemistry along historical lines. I will retain only those ideas that have stood the test of time and omit all of those dead ends and false turns which are part of the development of any science. Even with this restriction, it is impossible to cover all of the areas of isotope chemistry. The one area which relates most to all disciplines of isotope chemistry is the equilibrium in ideal gases. Other papers in this symposium will start from the ideal gas equilibrium to such topics as tunnelling in chemical kinetics, isotope separation, reaction mechanisms, condensed phase isotope chemistry and isotope biology.

Shortly after the discovery of isotopes Fajans (1) recognized that the thermodynamic properties of solids, which depend on the frequencies of atomic and molecular vibrations, must be different for isotopes. This idea was put into quantitative form independently by Stern (2) and Lindemann (3,4).

\* Much of the research reported in this article was supported by the U.S. Atomic Energy Commission.

\*\* A condensed summary of this article was presented at the Division of Chemical Education Symposium on "Isotopes and Chemical Principles", ACS National Meeting 3 April 1974, Los Angeles. The manuscript was prepared during the tenure of a John Simon Guggenheim Memorial Fellowship.

### Stern-Lindemann Formulation of Vapor Pressure Isotope Effect

Stern and Lindemann independently gave the first quantitative formulation of an isotope effect. They considered the equilibrium between a Debye solid and an ideal gas composed of monatomic substances. Further they introduced the following assumptions: 1) the oscillations in a solid lattice are harmonic, 2) the potential energy is isotope invariant, and 3) an oscillator has a zero point energy. Some of these assumptions represented a significant insight into physical processes at the time they were put forward. Anharmonic effects are of major importance in the equation of state of solids. However, neither experiment nor theory had advanced to the point where anharmonic effects needed to be considered in the analysis of the constant volume heat capacity, the enthalpy, the entropy, and the free energies of solids. The Bohr-Sommerfeld theory of the hydrogen atom shows a small dependence of the potential energy on the mass. The dependence of the Rydberg constant on the mass of the nucleus leads to a small difference in behavior of hydrogen and deuterium. The Born-Oppenheimer approximation to the solution of the Schrodinger equation for molecules inherently contains the assumption of an isotope independent potential energy. The small corrections to isotope chemistry from corrections to the Born-Oppenheimer approximation are currently being investigated by Wolfsberg and are reported in the paper in this symposium volume by Wolfsberg and Kleinman. Even before the development of quantum mechanics by Heisenberg and Schrödinger in 1925-'6, in which such concepts as zero point energy follow naturally, difficulties with the old quantum theory led scientists of 1920 to anticipate the existence of a zero point energy. It was, therefore, natural for Lindemann to develop the theory of the vapor pressure isotope effect both for the case of the existence of zero point energy and for the non-existence. For the former, he predicted that the isotope effect on vapor pressure would be a small effect, of the order of 0.02 % for  $^{206}\text{Pb}/^{208}\text{Pb}$  at 600° K (actually Lindemann has an error of a factor of 10 and his result should be reduced to 0.002 %) and that the effect is a "second order difference". Stern and Lindemann obtained for the monatomic Debye solid under the harmonic oscillator, Born-Oppenheimer approximations for a system with zero point energy,  $E = 1/2 h\nu$ ,

$$\ln P'/P = (3/40) (\theta/T)^2 \delta + \dots \quad (1)$$

where  $P'$  and  $P$  are the vapor pressures of a light and heavy isotope respectively,  $\theta$  is the Debye temperature,  $h\nu_m/k$ , of the heavy isotope and

$$\delta = [(M/M') - 1]$$

Equation (1) is the first term of a Taylor expansion valid for  $(\theta/T) < 2\pi$ . For the case of the non-existence of zero point energy, one predicts an isotope effect for the  $^{206}\text{Pb}/^{208}\text{Pb}$  vapor pressure ratio two orders of magnitude larger than the prediction from Eq. (1) at  $600^\circ\text{K}$ . In addition the no zero point energy case predicts the  $^{208}\text{Pb}$  to have the larger vapor pressure at  $600^\circ\text{K}$ .

Stern's estimate of the difference in vapor pressures of  $^{20}\text{Ne}$  and  $^{22}\text{Ne}$  at  $24.6^\circ\text{K}$  through Eq. (1) led to the first separation of isotopes on a macro scale by Keesom and van Dijk (2). The same theory, without the approximation  $(\theta/T) < 1$ , was used by Urey, Brickwedde, and Murphy (5) to design a Raleigh distillation concentration procedure to enrich HD in  $\text{H}_2$  five fold above the natural abundance level, which was adequate to demonstrate the existence of a heavy isotope of hydrogen of mass 2. It is interesting to note that as late as 1931 Keesom and van Dijk took their finding that there was a difference in vapor pressures of the neon isotopes and that the vapor pressure of  $^{20}\text{Ne}$  is greater than  $^{22}\text{Ne}$  to be an important experimental proof of the existence of zero point energy. It is fortunate that Urey had not yet discovered deuterium at the time of Keesom and van Dijk's work or they might have been misled by the discovery that the vapor pressure of deuterocarbons is generally larger than hydrocarbons. It is interesting to speculate what conclusions would have been drawn from such a finding in 1931.

It is important to look into the implications of Eq. (1) since the development of the quantum-statistical mechanical theory of isotope chemistry from 1915 until 1973 centers about the generalization of this equation and the physical interpretation of the various terms in the generalized equations. According to Eq. (1) the difference in vapor pressures of isotopes is a purely quantum mechanical phenomenon. The vapor pressure ratio approaches the classical limit, high temperature, as  $T^{-2}$ . The mass dependence of the isotope effect is  $\delta M/M^2$  where  $\delta M = M - M'$ . Thus for a unit mass difference in atomic weights of isotopes of an element, the vapor pressure isotope effect at the same reduced temperature  $(\theta/T)$  falls off as  $M^{-2}$ . Interestingly the temperature dependence of  $\ln P'/P$  is  $T^{-2}$  not  $\delta\lambda_0/T$  where  $\delta\lambda_0$  is the heat of vaporization of the heavy isotope minus that of the light isotope at absolute zero. In fact, it is the difference between  $\delta\lambda$ , the difference in heats of vaporization at the temperature  $T$  from  $\delta\lambda_0$ , that leads to the  $T^{-2}$  law.

From Eq. (1) we can write

$$\frac{(\Delta G^\circ - \Delta G^{\circ'})}{RT} = \ln(P'/P) = \frac{(\Delta S^\circ - \Delta S^{\circ'})}{R} = \frac{1}{2} \frac{(\lambda - \lambda')}{RT} T \quad (2)$$

where  $(\Delta G^\circ - \Delta G^{\circ'})_T$ ,  $(\Delta S^\circ - \Delta S^{\circ'})_T$ , and  $(\lambda - \lambda')_T$  are respectively the differences in standard free energies, entropies and heats of vaporization at the temperature  $T$ .



Within the approximation of Eq. (1) the entropy change in the process is equal to the change in  $\delta(\Delta G)/T$  and each are equal to one half the isotope effect on  $T^{-1}$  times the enthalpy change. The competition between entropy and enthalpy is independent of temperature and the sign of the difference in free energy change never changes. For the system under consideration, equilibrium between a gas and a solid, this conclusion is valid even if one includes the higher terms in Eq. (1). Later we shall see that the consideration of higher order terms in Eq. (1) leads to a temperature dependence on the enthalpy-entropy balance, but the difference in free energies of formation of any system from its atoms is always of the sign given by Eq. (2).

Although Keesom and van Dijk were led to the successful separation of the neon isotopes through predictions made by Professor Otto Stern based on Eq. (1), Keesom and Haantjes (6) interpreted their measurements of the vapor pressure ratio of  $^{20}\text{Ne}/^{22}\text{Ne}$  in terms of a  $\delta\lambda/T$  rather than a  $\delta\lambda/T^2$  temperature dependence. When I replotted their data in 1956 in accord with expectations from Eq. (1), I found that a linear extrapolation of the Keesom-Haantjes data predicted a significant difference in vapor pressures of the neon isotopes for the hypothetical solids at infinite temperature. There were no other direct confirmations of the  $T^{-2}$  law predicted by Eq. (1) and this led to a reinvestigation of the vapor pressures of the neon isotopes. Roth and Bigeleisen (7,8) not only confirmed Eq. (1) through their investigation of the vapor pressures of the neon isotopes, cf. Fig. 1, but also showed that the systematic investigation of the vapor pressure isotope effect in simple substances could give important new information on the lattice energy, the anharmonic vibrations in crystals, the melting process and the mean square force between molecules in the liquid state. The latter is related to the intermolecular potential and the radial distribution function in the liquid. Systematic investigation of the vapor pressures of the argon (9,10) and krypton (11) isotopes have in fact fulfilled these expectations (12,13,14).

Herzfeld and Teller (15) showed that a more general form of Eq. (1) could be derived through the use of the Wigner distribution function. For the vapor pressure isotope effect between a condensed phase and a monatomic vapor they obtained

$$\ln(P'/P) = (1/24) (\hbar/kT)^2 \left( \frac{1}{m} - \frac{1}{m'} \right) \langle \nabla^2 U \rangle \quad (3)$$

where  $\langle \nabla^2 U \rangle$  is the mean value of the Laplacian of the interaction potential in the condensed phase. In the harmonic oscillator approximation  $\langle \nabla^2 U \rangle$  is just  $f/m$ , the force constant. For a harmonic Debye lattice  $(\hbar/k)^2 \langle \nabla^2 U \rangle$  ( $\text{m}^{-1}$ ) is just  $\theta_D^2$ .

Although Equations (1) and (3) can provide significant insight into the behavior of polyatomic molecules, they are inadequate approximations to account for the role of molecular structure on the isotope chemistry of condensed phases (16).

Urey-Rittenberg Formulation of Isotope Exchange Equilibria

After he had succeeded in enriching deuterium by the Raleigh distillation of liquid hydrogen, Urey undertook both theoretical and experimental investigations of the differences in the chemistry of protium and deuterium compounds. On the theoretical side Urey and Rittenberg (17) utilized the methods developed for the calculation of the partition function and the free energy of a diatomic molecule from spectroscopic data. For an ideal gas

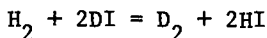
$$- (G^\circ - E_0^\circ)/T = 3/2R \ln M + 5/2R \ln T + R \ln Q_{\text{int}} - K(S-T) \quad (4)$$

where  $E_0^\circ$  is the standard molar internal energy of the molecule at  $0^\circ \text{K}$ ,  $Q_{\text{int}}$  is the internal partition function,  $K(S-T)$  is the Sackur-Tetrode constant.

$$Q_{\text{int}} = \sum_{\nu, J} P_J \exp(-E(\nu, J)/kT) \quad (5)$$

The internal partition function is a sum of Boltzmann factors, multiplied by their degeneracies,  $P_J$ , over the vibrational and rotational states of the molecule. In the summation over the rotational states it is necessary to consider symmetry selection rules. This leads to a factor  $S^{-1}$  in  $Q_{\text{int}}$  and  $R \ln S$  in Eq. (4) when the rotation is classical. In the calculation of the standard free energy change of a chemical reaction from spectroscopic data it is necessary to evaluate  $\Delta E_0^\circ$ , the energy change at absolute zero. In the general chemical reaction the difference in electronic binding energies between products and reactants dominates  $\Delta E_0^\circ$ . The latter are usually not known with sufficient accuracy for the calculation of  $\Delta G^\circ/RT$  to an absolute value of  $10^{-2}$  or better. Therefore, recourse is usually made to experimental thermodynamic data for the evaluation  $\Delta E_0^\circ$  (18). The dissociation of the halogens and other diatomic molecules are cases where  $\Delta E_0^\circ$  has been determined entirely from spectroscopic data to yield values of  $\Delta G^\circ/RT$  calculated from Eq. (4) in quantitative agreement with experiment.

For the isotope exchange reaction, e.g.,



$\Delta E_0^\circ$  electronic is identically zero under the Born-Oppenheimer approximation. The only contribution to  $\Delta E_0^\circ$  comes from the molecular vibrations.

$$E_0^\circ/Nhc = \sum_i (n + 1/2) \nu_i + \text{anharmonic corrections} \quad (6)$$

Thus once the spectroscopic rotational and vibrational constants are known for a pair of isotopic molecules it is possible to calculate the partition function ratio of a pair of isotopic molecules

$$Q_1/Q_2 = \exp [-(G_1^\circ - G_2^\circ)/RT] \quad (7)$$

from Equations (4) and (6).  $Q$  is the total partition function. The rotational and vibrational spectroscopic constants, moments of inertia and vibrational frequencies, of isotopic molecules are related through atomic masses, bond distances, and force constants (19). The spectroscopic constants used in the calculation of  $Q_1/Q_2$  must be consistent with the isotope relations for moments of inertia and vibrational frequencies of the molecules concerned. Frequently the spectroscopic constants for a set of isotopic molecules are best obtained from a least square fit of all available data to the molecular parameters of one isotopic species and the calculation of all the other isotopic species through the isotope rules. The equilibrium constant for an isotope exchange reaction is then the ratio of isotopic partition functions in two chemical species. For instance, for the protium-deuterium exchange between hydrogen and hydrogen iodide

$$K = (Q_{D_2} / Q_{H_2}) / (Q_{DI} / Q_{HI})^2$$

The experiments of Rittenberg and Urey (20) confirmed their calculations on this exchange reaction within the uncertainty of their calculations. Their calculation of the anharmonic correction to  $E_0^\circ$ , like many subsequent ones, is incomplete. In the exchange reaction of protium and deuterium between hydrogen gas and water vapor the deuterium favors the water molecule. At 25° C

$$K = (HDO/H_2O) / (HD/H_2) = 3.7$$

In the electrolysis of water deuterium is depleted by a factor of 3 to 9 compared with the liquid water. The precise difference depends on the electrode materials and the conditions of electrolysis. This fractionation is kinetically controlled.

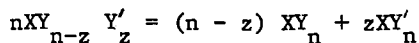
Urey and Greiff (20) extended the treatment given by Urey and Rittenberg for diatomic molecules to polyatomic molecules. In the approximation of harmonic oscillators and rigid rotors they obtained

$$(Q_1/Q_2) = \left( \frac{S_2}{S_1} \right) \left( \frac{A_1 B_1 C_1}{A_2 B_2 C_2} \right)^{1/2} \left( \frac{M_1}{M_2} \right)^{3/2} \pi e^{\Delta U_1/2} \frac{(1-e^{-U_{12}})}{(1-e^{-U_{11}})} \quad (8)$$

for the partition function ratio of polyatomic molecules.  $A$ ,  $B$ , and  $C$  are the principal moments of inertia,  $M$  is the molecular weight and  $U_i = h\nu_i/kT$ . (The factor  $S_2/S_1$  in Eq. (8) does not appear in Urey's and Greiff's Eq. (13) since they

restricted their calculations to isotopic molecules of the same symmetry,  $S_1 = S_2$ ). Whereas, Urey and Rittenberg found values of the total partition function ratio of several diatomic deuterides to the corresponding hydrides corrected for nuclear spin and symmetry of the order of 10 at 298° K, Urey and Greiff found values between 1.25 and 1.35 for the isotopic partition function ratios of a number of compounds of lithium, carbon, oxygen, and sulfur at 298° K. The partition function ratios calculated by them were either independent of temperature,  $^7\text{Li}/^6\text{Li}$ , or decreased with temperature. A summary of some of their calculations is given in Table I.

The chemical isotope fractionation factor,  $\alpha = (N_1/N_2)_a / (N_1/N_2)_b$ , where  $N_{ia}$  is the mole fraction of isotope  $i$  in compound of chemical species  $a$ , is just the ratio  $(Q_1/Q_2)_a / (Q_1/Q_2)_b$  for molecules of the same symmetry and with equal number of exchangeable atoms. When a molecule contains more than one equivalent exchangeable atom, e.g.,  $\text{CO}_2$ , it is sufficient to apply the rule of the mean (22), which states that for isotopic disproportionation reactions,



$$\Delta G^\circ/RT = n \ln (S_{xy_n} / S_{xy_{n-z}y'})$$

in the harmonic oscillator approximation. The fractionation factor for each atom exchanged is then calculated by the use of the appropriate power of the reduced partition function ratio, e.g.,  $(C^{18}\text{O}_2/C^{16}\text{O}_2)^{1/2}$ ,  $(C^{18}\text{O}_3/C^{16}\text{O}_3)^{1/3}$  for the exchange of one oxygen atom. The table of partition function ratios of Urey and Greiff predicts chemical fractionation factors for the isotopes of carbon and oxygen of the order of 1.0 - 1.1 at 25°C. Oxygen exchange between  $\text{CO}_2$  and  $\text{H}_2\text{O}(\text{g})$  is predicted to enrich  $^{18}\text{O}$  in  $\text{CO}_2$  over  $\text{H}_2\text{O}$  by a factor of 1.054 at 25°C. When such a fractionation is cascaded in a countercurrent column, it provides the basis of a practical economic isotope separation process. The requirements necessary for such a process are reviewed by Spindel in this monograph. Chemical exchange processes for the enrichment of  $^6\text{Li}$ ,  $^{13}\text{C}$ , and  $^{15}\text{N}$  were developed by Lewis and MacDonald (23), Hutchison, Stewart and Urey (24), and Thode and Urey (25), respectively.

For the development of nuclear energy for military purposes in World War II, the Manhattan Project of the U.S. Army Engineers Corps required large quantities of  $\text{D}_2\text{O}$ , highly enriched  $^{10}\text{B}$  and the fissionable isotope of uranium,  $^{235}\text{U}$ . The most difficult task was the production of kilograms of 90%  $^{235}\text{U}$  from the natural abundance of 0.7%. Many processes were

Table I  
Calculation of Ratios of Distribution Functions  
for Light Isotopes

H. C. Urey and Lotti J. Greiff (1935)

Ratio	298° K	600° K
${}^7\text{Li}/{}^6\text{Li}$	1.2601	1.2601
${}^7\text{LiH}/{}^6\text{LiH}$	1.2918	1.2707
<hr/>		
$\text{C}^{18}\text{O}/\text{C}^{16}\text{O}$	1.3200	1.2403
$(\text{C}^{18}\text{O}_2/\text{C}^{16}\text{O}_2)^{\frac{1}{2}}$	1.3342	1.2400
$\text{H}_2^{18}\text{O}/\text{H}_2^{16}\text{O}$	1.2663	1.2231
$(\text{S}^{18}\text{O}_2/\text{S}^{16}\text{O}_2)^{\frac{1}{2}}$	1.3018	1.2263
<hr/>		
${}^{13}\text{C}/{}^{12}\text{C}$	1.3289	1.2033
${}^{13}\text{CO}/{}^{12}\text{CO}$	1.2378	1.1686
${}^{13}\text{CO}_2/{}^{12}\text{CO}_2$	1.3437	1.2020
${}^{13}\text{CO}_3/{}^{12}\text{CO}_3$	1.3594	1.1987
<hr/>		

considered and several different types of production plants were built (26). In the end those processes for the enrichment of D,  $^{10}\text{B}$ , and  $^{235}\text{U}$  developed at the SAM Laboratories of Columbia University under the direction of H. C. Urey proved to be the most economical and reliable of all the processes developed.

### Reduced Partition Function Ratio of Bigeleisen and Mayer

I joined the SAM Laboratories in June 1943. I was assigned to a small short term basic research program to investigate the spectra of uranium compounds. The immediate goal was to see whether there were differences in the spectra of  $^{235}\text{U}$  and  $^{238}\text{U}$  which could lead to a photochemical separation of the uranium isotopes. A review of the program in the fall of 1943 led to the conclusion that it was unlikely that a photochemical separation process could be developed within the time schedules drawn up by the Manhattan District. It was decided to phase out the photochemical separation program. We did assemble a significant amount of spectroscopic data, much of which was analyzed by the late Maria Goeppert-Mayer. Under an administrative decision last in-last out, I was left at the end with closing out the program and the preparation of the final status report.

One of the processes which had been considered early in the OSRD program for the separation of the uranium isotopes was chemical exchange. It was dropped in favor of the calutron, centrifuges, gaseous and thermal diffusion. By the fall of 1943 all of these processes were in trouble and Urey was led to reconsider chemical exchange. He asked an assistant and former student, Dr. Isidor Kirschenbaum, to see whether I could calculate any useful guidelines for chemical exchange separation processes for uranium isotopes from our spectroscopic data. Recall that the chemical isotope fractionation factor  $\alpha$  is the ratio of two partition function ratios. If we use the Urey-Greif approximation to the partition function ratio,  $Q_1/Q_2$  Eq. (8), and eliminate the symmetry number factor, then the chemical exchange fractionation factor is a product of ratios

$$\alpha = \frac{(Q_1/Q_2)_a}{(Q_1/Q_2)_b} = \frac{(A_1 B_1 C_1 / A_2 B_2 C_2)_a^{1/2}}{(A_1 B_1 C_1 / A_2 B_2 C_2)_b^{1/2}} \cdot \frac{(M_1/M_2)_a^{3/2}}{(M_1/M_2)_b^{3/2}} \times \frac{\text{ZPE}_a}{\text{ZPE}_b} \cdot \frac{\text{Exc}(a)}{\text{Exc}(b)} \quad (9)$$

where the abbreviations ZPE and Exc stand for the zero point energy factor and Boltzmann excitation factors in Eq. (8),

respectively. For compounds of uranium we are dealing with a product of four numbers each of which differs from unity by the order of one per cent or less. The individual factors in Eq. (9) could be greater or less than unity and the absolute value of  $\ln \alpha$  is not expected to be larger than  $5 \times 10^{-3}$ . For some of the compounds of interest, it was not known whether  $A_1 B_1 C_1 / A_2 B_2 C_2$  was unity. Maria Mayer and I had not yet established that  $UF_6(g)$  had the regular octahedral structure. Since some of the factors in Eq. (9) are larger than unity and some are less than unity, it was obvious to me that it would be useful if some basis could be found to calculate  $(Q_1/Q_2)$ , or a quantity related to it, directly rather than the product of the ratio of four numbers. It was immediately obvious that the ZPE and Boltzmann factors in  $\ln(Q_1/Q_2)$  could be combined through a

Taylor series expansion to yield  $\sum_i (1/2 + \frac{1}{u_i - 1}) \Delta u_i$ .

The following day Maria Mayer visited me to find out how I was coming along with the summary of the spectroscopy program. I informed her that I had temporarily set that aside and was using what data we had to estimate chemical exchange factors. Maria Mayer knew all the difficulties in the calculation of partition function ratios from incomplete spectroscopic data. She had been through it in connection with the heavy water program. She was excited by my approach and said that I could now finish the whole matter by taking out the classical contribution to  $Q_1/Q_2$ . If we now added  $(-1/u_i) \Delta u_i$  to my Taylor series expansion, we would now have a function  $G_i$  related to  $(Q_1/Q_2)$  and useful for the calculation of chemical isotope separation factors. We define

$$G(u_i) = (1/2 - \frac{1}{u_i} + \frac{1}{e^{u_i} - 1}) \quad (10)$$

and a quantity  $(s/s')f$

$$(s/s')f = (Q/Q')_{qm} / (Q/Q')_{cl} \quad (11)$$

where the prime designates the light isotope.  $(s/s')f$  is a reduced partition function ratio, the partition function ratio of a pair of isotopic molecules calculated by quantum statistical mechanics divided by the corresponding ratio calculated by classical statistical mechanics. We shall presently show that these defined quantities are related by

$$\ln(s/s')f = \sum_i G(u_i) \Delta u_i + \dots \quad (12)$$

For most molecules the classical partition function is an adequate approximation for the translation and rotation in

ideal gases. These lead to the factors  $M^{3/2}$  and  $(ABC)^{1/2}$  respectively in Eq. (8). Only the molecular vibration is quantum mechanical and contributes to  $(s/s')f$ . We shall show shortly that the reduced partition function,  $(s/s')f$ , provides an absolute scale for the calculation of isotope separation factors.

Within the approximations that  $(Q_{\text{rot}})_{\text{qm}} = (Q_{\text{rot}})_{\text{cl}}$ ,  $(Q_{\text{trans}})_{\text{qm}} = (Q_{\text{trans}})_{\text{cl}}$  and that the molecular vibration is harmonic, then the reduced partition function is

$$(s/s')f = \prod_i \frac{3n-6}{u_i} e^{(u_i' - u_i)/2} \frac{(1 - e^{-u_i'})}{(1 - e^{-u_i})} \quad (13)$$

for ideal gases. The factor  $\prod_i u_i/u_i'$  is just  $(Q_i/Q_i')_{\text{cl}}^{-1}$  for a set of vibrations. The remaining factor in Eq. (13) is  $(Q/Q')$  for a set of harmonic oscillators. Development of Eq. (13)<sup>qm</sup> in a power series in  $\Delta u_i = (u_i' - u_i)$  gives Eq. (12).

We next show that  $(Q/Q')_{\text{cl}}$  depends only on the symmetry number ratio and a mass factor independent of chemical composition. Write the Hamiltonian of the molecule in Cartesian coordinates. Then the classical partition function

$$Q = (1/h^f s) \int \dots \int e^{-H(p,q)/kT} dp \dots dq \quad (14)$$

can be integrated over the momenta to give

$$Q_{\text{cl}} = (1/h^f s) \prod (2\pi m_i kT/h^2)^{3/2} \int \dots \int e^{-V(q)/kT} dq_1 \dots dq_{3n} \quad (15)$$

where  $n$  is the number of atoms in the molecule. Then

$$(Q/Q')_{\text{cl}} = (s'/s) \prod (m_i/m_i')^{3/2} \quad (16)$$

where  $m_i$  and  $m_i'$  are the masses of the isotopic atoms.

We now demonstrate that within the approximation of classical statistics there is no chemical isotope fractionation. The symmetry number ratio provides no mechanism for isotope concentration. Rather it is an important statistical factor that corrects for the a priori probabilities of forming symmetrical vs asymmetrical molecules of the same configuration. Consider the isotopes  $Y$  and  $Y'$  which form compounds of type  $A$  and  $B$ . Let there be isotopic exchange of  $Y$  and  $Y'$  between  $A$  and  $B$ . Define  $\beta = (Y/Y')_A$  and  $\gamma = (Y/Y')_B$  where  $(Y/Y')_A$  is the atom ratio in the species  $A$ . Then the isotope fractionation factor is

$$\alpha \equiv \beta/\gamma$$

For systems which obey the rule of the mean (22)



$$(Q/Q')_A = (s'/s)_A \beta$$

$$(Q/Q')_B = (s'/s)_B \gamma$$

Then

$$\alpha = (s/s')_A (Q/Q')_A / ((s/s')_B (Q/Q')_B)$$

If

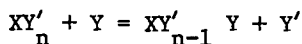
$$(Q/Q')_A = (Q/Q')_{Ac1} = (s'/s)_A \left(\frac{m}{m'}\right)^{3/2}$$

$$(Q/Q')_B = (Q/Q')_{Bc1} = (s'/s)_B \left(\frac{m}{m'}\right)^{3/2}$$

Then

$$\alpha \equiv 1$$

Now consider the exchange reaction



Let the chemical species A and B be  $XY'_n$  and Y respectively.

Since Y is an atom,  $s_B = s_{B'} = 1$  and  $n$

$$(Q/Q')_B = (Q/Q')_{Bc1} = (m/m')_Y^{3/2}$$

Recall

$$\begin{aligned} (s/s')_A f_A &= (Q/Q')_{Aqm} / (Q/Q')_{Ac1} \\ &= (s/s')_A (Q/Q')_{Aqm} / (Q/Q')_{Bc1} \\ &= \beta/\gamma = \alpha \end{aligned}$$

Thus the reduced partition function ratio,  $(s/s')f$ , is just the chemical isotope fractionation factor of the chemical species against the gaseous atom. With the convention prime is the light isotope it is easy to prove that  $\ln(s/s')f$  is always positive. This follows from the fact that  $u'_1 \geq u_1$ .

We return now to Eq. (10) and examine the  $G(u)$  function. It is a monotonic positive function. Its value is 1/2 as  $u$  goes to infinity and it approaches zero as  $u$  goes to zero. At small  $u$  it has the value  $u/12$ . For the case of small  $u$ , Eq. (11) becomes

$$\ln(s/s')f \approx \sum_i u_i \Delta u_i / 12 \approx \sum \delta u_i^2 / 24 \quad (17)$$

where  $\delta u_i^2 = u_i'^2 - u_i^2$ . But  $\sum u_i^2 = (\hbar/kT)^2 \sum h_{ii}$  where  $\sum h_{ii}$  is the trace of the secular equation of the molecular vibrations. The latter is independent of the coordinate system. For convenience we choose Cartesian coordinates and obtain

$$\sum h_{ii} = \sum \frac{1}{m_i} a_{ii} = \sum \frac{1}{m_i} \nabla^2 U$$

where  $a_{ii}$  is the sum of the three orthogonal Cartesian force constants equal to

$$\left( \frac{\partial^2}{\partial x_i^2} + \frac{\partial^2}{\partial y_i^2} + \frac{\partial^2}{\partial z_i^2} \right)$$

operating on the potential energy for the molecular vibrations. We then obtain

$$\ln(s/s')f \sim 1/24 (\hbar/kT)^2 \sum \left( \frac{1}{m_i} - \frac{1}{m_i} \right) \nabla^2 U \quad (18)$$

Maria Mayer prepared a summary of the above development in April 1944 (27) which was reviewed by Edward Teller at the request of H. C. Urey and M. Kilpatrick. Included in the summary paper were some applications of equations (12) and (18) to the possible chemical separation of the uranium isotopes. Edward Teller recognized that in Eq. (18) we had generalized the Herzfeld-Teller theorem to the case of chemical equilibrium in polyatomic molecules. A lucid summary of this development and some of the research it initiated is summarized by Clyde A. Hutchison, Jr. (29). Late in 1946 Maria Mayer and I were encouraged by W. F. Libby and H. C. Urey to prepare a summary of our work which could be published in the open literature (29). It was then that Libby called our attention to Waldmann's independent formulation of the reduced partition function ratio and the development of a mathematically equivalent form of Eq. (12) (30).

The  $\ln(s/s')f$  scale is a positive scale. The value of  $\ln(s/s')f$  of a compound is the maximum isotope fractionation that can be obtained if the heavy isotope is to concentrate in that compound. Detailed calculations show that values of  $\ln(s/s')f$  for a given isotopic substitution in a wide range of compounds lie within a narrow range at a given temperature. This is one of the reasons why isotope separation is difficult. In Table II we give some typical order of magnitude values of  $\ln(s/s')f$  at 300°K. A more detailed systematic discussion of the  $\ln(s/s')f$  scale and its relationship to isotope fractionation factors is given in London's book on isotope separation(31).

Table II

Approximate Values of  $\ln(s/s')$  at 300° K for Isotopes  
as a Function of Atomic Weight

<u>Isotopic Pair</u>	<u><math>\ln(s/s')</math> at 300° K</u>
D/H	2.3
$^{13}\text{C}/^{12}\text{C}$	0.1
$^{80}\text{Se}/^{78}\text{Se}$	0.01
$^{238}\text{U}/^{235}\text{U}$	0.002

The simplifications and insight that were introduced into isotope chemistry by the reduced partition function formulation led H. C. Urey in 1946 to revise and extend the pioneer calculations he had made with Rittenberg and Greiff. With the assistance of L. S. Myers, Urey calculated values of  $f$  for the isotopes of hydrogen, lithium, boron, carbon, nitrogen, oxygen, chlorine and bromine in a variety of compounds of each of these elements. The results were presented in the Liversidge lecture late in 1946 (32). In the course of this work, Urey was led to conceive of the isotopic paleotemperature scale. The latter is based on the temperature coefficient of the  $^{18}\text{O}/^{16}\text{O}$  fractionation between carbonate and water. The development of this method over the decades owes much to Epstein and has become an important method in geochemical science. In his paper Urey makes comparison between calculated values of equilibrium constants with experiment wherever possible.

For the calculation of the reduced partition function ratios of the isotopes of hydrogen, Urey found it necessary to introduce an anharmonic correction to the zero point energy difference, which in some cases led to corrections to the exchange equilibrium constants of the order of 5 - 10% at 300°K. The most extensive experimental data at the time were the exchange of tritium between hydrogen gas and water which covered the temperature range 273-600°K (33). For these calculations Urey made use of the extensive calculations of the vibrational frequencies and anharmonic corrections in the water molecules carried out by Libby (34). The experimental values are about 2-5% larger than the calculated values. Comparable agreement is found for other exchange reactions involving other elements and compounds.

The most important part of the anharmonic correction to isotope exchange equilibria is in the zero point energy term. The full theory of this correction was developed by Wolfsberg in 1967 (35). We shall outline here the theory for a diatomic molecule

$$H = 1/2 \dot{Q}^2 + 1/2 \lambda Q^2 + (a/\mu^{3/2})Q^3 + (b/\mu^2) Q^4 \quad (19)$$

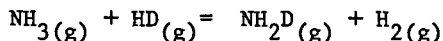
$$E/hc = G_0 + \omega_e (n + 1/2) - \chi_e \omega_e (n + 1/2)^2 + \dots \quad (20)$$

$$G_0 = \frac{B_e}{4} + \frac{\alpha_e \omega_e}{12B_e} + \left( \frac{\alpha_e \omega_e}{12B_e} \right)^2 \frac{1}{B_e} - \frac{\chi_e \omega_e}{4} \quad (21)$$

$$\alpha_e = \frac{24 B_e^3 r_e^3 a}{hc \omega_e^3} - \frac{6 B_e^2}{\omega_e} \quad (22)$$

$$B_e = h/8\pi^2 I_e c \quad (23)$$

In Eq.'s (19 - 23),  $Q$  is the normal coordinate and the other terms have the usual spectroscopic significance. The important new term introduced by Wolfsberg is  $G_0$ . This correction may be as large as the  $1/4 \chi_e^e$  correction in Eq. (20) and may be of the same or opposite sign. Wolfsberg has extended this method to the water and ammonia molecules. In Fig. II we reproduce the comparison of Bron and Wolfsberg's (36) calculation of exchange equilibrium

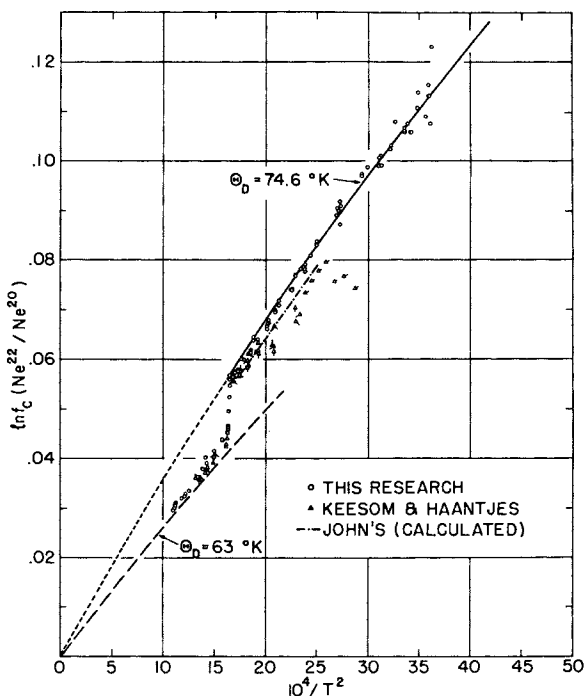


with experimental data over the temperature range 200-450°K. The agreement between theory and experiment is of the order of the precision of the experimental data, which is +1%. Even better agreement is obtained for  $^{18}\text{O}/^{16}\text{O}$  exchange between  $\text{CO}_2$  and  $\text{H}_2\text{O}$ . The results of Bottinga's (37) calculation are compared with the experimental data of Craig, Bottinga, O'Neil, Adami, and Truesdale in Fig. 3. The anharmonic correction is smaller for oxygen isotope exchange than hydrogen isotope exchange because of the smaller amplitude of vibration. Bottinga's calculation does not include Wolfsberg's  $G_0$  correction. In summary, we see that Eq. (13) when corrected for non-classical rotation and anharmonic effects leads to isotopic exchange equilibrium constants which agree within the order of one per cent of the experimental value of  $\ln K$ .

### Isotope Chemistry and Molecular Forces

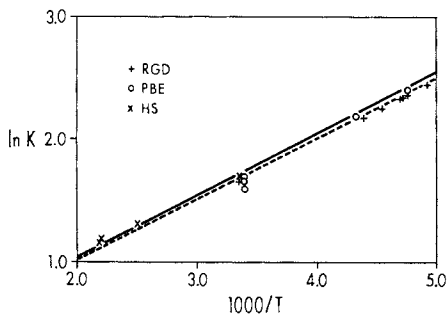
Much can be learned about the relationship between isotope chemistry and molecular structure and molecular forces by systematic calculations from Eq. (13). This can take the form of the study of real molecules or systematic variation in the properties of real molecules, e.g., bond lengths, force constants, substituents, etc., and determining the effect of such variations on  $\ln(s/s')f$ . This method has been employed to good effect by Wolfsberg and Stern (38) among others (39). An analytical approach to this central problem in isotope chemistry was initiated by Bigeleisen and Mayer (29) and further developed by Bigeleisen (22, 40-46), most recently in collaboration with Ishida and Spindel. The analytical approach consists in the series expansion of  $\ln(s/s')f$  in powers of

$\sum_i \delta u_i^{2j}$  ( $\delta u_i^{2j} = u_i^{2j} - u_i^{2j}$ ) and the explicit relations between  $\sum_i \delta u_i^{2j}$  and atomic masses and molecular force constants. The development over the years has involved extension of the range of validity of Eq. (18) first through alternate Taylor series expansions (40) and finally through the use of finite orthogonal polynomial expansions (41, 42, 45). The other



Journal of Chemical Physics

Figure 1. Plot of the logarithm of the reduced partition function of ( $^{22}\text{Ne}/^{20}\text{Ne}$ ) solid and liquid derived from vapor pressure data of Bigeleisen and Roth (8)



Journal of Chemical Physics

Figure 2. Comparison of theoretical calculations (36) of the equilibrium isotope exchange reaction  $\text{NH}_3(\text{g}) + \text{HD}(\text{g}) = \text{NH}_2\text{D}(\text{g}) + \text{H}_2(\text{g})$  with experimental data

aspect of the development has involved physical interpretation and numerical analysis of the various terms in the power series expansion of  $\ln(s/s')f$  in terms of  $\delta u_i^{2j}$ .

We now summarize the analytical extensions of Eq. (18).

$$\ln(s/s')f = \sum_i \sum_{j=1}^{\infty} (-1)^{j+1} \frac{B_{2j-1} \delta u_i^{2j}}{2j(2j)!} [u_i' < 2\pi] \quad (24)$$

$$= \sum_i \left( \frac{\delta u_i^2}{24} - \frac{\delta u_i^4}{2880} + \frac{\delta u_i^6}{181,440} \dots \right) [u_i' < 2\pi] \quad (25)$$

$$= \sum_i \sum_{j=1}^n W_j (-1)^{j+1} \frac{B_{2j} \delta u_i^{2j}}{2j(2j)!} [u_i' < \infty] \quad (26)$$

where  $B_{2j} - 1$  are the Bernoulli numbers ( $B_1 = 1/6$ ,  $B_3 = 1/30$ ,  $B_5 = 1/42$ , etc.) and  $W_j$  are finite orthogonal modulating coefficients. For convenience we will use the abbreviation  $A_j = (-1)^{j+1} B_{2j-1}/(2j)(2j)!$ . The finite orthogonal modulating coefficients are defined as (41, 42)

$$W_j = \sum_{k=1}^L \frac{T(n, j, R_k)}{k^{2j}} + T(n, j, R_{L+1}) \left[ z(j) - \sum_{k=1}^L \frac{1}{k^{2j}} \right]$$

$$= z(j)T(n, j, R_{L+1}) + \sum_{k=1}^L \frac{T(n, j, R_k) - T(n, j, R_{L+1})}{k^{2j}},$$

where

$$T(n, j, u') = \sum_{p=j}^n \frac{(-1)^p C_n^p}{R^p} / \sum_{p=0}^n \frac{(-1)^p C_n^p}{R^p}.$$

Here

$$R_k = R_1/k^2 = (u'/2\pi k)^2 \quad (k = 1, 2, \dots, L)$$

and

$z(j)$  is the Riemann zeta function.

Any value of the argument  $u'$  larger than the actual value will insure convergence of expansion (2). For a polyatomic molecule the modulating coefficient should be chosen in terms of the largest argument  $u_{\max}'$ , corresponding to the highest vibrational frequency, to ensure the convergence. The sums of the even

powers of  $u_i$  are obtained directly from the secular equation for the molecular vibrations:

$$\sum u_i^{2j} = \sum (\hbar/kT)^{2j} \lambda_i^j, \quad (27)$$

$$\sum \lambda_i^j = \text{Tr}[H^j], \quad (28)$$

$$H = F \cdot G, \quad (29)$$

$$|H - \lambda I| = 0, \quad (30)$$

where  $F$  and  $G$  are the Wilson potential- and kinetic-energy matrices, respectively. For brevity we will restrict our discussion to the implications from  $\sum \delta \lambda_i^2$  and  $\sum \delta \lambda_i^4$ .

The sums  $\sum \delta \lambda_i^2$  and  $\sum \delta \lambda_i^4$  are respectively

$$\sum \delta \lambda_i^2 = \sum_{\text{atoms}} (\mu_i' - \mu_i) a_{ii} \quad (31)$$

$$= \sum_{ij} \delta g_{ij} f_{ij} \quad (31a)$$

$$\sum \delta \lambda_i^4 = \sum_{\text{atoms}} (\mu_i'^2 - \mu_i^2) a_{ii}^2 + \sum_{\substack{\text{atoms} \\ i \neq j}} 2(\mu_i' - \mu_i) \mu_j a_{ij}^2 \quad (32)$$

$$\begin{aligned} &= \sum_i \delta g_{ii}^2 f_{ii}^2 + 2 \sum_{i \neq j} \delta (g_{ii} g_{jj}) f_{ij}^2 \\ &\quad + 2 \sum_{i \neq j} \sum \delta g_{ij}^2 (f_{ii} f_{jj} + f_{ij}^2) + 4 \sum_{i \neq j} \delta (g_{ii} g_{ij}) f_{ii} f_{ij} \\ &\quad + 4 \sum_{i \neq j \neq k} \delta (g_{ii} g_{jk}) f_{ij} f_{ik} \\ &\quad + 4 \sum_{i \neq j \neq k} \delta (g_{ij} g_{ik}) (f_{ij} f_{ik} + f_{ii} f_{jk}) \\ &\quad + 24 \sum_{i \neq j \neq k \neq l} \delta (g_{ij} g_{kl}) (f_{il} f_{kj} \end{aligned} \quad (32a)$$

where  $\delta (g_{ij} g_{kl}) = g'_{ij} g'_{kl} - g_{ij} g_{kl}$ . The summations in Eq. (32a) run over all different values of the distinct subscripts as



shown. In Equations (31) and (32),  $\mu'_i$  and  $\mu_i$  are reciprocal atomic masses of the light and heavy isotope respectively,  $a_{ij}$  is a Cartesian force constant,  $g_{ij}$  and  $f_{ij}$  are the elements of the Wilson G and F matrices,  $g_{ij}$  respectively.

The first order approximation of  $\ln(s/s')f$  through Eq.(26),  $j = 1$ , gives values of  $\ln(s/s')f$  within 10% of the exact solution, Eq. (13), even for D/H isotope effects at 300° K. Eq.(26) is an even better approximation to  $\ln(s/s')f$  of heavier elements. Within this limitation, we can now derive the first order rules of isotope chemistry by substitution of Equations (31) and (31a) into Eq. (26). They are:

- 1) Isotope effects,  $\ln(s/s')f$ , depend only on the masses of the isotopic atoms and the force constants bonding the atom at the site of isotopic substitution with other atoms in the molecule,  $a_{ij}$ .
- 2) Isotope effects between different compounds occur only when there are force constant changes at the site of isotopic substitution.
- 3) Isotope effects are additive.
  - a) isotopic additivity

$$\begin{aligned} \ln(s/s')f(D_2^{18}O/H_2^{16}O) &= \ln(s/s')f(D_2^{16}O/H_2^{16}O) \\ &+ \ln(s/s')f(H_2^{18}O/H_2^{16}O) \end{aligned}$$

- b) substituent additivity (47)

$$\begin{aligned} \ln(s/s')f(CHDFCl/CH_2FC1) &= \ln(s/s')f(CH_2DF/CH_3F) \\ &+ \ln(s/s')f(CH_2DC1/CH_3Cl) \\ &- \ln(s/s')f(CH_3D/CH_4) \end{aligned}$$

- 4) Isotope effects are cumulative (first rule of the geometric mean)

$$\ln(s/s')f(CH_2D_2/CH_4) = 2 \ln(s/s')f(CH_3D/CH_4)$$

- 5) Equivalent isomers have the same isotope chemistry.

$$\begin{aligned} \ln(s/s')f(C_6H_4D_2(O)/C_6H_6) &= \ln(s/s')f(C_6H_4D_2(m)/C_6H_6) \\ &= \ln(s/s')f(C_6H_4D_2(p)/C_6H_6) \end{aligned}$$

For the complete calculation of  $\ln(s/s')f$  directly from atomic masses and molecular structure, G matrices, and molecular forces, F matrices, it is necessary to relate the modulating coefficients,  $W_j$ , to these quantities. Each  $W_j$  is a positive

number in the range  $0 < W_i < 1$ . They have been tabulated as a function of  $u$  in the range  $0 < u < 25$  (48).  $W_i$  can be determined directly from the  $H' = G'F$  matrix by the row sum-column sum method (42). Through this method it is thus possible to calculate  $\ln(s/s')$  directly from the  $F$  and  $G$  matrices to any desired accuracy from Equations (26-28).

In Table III we summarize a correlation of exact values of  $\ln(s/s')$  at  $300^\circ \text{K}$  for  $^{13}\text{C}/^{12}\text{C}$  substitution in the two homologous series (1)  $\text{CO}$ ,  $\text{OCS}$ ,  $\text{CO}_2$  (2)  $\text{Br}_2\text{CO}$ ,  $\text{Cl}_2\text{CO}$ ,  $\text{F}_2\text{CO}$ . The correlation of  $\ln(s/s')$  with the sum of  $f_{ii}$  (stretch) plus  $f_{ii}$  (bend) is convincing evidence of the relationship between  $\ln(s/s')$  and force constants, as predicted from the simple one term expansion of Eq. (26).

From Eq. (32) we see that there are two types of effects which enter into the term  $W_2 A_2 \sum \delta u_i^4$ . The first term,  $W_2 A_2 (\mu_i'^2 - \mu_i^2) a_{ii}^2$ , is similar in form to the first order term  $W_1 A_1 (\mu_i' - \mu_i) a_{ii}$ . It is a statistical mechanical correction term corresponding to the harmonic motion of a mass ( $m_i, m_i'$ ) connected by a force  $a_{ii} X_i$  to an infinite mass. The second term,  $2W_2 A_2 (\mu_i' - \mu_i) \mu_j a_{ij}^2$ , is a kinetic energy coupling term which accounts for the fact that  $\mu_j$  is not zero and the  $j$ 'th atom shares some of the kinetic energy in the vibration (43). It is this term which explains why the isotope effect increases as the isotopic atom is successively bonded to a heavy rather than a light atom, e.g.,  $^{13}\text{C}/^{12}\text{C}$  in C-C vs C-H for equal force constant. Thus the C-C stretching force constant,  $5.09 \text{ mdyne } \text{\AA}^{-1}$ , contributes 0.035 to  $\ln(s/s')$  in ethane at  $300^\circ \text{K}$  while each of the three C-H stretching force constants,  $4.70 \text{ mdyne } \text{\AA}^{-1}$ , contributes but 0.016 to the same quantity. Up to terms in  $W_2 A_2 \sum \delta u_i^4$  we can write

$$\ln(s/s')f \approx \sum_i W_1 A_1 (\mu_i' - \mu_i) a_{ii} \left\{ 1 - \frac{W_2 |A_2|}{W_1 A_1} [(\mu_i' + \mu_i) a_{ii} + \sum_j 2\mu_j a_{ij}^2 / a_{ii}] \right\} \quad (33)$$

Inasmuch as the term in brackets in Eq. (33) is close to unity, Eq. (33) or the analogous one based on Equations (31a) and (32a) may be used to define effective bond force constants. Eq. (33) provides the theoretical basis for, and delimits the range of, applicability of Galimov's method for the calculation of  $\ln(s/s')$  from empirical bond values (49).

Within the framework of the first order approximation to  $\ln(s/s')$ , the isotope fractionation factor  $\ln \alpha = \ln(s/s')f_A - \ln(s/s')f_B$  always has the same sign, except for small differences which may arise from  $W_1(A) - W_2(B)$  as a function of

Table III

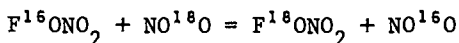
 $^{13}\text{C}/^{12}\text{C}$  Reduced Partition Function Ratio at 300° K <sup>a</sup>

Molecule	$f_{ii}$ Stretch <sup>b</sup>	$f_{ii}$ Bend	$\ln(s/s')f$
CO	18.5		0.0920
OCS	16.1, 7.1	0.64(2)	0.1356
CO <sub>2</sub>	15.6(2)	0.77(2)	0.1729
Br <sub>2</sub> CO	13.6, 2.5(2)	0.83(2), 1.13	0.1283
Cl <sub>2</sub> CO	13.7, 3.1(2)	0.94(2), 0.95	0.1391
F <sub>2</sub> CO	15.1, 6.5(2)	1.18(2), 1.52	0.1886

<sup>a</sup> See Reference (46).

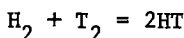
<sup>b</sup> Number in parenthesis, e.g., (2), gives the number of equivalent force constants with  $g'_{ij} \neq g_{ij}$ .

temperature. Within this approximation isotope fractionation factors do not change sign with temperature. Yet, they do. The latter, which is known as the cross over, is principally due to the  $W_2 A_2 \Sigma \delta u_i^4$  terms. To describe the cross over one must calculate  $2 \ln(s/s')$  for each compound at least through the second order terms. A convincing demonstration of the power of the finite orthogonal polynomial method for the calculation and understanding of the reduced partition function ratio of isotopic molecules was given by the calculation made by Ishida, Spindel, and Bigeleisen (42) of the cross over equilibrium in the exchange reaction

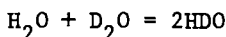


by a two term expansion of Eq. (26).  $W_1$  and  $W_2$  were obtained by the row sum-column sum method and Equations (31a) and (32a) gave  $\Sigma \delta u_i^2$  and  $\Sigma \delta u_i^4$ , respectively. A comparison with exact calculations from Eq. (13) is given in Fig. 4.

The  $W_2 A_2 \Sigma \delta u_i^4$  term in Eq. (26) allows one to predict the sign and magnitude of the deviation from the rule of the mean in the harmonic approximation. From this term we can derive the theorem: in an isotopic disproportionation reaction to form asymmetric molecules from symmetrical ones, the symmetry number corrected equilibrium constant is always less than unity. Only the term  $2(\mu'_i - \mu_i) \mu_j a_{ij}^2$  in  $\Sigma \delta u_i^4$  leads to deviations from the rule of the mean. Quantitative calculation of the deviations from the rule of the mean by Eq. (26) will require at least the term  $j = 3$ . The corrections are proportional to  $\mu_j a_{ij}^2$ . The largest deviations are expected for the equilibrium



for which the calculated value is  $\ln(K/4) = -0.441$  at  $298^\circ K$ . The corresponding value for  $H_2 + D_2 = 2HD$  is  $-0.204$ . On the other hand the values for



are  $-0.037$  and  $-0.038$  in the harmonic and fully corrected anharmonic approximations respectively (50). The experimental values of  $\ln(K/4)$  are some 50 per cent larger than the theoretical values, corresponding to a difference of 2.5 per cent between the experimental and theoretical values of  $K$ . This deviation may be real. The first order correction to  $\ln(K/4)$  for the isotopic disproportionation reaction with two equivalent atoms is, in the harmonic oscillator approximation,  $-W_2 |A_2| (\mu'_i - \mu_i) \mu_j a_{ij}^2$ . For the  $H_2$  molecule  $a_{ij}$  is the stretch-force constant. Transformation from Cartesian to valence force

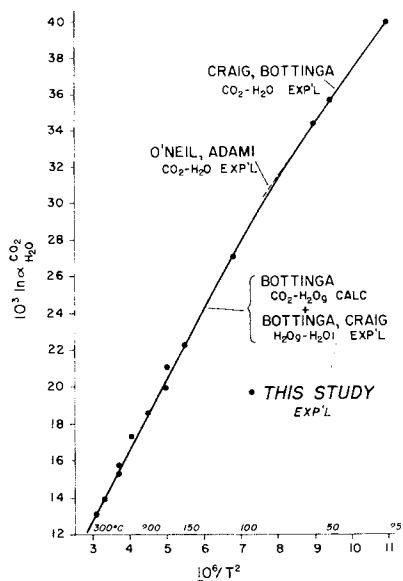
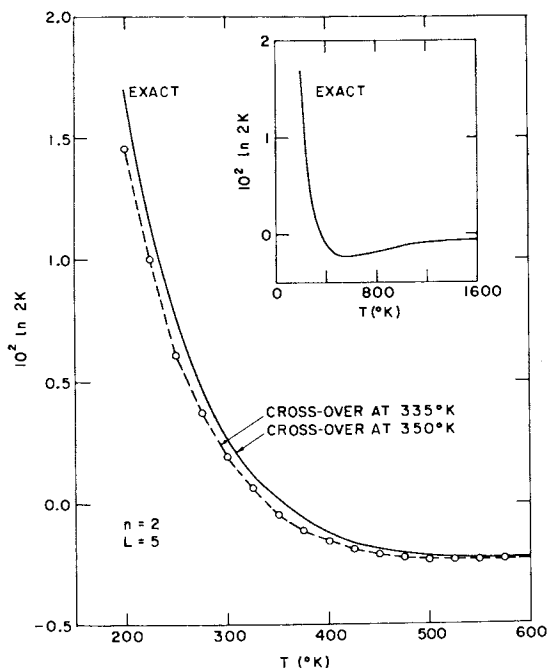


Figure 3. Comparison of theoretical calculations and experimental measurements for the equilibrium exchange of oxygen between  $\text{CO}_2(\text{g})$  and  $\text{H}_2\text{O}(\text{l})$



Advances in Chemistry Series

Figure 4. Exact and finite orthogonal polynomial expansion calculation of the equilibrium (42)  $\text{F}^{16}\text{ONO}_2 + \text{NO}^{18}\text{O} = \text{F}^{18}\text{ONO}_2 + \text{NO}^{16}\text{O}$

constants shows that  $(\mu'_1 - \mu_1)\mu_{1j}a_{ij}^2$  has a negligible contribution from the O-H stretching force constant in water. The deviation from the rule of the mean in the case of water and other polyatomic molecules has its origin in the bending force constants (41, 50). These theorems can be proven in detail from Eq. (32a). Since stretching force constants are approximately ten times those of bending force constants, it is apparent that the large deviations from the first rule of the mean for the isotopic disproportionation of the hydrogen molecules are unique.

The development of the finite orthogonal polynomial method provides the basis for the understanding of the total reduced partition function ratio,  $\ln(s/s')f$ , of a pair of isotopic molecules and each of the quantum terms,  $(h/kT)^{2j}$ , of order  $j$  to  $\ln(s/s')f$ . To this end Bigeleisen, Ishida, and Spindel have undertaken a systematic program for the correlation of  $\ln(s/s')f$  for isotopes of a number of elements in a variety of compounds with the molecular force constants in the compounds. It is of interest to compare the contributions of bending and stretching forces in a homologous series. This comparison is made in Table IV, taken from the recent work of Bigeleisen and Ishida (46), where the H/D isotope effects for the molecules  $\text{CH}_2\text{O}$ ,  $\text{CH}_4$ ,  $\text{C}_2\text{H}_6$ ,  $\text{C}_2\text{H}_4$ , and  $\text{C}_6\text{H}_6$  are intercompared. We can readily see the one to one correspondence of the contribution of the C-H stretching force constant to  $\ln(s/s')f$  with the magnitude of the C-H stretching force constant. In all cases the stretching force constant accounts for more than 65 per cent of the isotope effect even at room temperature. There is also a close parallelism of the sum of the contributions of the bending force constants to  $\ln(s/s')f$  with either the magnitude of the C-H stretching force constant or the sum of the bending force constants in a molecule are correlated. Small deviations from an exact linear relationship between force constants and contribution to  $\ln(s/s')f$  are associated with coupling effects, higher order terms, and geometrical effects in the case of some bending coordinates.

In recent years there has been significant progress in the quantum mechanical calculation of energies and wave functions of polyatomic molecules. Atomic force constants are related in a simple manner to molecular electron density functions (51). A significant beginning has been made in the calculation of atomic force constants (52) and their application to isotope chemistry (53).

The development of isotope chemistry has been closely connected with the development of quantum chemistry and quantum statistical mechanics. In many cases isotope chemistry has provided important guides to the development of quantum statistical mechanics. In other bases it has provided important and unique confirmations. We can confidently expect this pattern to continue into the future.

Table IV  
 Contributions of Stretching and Bending Forces to  $\ln(s/s')f(D/H)$  at 300° K

Coordinate	$\frac{CH_2O}{CH_4}$	$\frac{CH_4}{C_2H_6}$	$\frac{C_2H_6}{C_2H_4}$	$\frac{C_2H_4}{C_2H_6}$
C-H Stretch	1.478	1.600	1.556	1.675
$f$ (mdyne Å <sup>-1</sup> )	(4.31)	(4.92)	(4.70)	(5.03)
HCH bend (a)	0.130(1)	0.631(3)	0.464(2)	0.355(1)
HGX bend (p) <sup>b</sup>	0.352		0.289	0.202
HGX bend (o-p)	0.172			0.132
HGX bend (t)				0.100
$\Sigma$ "bend"	0.654	0.631	0.753	0.789
Total $\Sigma$	2.132	2.231	2.309	2.364
Exact	2.200	2.312	2.353	2.321
				$\frac{C_2H_6}{C_2H_4}$
				1.632
				(5.06)
				0.572
				0.266
				0.838
				2.470
				2.395

<sup>a</sup> Number of bending coordinates affected by the isotopic substitution.

<sup>b</sup> (p) means planar; (o-p) means out-of-plane; (t) means torsion.

## Literature Cited

1. Fajans, K., *Physik. Z.* (1915) 16, 456.
2. Stern, O., (1914), see Keesom, W. H. and Van Dijk, H., *Proc. Roy. Acad. Sci. Amsterdam* (1931) 34, 42.
3. Lindemann, F. A. and Aston, F. W., *Phil. Mag.* (1919) 37, 523.
4. Lindemann, F. A., *Phil. Mag.* (1919) 38, 173.
5. Urey, H. C., Brickwedde, F.G., and Murphy, G.M., *Phys. Rev.* (1931) 39, 164; (1932) 40, 1.
6. Keesom, W. H. and Haantjes, J., *Physica* (1935) 2, 986.
7. Roth, E. and Bigeleisen, J., *J. Chem. Phys.* (1960) 32, 612.
8. Bigeleisen, J. and Roth, E., *J. Chem. Phys.* (1961) 35, 68.
9. Lee, M. W., Fuks, S. and Bigeleisen, J., *J. Chem. Phys.* (1970) 53, 4066.
10. Phillips, J. T., Linderstrom-Lang, C. V. and Bigeleisen, J., *J. Chem. Phys.* (1972) 56, 5053.
11. Lee, M. W., Eshelman, D. M. and Bigeleisen, J., *J. Chem. Phys.* (1972) 56, 4585.
12. Mandel, F., *J. Chem. Phys.* (1972) 57, 3929.
13. Bigeleisen, J., Lee, M. W. and Mandel, F., *Ann. Rev. Phys. Chem.* (1973) 24, 407.
14. Bigeleisen, J., Lee, M. W. and Mandel, F., *Accounts of Chemical Research*, in press.
15. Herzfeld, K. F. and Teller, E., *Phys. Rev.* (1938) 54, 912.
16. Bigeleisen, J., *J. Chem. Phys.* (1961) 34, 1485; see also paper by Van Hook, W. A. in this monograph.
17. Urey, H. C. and Rittenberg, D., *J. Chem. Phys.* (1933) 1, 137.
18. Giauque, W. F., *J. Am. Chem. Soc.* (1930) 52, 4808.
19. Herzberg, G., "Infra-red and Raman Spectra of Polyatomic Molecules", Van Nostrand, New York, (1945).
20. Rittenberg, D. and Urey, H. C., *J. Am. Chem. Soc.* (1934) 56, 1885.
21. Urey, H. C. and Greiff, L. J., *J. Am. Chem. Soc.* (1935), 57, 321.
22. Bigeleisen, J., *J. Chem. Phys.* (1955) 23, 2264.
23. Lewis, G. N. and MacDonald, R. T., *J. Am. Chem. Soc.* (1936) 58, 2519.
24. Hutchison, C. A., Jr., Stewart, D. W. and Urey, H. C., *J. Chem. Phys.* (1940) 8, 532.
25. Thode, H. G. and Urey, H. C., *J. Chem. Phys.* (1939) 7, 34.
26. Smyth, H. D., "Atomic Energy for Military Purposes", Princeton University Press, Princeton, (1945).
27. Mayer, M. G., S.A.M. Report 4-M-159, April 8, 1944. See also reference No. 28.
28. Hutchison, C. A., Jr., "Chemical Separation of the Uranium Isotopes", NNES, Div. 3, Vol. 3, Oak Ridge, (1952).
29. Bigeleisen, J. and Mayer, M. G., *J. Chem. Phys.* (1947) 15, 261.



30. Waldmann, L., *Naturwiss.* (1943) 31, 205.
31. Bigeleisen, J., in London, H., "Separation of Isotopes", Geo. Newnes, Ltd., London, (1961).
32. Urey, H. C., *J. Chem. Soc.* (1947) 562.
33. Black, J. F. and Taylor, H. S., *J. Chem. Phys.* (1943) 11, 395.
34. Libby, W. F., *J. Chem. Phys.* (1943) 11, 101.
35. Wolfsberg, M., "Advances in Chemistry", (1969) 89, Am. Chem. Soc.
36. Bron, J. and Wolfsberg, M., *J. Chem. Phys.* (1972) 57, 2862.
37. Bottinga, Y., *J. Phys. Chem.* (1968) 72, 800.
38. Stern, M. J. and Wolfsberg, M., *J. Chem. Phys.* (1966) 45, 2618.
39. Hartshorn, S. R. and Shiner, V. J., Jr., *J. Am. Chem. Soc.* (1972) 94, 9002.
40. Bigeleisen, J., "Proc. Intern. Symp. Isotope Separation", North Holland Publishing Company, Amsterdam, (1958), 121.
41. Bigeleisen, J. and Ishida, T., *J. Chem. Phys.* (1968), 48, 1311.
42. Ishida, T., Spindel, W. and Bigeleisen, J., *Advan. Chem. Ser.* (1969) 89, 192.
43. Bigeleisen, J., Ishida, T. and Spindel, W., *Proc. Nat. Acad. Sci.* (1970) 67, 113.
44. Bigeleisen, J., Ishida, T. and Spindel, W., *J. Chem. Phys.* (1971) 55, 5021.
45. Bigeleisen, J. and Ishida, T., *J. Am. Chem. Soc.* (1973) 95, 6155.
46. Bigeleisen, J. and Ishida, T., *J. Chem. Phys.*, in press.
47. The substituent additivity rule holds in the approximation that off diagonal  $F$  matrix elements,  $f_{ij}$  ( $i \neq j$ ), are small. When isotope substitution is at an end <sup>$i$</sup>  atom, e.g.,  $C_2H_5D$  vs  $C_2H_6$ , only the interaction of adjacent bending coordinates have non-zero values of  $\delta g_{ij}$ , which reduces the above qualification on substituent <sup>$i$</sup>  additivity.
48. NAPS document O1022, National Auxiliary Publication Service, c/o CCM Information Corp., 909 Third Ave., New York, New York 10022.
49. Galimov, E. A., *Geochimica et Cosmochimica*, in press.
50. Wolfsberg, M., Massa, A. A. and Pyper, J. W., *J. Chem. Phys.* (1970) 53, 3138.
51. Anderson, A. B. and Parr, R. G., *J. Chem. Phys.* (1970) 53, 3375.
52. Gaughen, R. R. and King, W. T., *J. Chem. Phys.* (1972) 57, 4530.
53. King, W. T., *J. Phys. Chem.* (1973) 77, 2770.

# Isotope Effects and Spectroscopy

CHARLES P. NASH

Department of Chemistry, University of California, Davis, Calif. 95616

## Introduction

One of the most valuable techniques available to any kind of spectroscopist is that of isotopic substitution. This paper will discuss a few applications of the method to problems in the optical spectroscopy of atoms, diatomic and small polyatomic molecules, the vibrations of transition metal complexes, hydrogen bonding, solvation, and optical activity. We shall not treat either magnetic resonance or microwave spectroscopy.

Any review which treats optical spectroscopy must acknowledge at its outset the magnificent series of volumes on this subject by Herzberg (1,2,3,4). The textbooks by Walker and Straw (5), and King (6) also treat many of the subjects we shall discuss at a somewhat less advanced level.

## Atomic Spectra

In the domain of atomic spectroscopy, the first direct observation of deuterium was made in 1932 by Urey, Brickwedde, and Murphy (7), who observed weak satellites of four of the Balmer lines of hydrogen which were shifted to shorter wavelengths by amounts ranging from 1.79 Å for  $H_{\alpha}$  at 6536 Å to 1.12 Å for  $H_{\delta}$  at 4102 Å. Within experimental error the shifts were in exact agreement with the predictions of quantum mechanics for the effect of a mass "2" nucleus on the reduced mass of the atom. For multi-electron atoms, isotope effects are manifest not only in the changes in hyperfine structure arising from nuclear spin changes (1,8), but also in small shifts in the energies of s electrons which may be attributed to changes in the nuclear dimensions (9). Hindmarsh, Kuhn, and Ramsden (10) have attributed some of the irregularities found in atomic isotope shifts to the closing of nuclear shells.

### Diatomic Molecule Spectra

When two atoms are combined to form a diatomic molecule, isotope effects appear in the vibrational, rotational, and electronic spectra. To the extent that the Born-Oppenheimer approximation is valid, the potential function for a given electronic state is independent of the masses of the nuclei. The harmonic vibration frequencies of two isotopic variants of a diatomic molecule in the same electronic state are then related by the equation

$$\frac{\omega_2}{\omega_1} = \left( \frac{\mu_1}{\mu_2} \right)^{\frac{1}{2}} \quad (1)$$

where  $\omega_j$  is the harmonic vibration frequency of the  $j$ 'th isotopic variant, and  $\mu_j$  is the reduced mass of that molecule; i.e.,

$$\mu = \frac{M_A M_B}{M_A + M_B} \quad (2)$$

Here  $M_A$  and  $M_B$  are the atomic masses of the atoms comprising the molecule.

One obvious source of differences in the rotational spectra of isotopically-related diatomic molecules arises from the fact that the energy levels of the rigid rotor contain an explicit  $\mu^{-1}$  dependence. Another effect also occurs if one of the isotopic variants is a homonuclear molecule and the other is heteronuclear.

For a homonuclear diatomic molecule composed of even(odd) mass-number nuclei, the total wave function, which we assume to be a product of electronic, vibrational, rotational, and nuclear-spin functions, must be symmetric (antisymmetric). If the electronic wave function is symmetric, and if the nuclear spin is zero, as in the ground state of  $^{16}\text{O}_2$ , only even values of  $J$ , the rotational quantum number, are allowed. If the nuclear spin is not zero, both even and odd values of  $J$  (i.e., symmetric and antisymmetric rotational wave functions) are allowed, but with different statistical weights. These may be determined from the nuclear-spin part of the wave function.

For a nuclide of spin  $s_n$  the nuclear-spin degeneracy is  $g_n = (2s_n + 1)$ . For the molecule a total of  $g_n^2$  nuclear-spin functions are possible, of which  $g_n(g_n + 1)/2$  are symmetric (ortho), and  $g_n(g_n - 1)/2$  are antisymmetric (para). The ortho (or para) nuclear spin functions then combine exclusively with either even- $J$  or odd- $J$  rotational states to produce overall wave functions which have the proper symmetry.

For  $H_2$  ( $s_n = \frac{1}{2}$ ) the total wave function must be antisymmetric, the odd-J levels combine with the ortho spin-functions, and the statistical odd-J:even-J ratio is 3:1. For  $D_2$  or  $^{14}N_2$  ( $s_n = 1$ ) the total wave function must be symmetric. The even-J levels now combine with the ortho spin-states, and the statistical even-J:odd-J ratio is 6:3=2:1. For heteronuclear diatomic molecules the allowable values of J are not subject to symmetry constraints.

In accordance with these considerations, the pure-rotational Raman spectrum (selection rule  $\Delta J = \pm 2$ ) of  $^{16}O_2$  has every second line missing, whereas that of  $^{14}N_2$  has all lines present, but those arising from even-J states are more intense than those arising from odd-J states (2). Yoshino and Bernstein (11) have observed intensity alternations having statistical origins in both the pure-rotational Raman spectrum of  $H_2$ , and in the rotational fine-structure (selection rules  $\Delta J = 0, \pm 2$ ) of the vibrational band in the Raman spectra of both  $H_2$  and  $D_2$ .

If a high-resolution infrared spectrophotometer is available to them, undergraduates can obtain and analyze in detail the fundamental vibration-rotation spectra of the four common isotopic variants of hydrogen chloride ( $H, D, ^{35}Cl, ^{37}Cl$ ) (12,13). For these molecules the potential curve is significantly anharmonic, and a dependence of the rotational constant on the vibrational quantum number is immediately apparent, since the rotational lines are not evenly spaced. From their data our students have confirmed the constancy of the equilibrium internuclear distances in these four molecules to within  $\pm 0.001 \text{ \AA}$ , and they have confirmed the validity of Eq. 1 to four decimal places. It must be emphasized that when band-origins rather than harmonic frequencies are used in Eq. 1, disagreements occur in the second decimal place. Extensive comparison data are available in the literature for all these molecules (14,15,16,17,18).

It is of some interest to note here also that Connes *et al.* (19) have detected 8 lines of the R-branch of the  $\Delta v = 2$  vibration-rotation band of both  $H^{35}Cl$  and  $H^{37}Cl$  at about  $5700 \text{ cm}^{-1}$  in the spectrum of Venus. The agreement between the astronomical data and laboratory data was within  $\pm 0.01 \text{ cm}^{-1}$  for all lines. By comparing the relative intensities of the Venusian HCl and  $CO_2$  spectra they estimated a partial pressure of HCl  $\sim 10^{-4}$  torr, and from the relative intensities of the rotational lines they estimated a rotational temperature of 240 K.

The electronic spectra of isotopically varied diatomic molecules reflect the effects of changes in the vibrational and rotational energy levels of both the ground and the excited electronic states. This subject is of great historical importance, since the isotopes  $^{18}O$ ,  $^{17}O$ ,  $^{13}C$ , and  $^{15}N$  were all identified in 1929 on the basis of weak bands in the electronic spectra of diatomic molecules.

Giauque and Johnston (20,21) identified a weak band in the solar spectrum of oxygen near  $7595 \text{ \AA}$  as the (0,0) band of the b-X transition of  $^{18}\text{O}^{16}\text{O}$  on the basis of an isotopic shift of the band origin of  $-2.07 \text{ cm}^{-1}$  vs. the band origin of the (0,0) band of  $^{16}\text{O}_2$ , as well as the fact that the band envelope of the homonuclear molecule contained 13 lines whereas that of the heteronuclear molecule contained 26.

There then followed the identification of  $^{13}\text{C}^{12}\text{C}$  in the Swan bands of  $\text{C}_2$  by King and Birge (22);  $^{17}\text{O}^{16}\text{O}$  in the solar spectrum by Giauque and Johnston (23,24);  $^{15}\text{N}^{16}\text{O}$ ,  $^{14}\text{N}^{18}\text{O}$ , and  $^{14}\text{N}^{17}\text{O}$  by Naudé (25); and  $^{13}\text{C}^{14}\text{N}$  and  $^{13}\text{C}^{16}\text{O}$  by King and Birge (26).

### The Spectra of Small Polyatomic Molecules

Isotopic substitution has been an important tool in the solution of an enormous variety of problems in the spectroscopy of small polyatomic molecules. One such problem is the structure of the ethane molecule (27). The eclipsed form of this molecule, having symmetry  $D_{3h}$ , would have three Raman-active vibration-rotation bands, designated  $\nu_{10}$ ,  $\nu_{11}$  and  $\nu_{12}$ , for which the selection rule  $\Delta K = \pm 1$  would predict only one series of Q-branches. The corresponding vibration-rotation bands for the staggered conformation, having symmetry  $D_{3d}$ , would obey the selection rules  $\Delta K = \pm 1, \pm 2$ . Thus two sets of Q-branches would be observed. The CH stretching-region of the  $\text{C}_2\text{H}_6$  spectrum contains a complicated admixture of the lines of the  $\nu_{10}$  fundamental together with those of the  $\nu_1$  fundamental and three other combination bands. The  $\nu_{10}$  fundamental of  $\text{C}_2\text{D}_6$ , however, occurs free from any other interferences. Two well-defined sets of Q-branches were observed, and hence the staggered structure of ethane was confirmed beyond question.

If one wishes to determine the vibrational force constants for a polyatomic molecule, isotopic substitutions are essential. The general valence force field for a non-linear polyatomic molecule, expressed in internal coordinates, contains a total of  $\frac{1}{2}(3N-6)(3N-5)$  force constants. Some of these may equal others by the symmetry of the molecule, but a maximum of only  $(3N-6)$  vibration frequencies may be observed.

The well-known Wilson GF-matrix method (28,29) allows one to break down the  $(3N-6) \times (3N-6)$  secular determinant for the molecule into smaller blocks, the number and size of which depend on the symmetry of the molecule in question. Any  $n \times n$  block of the block-diagonal secular equation obtained by Wilson's method yields, of itself, an  $n \times n$  secular equation of the form

$$|\underline{GF} - \underline{\Lambda}| = 0 \quad (3)$$

The  $\underline{G}$  matrix elements are composed only of structural parameters of the molecule (its masses, bond distances, and bond angles), while the  $\underline{F}$  matrix elements, which are called symmetry force constants, are usually linear combinations of the general valence force constants. The roots,  $\lambda_i$ , of the secular equation, Eq. 3, are related to the harmonic vibration frequencies of the  $n$  normal modes of that symmetry type by

$$\lambda_i = 4\pi^2 c^2 \omega_i^2 \quad (4)$$

where the  $\omega_i$  are expressed in  $\text{cm}^{-1}$  and  $c$  is the speed of light.

Except when  $n=1$ , the number of independent  $\underline{F}$  matrix elements,  $\frac{1}{2}n(n+1)$ , exceeds the number of observable frequencies,  $n$ . Even when  $n=1$  the  $\underline{F}$  matrix element may still be a combination of general force constants.

If one or more isotopic substitutions are performed on the molecule, new frequencies will be obtained, as well as new  $\underline{G}$  matrix elements. Within the Born-Oppenheimer approximation, however, the  $\underline{F}$  matrix elements will transfer intact to the new molecule. The amount of new information which can be obtained about the elements in the  $\underline{F}$  matrix in this way is, however, limited by several isotope rules which the sets of harmonic frequencies of each symmetry type must obey. One of these, the form of the Teller-Redlich product rule which applies to two isotopic variants having the same molecular symmetry, may be deduced immediately from the secular equation itself. When the  $n \times n$  secular determinant is expanded in polynomial form, the constant term, which must be equal to the product of the roots,  $\prod_{i=1}^n \lambda_i$ , is simply the determinantal product  $|\underline{G}| \cdot |\underline{F}|$ . Thus, if we designate with superscript  $j$ 's and  $k$ 's the properties of two isotopic variants having the same molecular symmetry, we find

$$\frac{\prod_{i=1}^n \lambda_i^j}{\prod_{i=1}^n \lambda_i^k} = \frac{|\underline{G}^j|}{|\underline{G}^k|} = \left[ \frac{\prod_{i=1}^n \omega_i^j}{\prod_{i=1}^n \omega_i^k} \right]^2 \quad (5)$$

In addition to the product rule, there are also sum rules which further restrict the number of independent observables when more than two isotopic variants are available. This subject has been discussed in detail by Heicklen (30). One interesting conclusion he reaches is that for molecules with symmetry the full  $\underline{F}$  matrix can be determined by substituting for all but one of the sets of equivalent atoms. In principle, then,  $^{12}\text{CH}_4$  and  $^{13}\text{CH}_4$ ,  $\text{C}_6\text{H}_6$  and  $\text{C}_6\text{D}_6$ , or  $^{12}\text{C}_6\text{H}_6$  and  $^{13}\text{C}_6\text{H}_6$ , should suffice to

determine the force-fields for methane or benzene. In practice, however, such a minimum set of data is rarely enough. For methylamine,  $\text{H}_3\text{CNH}_2$ ,  $\text{D}_3\text{CND}_2$ ,  $\text{D}_3\text{CNH}_2$ , and  $\text{H}_3\text{C}^{15}\text{NH}_2$  have all been studied, but almost half the elements of the general force-constant matrix are still undetermined (31). Hirakawa, Tsuboi, and Shimanouchi (31) point out that  $^{13}\text{C}$  substitution would be very helpful in analyzing this particular molecule.

The vibration frequencies of a molecule are not the only sources of information about the elements of the symmetry force-constant matrix. In the vibration-rotation spectra of polyatomic molecules, especially those with degenerate vibrational modes, e.g., symmetric tops, there occur certain anomalies in the spacings of the rotational lines which may be attributed to the Coriolis interaction (32). This phenomenon, which is a coupling between the rotational angular momentum of the molecule and its vibrational angular momentum, is expressed in terms of coupling constants called zeta constants. The  $\zeta$ -constants are directly related to the  $\underline{F}$  and  $\underline{G}$  matrices for the molecule in question. The  $\zeta$ -constants for a given molecule must have a sum which may be inferred from the molecular structure, and for all symmetric tops, except those which belong to the  $S_4$  and  $D_{2d}$  point groups, there is also an isotope rule which they must obey, namely

$$m \sum_i \omega_i^2 (1 - \zeta_i) = \text{constant} \quad (6)$$

Here  $m$  is the mass of the off-axis atom,  $\omega_i$  is the harmonic vibration frequency of the  $i$ -th degenerate normal mode, and  $\zeta_i$  is the Coriolis constant for that mode. The summation extends over all the normal modes belonging to a given degenerate species.

The work of Aldous and Mills (33,34) on the methyl halides provides an excellent example of the determination of force constants. For one of these molecules there are six independent vibrations -- three of class  $A_1$  and three of class E. There are 16 different force constants in the general valence force field expressed in internal coordinates, and 12 force constants in the symmetrized  $\underline{F}$  matrix, all but two of which are linear combinations of the original 16. For  $\text{CH}_3\text{X}$  and  $\text{CD}_3\text{X}$  together there are 12 observed frequencies, but the product rule states that within each class only five of the six frequencies are independent observables. For the E-vibrations of either  $\text{CH}_3\text{X}$  or  $\text{CD}_3\text{X}$  three  $\zeta$ -constants can be measured. However each molecule must obey a  $\zeta$ -sum rule, and together they must obey the isotope rule, so that only three of the six  $\zeta$ -constants are truly independent.

In addition to the vibration frequencies and the zeta constants, Aldous and Mills included in their determination of the force field the data then available on the centrifugal-

distortion constants, two of which are possible for one of these molecules. These constants are related to derivatives of the moment-of-inertia tensor and the elements of the inverse of the  $F$  matrix for both the  $A_1$  and the  $E$  vibrations (35,36). Thus, up to 22 experimental values for each isotopic pair were used by Aldous and Mills to determine the 12 elements of the  $F$  matrices for all the methyl halides, together with estimates of their probable errors.

The effects of isotopic substitution on the vibrational spectra of small polyatomic molecules have resulted in two recent astrophysical observations of considerable interest. The first extra-terrestrial detection of deuterium was reported in 1972 by Beer *et al.* (37), who found 11 lines of the P-branch of the  $2\nu_3$  vibration-rotation band of  $CH_3D$  in the spectrum of Jupiter. More recently Beer and Taylor (38) have examined the intensities of these lines and concluded that the D/H ratio in the atmosphere of Jupiter is between 1/2 and 1/6 the terrestrial value.

In 1969 Young (39) published a high-resolution spectrum (which had actually been obtained earlier by Connes' group) showing a very complete vibration-rotation band comprising the  $2\nu_3$  transition of  $^{13}C^{16}O^{18}O$  centered at  $4508\text{ cm}^{-1}$  in the spectrum of Venus. This molecule, unknown in the laboratory, could be detected in spite of the abundance of  $CO_2$  in the earth's atmosphere, because for all the symmetrical isotopes of carbon dioxide (symmetry  $D_{\infty h}$ ) this overtone is symmetry forbidden. On the basis of a painstaking analysis of the intensities of the rotational lines Young deduced a rotational temperature of  $245 \pm 3$  K, in excellent agreement with the value of 240 K obtained by Connes *et al.* (19) from the spectra of the HCl species.

While it is common knowledge that isotopic substitution alters the vibration frequencies of normal modes, it may be less well known that the intensity of the corresponding infrared absorption band must be affected as well. Crawford (40) has shown that within the harmonic approximation the integrated intensity of an infrared absorption band,  $\Gamma_i$ , is given by

$$\Gamma_i \equiv \frac{1}{nl} \int_{\text{band}} \ln \left( \frac{I_0}{I} \right) d\ln \omega = \frac{N_A \pi}{3c^2 \omega_i} \left( \frac{\partial \bar{u}}{\partial Q_i} \right)^2 \quad (7)$$

Here  $n$  is the concentration of the absorber,  $l$  is the path length,  $I_0$  and  $I$  are the incident and transmitted intensities respectively,  $\omega_i$  is the harmonic frequency of the  $i$ 'th absorption band,  $N_A$  is Avogadro's number,  $c$  is the speed of



light,  $\vec{\mu}$  is the dipole moment of the molecule, and  $Q_i$  is the  $i$ 'th normal coordinate. Now  $\vec{\mu}$  is invariant to isotopic substitution, but both  $\omega_i$  and  $Q_i$  are mass-dependent, and hence the intensity of the band must be mass-dependent as well.

Crawford (41) has also shown that the integrated intensities of the infrared absorption bands of isotopically related molecules must obey two sum-rules, one of which, the so-called F-sum rule, may be written  $\sum_i \frac{\mu_i^2}{\omega_i} = \text{constant}$ . Here the summation extends over all vibrations of the same symmetry class.

Dickson, Mills, and Crawford (42) have made an extensive study of the vibrational intensities of the proto and deuteromethyl chlorides, bromides, and iodides. Among other things, they found that the  $A_1$  vibrations of the methyl bromides and methyl iodides showed excellent agreement with the F-sum rule, but the agreement for the methyl chlorides was less satisfactory.

In his excellent recent monograph based on his Baker lectures, Herzberg (43) describes the way in which isotopic studies contributed to the identification of two transient species. In the spectrum of a comet, a band system was found near 4050 Å which Herzberg, in 1942, attributed to the  $\text{CH}_2$  radical. He also found the same bands in the spectrum of a discharge through methane. In 1949, however, Monfils and Rosen (44) found the identical spectrum from a discharge through  $\text{CD}_4$ , and hence the entity responsible for it could not have been  $\text{CH}_2$ . In 1951 Douglas (45) reported the spectrum of a discharge through an equimolar mixture of  $^{12}\text{CH}_4$  and  $^{13}\text{CH}_4$ . There appeared six bands, and hence the species in question must have contained three carbon atoms. In 1954 Clusius and Douglas (46) reported the spectrum of a discharge through pure  $^{13}\text{CH}_4$ . They found an intensity alternation in the rotational lines having a 3:1 ratio, and they also inferred that in the spectrum of the  $^{12}\text{CH}_4$  discharge every-other rotational line was missing. This kind of behavior, analogous to that cited earlier for diatomic molecules, is diagnostic for a linear triatomic molecule. Thus the species responsible for the 4050 Å band was identified as linear  $\text{C}_3$ .

Herzberg (43) then describes the actual discovery of the  $\text{CH}_2$  radical, which was produced by the flash photolysis of diazomethane. The absorption band, which appeared at 1415 Å, shifted when  $\text{CD}_2\text{N}_2$  rather than  $\text{CH}_2\text{N}_2$  was photolyzed. In subsequent experiments the photolysis of  $^{13}\text{CH}_2\text{N}_2$  confirmed the presence of a carbon atom in the radical.

Very recently Katayama, Huffman, and O'Bryan (47) have studied the absorption and photo ionization spectra of several isotopic water molecules in the vacuum ultraviolet. As part of this investigation they used the spectra of  $\text{H}_2^{16}\text{O}$  and  $\text{H}_2^{18}\text{O}$  to establish that the first electronic excited state of  $\text{H}_2\text{O}^+$  is linear.

### The Vibrational Spectra of Metal Complexes.

In recent years Nakamoto (48) has pioneered in the use of isotopes of the transition metals in order to make assignments of the vibrational bands of their complexes. By studying the spectra of  $^{50}\text{Cr}(\text{acac})_3$  and  $^{53}\text{Cr}(\text{acac})_3$ , Nakamoto, Udovich, and Takemoto (49) were able to assign a band at  $460\text{ cm}^{-1}$  to a Cr-O stretching mode and one at  $592\text{ cm}^{-1}$  to an out-of-plane ring mode. On the basis of  $^{16}\text{O} \rightarrow ^{18}\text{O}$  isotopic substitution, the  $592\text{ cm}^{-1}$  band had previously been misassigned as the Cr-O stretch (50).

For tetrahedral  $\text{XY}_4$  species the totally symmetric  $A_1$  stretching mode involves no motion of the central atom, and hence should yield virtually no isotope shift when that atom is substituted. The triply-degenerate  $F_2$  mode, however, should display an isotope effect. Thus Takemoto and Nakamoto (51) were able to assign bands in the Raman spectra of  $\text{Zn}(\text{NH}_3)_4$  at  $430\text{ cm}^{-1}$  and  $410\text{ cm}^{-1}$  to the  $A_1$  and  $F_2$  modes respectively. In this instance the isotopes  $^{64}\text{Zn}$  and  $^{68}\text{Zn}$  were used. The ordering of these two levels in this complex is somewhat unexpected, since in the vast majority of the  $\text{XH}_4$ , tetrahalogeno, or  $\text{XO}_4$  species which have been examined the  $F_2$  band occurs at the higher frequency (52).

As a final example of the use of isotopic substitution in the study of metal complexes, we cite the use of  $^{15}\text{NO}$  as a ligand by Collman, Farnham, and Dolcetti (53), who found what they termed "hybridization tautomerism" in several cobalt-nitrosyl complexes. From their infrared spectra they inferred a rapid equilibrium between a trigonal-bipyramidal Co(I) species having a linear Co-nitrosyl geometry, and a square-pyramidal Co(III) species, in which the Co-nitrosyl moiety is bent.

### Hydrogen Bonding Studies.

Much current interest in the spectroscopy of hydrogen bonded systems attaches to the question of how one might infer the shape of the potential function from the vibrational spectrum of the entity. In this connection Wood and his collaborators have recently made major contributions. They have examined the infrared and Raman spectra of a great number of cations of the form  $(\text{BPB}')^+$ , where B and B' are nitrogen bases or perdeutero-nitrogen bases, and P is either hydrogen or deuterium.

When B and B' were both trimethylamines (54) the  $\text{NH}^+$  stretching band and the  $\text{ND}^+$  stretching band were both singlets. The same behavior obtained also when B and B' were trimethylamine and pyridine (55). When  $\text{B}=\text{B}'=\text{pyridine}$  (56), or substituted pyridines (57), and  $\text{P}=\text{H}$ , the  $\text{NH}^+$  band was split into a

broad doublet. The  $\text{ND}^+$  stretch, however, was a singlet. Also in these ions the N--N stretching motion, which was observed in the infrared spectrum, showed only a small frequency shift when the bridge was deuterated.

When  $\text{B} \neq \text{B}'$ , but both bases were various pyridines or quinoline, the  $\text{NH}^+$  band could be characterized as a doublet with an intensity ratio of the components which varied between 1.2 and zero as the  $\text{pK}_\text{A}$  difference of the bases varied between zero and eight (58). The N--N stretching mode in these unsymmetrical ions was not substantially more intense than that found when  $\text{B} = \text{B}'$ . Another remarkable feature of the spectra of this set of unsymmetrical ions was the appearance of a new band in the  $500\text{--}600\text{ cm}^{-1}$  region whose frequency increased when the bridge was deuterium substituted.

Wood (59) analyzed all these results in a semi-theoretical paper in which may be found, at least schematically, the spectral consequences (including deuterium isotope effects) to be expected for linear or bent H-bonded systems having potential functions with single minima, or double minima with either low or high barriers. He interprets those of his  $(\text{BPB}')^+$  systems which show a splitting of the  $\text{NH}^+$  band as having low-barrier double-minimum potential functions. Wood also shows that the anomalous frequency shift of the  $550\text{ cm}^{-1}$  band on deuteration can be explained on the basis of a well-to-well proton transition occurring in a low-barrier double-minimum potential which is markedly asymmetric.

Laane (60) has made calculations which show that for double-minimum, symmetric, but possibly anharmonic, potentials the frequency ratio  $\omega_\text{H}/\omega_\text{D}$  varies depending on the relative sizes of the height of the barrier and the energy of the transition. For a high barrier the frequency ratio is about 1.4. As the barrier height decreases the ratio falls, attaining a minimum value of about 1.2 when the upper level is near the top of the barrier. With a further decrease in the barrier the ratio increases again, passing through a maximum value of about 1.6 for a flat-bottomed well. For a single-minimum harmonic potential the ratio becomes 1.4 again. On the basis of his calculations Laane has questioned the frequency assignments which Berney *et al.* (61) have made for acetic acid. These authors have correlated two bands for which  $\omega_\text{H}/\omega_\text{D} = 0.93$ .

Very recently Bournay and Marechal (62) have studied the integrated intensities of the infrared absorption bands of the dimers of acetic acid and acetic acid- $\text{d}_1$ . For these molecules they find that the intensity of the band attributed to the OH--O antisymmetric stretching mode is twice that of the corresponding OD--O band, whereas the intensity ratio in the

harmonic approximation should be more nearly  $\sqrt{2}$ . In their discussion of this anomolous result they conclude that anharmonicity is not a dominant factor. Rather, they suggest that in this hydrogen bonded system the Born-Oppenheimer approximation is invalid; i.e., they propose that the motion of the H atom along the bond induces an electronic transition in the molecule, and the vibrational spectra have borrowed some intensity from that electronic transition.

### Ionic Solvation.

In recent years isotopic substitution has been used to identify the vibrational modes of cation solvates in both aqueous and nonaqueous media. Da Silveira, Marques, and Marques (63) obtained the Raman spectra of various salts of  $Mg^{2+}$ ,  $Zn^{2+}$ , and  $Al^{3+}$  in both  $H_2O$  and  $D_2O$ . They observed one polarized and two depolarized lines in each case, which they attributed to the  $A_{1g}$ ,  $E_g$ , and  $F_{2g}$  vibrational modes of octahedral solvates. The frequencies of the  $A_{1g}$  and  $E_g$  vibrations were decreased by a factor of 1.04-1.05 when  $D_2O$  was used as the solvent, whereas that of the  $F_{2g}$  vibration decreased by a factor of 1.08. These values are those which would be expected for species having octahedral symmetry.

In our own laboratory we have obtained the Raman spectra of aqueous solutions of  ${}^6LiCl$  and  ${}^7LiCl$  (64). In addition to three depolarized librational bands of water at  $720\text{ cm}^{-1}$ ,  $585\text{ cm}^{-1}$ , and  $462\text{ cm}^{-1}$ , we find two other bands in the low frequency region. One of these is a polarized band at  $420\text{ cm}^{-1}$ , independent of the lithium isotope used, which the other is a depolarized band which occurs at  $355\text{ cm}^{-1}$  in the  ${}^7LiCl$  solutions or  $385\text{ cm}^{-1}$  in the  ${}^6LiCl$  solutions. We interpret these bands as the  $A_1$  and  $F_2$  modes of vibration of  $Li^+$  tetrahedrally solvated by water molecules. Singh and Rock (65) had earlier noted that if the lithium ion were tetrahedrally solvated, and if the  $F_2$  vibration frequencies of the solvates were  $384\text{ cm}^{-1}$  and  $358\text{ cm}^{-1}$  for  ${}^6Li(OH_2)_4^+$  and  ${}^7Li(OH_2)_4^+$  respectively, the experimental value of the equilibrium constant of  $1.046$  for the exchange reaction  ${}^7Li(s) + {}^6LiCl(aq) = {}^6Li(s) + {}^7LiCl(aq)$  could be explained.

In an extensive series of papers Popov and his collaborators have studied the solvation of alkali metal cations in various nonaqueous media, using  ${}^{23}Na$  magnetic resonance shifts (66), and far-infrared spectroscopy. The ion-solvent vibrational bands which they find fall in the  $100\text{-}500\text{ cm}^{-1}$  range.

In dimethylsulfoxide the bands were identified by using  $DMSO-d_6$  as solvent (67). In acetone (68) both  ${}^7Li^+ \rightarrow {}^6Li^+$  and acetone- $d_6$  substitutions were used. In this solvent the frequencies of the "lithium" vibrations showed an anion

dependence, indicative of ion pairing, when the mole ratio of acetone to lithium was less than four. In pyridine and substituted pyridines (69) lithium isotopes were again used. In these solvents also, lithium halide contact ion pairing was inferred.

Concurrently with Popov's work, Roche and Huong (70) reported the cage vibrations of  $\text{Ca}^{2+}$ ,  $\text{Mg}^{2+}$ , and  $\text{Li}^+$  in acetonitrile. These authors employed both  ${}^7\text{Li}^+ \rightarrow {}^6\text{Li}^+$  and  $\text{CH}_3\text{CN} \rightarrow \text{CD}_3\text{CN}$  substitutions to identify the absorption bands of the solvates.

### Optical Activity Induced by Isotopic Substitution.

The first example of optical activity in a compound of the type  $\text{R}_1\text{R}_2\text{CHD}$  was reported in 1949 by Alexander and Pinkus (71). They measured a specific rotation for 2,3-dideutero-trans-menthane of  $[\alpha]_{\text{D}}^{25} = -0.09^\circ$ . They could not, however, establish the origin of the optical activity, owing to the presence of four asymmetric carbons in the molecule.

In the same year Eliel (72) reported the synthesis of ethylbenzene with one deuterium in the  $\alpha$  position. The optical activity of this compound ( $[\alpha]_{\text{D}}^{25} = -0.30^\circ$ ) clearly derives from the asymmetry between D and H. Subsequently Streitweiser and Wolfe (73) characterized a number of other benzyl- $\alpha$ -d-derivatives.

In 1963 Stirling (74) reported the preparation of (-)-benzyl-p-tolyl- $[\text{C}^{16}\text{O}^{18}\text{O}]$ -sulfone, whose rotation ( $[\alpha]_{\text{D}} = -0.16^\circ$ ) arises from the presence of two different oxygen isotopes bonded to sulfur. A number of other  ${}^{16}\text{O}^{18}\text{O}$  sulfones have since been prepared (75,76).

Anderson, Colonna, and Stirling (77) have recently reported (R)-dibenzyl- $[\text{C}^{12}\text{CH}_2\text{C}^{13}\text{CH}_2]$ -sulfoxide. In this compound the optical activity ( $[\alpha]_{280} = +0.71$ ) originates from having two carbon isotopes bonded to sulfur.

There have also appeared very recently the studies of Kokke and Osterhoff (78,79). These authors have prepared (1R)- $[\text{C}^{18}\text{O}]$ - $\alpha$ -fenchocamphoronequinone and (1R)- $[\text{C}^{18}\text{O}]$ - $\alpha$ -fenchocamphoronequinone. In these molecules the sole source of asymmetry was either an  ${}^{18}\text{O}$  in the  $\alpha$ -diketone function, or a single deuterium atom at a bridgehead. The circular dichroism spectra of these two compounds in the visible are remarkably different.

### Literature Cited.

1. Herzberg, G., "Atomic Spectra and Atomic Structure," Dover Publications, New York, 1944.
2. Herzberg, G., "Spectra of Diatomic Molecules," 2nd ed., Van Nostrand Reinhold, New York, 1950.

3. Herzberg, G., "Infrared and Raman Spectra of Polyatomic Molecules," Van Nostrand Reinhold, New York, 1945.
4. Herzberg, G., "Electronic Spectra and Electronic Structure of Polyatomic Molecules," Van Nostrand Reinhold, New York, 1966.
5. Walker, S. and Straw, H., "Spectroscopy," Vol. II, Chapman and Hall Ltd., London, 1962.
6. King, G. W., "Spectroscopy and Molecular Structure," Holt, Rinehart and Winston, Inc., New York, 1964.
7. Urey, H. C., Brickwedde, F. G., and Murphy, G. M., *Phys. Rev.* (1932), 40, 1.
8. Candler, C., "Atomic Spectra," Ch. 19, Van Nostrand Reinhold, New York, 1964.
9. Willets, L., Hill, D. L., and Ford, K. W., *Phys. Rev.* (1953), 91, 1488.
10. Hindmarsh, W. R., Kuhn, H., and Ramsden, S. A., *Proc. Phys. Soc. (London)*(1954), A67, 478.
11. Yoshino, T. and Bernstein, H. J., *J. Mol. Spectry.* (1958), 2, 213.
12. Daniels, F., Williams, J. W., Bender, P., Alberty, R. A., Cornwell, C. D., and Harriman, J. E., "Experimental Physical Chemistry," 7th ed., pp. 247-256, McGraw-Hill Inc., New York, 1970.
13. Shoemaker, D. P., Garland, C. W., and Steinfeld, J. L., "Experiments in Physical Chemistry," 3rd ed., pp. 450-459, McGraw-Hill Inc., New York, 1974.
14. Levy, A., Rossi, I., and Haeusler, C., *J. Physique* (1966), 27, 526.
15. Levy, A., Rossi, I., Joffrin, C., and Van Thanh, N., *J. Chim. Physique* (1965), 62, 601.
16. Rank, D. H., Eastman, D. P., Rao, B. S., and Wiggins, T. A., *J. Opt. Soc. Am.* (1962), 52, 1.
17. Van Horne, B. H. and Hause, C. D., *J. Chem. Phys.* (1956), 25, 56.
18. Pickworth, J. and Thompson, H. W., *Proc. Roy. Soc. (London)* (1953), 218, 37.
19. Connes, P., Connes, J., Benedict, W. S., and Kaplan, L. D., *Astrophys. J.* (1967), 147, 1230.
20. Giaque, W. F. and Johnston, H. S., *Nature* (1929), 123, 318.
21. Giaque, W. F. and Johnston, H. S., *J. Amer. Chem. Soc.* (1929), 51, 1436.
22. King, A. S. and Birge, R. T., *Nature* (1929), 124, 127.
23. Giaque, W. F. and Johnston, H. S., *Nature* (1929), 123, 831.
24. Giaque, W. F. and Johnston, H. S., *J. Amer. Chem. Soc.* (1929), 51, 3528.
25. Naudé, S. M., *Phys. Rev.* (1929), 34, 1499.
26. King, A. S. and Birge, R. T., *Astrophys. J.* (1930), 72, 19.
27. Weber, A., in Anderson, A., Ed., "The Raman Effect," Vol. II, pp. 637-640, Marcel Dekker, Inc., New York, 1973.

28. Wilson, E. B., Decius, J. C., and Cross, P. C., "Molecular Vibrations," McGraw-Hill Inc., New York, 1955.
29. A detailed application of the method to the chloroform molecule has been given by Colthup, N. B., Daly, L. H., and Wiberley, S. E., "Introduction to Infrared and Raman Spectroscopy," Ch. 14, Academic Press Inc., New York 1964.
30. Heicklen, J., *J. Chem. Phys.* (1962), 36, 721.
31. Hirakawa, A. Y., Tsuboi, M., and Shimanouchi, T., *J. Chem. Phys.* (1972), 57, 1236.
32. Weber, A., in ref. 27, pp. 690-705.
33. Aldous, J. and Mills, I. M., *Spectrochim. Acta* (1962), 18, 1073.
34. Aldous, J. and Mills, I. M., *Spectrochim. Acta* (1963), 19, 1567.
35. Kivelson, D. and Wilson, E. B., *J. Chem. Phys.* (1953), 21, 1229.
36. Wilson, E. B., *J. Chem. Phys.* (1957), 27, 986.
37. Beer, R., Farmer, C. B., Norton, R. H., Martonchick, J. V., and Barnes, T. G., *Science* (1972), 175, 1360.
38. Beer, R. and Taylor, F. W., *Astrophys. J.* (1973), 179, 309.
39. Young, L. G., *Icarus* (1969), 11, 66.
40. Crawford, B., *J. Chem. Phys.* (1958), 29, 1042.
41. Crawford, B., *J. Chem. Phys.* (1952), 20, 977.
42. Dickson, A. D., Mills, I. M., and Crawford, B., *J. Chem. Phys.* (1957), 27, 445.
43. Herzberg, G., "The Spectra and Structures of Simple Free Radicals," pp. 10-16, Cornell University Press, Ithaca, N. Y., 1971.
44. Monfils, A. and Rosen, B., *Nature* (1949), 164, 713.
45. Douglas, A. E. *Astrophys. J.* (1951), 114, 466.
46. Clusius, K. and Douglas, A. E., *Can. J. Phys.* (1954), 32, 319.
47. Katayama, D. H., Huffman, R. E., and O'Bryan, C. L., *J. Chem. Phys.* (1973), 59, 4309.
48. Nakamoto, K., *Angew. Chem. internat. Edit.* (1972), 11, 666.
49. Nakamoto, K., Udovich, C., and Takemoto, J., *J. Amer. Chem. Soc.* (1970), 92, 3973.
50. Pinchas, S., Silver, B. L., and Laulicht, I., *J. Chem. Phys.* (1967), 46, 1506.
51. Takemoto, J. and Nakamoto, K., *Chem. Commun.* (1970), 1017.
52. Nakamoto, K., "Infrared Spectra of Inorganic and Coordination Compounds," 2nd ed., pp. 106-112, Wiley-Interscience, New York, 1970.
53. Collman, J. P., Farnham, P., and Dolcetti, G., *J. Amer. Chem. Soc.* (1971), 93, 1788.
54. Masri, F. N. and Wood, J. L., *J. Mol. Struct.* (1972), 14, 217.
55. Masri, F. N. and Wood, J. L., *J. Mol. Struct.* (1972), 14, 201.
56. Clements, R. and Wood, J. L., *J. Mol. Struct.* (1973), 17, 265.

57. Clements, R. and Wood, J. L., *J. Mol. Struct.* (1973), 17, 283.
58. Clements, R., Dean, R. L., and Wood, J. L., *J. Mol. Struct.* (1973), 17, 291.
59. Wood, J. L., *J. Mol. Struct.* (1973), 17, 307.
60. Laane, J., *J. Chem. Phys.* (1971), 55, 2514.
61. Berney, C. V., Redington, R. L., and Lin, K. C., *J. Chem. Phys.* (1970), 53, 1713.
62. Bournay, J. and Marechal, Y., *J. Chem. Phys.* (1973), 59, 5077.
63. da Silveira, A., Marques, M. A., and Marques, N. M., *Mol. Phys.* (1965), 9, 271.
64. Nash, C. P., Donnelly, T. C., and Rock, P. A., unpublished results.
65. Singh, G. and Rock, P. A., *J. Chem. Phys.* (1972), 57, 5556.
66. Greenberg, M. S., Wied, D. M., and Popov, A. I., *Spectrochim. Acta* (1973), 29A, 1927, and earlier papers cited there.
67. Maxey, B. W. and Popov, A. I., *J. Amer. Chem. Soc.* (1969), 91, 20.
68. Wong, M. K., McKinney, W. J., and Popov, A. I., *J. Phys. Chem.* (1971), 75, 56.
69. Handy, P. R. and Popov, A. I., *Spectrochim. Acta* (1972), 28A, 1545.
70. Roche, J.-P. and Huong, P. V., *Bull. Soc. Chim. France* (1972), 4521.
71. Alexander, E. R. and Pinkus, A. G., *J. Amer. Chem. Soc.* (1949), 71, 1786.
72. Eliel, E. L., *J. Amer. Chem. Soc.* (1949), 71, 3970.
73. Streitweiser, A. and Wolfe, J. R., *J. Amer. Chem. Soc.* (1959), 81, 4912.
74. Stirling, C.J.M., *J. Chem. Soc. (London)*(1963), 5741.
75. Sabol, M. A. and Andersen, K. K., *J. Amer. Chem. Soc.* (1969), 91, 3603.
76. Annunziata, R., Cinquini, M., and Colonna, S., *J. Chem. Soc. Perkin Trans. I* (1972), 2057.
77. Andersen, K. K., Colonna, S., and Stirling, C.J.M., *J. Chem. Soc. Sec. D* (1973), 645.
78. Kokke, W.C.M.C. and Oosterhoff, L. J., *J. Amer. Chem. Soc.* (1972), 94, 7583.
79. Kokke, W.C.M.C. and Oosterhoff, L. J., *J. Amer. Chem. Soc.* (1973), 95, 7159.



# 3

## Isotope Effects and Quantum-Mechanical Tunneling

RALPH E. WESTON, JR.

Department of Chemistry, Brookhaven National Laboratory, Upton, L. I., N. Y. 11973

### Introduction

The phenomenon of quantum-mechanical tunneling is not observable in the macroscopic world which we experience directly. Suppose that a ball is rolled along the ground towards a small ridge. If its kinetic energy is greater than the potential energy of the ball at the top of the ridge it will surmount the barrier; if the kinetic energy is less than this, the ball will not get over the hill.

However, a moving particle of atomic or electronic mass does not obey Newtonian mechanics. Instead, it behaves as a wave packet with a wavelength given by the de Broglie expression

$$\lambda = h/mv \quad (1)$$

where  $h$  is Planck's constant,  $m$  is the mass of the particle, and  $v$  its velocity. For purposes of calibration, it is convenient to remember that a hydrogen atom, moving with thermal velocity at 300 K, has a wavelength of about  $1 \text{ \AA}$  (0.1 nm).

When such a particle encounters a barrier, represented by an increase in potential energy, it does not behave like a macroscopic particle. Instead, there is a finite probability of "leakage" or "tunneling" through the barrier even if the kinetic energy is less than the potential energy at the barrier summit; conversely, there is a finite probability of reflection even if the kinetic energy is greater than this. The extent of tunneling, the transmission probability  $\kappa$ , is defined by  $\kappa = (A_t/A_i)^2$ , where  $A_i$  and  $A_t$  are the wave function amplitudes for the incident and transmitted waves (Fig. 1).

As one would expect,  $\kappa$  depends on the mass of the particle, its velocity, and the shape and height of the barrier. Two convenient parameters are

$$\alpha = 2\pi V^*/h\nu^* \quad \text{and} \quad \epsilon = E/V^* \quad (2)$$

where  $V^*$  is the barrier height and  $\nu^*$  is a "vibrational frequency" defined by

$$\nu^* = (2\pi)^{-1} \{-\mu^{-1} [d^2V(x)/dx^2]\}^{1/2} \quad (3)$$

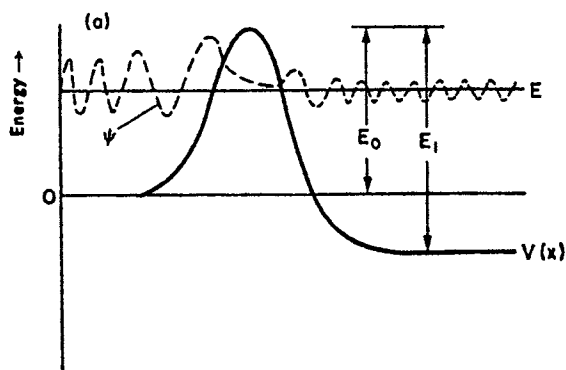
where  $\mu$  is the reduced mass appropriate to motion in the  $x$  direction. For a particular form of the potential barrier,  $V(x)$ , known as the Eckart barrier (see below), the dependence of  $\kappa$  on  $\epsilon$  and  $\alpha$  is shown in Fig. 2. The classical limit is simply a step function at  $\epsilon = 1$ , i.e. when the kinetic energy of the particle is equal to the potential energy at the barrier summit. Large values of  $\alpha$ , corresponding to high, or nearly flat, barriers lead to a similar form of  $\kappa$ . Low values of  $\alpha$ , on the other hand, lead to finite values of  $\kappa$  with  $\epsilon$  much less than unity, and to values of  $\kappa$  less than unity even when  $E$  is greater than  $V^*$ .

The physical significance of quantum-mechanical tunneling was recognized very early in the development of wave mechanics, and there are many examples of physical phenomena in which tunneling is important. Here is a very incomplete list of examples, chosen principally on the basis of historical interest:

1. The cold emission of electrons from a metal cathode at a high negative voltage (1).
2. The emission of  $\alpha$ -particles from an atomic nucleus (2,3).
3. The effect of the double minimum in the potential energy for  $\text{NH}_3$  on vibrational energy levels (4).
4. The possibility of tunneling in a chemical reaction involving motion of a proton or a hydrogen atom, which seems to have been first recognized by R. P. Bell (5).
5. The tunnel diode, a semiconductor device of considerable practical importance. The discovery of this by L. Esaki in 1956-58 (6) led to his sharing in the 1973 Nobel prize for physics (7). In fact, it is interesting to note that the other two recipients of the Nobel prize in physics for that year, B. D. Josephson and I. Giaever, were also honored for discoveries involving tunneling in solids (8,9). The Nobel prize awards should, in themselves, provide ample proof of the reality and the practical significance of tunneling!

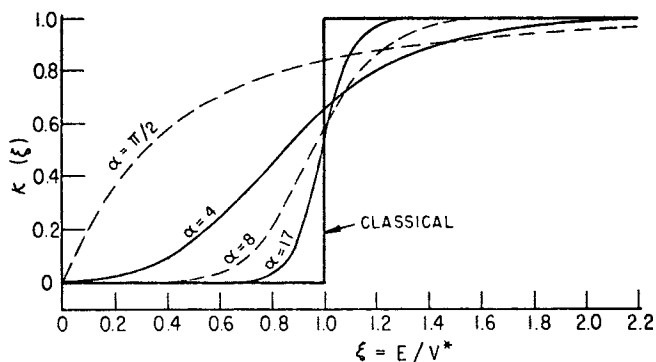
#### Tunneling in Chemical Reactions

Now that it has been made evident that tunneling is predicted by quantum mechanics, and that there are a number of physical manifestations of it, what about the particular area of chemical reactions?



## Theory of Elementary Gas Reaction Rates

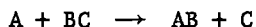
Figure 1. Permeability of a barrier to a particle with kinetic energy less than barrier height. The dashed line represents the wave function for a particle of energy,  $E$ , moving from the left and interacting with an Eckart barrier (solid line) (29).



## Gas Phase Reaction Rate Theory

Figure 2. Transmission probability  $\kappa(\epsilon)$  as a function of reduced energy  $\epsilon (= E/V^*)$  and  $\alpha (= 2\pi V^*/h\nu^*)$  for a symmetrical Eckart barrier (30)

The potential energy of interaction for the reactants in a hypothetical reaction such as



can be represented by a contour map (Fig. 3). Along the reaction path, the potential energy has the form of a one-dimensional barrier, similar to that in Fig. 1. If the mass of the atom being transferred (B in this example) is sufficiently small, and if the barrier has suitable dimensions, tunneling may become important. I am deliberately evading here some subtle questions, such as:

1. What is the precise reaction path that should be used to obtain the one-dimensional potential?

2. Is it correct to treat the problem as one-dimensional, when the potential energy is a function of two dimensions?

These and related questions have been discussed in detail by others (10,11).

For a one-dimensional barrier of arbitrary shape, numerical methods can be used to calculate the transmission probability  $\kappa$  (12). Before the availability of large computers, this problem was often circumvented by approximating the barrier with an Eckart function (13). The symmetric form of this, which I shall use later, is

$$V(x) = V^*/\cosh^2[(2\mu V^*)^{1/2}\pi v^* x] \quad (4)$$

This potential has the great advantage of leading to analytical solutions of the resulting Schrödinger equation, so that much less computational effort is required to calculate  $\kappa$  than is required for an arbitrary barrier shape. It is ideally suited for testing the qualitative effects of changing properties of the barrier. With an Eckart barrier, the transmission probability for a particle with energy  $E$  is found to be

$$\kappa(E) = [\cosh(2\alpha\epsilon^{1/2}) - 1] / [\cosh(2\alpha\epsilon^{1/2}) + \delta] \quad (5)$$

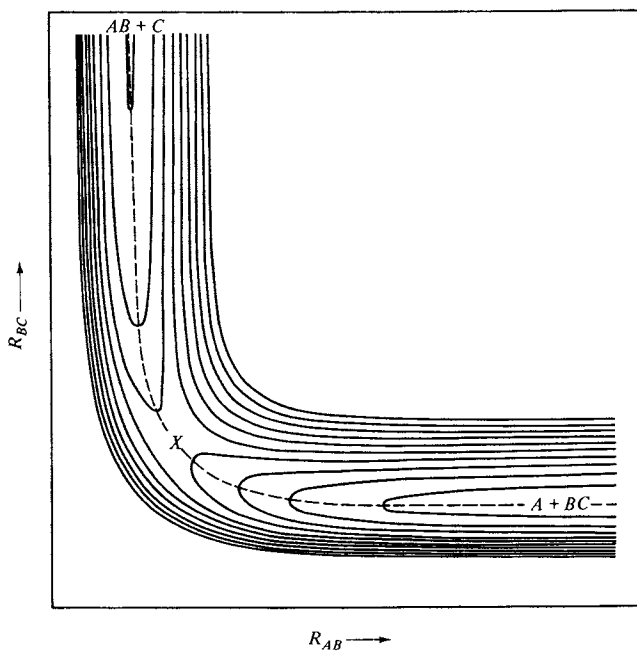
where  $\delta = \cosh(4\alpha^2 - \pi^2)^{1/2}$  ( $\alpha > \pi/2$ )  
 or  $\delta = \cos |4\alpha^2 - \pi^2|^{1/2}$  ( $\alpha < \pi/2$ ),  
 and the other quantities have already been defined.

In a chemical reaction system at thermal equilibrium, the Boltzmann distribution of molecular energies must be taken into account in obtaining the average transmission probability. The tunneling factor is usually defined as the ratio of this averaged transmission probability to that obtained with the classical values

$$\kappa(E) = 0, \quad E < V^*; \quad \kappa(E) = 1, \quad E \geq V^* \quad .$$

American Chemical  
Society Library

1155 16th St. N.W.



Chemical Kinetics

Figure 3. Hypothetical potential energy surface for the collinear reaction  $A + BC \rightarrow AB + C$ . The solid lines are equipotentials and the dashed line is the reaction path (31).

That is,

$$\Gamma^*(T) = \frac{\int_0^{\infty} \kappa(E) \exp(-E/RT) dE}{\int_{V^*}^{\infty} \exp(-E/RT) dE} \quad (6)$$

or

$$\Gamma^*(T) = \exp(V^*/RT) \int_0^{\infty} \kappa(E) \exp(-E/RT) d(E/RT) \quad (7)$$

This expression must be numerically integrated over the appropriate energy range.

### Tunneling and Kinetic Isotope Effects

The Magnitude of Primary Hydrogen Isotope Effects. As Eq.(1) illustrates, the wavelength associated with a moving particle is inversely proportional to the mass. In a comparison of two isotopic species in a chemical reaction, this mass dependence leads to different values of  $v^*$  and  $\alpha$ . Since  $\alpha$  is larger ( $v^*$  smaller) for the heavier species, the values of  $\kappa(E)$  are closer to the classical values, and this shows up in  $\Gamma^*(T)$ . Since relative differences in mass are greatest for the isotopes of hydrogen, one might expect important differences in the tunneling corrections for reactions involving the motion of H, D, or T atoms or ions. In fact, almost since the discovery of deuterium, such reactions have been studied in an attempt to find evidence for tunneling in a chemical reaction (14).

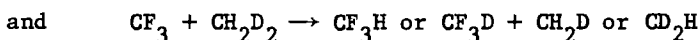
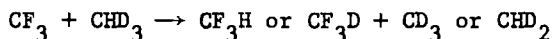
To find evidence for tunneling, one must first account for kinetic isotope effects that do not depend on tunneling. The most direct method of doing this is by means of activated complex theory, which leads to a formulation of the rate constant in terms of partition functions of the reactants and the activated complex. Arguments concerning the validity of activated complex theory are easy to provoke and difficult to settle, and I shall not consider this question here. It can then be shown (15,16) that the ratio of rate constants for two isotopic forms of the same reactant ( $AX_1$  and  $AX_2$ ) is given by

$$\frac{k_1}{k_2} = \frac{v_1^* \Gamma_1^*}{v_2^* \Gamma_2^*} \prod_{i=1}^{3r-7} \frac{\Gamma_i(A\overset{\ddagger}{X}_1)}{\Gamma_i(A\overset{\ddagger}{X}_2)} \prod_{j=1}^{3r-6} \frac{\Gamma_j(A\overset{\ddagger}{X}_2)}{\Gamma_j(A\overset{\ddagger}{X}_1)} \quad (8)$$

Here  $\Gamma_1 = u_1 e^{-u_1/2} / (1 - e^{-u_1})$ ,  $u_1 = hv_1/kT$ , and  $3r-6$  ( $3r-7$ ) is the number of real vibrations in the reactant (activated complex).

Given the details of the relevant potential energy surface, or some empirical scheme for predicting the force constants needed to calculate the vibrational frequencies upon which the  $\Gamma_1$ 's depend, one can evaluate Eq. (8) with or without the tunneling contribution  $\Gamma_1^*/\Gamma_2^*$ . A comparison with experiment should then reveal whether the tunneling correction is indeed important.

A good example of this approach is provided by the gas-phase reaction systems



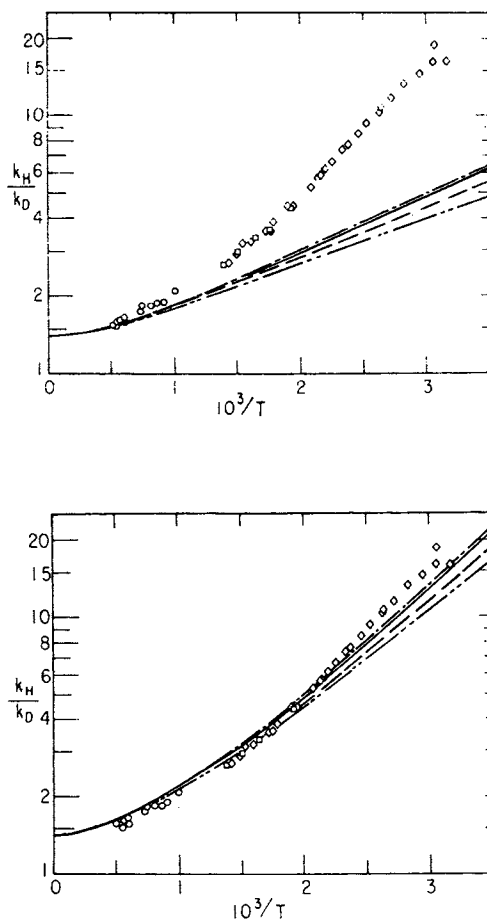
which have been examined in detail by H. S. Johnston and coworkers (17,18). A comparison of experimental isotope effects and those calculated with and without tunneling is given in Fig. 4; evidently the calculations which include tunneling are in better agreement with experiment.

This approach depends for its validity on the accuracy with which Eq. (8) can be evaluated. As potential energy surfaces for larger and larger reaction systems become available, the confidence with which one can utilize this method will increase; obviously it is only as good as the force constants that go into Eq. (8). However, in some cases even the magnitude of the experimental isotope effect is so large that it seems difficult to explain without a contribution from the tunneling correction. For example, the isotopic rate constant ratio  $k_H/k_D$  for the proton (deuteron) transfer from 4-nitrophenylnitromethane to tetramethylguanidine has been found to be as high as 45 at 25°C (19).

Arrhenius Pre-exponential Factors in Primary Hydrogen Kinetic Isotope Effects. A second diagnostic test for tunneling in chemical reactions is based on the temperature dependence of tunneling. Returning again to Eq. (1), we see that as the momentum of a particle increases (due to increased thermal energy, for example) its wavelength decreases. This, in turn, leads to a temperature dependence of  $\Gamma^*$ , which approaches unity at high temperatures.

The way this has been expected to influence an isotopic rate constant ratio has been discussed frequently in the literature (14), and is illustrated in Fig. 5. Kinetic-isotope-effect data can be expressed in the form

$$k_H/k_D = A_Q(T) e^{B(T)/T} \quad (9)$$



Journal of Chemical Physics

Figure 4. Rate constant ratio  $k_H/k_D$  for the abstraction of H or D from  $CHD_3$  or  $CH_2D_2$ . The points are experimental values, and the lines are values calculated from different reaction models. (a) No tunneling correction included. (b) Tunneling correction included (18).



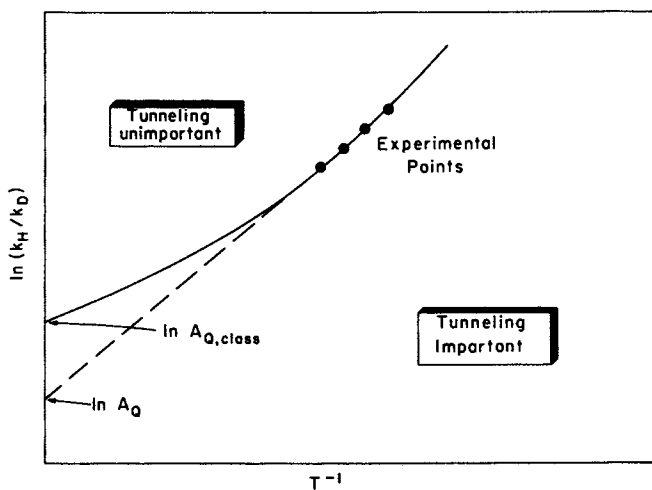
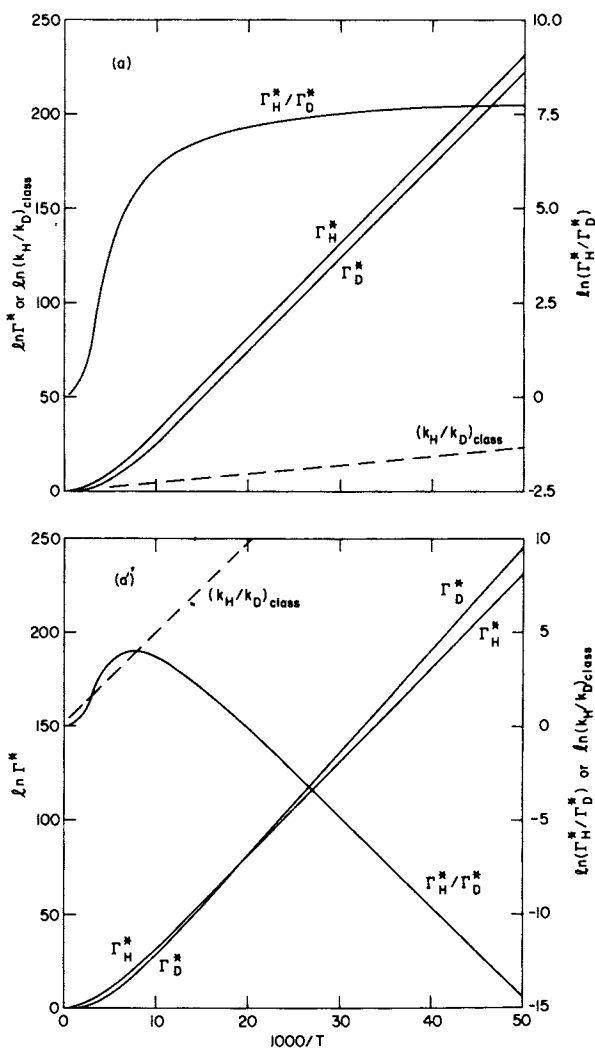


Figure 5. Qualitative portrayal of the temperature dependence of an isotopic rate constant ratio in a reaction where tunneling is important. The Arrhenius intercept which would be obtained at high temperatures ( $A_{Q,class}$ ) and the intercept obtained by extrapolation from low temperatures ( $A_Q$ ) are indicated.

where both  $A_Q$  and  $B$  are written as temperature-dependent, for the sake of generality. If tunneling is unimportant, i.e., at high temperatures, this expression will behave like the Arrhenius expression for individual rate constants, with  $A_Q$  and  $B$  independent of temperature. Then a plot of  $\ln(k_H/k_D)$  vs  $T^{-1}$  will be linear, or very nearly so. As the temperature is decreased and the tunneling component of the isotope effect becomes more important,  $\ln(k_H/k_D)$  will curve upwards, so that  $B(T)$  is larger and  $A_Q(T)$  is smaller than they would be without tunneling (Fig. 5). Bell (20), and more recently Schneider and Stern (21), have investigated the temperature dependence of  $A_Q$  for model reactions. The latter workers carried out calculations of  $k_H/k_D$  with Eq. (8) (without the tunneling correction), and by fitting these values to the form of Eq. (9), they obtained  $A_Q$  as a function of temperature. For several model reactions with large primary hydrogen isotope effects, they attempted to force  $A_Q$  values as low as possible by adjusting force constants of the model activated complexes. Over a temperature range of 20–1000°K, values of  $A_Q$  below 0.7 could not be attained. This answers part of the question: In the absence of tunneling,  $A_Q$  is restricted to a rather narrow range. The remaining part of the question is the converse: In the presence of tunneling, does  $A_Q$  lie outside this range?

To answer this, Stern and I (22) used the same model systems previously investigated by Schneider and Stern, but included the tunneling correction in the isotope effect. Values of  $v^*$  were those calculated in their work; barrier heights  $V^*$  were not needed in their work, and we have simply assumed values of 1, 5, 10, 20, and 30 kcal/mole for  $V_H^*$ . A symmetrical Eckart potential was used. For reasons discussed in our paper (22), two sets of calculations were made: one with  $V_D^* = V_H^*$  and one with  $V_D^* = V_H^* + 1$  kcal/mole. Although we examined all of the models used by Schneider and Stern, I shall discuss here only the results obtained from the model for the reactions  $CF_3 + C_2H_6$  or  $C_2H_5D \rightarrow CF_3H$  or  $CF_3D + C_2H_5$ .

First, the individual tunneling corrections,  $\Gamma_H^*$  and  $\Gamma_D^*$ , are shown in Fig. 6 as functions of  $T^{-1}$ . These are well-behaved, smooth, functions, although if  $V_H^*$  is not equal to  $V_D^*$  there is a crossover temperature below which  $\Gamma_H^* < \Gamma_D^*$ . This arises from the term  $\exp(v^*/RT)$  in Eq. (7); thus,  $\exp[(V_H^* - V_D^*)/RT]$  is more important than the integral at low temperatures. For the isotope-independent barrier, the ratio  $\Gamma_H^*/\Gamma_D^*$  is almost constant at low temperatures because the individual lines are parallel. At high temperatures,  $\ln(\Gamma_H^*/\Gamma_D^*)$  approaches zero with a positive curvature, so that the complete  $\ln(\Gamma_H^*/\Gamma_D^*)$  vs  $T^{-1}$  curve is sigmoid shaped. When the barrier height is isotope dependent, the shape of  $\ln(\Gamma_H^*/\Gamma_D^*)$  is similar at high temperatures, but ultimately the values are decreased because of the exponential term discussed above, and the curve is almost a straight line with slope



Journal of Chemical Physics

Figure 6. Arrhenius-type plots of  $\Gamma_H^*$ ,  $\Gamma_D^*$ ,  $\Gamma_H^*/\Gamma_D^*$  and  $(k_H/k_D)_{\text{class}}$  for a model hydrogen-atom abstraction with (a)  $V_H^* = V_D^* = 10$  kcal/mole, (a')  $V_H^* = 10$ ,  $V_D^* = 11$  kcal/mole (22)

$(V_H^* - V_D^*)/R$ . However, since this term has an exponential temperature dependence, it does not affect  $A_Q$ . The temperature dependence of  $\ln A_Q$  (for tunneling alone) can be qualitatively assessed from Fig. 6 by linear extrapolation from a particular temperature region. This was done more precisely by using a least-squares fit to  $\ln(\Gamma_H^*/\Gamma_D^*)$  or  $\ln(k_H/k_D)$  at four temperatures, and the resulting values of  $A_Q$  for various barrier heights are plotted in Fig. 7a. The infinite-temperature limit of  $\ln A_{Q,tun}$  is zero. At high temperatures,  $\ln A_{Q,tun}$  will decrease to negative values with decreasing temperature. As the temperature is further decreased,  $\ln A_{Q,tun}$  will go through a minimum at the temperature of the inflection point in the  $\ln(\Gamma_H^*/\Gamma_D^*)$  curve, and then increase again as the temperature decreases further. At very low temperatures,  $\ln A_{Q,tun}$  is approximately equal to  $\ln \Gamma_H^* - \ln \Gamma_D^*$ , which is a very large quantity. As mentioned above, there is not a significant difference between the cases with isotope-dependent and isotope-independent barrier heights.

When the tunneling correction is combined with the rest of the rate constant ratio,  $(k_H/k_D)_{class}$ , the resultant form of  $\ln A_Q$  is almost identical with that for tunneling only. This is because  $\ln(k_H/k_D)_{class}$  has almost exactly the Arrhenius form, with  $\ln(A_{Q,class})$  virtually independent of temperature (see the curves labelled "NT" in Figs. 7a' and 7a").

Figs. 7a' and 7a'' illustrate the following important features:

1. Regardless of the barrier height, there is a fairly small temperature region in which  $\ln A_Q$  is below the limit of  $-0.69$  predicted by Bell's model in the absence of tunneling (indicated by the lower dashed line). The extent of the excursion below this limit increases with increasing barrier height. It is in this temperature region that most experiments have been done, and earlier calculations of tunneling were made.

2. At lower temperatures,  $\ln A_Q$  exceeds the upper limit of  $0.35$  predicted by Bell in the absence of tunneling (indicated by the upper dashed line). This is contrary to what had been expected before our calculations were made, because earlier calculations concentrated on the region to the left of the inflection point in Fig. 6.

3. The value of  $A_Q$  does not correlate simply with the extent of tunneling, which is indicated by values of  $\ln \Gamma_H^*$  for  $V_H^* = 10$  on the top of Fig. 7.

In our work, we also examined other model reactions, and a few other barrier shapes, with similar results.

Thus, we conclude that experimental  $A_Q$  values can be used as quantitative indicators of quantum-mechanical tunneling only in conjunction with model calculations. Although  $A_Q$  values outside of Bell's range of  $0.5\text{--}\sqrt{2}$  probably cannot be found in the absence of tunneling,  $A_Q$  values inside this range do not necessarily indicate the absence of large tunneling factors. In spite of this somewhat uncertain situation, it is interesting to see if there are experimental values of  $A_Q$  outside the "non-tunneling" range. Data from reactions in which tunneling has been invoked are given in Table I. (This does not mean that tunneling is unimportant in other reactions, but only that it has not been specifically searched for). Without critically evaluating the experimental data of Table I, I simply point out that there are several reactions in which abnormally low  $A_Q$  values have been observed.

Relative Tritium-Deuterium Isotope Effects. Because some isotope experiments are best done with D substitution and others with T substitution, there has been for some time an interest in, and a necessity for, the correlation of the rate constant ratios  $k_H/k_D$  and  $k_H/k_T$ . This correlation may be defined as

$$\underline{r} = \frac{\ln(k_H/k_T)}{\ln(k_H/k_D)}$$

Several theoretical investigations of the allowable range in  $\underline{r}$  in the absence of tunneling have been made. Using a simplified model for a hydrogen-transfer reaction, Swain and coworkers (23) obtained a value of 1.442, considering only zero-point-energy effects.

Bigeleisen (24), using a more complete model, proposed a range of 1.33-1.58 for the relative isotope effects, including Wigner tunneling (valid if  $\kappa$  is close to unity). He stated that extensive tunneling should lead to abnormally low values of  $\underline{r}$ . More O'Ferrall and Kouba (25) calculated isotope effects for some model proton-transfer reactions involving linear four- and five-atom transition states. They found deviations of only 2% from the Swain value of  $\underline{r}$  (1.442), even when tunneling corrections for a parabolic barrier were included. It has also been shown by Lewis and Robinson (26) that tunneling corrections do not necessarily produce significant changes in the relative isotope effect.

Recently, Stern and Vogel (27) investigated relative tritium-deuterium isotope effects for 180 model reaction systems. They found that, within the temperature range 20-1000°K,  $\underline{r}$  was restricted to the range  $1.33 \leq \underline{r} \leq 1.58$  provided that:

1.  $k_H/k_T$  and  $k_H/k_D$  reflect significant force-constant changes between reactant and transition state at the isotopic position(s).

Table I. Arrhenius Preexponential Factors and Relative Tritium-Deuterium Isotope Effects

<u>Reaction</u>	<u>A<sub>Q</sub></u>	<u>κ</u>	<u>Ref.</u>
1. 4-Nitrophenylnitromethane + tetramethylguanidine (in toluene)	0.032	-	a
2. Same reaction in dichloromethane	0.45	-	a
3. Leucocrystal violet + chloranil	0.04	1.31	b
4. 2-Carboethoxycyclopentanone + F <sup>-</sup>	0.042	1.32	c,d
5. 2-Nitropropane + 2,4,6-trimethyl- pyridine	0.15	1.39	b
6. Oxidation of 1-phenyl-2,2,2-tri- fluoroethanol	0.25	1.46	b
7. 2-Carboethoxycyclopentanone + chloracetate ion	0.35	1.72	c,d
8. Acetophenone + OH <sup>-</sup>	0.38	1.38	e
9. 1-Bromo-2-phenylpropane + ethoxide	0.40	1.48	f,g
10. 2-Carboethoxycyclopentanone + D <sub>2</sub> O	0.44	1.48	c,d
11. Pyridinediphenylborane + H <sub>2</sub> O	0.94	1.38	h
12. 2,2-Diphenylethylbenzene- sulfonate + methoxide	1.1	1.48	i

<sup>a</sup>Ref. 19

<sup>b</sup>Ref. 26

<sup>c</sup>Bell, R. P., Fendley, J. A., and Hulett, J. R., Proc. Roy. Soc. Ser. A (1956), 235, 453.

<sup>d</sup>Jones, J. R., Trans. Faraday Soc. (1969), 65, 2430.

<sup>e</sup>Jones, J. R., *ibid.* (1969), 65, 2138.

<sup>f</sup>Shiner, V. J., Jr. and Smith, M. L., J. Amer. Chem. Soc. (1961), 83, 593.

<sup>g</sup>Shiner, V. J., Jr. and Martin, B., Pure Appl. Chem. (1964), 8, 371.

<sup>h</sup>Lewis, E. S. and Grinstein, R. H., J. Amer. Chem. Soc. (1962), 84, 1158.

<sup>i</sup>Willi, A. V., J. Phys. Chem. (1966), 70, 2705.

2.  $k_H/k_T$  and  $k_H/k_D$  are both greater than unity.

3.  $k_H/k_T$  and  $k_H/k_D$  exhibit "regular" temperature dependences at all temperatures, "regular" being defined in their paper.

Stern and I (28) re-examined the model reactions meeting the above three criteria, to see what effect the inclusion of tunneling would have on the relative isotope effect. The tunneling corrections were calculated as described in the preceding sub-section. Although this was done for a large number of model reactions, I shall discuss here only the model for hydrogen-atom abstraction that has already been mentioned in the preceding sub-section. Again, two variations were considered: in one,  $V_H^* = V_D^* = V_T^*$ ; in the other,  $V_D^* = V_H^* + 1$ ,  $V_T^* = V_H^* + 1.45$ . Figs. 8a and 8b show the ratios of tunneling corrections,  $\Gamma_H^*/\Gamma_D^* \equiv T_{H/D}$  and  $\Gamma_H^*/\Gamma_T^* \equiv T_{H/T}$ , for the two cases. In addition, the relative tritium-deuterium tunneling correction

$$\underline{t} \equiv \ln T_{H/T} / \ln T_{H/D}$$

is indicated. The slightly different shapes of  $\ln T_{H/T}$  and  $\ln T_{H/D}$  vs.  $\log T$  result in a temperature dependence of  $\underline{t}$ . At high temperatures,  $\Gamma^*$  is given by the Wigner expression, and it can be shown (24) that

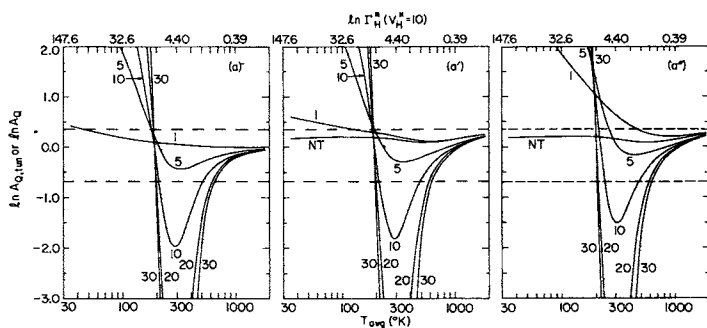
$$\underline{t} \rightarrow \frac{1 - (v_T^*/v_H^*)^2}{1 - (v_D^*/v_H^*)^2} \quad \text{as } T^{-1} \rightarrow 0 \quad .$$

If the barrier height depends on isotopic substitution, there is a temperature at which  $T_{H/T}$  is unity and  $\underline{t}$  is zero. At a slightly higher temperature,  $T_{H/D}$  becomes unity and  $\underline{t}$  has a pole ( $\pm\infty$ ).

The relative isotope effect including the tunneling correction, which we designate as  $\underline{r}'$ , can be expressed in terms of  $\underline{t}$  and  $\underline{r}$ , the relative isotope effect without tunneling:

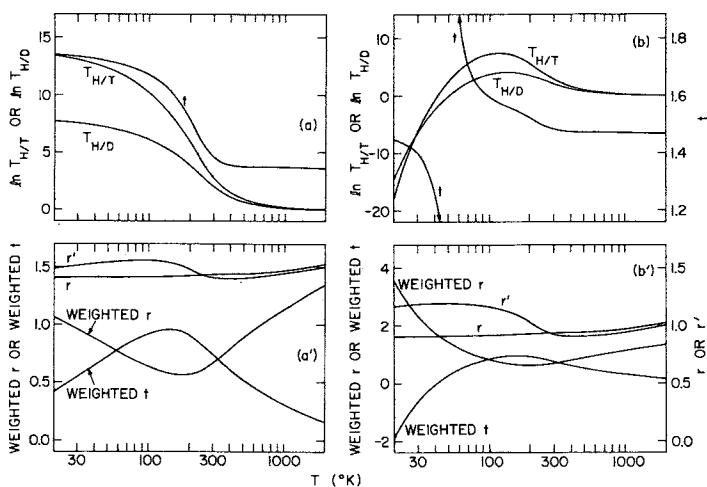
$$\underline{r}' = \frac{\ln R_{H/D}}{\ln R'_{H/D}} \underline{r} + \left[ 1 - \frac{\ln R_{H/D}}{\ln R'_{H/D}} \right] \underline{t} \quad .$$

In this expression,  $R_{H/D}$  is the rate constant ratio with no tunneling correction, and  $R'_{H/D}$  the same ratio including tunneling. It is apparent that the weighting factors multiplying  $\underline{r}$  and  $\underline{t}$  are complementary; as a result, plots of the weighted  $\underline{r}$  and weighted  $\underline{t}$  contributions vs.  $\log T$  will be, approximately, displaced "mirror images" (cf. Figs. 8a' and 8b'). Because the two contributions are not exactly out of phase, a slight temperature dependence of  $\underline{r}'$  remains. Fig. 9 illustrates the effect on  $\underline{t}$  and on  $\underline{r}'$  of



Journal of Chemical Physics

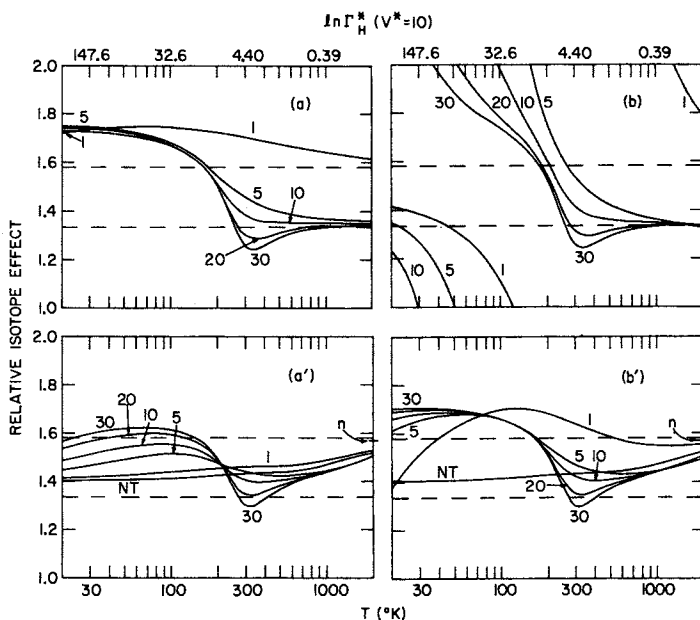
Figure 7. Arrhenius pre-exponential factors as functions of temperature for a model hydrogen-atom abstraction with various barrier heights: (a), tunneling correction only,  $V_D^* = V_H^*$ ; (a'), complete isotope effect,  $V_D^* = V_H^*$ ; (a''), complete isotope effect,  $V_D^* = V_H^* + 1$ . The curves are labeled with  $V_H^*$  in kcal/mole. (NT indicates that no tunneling correction is included.) Numbers at the top of each graph are  $\ln \Gamma_H^*$  for  $V_H^* = 10$ , as a function of  $T_{eq}$ . Dashed lines are at  $A_0 = 1/2$  and  $\sqrt{2}$  (22).



Journal of Chemical Physics

Figure 8. Relative tritium-deuterium kinetic isotope effect  $r'$  and individual contributors to  $r'$  for a model hydrogen-atom abstraction: (a), (a'),  $V_H^* = V_D^* = V_T^* = 10$  kcal/mole; (b), (b'),  $V_H^* = 10$ ,  $V_D^* = 11$ ,  $V_T^* = 11.45$  kcal/mole (28)





Journal of Chemical Physics

Figure 9. Relative tritium-deuterium kinetic isotope effects as functions of temperature with various barrier heights: (a),(b), tunneling only; (a'),(b'), complete isotope effect. Unprimed letters are for isotope-independent barrier heights, and primed letters are for  $V_D^* = V_H^* + 1$ ,  $V_T^* = V_H^* + 1.45$  kcal/mole. The curves are labeled with  $V_H^*$  in kcal/mole. Numbers at the top of the graphs are  $\ln \Gamma_H^*$  for  $V_H^* = 10$  kcal/mole, as a function of  $\log T$ . Dashed horizontal lines are the "nontunneling limits," 1.33 and 1.58. The infinite-temperature limit of the relative isotope effect is indicated by "n" at right border (28).

changes in  $V^*$ ; note that deviations of  $\underline{r}'$  vs  $\log T$  from a smooth, monotonic curve increase as the barrier height increases.

The important point, however, is that even when tunneling is very significant (cf. legend at top of Fig. 9),  $\underline{r}'$  does not greatly exceed the "nontunneling" range of 1.33-1.58. Furthermore, contrary to the assumptions of earlier authors,  $\underline{r}'$  drops below the lower limit only for the highest barrier tested, and over a narrow temperature range. Although tunneling is important at these temperatures, the tunneling correction is even larger at lower temperatures where  $\underline{r}'$  exceeds the upper range of 1.58. Except for the lowest barrier, where relative differences between  $V_H^*$ ,  $V_D^*$ , and  $V_T^*$  are large, the conclusions for the case when the barrier height is isotope-dependent are very similar. Note that the abnormal behavior of  $\underline{t}$  in Fig. 8b and 9b is removed by the weighting factor to give the smooth curves of Figs. 8b' and 9b'. The only cases for which the discontinuity in  $\underline{r}'$  is retained are physically unrealistic models in which secondary isotope effects are combined with an isotope-dependent barrier height.

The large number ( $\sim 60$ ) of other model reaction systems we investigated all gave results qualitatively similar to those discussed above, but with subtle differences dependent on the particular model. We conclude from this work that:

1. Even when quantum-mechanical tunneling is important, the limits  $1.33 \leq \underline{r} \leq 1.58$  are not likely to be exceeded, if they would not be exceeded in the absence of tunneling.
2. There is no general correlation between the magnitude of  $\underline{r}$  and the importance of tunneling.
3. The temperature dependence of  $\underline{r}$  is qualitatively the same for a wide range of barrier heights and reaction models.

Experimental data for some systems in which both deuterium and tritium isotope effects have been measured are given in Table I. Again, the warning must be issued that other reactions undoubtedly exist in which tunneling is important but has not been searched for by this method. Nevertheless, there is only one reaction listed (No. 7) where the experimental value of  $\underline{r}$  is significantly outside the range of 1.33-1.58. Interestingly, the temperatures at which this reaction was studied are close to the temperature at which a minimum value of  $\underline{r}'$  is calculated from the model discussed above.

#### Conclusion: What About Chemical Principles?

I hope that the details of the preceding sections have not diverted the reader's attention from the general subject of this

symposium: "Isotopes and Chemical Principles". Let me reiterate the principle that underlies these details:

*Classical mechanics cannot be relied upon to provide an adequate and accurate description of the motion of light atoms (particularly isotopes of hydrogen) during a chemical reaction. The wave nature of the moving particle must be taken into account because it permits "tunneling" through the potential energy barrier separating reactants from products. Because the wavelength (and hence the extent of tunneling) of the moving atom is mass-dependent, kinetic isotope effects will reflect this wave-mechanical property.*

Unfortunately, the diagnostic methods that have been used to search for tunneling in actual experiments have not led to unequivocal proof. In effect, the foundation is solid, but the structure that has been built on it is somewhat rickety. Anticipated developments that will improve the sturdiness of this structure over the next few years are:

1. The calculation of accurate potential energy surfaces for reacting systems consisting of a few atoms.
2. Complete wavemechanical calculations, with these potential energy surfaces, of reactive cross sections and other details of reaction dynamics.
3. Precise measurements of cross sections for these reaction systems, with reactants in well-defined states.

#### Acknowledgement

The tragic death of Marvin Stern brought to an untimely end the promising career of a good friend and respected colleague. His contributions to our calculations described here and in more detail elsewhere (22,28) cannot be overestimated. To this work he brought his insight into the significant features of the problem and his uniquely high standards of meticulous attention to detail.

This paper is based on research supported by the U. S. Atomic Energy Commission.

#### Literature Cited

1. Fowler, R. H. and Nordheim, L., Proc. Roy. Soc. Ser. A (1928), 119, 173.
2. Gamow, G., Z. Phys. (1928), 51, 204.

3. Gurney, R. W. and Condon, E. U., *Nature* (1928), 122, 439.
4. Morse, P. M. and Stueckelberg, E. C. G., *Helv. Phys. Acta* (1931), 4, 335.
5. Bell, R. P., *Proc. Roy. Soc. Ser. A* (1933), 139, 466.
6. Esaki, L., *Phys. Rev.* (1958), 109, 603.
7. Esaki, L., *Science* (1974), 183, 1149.
8. Josephson, B. D., *ibid.* (1974), 184, 527.
9. Giaever, J., *ibid.* (1974), 183, 1253.
10. Truhlar, D. G. and Kuppermann, A., *J. Am. Chem. Soc.* (1971), 93, 1840.
11. Truhlar, D. G. and Kuppermann, A., *J. Chem. Phys.* (1972), 56, 2232.
12. Le Roy, R. J., Quickert, K. A., and Le Roy, D. J., *Trans. Faraday Soc.* (1970), 66, 2997.
13. Eckart, C., *Phys. Rev.* (1930), 35, 1303.
14. For a review, cf. Caldin, E. F., *Chem. Rev.* (1969), 69, 135.
15. Bigeleisen, J., *J. Chem. Phys.* (1949), 17, 675.
16. Weston, R. E. and Schwarz, H. A., "Chemical Kinetics", p. 109, Prentice-Hall, Englewood Cliffs, N. J., 1972.
17. Johnston, H. S. and Tschuikow-Roux, E., *J. Chem. Phys.* (1962), 36, 463.
18. Sharp, T. E. and Johnston, H. S., *J. Chem. Phys.* (1962), 37, 1541.
19. Caldin, E. F. and Mateo, S., *J. Chem. Soc. Chem. Comm.* (1973), 854.
20. Bell, R. P., "The Proton in Chemistry", Chap XI, Cornell Univ. Press, Ithaca, N. Y., 1959.
21. Schneider, M. E. and Stern, M. J., *J. Am. Chem. Soc.* (1972), 94, 1517.
22. Stern, M. J. and Weston, R. E., Jr., *J. Chem. Phys.* (1974), 60, 2808.
23. Swain, C. G., Stivers, E. C., Reuwer, J. F., Jr., and Schaad, L. J., *J. Amer. Chem. Soc.* (1958), 80, 5885.
24. Bigeleisen, J., "Tritium in the Physical and Biological Sciences", International Atomic Energy Agency, Vienna, 1962, vol. 1, p. 161.
25. More O'Ferrall, R. A., and Kouba, J., *J. Chem. Soc. B* (1967), 985.
26. Lewis, E. S. and Robinson, J. K., *J. Amer. Chem. Soc.* (1968), 90, 4337.
27. Stern, M. J. and Vogel, P. C., *ibid.* (1971), 93, 4664.
28. Stern, M. J. and Weston, R. E., Jr., *J. Chem. Phys.* (1974), 60, 2815.
29. Bunker, D. L., "Theory of Elementary Gas Reaction Rates", in "The International Encyclopedia of Physical Chemistry and Chemical Physics", Topic 19, vol. 1, p. 30, Pergamon Press, Oxford, 1966.
30. Johnston, H. S., "Gas Phase Reaction Rate Theory", p. 45, The Ronald Press Co., New York, 1966.
31. Ref. 16, p. 36.

# 4

## Corrections to the Born–Oppenheimer Approximation in the Calculation of Isotope Effects on Equilibrium Constants

MAX WOLFSBERG and LAWRENCE I. KLEINMAN

Department of Chemistry, University of California, Irvine, Calif. 92664

### Introduction

The Born-Oppenheimer (B.O.) approximation is the cornerstone of most theories dealing with the effect of isotopic substitution on molecular properties. Within the framework of this approximation, the potential energy surface for the vibrational-rotational motions of a molecular system depends on the nuclear charges of the substituent atoms and on the number of electrons in the system but is independent of the masses of the nuclei. Thus isotope effects arise from the fact that nuclei of different mass move differently on the same potential surface.

Among the theories into which the B.O. approximation has been incorporated are the theory of isotope effects on the rotational-vibrational energy levels of a molecule, the theory of isotope effects on chemical equilibria, and various theories of isotope effects on chemical rates. The relative success of these theories in the interpretation of experimental results suggests that the B.O. approximation must be a relatively "good" approximation.

The first-order correction to the B.O. approximation has been formulated by Van Vleck (1) for diatomic molecules. Subsequent quantitative calculations have been largely restricted to one and two electron molecules. When corrections to the B.O. approximation are introduced, the energy of the non-rotating -- non-vibrating molecule will generally depend on isotopic substitution. Thus the energy difference between the non-rotating -- non-vibrating products and the corresponding reactants in the gas phase isotopic exchange reaction



need no longer vanish. This energy difference will be designated here as  $\Delta\text{ELEC}$ . If  $\Delta\text{ELEC}$  is not equal to zero, the value of the equilibrium constant calculated by the usual methods within the framework of the B.O. approximation must be multiplied by a factor differing from unity which is called here  $K(\text{BOELE})$ .  $K(\text{BOELE})$  will be referred to as the electronic isotope effect although it is actually the deviation of this quantity from unity which is important. It follows, however, from the work of Van Vleck and others that, to first order, this energy difference is still zero for the reaction  $2\text{HD} = \text{H}_2 + \text{D}_2$ . On the other hand, it also follows from Van Vleck's calculations, that the failure of the B.O. approximation favors the reactants of the reaction  $\text{H}^+ + \text{HD} = \text{D}^+ + \text{H}_2$  by  $29 \text{ cm}^{-1}$  (i.e.  $\Delta\text{ELEC} = 29 \text{ cm}^{-1}$ ). At  $300^\circ\text{K}$ , the consequent  $K(\text{BOELE})$  value for this reaction is about 0.87.

We decided to investigate corrections to the B.O. approximation for a number of diatomic hydrides and deuterides in order to obtain information about electronic isotope effects on the gas phase isotopic exchange reactions (1). Such calculations require a knowledge of electronic wave functions for molecules and the evaluation of a number of integrals. While such calculations would at one time have been very difficult, the availability of a large digital computer makes such calculations feasible now. The results of some of these calculations will be reported in the following sections; they are reported in more detail elsewhere (2, 3, 4).

### Theory

The theory here follows the development of Van Vleck (1) and Born (5). In atomic units ( $\hbar=1$ , mass of electron=1), the nonrelativistic Schroedinger equation for a diatomic molecule with  $n$  electrons and nuclei of masses  $M_a$  and  $M_b$  is

$$\left[ -\frac{1}{2M_a} \nabla_a^2 - \frac{1}{2M_b} \nabla_b^2 - \frac{1}{2} \sum_{i=1}^n \nabla_i^2 + V \right] \Phi_T = E_T \Phi_T \quad (2)$$

where all coordinates are relative to an arbitrary but fixed laboratory origin and  $\nabla^2$  is the Laplacian operator. The potential  $V$  consists of coulomb interactions among the charged particles (and possibly may contain spin terms) but it does not depend on nuclear masses. After the motion of the center of mass is separated out and the electronic coordinates are

transformed to the center of mass of the nuclei (CMN) system, the Schrodinger equation becomes

$$\left[ -\frac{1}{2\mu} \nabla_{\underline{R}}^2 - \frac{1}{2} \sum_{i=1}^n \nabla_{\underline{r}_i}^2 - \frac{1}{2(M_a + M_b)} \sum_{i,j=1}^n \nabla_{\underline{r}_i} \cdot \nabla_{\underline{r}_j} + V(\underline{R}, \underline{r}_i) \right] \Phi = E\Phi \quad (3)$$

where  $\underline{R}$  is the relative position vector of the two nuclei, the  $\underline{r}_i$  are electronic coordinates relative to axes whose origin is at the CMN and  $\mu = M_a M_b / (M_a + M_b)$ . The  $\underline{r}_i$  coordinates are taken to be molecule fixed here but the  $\nabla_{\underline{R}}^2$  differentiations must be carried out with the coordinates of the electrons held constant with respect to space fixed CMN axes. The B.O. electronic wavefunctions and energies are defined as the normalized eigenfunctions and eigenvalues of the following Schrodinger equation:

$$\left[ -\frac{1}{2} \sum_{i=1}^n \nabla_{\underline{r}_i}^2 + V \right] \Psi_{\Gamma}(\underline{r}_i; \underline{R}) = E_{\Gamma}^e(\underline{R}) \Psi_{\Gamma}(\underline{r}_i; \underline{R}). \quad (4)$$

This is the usual electronic Schrodinger equation for a diatomic molecule used by quantum chemists. Neither  $E^e$  nor  $\Psi$  (except insofar as the origin of the electronic coordinate system here reflects the nuclear masses) will depend on the masses of the nuclei. Since the B.O. wavefunctions form a complete set in the space of the electronic coordinates, it is possible to expand the total wavefunction in terms of the B.O. states:

$$\Phi(\underline{r}_i, \underline{R}) = \sum_{\Gamma} F_{\Gamma}(\underline{R}) \Psi_{\Gamma}(\underline{r}_i; \underline{R}). \quad (5)$$

Substitution of this expansion into (3), left multiplication by a particular  $\Psi_{\Gamma}^*$  and integration over all electronic coordinates yields the coupled equations for  $F_{\Gamma}(\underline{R})$

$$\left[ -\frac{1}{2\mu} \nabla_{\underline{R}}^2 + E_{\Gamma}^e(\underline{R}) - E \right] F_{\Gamma}(\underline{R}) + \sum_{\Gamma'} C_{\Gamma\Gamma'} F_{\Gamma'}(\underline{R}) = 0, \quad (6)$$

with

$$C_{\Gamma\Gamma'} = \frac{-1}{2\mu} [2 \int \Psi_{\Gamma'}^* \nabla_{\underline{R}} \Psi_{\Gamma} \, d\underline{r} \cdot \nabla_{\underline{R}} + \int \Psi_{\Gamma'}^* \nabla_{\underline{R}}^2 \Psi_{\Gamma} \, d\underline{r}] - \frac{1}{2(M_a + M_b)} \int \Psi_{\Gamma'}^* \sum_{i,j=1}^n \nabla_{\underline{r}_i} \cdot \nabla_{\underline{r}_j} \Psi_{\Gamma} \, d\underline{r}. \quad (7)$$

The zeroth-order approximation consists of neglecting all  $C$  terms so that

$$\left[ -\frac{1}{2\mu} \nabla_{\underline{R}}^2 + E_{\Gamma}^e(\underline{R}) \right] F_{\Gamma}(\underline{R}) = E F_{\Gamma}(\underline{R}). \quad (8)$$

This is the Born-Oppenheimer approximation.  $F_{\Gamma}(\underline{R})$  is the wavefunction for rotational-vibrational motion. The potential energy in the Schroedinger equation (8) for rotational-vibrational motion is the electronic energy as a function of  $\underline{R}$ ,  $E_{\Gamma}^e(\underline{R})$ , which is independent of the masses of the nuclei.

The first-order approximation to eq. (6), the so-called adiabatic approximation, consists of neglecting the off-diagonal matrix elements of  $C$  (i.e.  $C_{\Gamma\Gamma'} = 0$  when  $\Gamma \neq \Gamma'$ ). It can be shown (6, 7) that, for the ground state of  $\text{H}_2^+$ , the adiabatic correction accounts for 99.8% of the total correction to the B.O. approximation. A similar statement is correct (8, 9) for the ground state of  $\text{H}_2$ . We expect that the adiabatic correction is sufficient for all the systems considered here and subsequent discussion will be restricted to the adiabatic correction.

In order to simplify the notation, the subscripts on  $E^e(\underline{R})$ ,  $F(\underline{R})$ ,  $\Psi$ , and  $C$  are henceforth omitted. Then, in the adiabatic approximation,

$$\left[ -\frac{1}{2\mu} \nabla_{\underline{R}}^2 + E^e(\underline{R}) + C \right] F(\underline{R}) = E F(\underline{R}). \quad (9)$$

It should be noted that  $C$  is in general a function of  $\underline{R}$  since  $\Psi$  is a function of  $\underline{R}$ .  $F(\underline{R})$  is the rotational-vibrational wavefunction of the molecule and eq. (9) is the Schroedinger equation for this wavefunction. The potential energy term in eq. (9) is the sum of  $E^e(\underline{R})$ , the B.O. electronic energy as a function of  $\underline{R}$ , which is independent of nuclear masses, and the adiabatic correction  $C$ , which does depend on nuclear masses. It is clear that the subsequent interest of the present discussion centers on  $C$ , which is sometimes referred to as the diagonal nuclear motion



correction.

$F(\underline{R})$  may be approximated in the usual manner (10) by the product of a vibrational and a rotational wavefunction

$$F(\underline{R}) = \frac{1}{R} f(R) Y_{JM}(\Theta, \phi).$$

$f(R)$  is then found to satisfy the vibrational wave equation

$$\left[ -\frac{1}{2\mu} \frac{d^2}{dR^2} + \frac{J(J+1)}{2\mu R^2} + E^e(R) + C \right] f(R) = E f(R) \quad (10)$$

The term involving  $J$  is the rotational energy of the molecule. The  $R$  dependence of this term gives rise to rotational-vibrational interaction.

The interest here will be restricted to  $^1\Sigma$  states. It can be shown that the first term in eq. (7) for  $C_{\Gamma\Gamma}$  must vanish. The differentiation  $\nabla_{\underline{R}}^2 \Psi$  in the second term must be performed with the coordinates of the electrons held constant with respect to space fixed axes whose origin is at the CMN. This term can be further simplified as is described elsewhere (10, 2).

In all the calculations discussed here, the electronic wavefunctions of the  $^1\Sigma$  states are filled shell single determinant LCAO-MO wavefunctions. The integrals which occur in  $C$  can then be expressed first as integrals over molecular orbitals and subsequently as integrals over atomic orbitals.

As a first approximation, one may assume that  $C$  is independent of  $R$ .  $C$  is calculated at the experimental equilibrium internuclear distance and is then the adiabatic correction to the zero of vibrational energy. In this approximation, the only contribution of the corrections to the B.O. approximation to the equilibrium constant of exchange reaction (1) will result from the quantity designated as  $\Delta E_{LEC}$  in the Introduction (See also eqs. (12) and (13)). In our later calculations (4), which will not be discussed in detail here, we have calculated  $C$  at several internuclear distances. We have found that  $C$  then will contribute not only to the zero of vibrational energy but will also lead to an isotope dependent shift of the equilibrium internuclear distance and of the various vibrational constants. However, the distance dependence of  $C$  is such in our calculations that the correction to the zero of vibrational energy so calculated at the new equilibrium internuclear distance is,

within the significance of the calculations, equal to the value of  $C$  calculated at the original equilibrium internuclear distance. Moreover, the isotope dependent shifts of equilibrium internuclear distance and of vibrational constants are sufficiently small so that the contribution of these shifts to the equilibrium constant of (1) appears negligible. The emphasis in the following section will therefore be on the evaluation of  $C$  at the experimental equilibrium internuclear distance of a molecule and the subsequent evaluation of  $\Delta ELEC$  and the electronic isotope effect  $K(BOELE)$  on the equilibrium constant.

### Calculations

Calculations were originally carried out (2) for the lowest  $^1\Sigma$  states of  $H_2$ ,  $LiH$ ,  $BH$ ,  $NH$ , and  $HF$  and the corresponding deuterated molecules with the LCAO-MO wavefunction of Coulson for  $H_2$  (11) and the LCAO-MO-SCF functions of Ransil (12) for the other molecules. These wavefunctions contain a minimum basis set of inner and valence shell Slater-type orbitals with the orbital exponents optimized at the experimental equilibrium internuclear distance. The  $^1\Sigma$  states are the ground states of the respective molecules except in the case of  $NH$ . The normalized molecular orbitals  $\psi_i$  are expressed in terms of atomic orbitals  $\phi_j$ ,

$$\psi_i = \sum_j c_{ij} \phi_j \quad (11)$$

The  $c_{ij}$  coefficients are available in the published literature only at the experimental internuclear distance of the respective molecules. Thus, in the calculation of  $C$  at the equilibrium internuclear distance, contributions which arise from the variations of the  $c_{ij}$  coefficients with distance were ignored except for the contribution which arises from the fact that  $\psi_i$  must remain normalized as a function of distance. We will designate as  $\mathcal{A}$  the contributions to  $C$  from the variations of such coefficients;  $\mathcal{A}$  was thus evaluated incompletely in these calculations.

With the minimum basis set wavefunctions, we calculated  $C$ ,

$$\Delta C = C(HX) - C(DX) \quad (12)$$

and

$$\begin{aligned}\Delta \Delta C &= -\Delta E_{\text{LEC}} = C(\text{HX}) + C(\text{HD}) - C(\text{DX}) - C(\text{H}_2) \\ &= \Delta C(\text{HX}) - \Delta C(\text{H}_2).\end{aligned}\quad (13)$$

The electronic isotope effect on the equilibrium constant of equilibrium (1) is then calculated as

$$K(\text{BOELE}) = \exp(\Delta \Delta C/kT).\quad (14)$$

In these calculations, we found (2) varying effects with a maximum effect,  $K(\text{BOELE}) = 1.10$ , in the case of  $X = B$ .

It was decided to improve these calculations by using better electronic wavefunctions (3). Single configuration molecular orbital wavefunctions were still used. However, the molecular orbitals were expressed in terms of a so-called extended basis set of gaussian atomic orbitals (for details see reference (3)). The Hartree-Fock-self-consistent-field (HFSCF) procedure was carried out with the digital computer program POLYATOM. The quality of the wavefunctions is not quite what would be called Hartree-Fock limit wavefunctions. Calculations were carried out at several internuclear distances and  $C$  was calculated with the inclusion of the factor  $\mathcal{A}$  correctly calculated. The calculations were extended to include the  $^1\Sigma$  ground states of several ions and also of HCl.

Cade and Huo (13) have calculated near Hartree-Fock limit wavefunctions for  $\text{LiH}$ ,  $\text{BH}$ ,  $\text{HF}$  and  $\text{HCl}$ . The molecular orbital coefficients  $c_{ij}$  are available in the literature again at only the equilibrium internuclear distance. Thus again  $\mathcal{A}$  values cannot be completely calculated. In Table I, the  $C$  values at the experimental equilibrium internuclear distances calculated for  $\text{LiH}$ ,  $\text{BH}$ ,  $\text{HF}$ , and  $\text{HCl}$  with (1) minimum basis set wavefunctions, with (2) our extended basis set wavefunctions and with (3) the near Hartree-Fock limit wavefunctions are compared. In order to assess the quality of the various wavefunctions, the respective electronic energies are compared with those of the corresponding near Hartree-Fock limit wavefunctions. For the minimum basis set and the near Hartree-Fock limit calculations, the correct  $\mathcal{A}$  values of the extended basis set calculations were employed to calculate  $C$ . It is seen that both the  $C$  values and the  $\Delta C$  values for the extended basis set calculations approach closely those of the near Hartree-Fock limit calculations. For  $\text{H}_2$ , we carried out calculations not only for an extended basis set but also for a large extended basis set which

Table I  
Adiabatic Corrections with Different Wavefunctions

Molecule	R(Å)	Wavefunction	$\Delta E^*$	$(\frac{\Delta E^*}{E}) \times 10^5$	C(cm <sup>-1</sup> )	$\Delta C(\text{cm}^{-1})^{***}$
<sup>7</sup> LiH	1.60	Minimum	0.017	218	189.55	31.56
		Extended	0.001	11	189.06	31.24
		Near H. F.	-----	---	188.27	30.81
BH	1.24	Minimum	0.057	226	364.63	49.74
		Extended	0.002	8	359.05	47.68
		Near H. F.	-----	---	360.06	48.30
HF	0.92	Minimum	0.534	534	646.17	35.47
		Extended	0.007	7	600.82	17.55
		Near H. F.	-----	---	598.54	16.46
HCl	1.27	Extended	0.023	5	1346.96	22.07
		Near H. F.	-----	---	1349.81	23.59

\*  $\Delta E$  (hartree units) =  $E_e - E^e$  (Near H. F.) Here  $E^e$  is the electronic energy of the molecule calculated with the given wavefunction and  $E_e$  (Near H. F.) is the electronic energy of the molecule calculated with the near Hartree-Fock limit wavefunction.

\*\*  $\Delta E/E = \Delta E^*/E^e$  (Near H. F.)

\*\*\*  $\Delta C = C(\text{HX}) - C(\text{DX})$

yields results of near Hartree-Fock limit quality. In the case of  $H_2$ , the results of the calculation of  $C$  and  $\Delta C$  with the almost exact wavefunctions of Kolos and Wolniewicz (8) are also available. The latter type of wavefunction can be reproduced in a molecular orbital type of calculation only if configuration interaction is included. Table II compares the results of the various calculations. For the minimum basis set calculation, the  $\alpha$  value calculated with the minimum basis set was employed since the relative  $c_{ij}$  values in the molecular orbital are determined by symmetry. This procedure may be termed somewhat arbitrary (3). The extended basis set and the large extended basis set yield very similar results (as does even the minimum basis set). Table II does emphasize that configuration interaction may be significant for the calculation of  $\Delta C$  values. Configuration interaction has not been employed in the subsequent calculations here and this neglect may be a source of error. Hopefully, the consistent neglect of configuration interaction leads to cancellation. We intend to undertake configuration interaction calculations at a later time.

Table II  
Adiabatic Corrections for  $H_2$  at  $R = 0.74\text{\AA}$  with  
Different Wavefunctions

Wavefunction	$C(\text{cm}^{-1})$	$\Delta C^* (\text{cm}^{-1})$
Minimum	99.07	24.75
Extended	100.94	25.22
Large Extended	101.31	25.31
Kolos and W.	114.59	28.63

\*  $\Delta C = C(H_2) - C(HD)$

Table III summarizes the results calculated with the extended basis set wavefunctions (except for  $H_2$  where the large extended basis set was employed). The calculations are at the respective equilibrium internuclear distances. As a matter of interest,  $\alpha$  values are listed to show that they need not be negligible. For the X atom in HX the nuclear mass of the most abundant isotope was employed unless otherwise stated. The

Table III  
Adiabatic Corrections (in  $\text{cm}^{-1}$ )

Molecule	R(Å)	$\alpha$	C	$\Delta C^*$
H <sub>2</sub>	0.74	7.63	101.31	
HD		5.72	76.00	25.31
<sup>6</sup> LiH	1.60	1.49	210.12	
<sup>6</sup> LiD		0.69	178.89	31.24
<sup>7</sup> LiH		1.50	189.06	
<sup>7</sup> LiD		0.71	157.82	31.24
BeH <sup>+</sup>	1.31	3.40	245.74	
BeD <sup>+</sup>		1.78	217.61	28.12
BH	1.24	8.60	359.05	
BD		4.14	311.37	47.68
CH <sup>+</sup>	1.13	4.76	454.12	
CD <sup>+</sup>		2.40	409.74	44.37
NH	1.05	4.07	515.78	
ND		2.27	478.07	37.71
HF	0.92	6.41	600.82	
DF		3.46	583.27	17.55
HCl	1.27	4.76	1346.96	
DCl		2.37	1324.89	22.07

\*  $\Delta C = C(\text{HX}) - C(\text{DX})$

lithium hydride calculations demonstrate that, while C does depend on the nuclear mass of X,  $\Delta C$  is independent of the X mass.

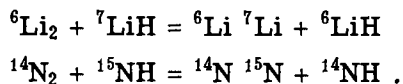
It is now easy to evaluate the electronic isotope effects on the equilibria (1). The results at 300 K are shown in Table IV. The electronic isotope effects on the various equilibrium constants vary from 0.96 to 1.11.

Table IV  
The Electronic Isotope Effect  
K(BOELE) at 300 K

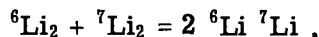
Reaction (X)	$\Delta \Delta C^*$ (cm <sup>-1</sup> )	K(BOELE) <sup>**</sup>
D	0.0	1.00
Li	5.92	1.029
Be <sup>+</sup>	2.81	1.014
B	22.36	1.113
C <sup>+</sup>	19.06	1.096
N	12.40	1.061
F	-7.77	0.963
Cl	-3.25	0.985

\*  $\Delta \Delta C = [ C(HX) - C(DX) ] - [ C(H_2) - C(HD) ]$   
 \*\*  $K(BOELE) = \exp (\Delta \Delta C/kT)$

We have evaluated the electronic isotope effect for some gas phase heavy atom exchange reactions only with minimum basis set wavefunctions,



We find K(BOELE) in these two cases at 300 K to be 1.001 and 0.999 respectively. For self-exchange equilibria like



one finds again that  $K(\text{BOELE})$  is unity. The deviation of  $K(\text{BOELE})$  from unity in heavy atom isotope effects is quite small as expected.

We have also calculated the isotope dependent changes in the equilibrium internuclear distances and the isotope dependent changes in the vibrational constants due to the corrections to the B.O. approximation. In Table V, we list some  $\Delta R_e$  values and also some  $\Delta\omega$  values (the changes in the harmonic vibrational frequencies). These changes are expected to lead only to very small effects on the exchange equilibrium constants. They are discussed in more detail elsewhere (4).

Table V  
Adiabatic Corrections to  $R_e$  and  $\omega$

Molecule	$\Delta^* R_e (\text{\AA})$	$\Delta^* \omega (\text{cm}^{-1})$
H <sub>2</sub>	$2.2 \times 10^{-4}$	-2.1
HD	$1.6 \times 10^{-4}$	-1.4
D <sub>2</sub>	$1.1 \times 10^{-4}$	-0.7
LiH	$3.8 \times 10^{-4}$	-0.5
LiD	$2.2 \times 10^{-4}$	-0.2

\*  $\Delta$  = Adiabatic - Born Oppenheimer

### Conclusions

We have found that corrections to the B.O. approximation may lead to measurable effects on isotopic exchange equilibrium constants involving hydrogen and deuterium. While our calculations do not yet include the effect of configuration interaction, there is no reason to expect agreement between theoretical and experimental isotope effects on equilibrium constants to be better than a few percent unless corrections to the B.O. approximation are included in the theoretical calculation. We hope to be able to report in the very near future on the comparison between a very accurately experimentally determined equilibrium constant involving diatomic hydrides and deuterides and a corresponding theoretical calculation including the corrections



to the B.O. approximation.

### Acknowledgements

We are indebted to Professor H. F. Schaefer III for making available to us his version of the program POLYATOM. This work was supported by the U.S. Atomic Energy Commission under Contract No. AT(04-3)-34, Project Agreement No. 188.

### Literature Cited

1. Van Vleck, J.H., J. Chem. Phys. (1936) 4, 327.
2. Kleinman, L.I., and Wolfsberg, M., J. Chem. Phys. (1973) 59, 2043.
3. Kleinman, L.I., and Wolfsberg, M., J. Chem. Phys. (1974) 60, 4740.
4. Kleinman, L.I., and Wolfsberg, M., J. Chem. Phys. (1974) 60, 4749.
5. Born, M., and Huang, K., "Dynamical Theory of Crystal Lattices" pp. 406-407 (Oxford University Press, New York 1954).
6. Hunter, G., and Pritchard, H.O., J. Chem. Phys. (1967) 46, 2146, 2153.
7. Kolos, W., and Wolniewicz, L., J. Chem. Phys. (1965) 43, 2429.
8. Kolos, W., and Wolniewicz, L., J. Chem. Phys. (1964) 41, 3663, 3674.
9. Poll, J.D., and Karl, G., Can. J. Phys. (1966) 44, 1467.
10. Kronig, R. de L., "Band Spectra and Molecular Structure" pp. 6-16 (Cambridge University Press, London 1930).
11. Coulson, C.A., Trans. Faraday Soc. (1937) 33, 1479.
12. Ransil, B.J., Rev. Mod. Phys. (1960) 32, 245.
13. Cade, P.E., and Huo, W.H., J. Chem. Phys. (1967) 47, 614, 649.

# Isotope Separation Processes

WILLIAM SPINDEL

Department of Chemistry, Yeshiva University, New York, N. Y. 10033

Stable isotopes can be separated by a variety of methods. A few of the methods which have been used or proposed for concentrating isotopes are listed in Table 1, which is neither complete nor exhaustive.

---

Table 1. Methods of Isotope Separation (1-8)

Electromagnetic
Thermal diffusion
Gaseous diffusion
Mass and sweep diffusion
Gas centrifuge
Separation nozzle
Chemical exchange
Chromatographic and ion exchange
Distillation and exchange distillation
Electrolysis and electromigration
Photochemical

---

An appreciation of the variety of conceivable separation processes for a particular task can be gleaned from the fact that a survey (9) carried out in 1953 by a group at the Esso Research and Engineering Company for the U.S. Atomic Energy Commission, of possible methods for the production of heavy water (D<sub>2</sub>O), examined 98 potential processes. In a similar vein, an advisory committee of the AEC in 1971 examining the potential merits of known processes for the separation of uranium isotopes, evaluated at least 25 processes other than gaseous diffusion and gas centrifuge methods (10). Almost all of the processes listed in the table are probably useful in varying degrees for separating isotopes of any of the elements in the periodic table. None of the processes listed is clearly superior to all the others for every isotope separating purpose.

Although the single-stage separation factor is the best single

measure of the relative ease of separation, it alone does not determine the optimum process for a specific separation task. The best method of separation depends on the properties of the element, the degree of separation desired, and the scale of the operation. Even for a given isotope, there is not one best method.

Some general conclusions regarding isotope separation methods drawn by Manson Benedict (11) almost twenty years ago, have not been invalidated to date by any direct experimental demonstration.

1. The most versatile means for the production of research quantities of isotopes is the electromagnetic method.
2. The simplest and most inexpensive means for small-scale separation of many isotopes is the Clusius Thermal-diffusion column.
3. Distillation and chemical exchange are the most economical methods for the large-scale separation of the lighter elements.
4. Gaseous diffusion and the gas centrifuge are most economical for the large-scale separation of the heaviest elements.

In this paper a number of isotope separating processes will be examined, particularly those utilized on a large industrial scale, and the bases for the above conclusions will be presented. Finally, the fundamental principles of a photochemical method of isotope separation based upon excitation by laser light, which has excited a great deal of current interest, will be outlined.

### Electromagnetic Separators

Electromagnetic separators, really large-scale mass spectrometers, called Calutrons because of their early development at the University of California Cyclotron Laboratory, were originally constructed for the Manhattan District during the second world war in order to separate  $^{235}\text{U}$  in kilogram quantities. At the height of this effort some 1100 units were in operation, in two sizes, a 48-inch radius unit called an alpha Calutron and a 24-inch radius unit, the beta Calutron. Figure 1 shows a schematic view of a beta separator. In 1945 production of  $^{235}\text{U}$  by this method was discontinued because the gaseous diffusion process could be operated at much lower cost and most of the Calutrons were dismantled. Only two of the alpha units and 72 of the beta units remain in operation today at the Oak Ridge National Laboratory. These have been devoted for the past 25-30 years to the separation of a most amazing variety of isotopes, both stable and radioactive. Some 200 kilograms of enriched isotopes including over 250 nuclidic species have been produced by the facility. A recent retrospective paper by W. O. Love (12) outlined the accomplishments of the Oak Ridge Electromagnetic Separations Department over

the past three decades. Figure 2 and Table 2 summarize the production of separated isotopes by this facility, and indicate the levels of isotopic purities obtainable by the electromagnetic method. The highly purified samples listed in Table 2. required two or at most three passes through the separator.

These results elegantly demonstrate the extreme versatility of the electromagnetic method.

Table 2. Uranium and plutonium isotope separations. (12)

Mass	Weight Collected (g)	Assay range (%)
Uranium		
233	220	99.99-99.9986
234	16	30.86-94.49
235	530	98.64-99.9988
236	280	85.07-99.996
Plutonium		
238	5	99.48-99.9988
239	232	95.4-99.999
240	238	97.03-99.993
241	120	83.31-99.997
242	360	81.45-99.987
244	3	0.61-99.06

Science

### Thermal Diffusion

The thermal diffusion effect, namely that in a gaseous mixture subjected to a temperature gradient, as for example in a vessel with walls at different temperatures, a concentration gradient is established, was first predicted theoretically by Enskog (13) and by Chapman (14) and confirmed experimentally by Chapman and Dootson (15). It remained for Clusius and Dickel (16) in 1938 to transform the thermal diffusion effect from a laboratory curiosity into a useful and simple method for separating gaseous, liquid, and isotopic mixtures by devising the thermal-diffusion (or thermo-gravitational) column whose operational principle is illustrated in Figure 3.

Heating the inner wire (or tube) and cooling the outer wall of a column produces a convective flow pattern, as shown, descending along the cold wall and rising along the heated wire. This convective flow is super-imposed upon the radial concentration gradient produced by the thermal diffusion effect. The

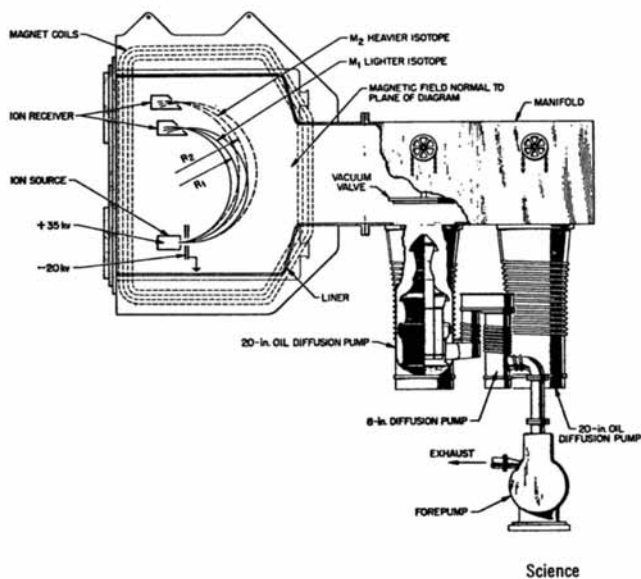


Figure 1. Diagram of a beta calutron separator (12)

H									He				
Li 2889 35.2	Be 0.003 1.3	B 85 9.3	C 150 10.3	N 41 2.9	O 0.022 0.5	F		Ne					
Na	Mg 2889 47.7	Al	Si 5757 146	P	S 3447 127	Cl 431 26.1		Ar					
K 2200 45.5	Ca 46,342 355	Sc	Ti 2561 41.5	V 186 5.8	Cr 4088 55.3	Mn	Fe 30,900 224	Co	Ni 11,06 123				
Cu 3317 43.6	Zn 1626 18.2	Ga 713 14.6	Ge 1663 22.1	As 784 31.0	Se 784 31.0	Br 572 22.8	Kr						
Rb 658 15.2	Sr 8985 75.9	Y	Zr 2314 59.7	Nb 9603 150	Mo 9603 150	Tc	Ru 64 7.1	Rh	Pd 97 12.2				
Ag 801 12.4	Cd 2163 30.5	In 531 7.1	Sn 4932 109	Sb 384 5.4	Te 2271 27.9	I	Xe						
Cs 648 122	Ba 1963 40.9	La 294 8.6	Hf 602 24.5	Ta 1427 28.7	W 9576 92.9	Re 370 6.7	Os 48 2.8	Ir 6.7 3.7	Pt 73 4.8				
Fr	Ra	Ac											
Ca 2123 51.1	Pr 2574 59.5	Nd 2574 59.5	Pm	Sm 2666 39.5	Eu 627 14.7	Gd 1911 90.6	Tb 2.1 0.8	Dy 1178 32.5	Ho	Er 4664 40.0	Tm	Yb 2467 63.2	Lu 378 3.7
Th 33 1.5	Pa	U 6653 51.7	Np	Pu 1506 24.5	Am 0.1 0.1	Cm 0.3 0.3	TOTAL ESTIMATED WEIGHT (grams) THOUSANDS OF TANK-HOURS						

Science

Figure 2. Summary of isotope separations by Oak Ridge Electromagnetic Separations Department through 1972 (12)

counter-current flow multiplies the single-stage separation effect and concentrates the component which diffuses preferentially toward the hot wall at the top of the column, while the component which diffuses preferentially toward the cold wall concentrates at the bottom. This multi-stage separation is essential because the concentration difference between hot and cold walls is quite small ( $\sim 10^{-2}$ ) for isotopic mixtures.

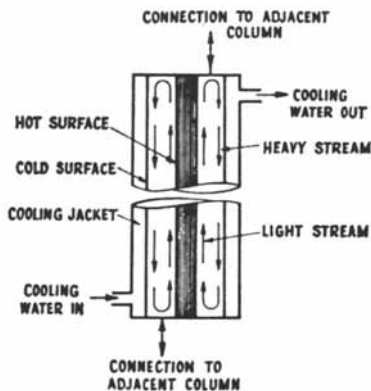
Usually rather than separating isotopes in a single long column, a series or series-parallel arrangement of columns (a cascade) is constructed with individual units perhaps 3-5 meters in length, and appropriate interconnections to permit flow from the top of one unit to the bottom of a succeeding unit. A typical cascade of eleven thermal diffusion columns used at the Mound Laboratory of the U.S.A.E.C. for separating the isotopes of argon (17) is illustrated in Figure 4. The separations obtained and the rate of production of enriched material is indicated. It is worth noting that  $^{38}\text{Ar}$  concentrates in the middle of the cascade. This is typical behavior for an isotope intermediate in mass between two others.

The versatility of the thermal diffusion method and the separations achieved with simple laboratory cascades by Clusius' laboratory for various isotopes is elegantly demonstrated by the data in Table 3.

**Table 3. Isotopes Separated by K. Clusius by Thermal Diffusion (8)**

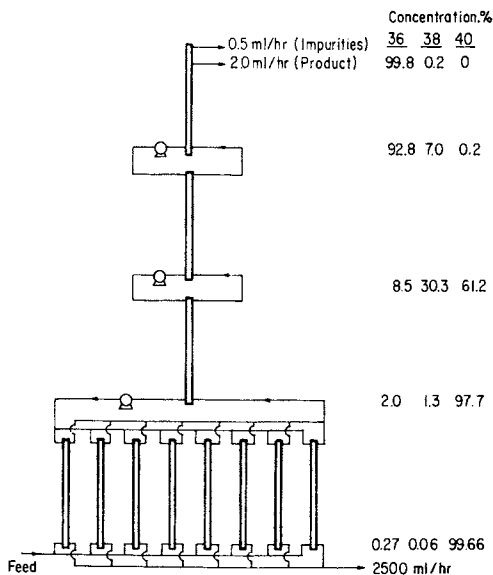
<i>Year</i>	<i>Isotopes</i>	<i>Natural Abundance</i>	<i>Separation Factor</i>	<i>Final Purity</i>
1939	$^{38}\text{Cl}$	75.7	53	99.4
1939	$^{37}\text{Cl}$	24.3	775	99.6
1942	$^{84}\text{Kr}$	57.1	45	98.3
1942	$^{86}\text{Kr}$	17.5	940	99.5
1950	$^{20}\text{Ne}$	90.5	210	99.95
1950	$^{15}\text{N}$	0.37	135,000	99.8
1953	$^{13}\text{C}$	1.09	45,000	99.8
1955	$^{136}\text{Xe}$	8.9	810	99.0
1956	$^{21}\text{Ne}$	0.275	96,500	99.6
1959	$^{18}\text{O}$	0.204	200,000	99.75
1959	$^{38}\text{Ar}$	0.064	9,750,000	99.984
1960	$^{22}\text{Ne}$	9.21	12,500	99.92
1962	$^{36}\text{Ar}$	0.37	3,300,000	99.991

Adv. Chem.



Countercurrent Separation Processes

Figure 3. Thermal diffusion column (7)



Gaseous Isotope Separation at Mound Lab.

Figure 4. Hot wire thermal diffusion cascade for separating argon isotopes (17)

The foregoing discussion fairly well demonstrates that on a small scale any desired isotope can be separated either by the electromagnetic or the thermal diffusion method. In contrast to these laboratory-scale processes, the separations of the heavier isotope D, of the lightest element, hydrogen, and of the lighter isotope  $^{235}\text{U}$ , of the heaviest natural element uranium, are carried out on a literally enormous industrial scale.

#### Uranium Enrichment by Gaseous Diffusion

The United States has three gaseous diffusion plants (18) for separating  $^{235}\text{U}$  located at Oak Ridge, Tenn., Paducah, Kentucky; and Portsmouth, Ohio. The total cost of these plants is about 2.4 billion dollars and the annual operating costs (at full capacity) is about 460 million dollars. Electrical power consumption is about 6000 megawatts, which correspond to an annual electrical energy cost of over 300 million dollars. The production capacity of these plants is the equivalent of 75000 kg. (75 metric tons) of 90%  $^{235}\text{U}$  per year. Further, the AEC has estimated that even if the existing plants are upgraded with newer technology and operated at a higher power level, to produce an additional 60% of enriched uranium, by 1980 additional enriching capacity will be required if the U.S. is to supply most of the free-world needs for uranium enrichment. A new plant is projected at a cost of 1-1.2 billion dollars with an annual production capacity equivalent to 38.5 metric tons of 90%  $^{235}\text{U}$ .

Figure 5 shows an aerial view of the Portsmouth, Ohio plant (the newest one), typical of the three in size. The buildings cover 93 acres of ground but have a floor area about three times as great. The larger two buildings (x-330 and x-333) are each about a half mile long by 550 feet wide!

The operating principles of multi-stage isotope separating processes, such as the gaseous diffusion process, were first developed by Karl Cohen (19), and further exposed in a form more directly useful to chemical engineers by Benedict and Pigford (1). Bigeleisen has presented a concise summary of the theory in his review (8).

At the heart of an isotope separation cascade is the elementary separating unit, or stage which separates a feed stream carrying  $F$  moles/time of an isotopic mixture containing a mole fraction  $x_f$  of the desired isotope, into a product (enriched) stream,  $P$  at mole fraction  $x_p$ , and a waste (depleted) stream,  $W$  at mole fraction  $x_w$ . For that matter, the same separation process is carried out by the entire cascade. Two material balance equations govern the operation of a separating unit or an entire cascade.



$$\text{Total: } F = P + W \quad (1)$$

$$\text{Isotopic: } Fx_f = Px_p + Wx_w \quad (2)$$

The elementary separation factor for a single-separating unit on a two component mixture is defined as

$$\text{Elementary factor: } \alpha \equiv \frac{(x/1-x)_{\text{enriched}}}{(x/1-x)_{\text{depleted}}} \quad (3)$$

For the separation of uranium isotopes by gaseous diffusion of  $\text{UF}_6$ , the theoretical limiting value of  $\alpha$  is given by Graham's law

$$\alpha = \sqrt{\frac{238_{\text{UF}_6}}{235_{\text{UF}_6}}} = \sqrt{\frac{352}{349}} = 1.0043 \quad .$$

The stages of a cascade are usually combined as shown in Figure 6. The feed to each stage is made-up by combining the depleted stream from the stage above with the enriched stream from the stage below. A material balance anywhere inside the cascade shows that the depleted flow from the  $(n+1)$ th stage is just equal to the enriched flow from the  $n$ th stage minus the product withdrawn at the top of the cascade. From the material balance equations 1 and 2, and material balances within the cascade, the operating parameters for an isotope separating cascade can be determined (1,8,19). The minimum number of separating stages,  $N$ , required to achieve a given overall separation at total reflux (no enriched product withdrawn) is

$$\text{Separation, } S \equiv \frac{(x_p/1-x_p)}{(x_w/1-x_w)} = \alpha^N \quad , \quad (4)$$

$$N_{\min} = \ln S / \ln \alpha \quad (5)$$

The minimum reflux ratio required, at the feed point, to produce a given product rate  $P$  of material at isotopic composition  $x_p$ , in systems where  $\alpha$  is close to 1, is

$$(L/P)_{\min} \cong \frac{x_p - x_f}{(\alpha-1)x_f(1-x_f)} \quad (6)$$

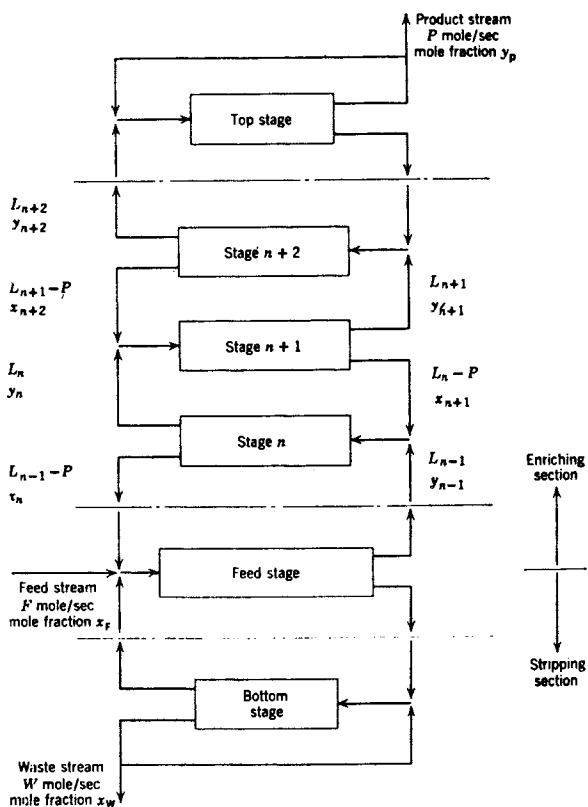
This minimum feed/product rate would require an infinite number of separating stages in the cascade.

Neither of these limiting cascade parameters are suitable for an actual isotope production task; the minimum stage cascade



AEC Gaseous Diffusion Plant Operations

Figure 5. Aerial view of Portsmouth, Ohio gaseous diffusion plant (18)



Encyclopedia of Chemical Technology

Figure 6. Separation stages arranged to form a simple cascade (6)

produces no material at the desired concentration, the minimum flow cascade requires an infinite number of stages. The ideal cascade is one in which the separation achieved per stage is just sufficient to make the composition of the depleted stream from the  $n+1$  stage exactly equal to that of the enriched stream from the  $n-1$  stage. Thus no entropy of remixing is produced when these streams are combined to form the feed of the  $n$ th stage. This cascade is often called the "no-remixing" cascade. In the ideal cascade,

$$x_w^{n+1} = x_p^{n-1} = x_f^n$$

$$N_{\text{ideal}} = 2 N_{\text{min}} \quad (7)$$

$$(L/P)_{\text{ideal}} = 2(L/P)_{\text{min}} .$$

Since the reflux ratio (flow/product) required at each stage in a cascade (eqs. 6 and 7) is related to the isotopic concentration at that point, the size of the separating units are tapered from the feed point towards the ends of the cascade in order to minimize the size and cost of the plant, the pumping energy consumed, the hold-up of enriched material, and the time required to reach steady-state enrichment. The characteristic shape of an ideal cascade is indicated in Figure 7 which *diagrammatically* depicts the parameters for an ideal gaseous diffusion cascade to produce 1 kg of 90%  $^{235}\text{U}$  from natural  $\text{UF}_6$  containing 0.711%  $^{235}\text{U}$  and discarding waste  $\text{UF}_6$  at 0.200%  $^{235}\text{U}$ . The vertical height at any point in the figure is proportional to the stage number measured from the waste end of the cascade, the width is proportional to the total interstage flow at that stage. The quantities of uranium feed required and waste produced, the numbers of stages in the enriching and stripping sections (above and below the feed point), and the inter-stage flow at any stage are all calculated by eqs. 1-7 and the elementary factor 1.0043. Thus, from eq. 7, and the product and feed isotope concentrations, the interstage flow at the feed point is calculated

$$(L/P)_{\text{ideal}} = 2 \cdot \frac{(0.9-0.00711)}{(.0043) (.00711) (1-.00711)} = 58,829 \quad (8)$$

Almost 60,000 moles of natural abundance uranium flow through the cascade, at the feed stage for each mole of 90%  $^{235}\text{U}$  withdrawn.

The total interstage flow,  $J$ , in the cascade, i.e. the total area enclosed in Figure 7, is (20)

$$J = \frac{8}{(\alpha-1)^2} [P \cdot V(x_p) + W \cdot V(x_w) - F \cdot V(x_f)] \quad (9)$$

where  $V(x)$  is the function  $(2x-1) \ln x/(1-x)$ , often called the value function or separation potential. The separation potential is a function of composition only and is dimensionless. It has a value of zero at  $x = 0.5$  and is positive for all other values of  $x$ , symmetrically about the minimum at  $x = 0.5$ .

Eq. 9 is of major importance for estimating the size and cost of an isotope separation plant. It indicates that the total flow is a product of two factors; the first of these, proportional to  $1/(\alpha-1)^2$  is a function only of the elementary separation factor which is determined by the separation process used. The second factor [in square brackets], which is usually called the separative duty or separative work units (S.W.U.) is a function only of quantities and concentrations of feed, product, and waste. It has the same dimensions as those used for the quantities of material, and its value is independent of the process used to accomplish the separation task. The significance of the magnitude of the elementary factor is immediately apparent; a two-fold reduction in  $(\alpha-1)$  requires an increase in the total flow by a factor of 4. Since for a gaseous diffusion process, the total flow rate is closely related to the total area of porous barriers, the total pumping capacity and the total power consumption required, all the associated costs vary proportionately.

The S.W.U. provides a quantitative measure of the isotope separation task for any conceivable process. For the task described in Figure 7, 227.3 kg S.W.U. are required per kg of 90%  $^{235}\text{U}$ . For gaseous diffusion, with  $(\alpha-1) = .0043$ , 98.2 million kg U must be pumped through the cascade in order to produce 1 kg of product.

It is most interesting to note from the shape of the ideal cascade in Figure 7, and from eq. 9, that most of the area in the figure, and therefore most of the volume of the cascade, and the energy which must be supplied, is associated with enriching the isotope from natural abundance by the first factor of ten, say from 0.711% to 7%  $^{235}\text{U}$ . To prepare 1 kg of  $^{235}\text{U}$  at 7% concentration requires 77% of the S.W.U. required to produce a kg of  $^{235}\text{U}$  at 90% enrichment. The cost of enrichment by any combination of processes is essentially determined by the process used at the base of the cascade.

To give some feeling for the magnitude of cost of enriching uranium, the A.E.C. estimates (18) that in the most efficient projected gaseous diffusion plants, 0.266 kW of continuous electrical energy will be consumed per S.W.U.·yr. This corresponds to a consumption of 530,000 kW·hr per kg of 90%  $^{235}\text{U}$ . At 5.5 mills per kW·hr the cost of electrical energy is \$2900 per kg of 90%  $^{235}\text{U}$ .

The essential elements of a gaseous diffusion cascade for  $^{235}\text{U}$  enrichment, their physical arrangement and inter-connections are indicated in Figure 8. The inter-relationships between the motors, compressors, heat exchangers, diffusion membranes, and stage control valves are all shown. The largest size diffusion stages used in one of the AEC plants are seen in the photograph in Figure 9, which shows the equipment size in comparison to a man.

### Deuterium Enrichment by Exchange and Distillation

Now let us examine deuterium enrichment--first the scale of the current effort, and a projection of the deuterium requirements in the future. The United States has constructed two plants, each capable of producing 500 tons of  $\text{D}_2\text{O}$  per year. One of these plants is dismantled, and the second plant is currently operating at about one third of its capacity, producing 180 tons of  $\text{D}_2\text{O}$  per year. In Canada, two plants with a combined output of 1600 tons  $\text{D}_2\text{O}$  per year have recently been completed (21).

$\text{D}_2\text{O}$  is used as a neutron moderator and heat transfer medium for power reactors. The  $\text{D}_2\text{O}$  requirement is about one ton  $\text{D}_2\text{O}$  per megawatt of electrical capacity. In the United States the development of power reactors has moved toward reactors fuelled with enriched  $^{235}\text{U}$ , using light water as moderator and either gas or liquid metals as coolants. In Canada the direction has been toward the use of natural abundance uranium (0.7%  $^{235}\text{U}$ ) as fuel, with  $\text{D}_2\text{O}$  as moderator.

It is of interest to project the deuterium requirements for use as a fusion fuel in controlled thermonuclear reactors (CTR). Robert Hirsch, Director of the U.S.A.E.C. Division of Controlled Thermonuclear Research has predicted the production of significant amounts of fusion energy by 1980, and fusion power commercialization before the turn of the century (22). A report prepared by a group at Brookhaven National Laboratory (23) can be used for estimating energy and deuterium requirements in a future fusion-based energy regime, in which all fossil fuels (except for ship and petrochemical feed requirements) are replaced with synthetic fuels produced by D-D fusion reactors, and all electricity production is by CTR. They estimate that by the year 2020,  $500 \times 10^{15}$  BTU of fusion energy would be required to supply all U.S. energy needs (with exceptions noted above). The total amount of deuterium needed to produce this energy (assuming 100% efficiency for the D-D fusion reaction) would be only 1000 tons  $\text{D}_2$  per year (5000 tons  $\text{D}_2\text{O}$ ). If the technical problems can be overcome, the fusion process promises to be astonishingly efficient from the standpoint of resource consumption!

Four, of the many processes proposed and used for deuterium

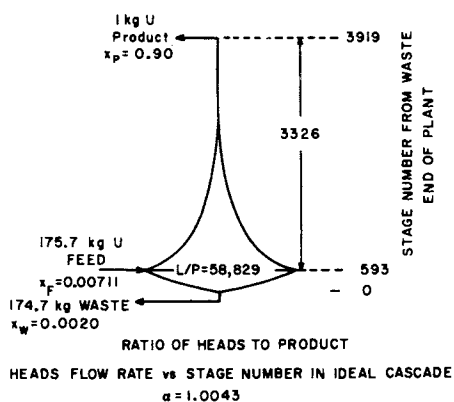
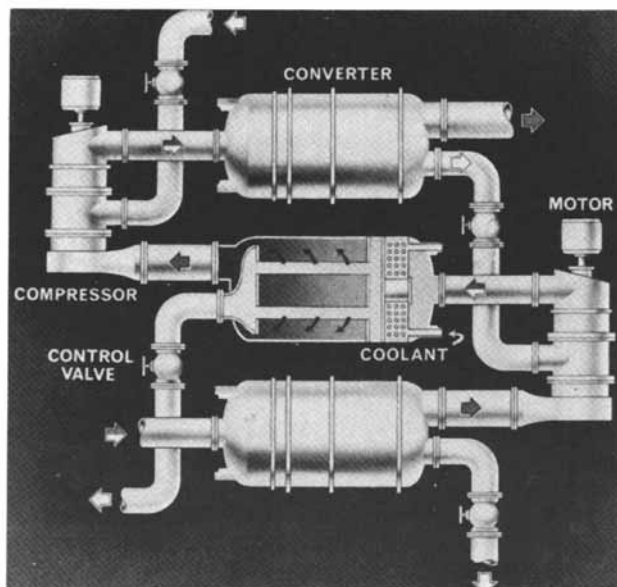


Figure 7. Parameters of an ideal separation cascade for uranium isotope separation



AEC Gaseous Diffusion Plant Operations

Figure 8. Arrangement of gaseous diffusion stages (18)

enrichment, will now be examined. Two are distillation processes and the remaining two are chemical exchange processes. The basic operational parameters of the distillation processes, water distillation and hydrogen distillation, are compared in Table 4. The water distillation system was actually used in early plants

Table 4. Distillation process requirements to produce deuterium at 99.8% D from natural feed at 0.0149% D. (4,24)

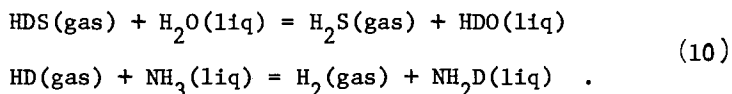
	<u>Water Distillation</u>	<u>Hydrogen Distillation</u>
effective $\alpha$	1.05	1.52
temperature	50°C	23 K
pressure	~100 mm	~1.6 atm
min.no.stages	308	41
min.reflux ratio	141,000	19,600
percent recovery	5	90
moles feed/moles product	133,940	7442
Operating Cost (\$/lb D <sub>2</sub> O)	176	16

built and operated in the U.S. between 1943 and 1945. These plants were shut down in 1945 because of the high operating costs. The hydrogen distillation process appears extremely favorable because of the large effective fractionation factor, and the total energy cost for producing deuterium by this process has been estimated (24) to be about 1700 kW·hr per pound of D<sub>2</sub>O. This corresponds to an energy cost of \$9.30 per pound of D<sub>2</sub>O (at 5.5 mills/kW·hr); the energy consumption is probably the lowest of any of the deuterium separating processes. Several plant designs for producing deuterium by distillation of liquid hydrogen were actually carried out during the decade 1941-1951 (25-27). Because of the technical problems of handling large amounts of liquid hydrogen at cryogenic temperatures of ~20 K, and because of the unavailability of sufficiently large quantities of hydrogen gas to serve as feed for a large-scale deuterium enriching plant, no hydrogen distillation plant has ever been constructed in the U.S. Several relatively small hydrogen distillation plants have been constructed and operated in the past 15 years in France, Germany, India and the Soviet Union. The reported magnitude of D<sub>2</sub>O production in these plants is in the range 3-14 tons D<sub>2</sub>O per year.

It seems of interest to re-examine the hydrogen distillation system, now, in light of current liquid hydrogen technology, and of projected hydrogen production as a synthetic fuel. At present, the U.S. production capacity for liquid hydrogen, mainly for use in the space program, is about 150 tons of liquid hydrogen per day. This, by itself, would permit the extraction of 15

tons deuterium (75 tons D<sub>2</sub>O) per year. More to the point is a developing interest in the use of liquid hydrogen as an aircraft fuel, particularly for hypersonic aircraft. Design studies have shown that the flying range of a large transport could be increased 30-40% using liquid hydrogen as fuel (28). Projections regarding liquid hydrogen consumption by aircraft (29) indicate that if only ~3.5% of air transport in the U.S. in the year 2000 were hydrogen fuelled, liquid hydrogen production would be 4.25 million tons per year, and the extractable deuterium, by distillation, would be 1100 tons per year. It should be noted that the energy consumption for the extraction of deuterium from liquid hydrogen, by a distillation process *operating parasitically* on a liquid hydrogen plant, would probably be lower by one or two orders of magnitude than the energy consumption previously estimated for hydrogen distillation systems. Previous estimates were based on using gaseous hydrogen as feed, where all refrigeration energy would be supplied for the purpose of isotope extraction; in parasitic operation on a liquid hydrogen facility only the heat losses from the distillation columns would correspond to energy required for the deuterium extraction.

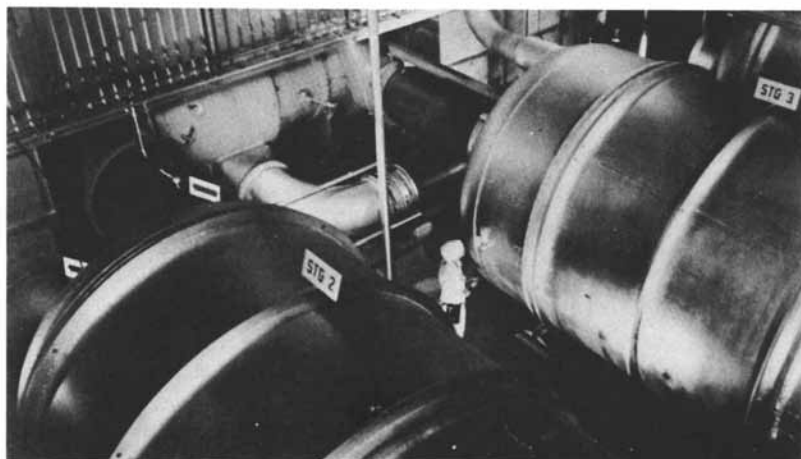
Two significant chemical exchange reactions useful for the concentration of deuterium are



A simple system for utilizing these exchange reactions for deuterium concentration is illustrated in Figure 10. In both the exchange reactions listed above, the desired isotope, deuterium concentrates in the liquid phase, so the phase conversion unit in Figure 10 consists of a chemical reactor which converts the enriched compound (HDO or NH<sub>2</sub>D respectively for the reactions listed) into the isotopically depleted compound (hydrogen gas or hydrogen sulfide gas). The exchange tower must contain sufficient separating stages to multiply the single stage enriching factor,  $\alpha$  to produce the desired degree of overall separation.

As indicated earlier, interstage flows are very large in isotope separation processes, and the quantities of processing chemicals required for reflux reactions (phase conversion) represent a major expense in any chemical exchange separation system, unless the process is parasitic on a chemical manufacturing process and/or the by-products of the reflux reactions upgrade the value of the reflux chemicals. An elegant way to avoid the need for reflux chemicals is provided by using a dual-temperature exchange system of the type first proposed, independently by Spevack (30) and by Geib (31). Such a system uses the variation of the exchange equilibrium constant with temperature, to substi-





AEC Gaseous Diffusion Plant Operations

Figure 9. Close-up view of actual equipment (diffusers and compressor) in a gaseous diffusion plant (18)

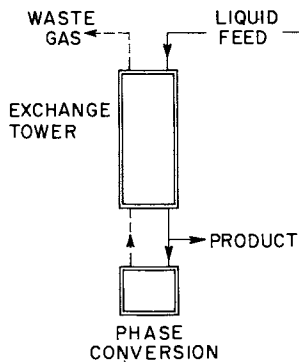


Figure 10. Simple chemical exchange system for isotope separation for an isotope concentrating in the liquid phase

tute thermal reflux instead of chemicals for returning the desired isotope from the enriched compound to the isotopically depleted compound. The magnitude of the exchange constants for deuterium exchange, and their variation with temperature, make a dual-temperature exchange process particularly suitable for concentrating isotopes of hydrogen.

Figure 11 illustrates a simplified arrangement of components and the magnitude of operating parameters for the concentration of deuterium by dual-temperature exchange between hydrogen sulfide gas and liquid water.  $H_2S$  is circulated in a closed loop counter-current to a descending stream of water. In the colder column deuterium concentrates in the liquid phase; the equilibrium constant for the exchange at the cold temperature,  $30^\circ C$ , is 2.20. In the hotter column, at  $130^\circ C$ , the exchange equilibrium constant is 1.69, and deuterium is returned from the aqueous phase to the gaseous phase. Thus, dual-temperature operation avoids the need for a chemical reaction to return the desired isotope from the phase in which it enriches to the phase in which it is depleted. In operation, feed water at the natural deuterium abundance of 145 ppm is fed to the top of the cold column, depleted water at 120 ppm deuterium is discarded from the bottom of the hot column, and enriched  $D_2O$  is withdrawn between the cold and hot columns. The effective single-stage enrichment factor is simply the ratio of  $\alpha_{cold}/\alpha_{hot} = 1.26$ , for this process at the indicated operating temperatures. This effective single-stage enrichment factor determines the number of separating stages required in the hot and cold columns respectively, to achieve the desired degree of enrichment. The maximum fraction of the isotope which is extractable from the feed in this operating mode, is simply the difference in the  $\alpha$ 's at the two operating temperatures divided by the larger of the two values. These relationships effectively limit the use of a dual temperature system to the separation of hydrogen isotopes. The operating temperatures shown in Figure 11 for the  $H_2S$ -water exchange system are determined by the practical considerations that  $H_2S$ -hydrate precipitates in the low temperature column below  $30^\circ C$ , and at the operating pressure of 300 psi, the mole fraction of water in the gaseous phase becomes excessive above  $130^\circ C$ .

A dual-temperature system requires twice the number of separating stages (hot and cold columns) needed for a single temperature system with the same effective  $\alpha$ , but the need for refluxing chemicals is eliminated, and the heat energy required to maintain the temperature difference can be greatly reduced by the use of heat exchangers at appropriate points to pre-heat the gas and liquid streams entering the hot column, and to pre-cool the gas entering the cold column.

All of the major plants currently producing deuterium in

quantities >20 tons D<sub>2</sub>O per year utilize the H<sub>2</sub>S-water dual-temperature exchange system. Figure 12 shows schematically the cascade arrangement used at the Savannah River plant for the production of 500 tons of D<sub>2</sub>O per year (32). Concentration of deuterium from the 15% level produced by exchange, to the final product concentration of 99.8% D is accomplished by vacuum distillation of water. It should be noted however, that practically all of the separative work is expended in getting from the feed concentration of 145 ppm to 15% D. This task requires 7383 SWU; about 0.7% additional SWU are needed to produce the final product. The economics of the process is determined at the base of the cascade!

Fundamental parameters for the ammonia-hydrogen exchange reaction which is listed in eq. 10, are much more favorable than the equivalent factors for the H<sub>2</sub>S-water system. The discovery by Claeys, Dayton and Wilmarth (33) that amide ion serves as an efficient homogeneous catalyst for the exchange immediately stimulated a group at Brookhaven National Laboratory, led by Bigeleisen to carry out extensive experimental and theoretical studies of this system (34,35). They determined that a dual-temperature system operating with hot column at 70°C ( $\alpha = 2.9$ ) and a cold column at -40°C ( $\alpha = 5.9$ ) would have an effective  $\alpha = 2.0$ , and would permit extraction of 50% of the deuterium from the ammonia feed. They also showed that the exchange, when catalyzed by NaNH<sub>2</sub> dissolved in the liquid, was sufficiently rapid even at the lower temperature to reach equilibrium in reasonably sized exchange columns. To date, this system is being used in a single-temperature plant in France producing about 20 tons D<sub>2</sub>O per year, about which only few details have been published. The major limitation on the use of this process has been the availability of sufficient quantities of ammonia for plant feed. Even a plant producing 1000 tons ammonia per day would only provide sufficient feed to permit production of 60-70 tons D<sub>2</sub>O per year. Again, one sees the interplay between science and technology, and one is faced with the fact that technological rather than scientific considerations are often the over-riding determinants for *large scale* isotope separation.

#### Photochemical Isotope Separation Processes

For many years attempts have been made to use photochemical processes for the separation of isotopes. The basic idea is to utilize the difference in the absorption spectra of different isotopic species, and by use of sufficiently monochromatic light of an appropriate wavelength to excite only one of the species to an upper energy level. The excited species may then be separated by chemical or physical means from its isotopic partners; the separating process need not have any inherent isotopic selectivity. A particularly successful application of the method was to the separation of Hg isotopes by Gunning et al. (36,37). For example,

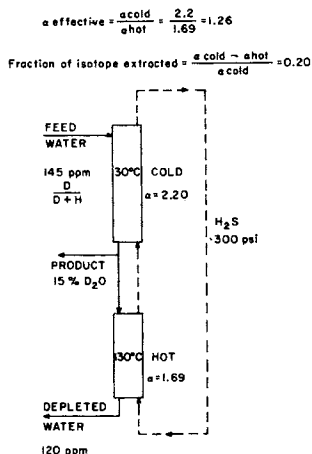
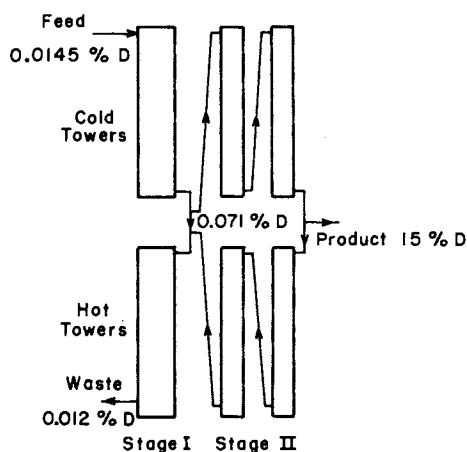


Figure 11. Simplified flow sheet for a dual-temperature exchange system for concentrating deuterium



Chemical Engineering Progress

Figure 12. Simplified schematic of Savannah River exchange unit showing principal towers and liquid flow paths. There are 24 such units (500 tons  $D_2O$ /year). Stage 1: hot towers, 12' dia.  $\times$  70 trays; cold towers, 11' dia.  $\times$  70 trays. Stage 2: hot towers, 2  $\times$  6.5' dia.  $\times$  70 trays ea.; cold towers, 2  $\times$  6.5' dia.  $\times$  85 trays ea. (32).

a monoisotopic  $^{202}\text{Hg}$  resonance lamp was used to illuminate mercury vapor containing the natural abundance mixture of Hg isotopes (196, 198-202, 204). Essentially only  $^{202}\text{Hg}$  isotopes were excited to an upper electronic state, in which they reacted with an added gas such as  $\text{H}_2\text{O}$ , to form  $\text{HgO}$  which could then be separated easily from unreacted Hg. Values of  $\alpha$  as high as 3 were obtained for  $^{202}\text{Hg}$ .

The essential requirements for any photochemical isotope separation scheme follow:

1. Absorption spectrum with a well resolved isotope shift (vibrational-rotational or vibronic for molecules, electronic for atoms)

2. A light source sufficiently monochromatic and tunable to excite absorption by one isotope and not the other, sufficiently intense to excite a substantial fraction of the isotopic species in the gas mixture.

3. Deactivation of excited species by collisions with other species must be minimized; energy transfer from one isotopic species to another must not occur before step 4.

4. A chemical or physical process which separates excited species from the others.

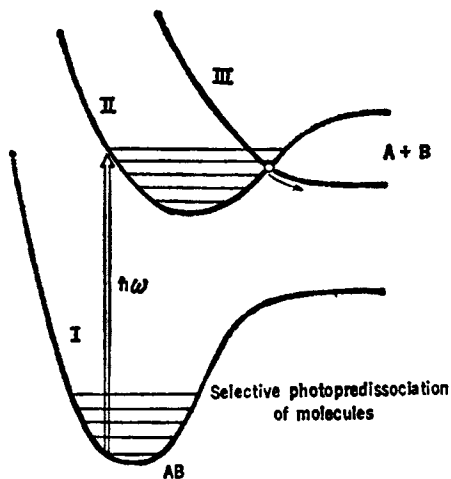
The first and last of these requirements are dependent on the specific isotopes, molecular species and chemical or physical processes. They cannot be changed, but the appropriate selection depends on the ingenuity of the investigator. Requirements two and three, on the other hand, have been virtually unobtainable until the development of lasers, which produce very large outputs of radiant energy with an extremely narrow band width. Also, the ability of a laser to emit this large amount of monochromatic radiant energy within a time interval as short as several nanoseconds is important in meeting the energy transfer requirements.

Two recent papers by Letokhov (38) and by Moore (39) contain excellent and detailed discussions of the application of lasers to isotope separation. The approaches fall into two broad categories which may be characterized as one-step and two-step processes. The one-step process is particularly simple conceptually but not as generally applicable. It involves selective excitation of a suitable molecule to an upper pre-dissociative state. This upper state is a non-dissociative one whose potential energy surface intersects another surface corresponding to a dissociative state. Such a system is illustrated in Figure 13. If the dissociative lifetime is shorter than the radiative lifetime, then selective photo-excitation can produce isotopically enriched

dissociation products. Yeung and Moore (40) irradiated an equimolar mixture of  $D_2CO$  and  $H_2CO$  using a frequency-doubled Ruby laser (3472 Å). The hydrogen gas formed by photo-dissociation of the formaldehyde showed a 6:1 D to H ratio! To maximize isotopic separation, the compound should be irradiated with a narrow line in a spectral region where the undesired isotopic species is relatively transparent. Moore (41) has observed the absorption spectra of the isotopic ( $^{13}C$  and  $^{12}C$ ) formaldehydes and concluded that irradiation with light of an appropriate wavelength should yield  $^{13}CO$  preferentially as a dissociation product.

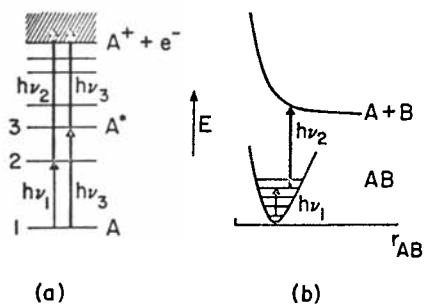
Selective two-step processes are more generally applicable to isotope separation. Several approaches are indicated in Figure 14. The diagram on the left (a) shows approaches to selective *photo-ionization*. A photon  $\nu_1$  selectively excites isotopic atoms to the upper state, 2, and a second photon  $\nu_2$ , with sufficient energy to ionize atoms in state 2, but insufficient to ionize those in the ground state, then ionizes the excited atoms. It should be noted that the second photon,  $\nu_2$  need not be highly monochromatic. Alternatively, the frequencies  $\nu_1$  and  $\nu_2$  may be identical, as indicated by  $\nu_3$ . The  $\nu_3$  frequency must be resonant with a transition of one of the isotopic species, and of sufficiently high frequency to ionize the excited atom. The diagram on the right of Figure 14, illustrates a two-step *photo-dissociation process*. The selective photon,  $\nu_1$  excites a vibrational transition. The level excited should be sufficiently high so that its thermal population is negligible, and its absorption coefficient for  $\nu_2$  is appreciable, while the corresponding coefficient from the thermally populated state is negligible. If the A and B fragments are chemically stable, one need only separate isotopically enriched A or B species from the remaining AB molecules by a simple chemical separation. If the fragments are reactive, a chemical trapping scheme which does not induce isotopic scrambling must be devised. Notice that the two-step processes are really limited to laser light sources, because the two light pulses must be closely synchronized to avoid energy transfer.

One can only estimate very crudely at this time the energy requirements for laser isotope separation. Moore has pointed out (39) that a process yielding one separated atom for each 3300 Å photon absorbed, requires 0.1 kw. hr. of light energy per mole of separated isotope. Assuming a laser efficiency of  $10^{-4}$  this corresponds to an energy consumption of 1000 kw. hr. per mole. Naturally, these calculations essentially represent a theoretical minimum goal to be approached. To date, the experimentally demonstrated feasibility of uranium isotope separation has been limited to the preparation of about  $10^5$   $^{235}U$  atoms per second (42), but the magnitude of the industrial enterprise involved in isotope separation certainly appears to justify an expanded level of fundamental research in this direction.



Science

Figure 13. Schematic diagram of molecular photo-predissociation process (38)



(a)

(b)

Accounts of Chemical Research

Figure 14. Schematic diagram of selective two-step processes: (a) photo-ionization, (b) photo-dissociation (39)

Acknowledgement

The author is most pleased to acknowledge the assistance of his colleagues, George W. Flynn and Ralph E. Weston through numerous discussions of isotopic separation by laser excitation.

Literature Cited

1. Benedict, M., and Pigford, T. H., "Nuclear Chemical Engineering", McGraw-Hill, New York, 1957.
2. Kistemaker, J., Bigeleisen, J., Nier, A.O.C., (Eds.), "Proceedings of the International Symposium on Isotope Separation", North-Holland Publ. Co., Amsterdam, 1958.
3. Koch, J., (Ed.), "Electromagnetic Isotope Separators and Applications of Electromagnetically Enriched Isotopes", North-Holland Publ. Co., Amsterdam, 1958.
4. London, H., (ed.), "Separation of Isotopes", George Newnes, Ltd., London, 1961.
5. J. Chim. Phys., (1963), 60, (1 and 2), Symposium on "Physical Chemistry of Isotope Separation".
6. Schacter, J., Von Halle, E., Hoglund, R. L., "Encyclopedia of Chemical Technology", Standen, A., (Ed.), 7, 91, Wiley and Sons, New York, 1965.
7. Pratt, H. R. C., "Countercurrent Separation Processes", Elsevier Publ. Co., Amsterdam, 1967.
8. Bigeleisen, J., in "Isotope Effects in Chemical Processes", Advances in Chemistry Series, 89, Am. Chem. Soc., Washington, D. C., 1969, Chapter 1.
9. Barr, F. T., Drews, W. P., Chemical Engineering Progress, (1960), 56, 49.
10. Benedict, M., Berman, A. S., Bigeleisen, J., Powell, J. E., Shacter, J., Vanstrum, P. R., "Report of Uranium Isotope Separation Review Ad Hoc Committee", ORO-694, Oak Ridge, Tenn., June 1972.
11. Ref. 1, p. 516.
12. Love, L. O., Science, (1973), 182, 343.
13. Enskog, D., Z. Physik, (1911), 12, 56, 533.
14. Chapman, S., Phil. Trans, Roy. Soc. London Ser. A, (1916), 216, 279.
15. Chapman, S., Dootson, F. W., Phil. Mag., (1917), 33, 248.
16. Clusius, K., Dickel, G., Naturwiss., (1938), 26, 546.
17. Haubach, W. J., Eck, C. F., Rutherford, W. M., Taylor, W. L., "Gaseous Isotope Separation at Mound Laboratory-1963", MLM-1239, Miamisburg, Ohio, June 1965.
18. "AEC Gaseous Diffusion Plant Operations", ORO-684, Washington, D. C., January 1972.
19. Cohen, K., "The Theory of Isotope Separation", McGraw-Hill, New York, 1951.
20. Ref. 1, p. 396.



21. Bancroft, A. R., "The Canadian Approach to Cheaper Heavy Water", AECL-3044, Chalk River, Ontario, February, 1968.
22. New York Times, February 28, 1974.
23. Powell, J., Salzano, F., Sevian, W., Hoffman, K., Bezler, P., "An Evaluation of the Technical, Economic and Environmental Features of a Synthetic Fuels Economy Based on Fusion Reactors", BNL-18430, Upton, N. Y., November 1973. (Figure 3.5).
24. Benedict, M., "Survey of Heavy Water Production Processes", Proc. Int'l Conf. on Peaceful Uses of Atomic Energy, (1956), 8, 377, United Nations, N. Y.
25. Clusius, K., Starke, K., Z. Naturforschung, (1949), 4A, 549.
26. Hydrocarbon Research, Inc., "Low Temperature Heavy Water Plant", NYO-889, N. Y., N. Y., March 1951.
27. Murphy, G. M., (Ed.), "Production of Heavy Water", N.N.E.S. III, 4F, McGraw-Hill, New York, 1955.
28. TID-26136, "Hydrogen and Other Synthetic Fuels--A Summary of the Work of the Synthetic Fuels Panel", September, 1972, Superintendent of Documents, Washington, D. C.
29. AET-8, "Reference Energy Systems and Resource Data for use in The Assessment of Energy Technologies", April, 1972, Assoc. Univ. Inc. Upton, New York.
30. Spevack, J., Report MDDC-891 (1947).
31. Clusius, K., et al., FIAT Review of German Science (1939-1946), Physcial Chemistry, p. 19ff.
32. Bebbington, W. P., Thayer, V. R., Chem. Eng. Progress, (1959) 55, 70.
33. Claeys, Y., Dayton, J. C., Wilmarth, W. K., J. Chem. Phys., (1950), 18, 759.
34. Perlman, M., Bigeleisen, J., Elliot, N., J. Chem. Phys., (1953), 21, 70.
35. Bigeleisen, J., Ref. 2., p. 121.
36. Pertel, R., Gunning, H. E., Can. J. Chem., (1959), 37 35.
37. Gunning, H. E., Strausz, O. P., Adv. in Photochem., (1963), 1, 209.
38. Letokhov, V. S., Science, (1973), 180, 451.
39. Moore, C. B., Accounts of Chem. Res., (1973), 6, 323.
40. Yeung, E. S., Moore, C. B., Appl. Phys. Lett., (1972), 21, 109.
41. Moore, C. B., private communication.
42. Chem. and Eng. News, (1974), 52, No. 27, p. 24 (July 8).

\*Research supported by U.S.A.E.C. under Contract AT(11-1)-3581.

†Present address: Division of Chemistry and Chemical Technology  
National Academy of Sciences-National Research  
Council, 2101 Constitution Avenue, Washington,  
D. C. 20418

# Condensed Phase Isotope Effects, Especially Vapor Pressure Isotope Effects: Aqueous Solutions

W. ALEXANDER VAN HOOK

Chemistry Department, University of Tennessee, Knoxville, Tenn. 37916

## Abstract

The theory of isotope effects in condensed phase systems, especially vapor pressure isotope effects (VPIE) is briefly reviewed. It is pointed out that the VPIE can be employed as one measure of the effect of intermolecular forces on the motions of molecules in condensed phases. This is illustrated with a number of examples from the recent literature and from our own laboratory. A more detailed description of our recent work on thermodynamic solvent isotope effects in aqueous systems is presented. Experiments on vapor pressures, freezing points, and heats of solution and dilution of solutions of electrolytes in HOH and DOD are described. Implications are discussed with respect to the aqueous solvent structure problem.

## A. Introduction

This symposium has revealed a number of different aspects of the physical and theoretical bases of isotope effects. Generally, we are interested in the effect of isotopic substitution on some process. In the direct approach one formulates a description of the process in terms of a set of energy levels describing the "before" and "after" states of each isotopic isomer which enters. With those energy states as input information one then calculates population distributions, and isotope effects on population distributions, evaluates partition functions, takes ratios, and thereby determines the isotope effects (IEs). More commonly, detailed information concerning energy level distributions is not available, so one is forced to the alternate point of view that the measured bulk property IEs serve as probes to investigate IEs on the energy level distributions. Further, we note that energy level distributions can often be theoretically calculated to sufficient precision from appropriate potential energy functions. These functions relate the potential energy to interparticle geometry. It is well established that properly evaluated potential

functions are independent of isotopic substitution to a good approximation (but see the paper by Wolfsberg (1)). It follows that measured isotope effects can serve as probes in investigations of some details of the nature of a given potential energy surface. This is the basic reason for scientific interest in isotope effects; thus, kineticists make certain deductions about the nature of transition states by reasoning from observed kinetic isotope effects (2); in a similar vein we will interpret measured isotope effects on condensed phase properties in terms of the intermolecular forces on the motions of molecules in condensed systems.

Most of the material in the present talk will be concerned with the Vapor Pressure Isotope Effect (VPIE). This is for two good reasons. First, the VPIE is the most thoroughly studied of all condensed phase effects and therefore a good deal of information is available to exemplify various points of interest. Second, the methods used to formulate a description of the VPIE can to a large extent be carried over and applied to other kinds of condensed phase effects, so a certain generality is present. More superficial, but equally useful is the fact that it is only with the VPIE that one is naturally led to employ the attenuated vapor as the reference standard state. This simplifies things and also has a good deal of appeal to anyone brought up on Lewis and Randall (3). A number of recent reviews containing significant amounts of material on the VPIE are available. Among these, the recent ones by Bigeleisen, Lee and Mandel (4) and by Jancso and Van Hook (5), afford convenient access to the literature.

The effect of isotopic substitution on the vapor pressure is an old problem -- the first theoretical calculations were carried out by Lindeman (6) for monatomic Debye solids. On the basis of this work it was suggested that experimental investigation of the VPIE might prove a powerful tool in settling the then controversial question of the existence of the zero point energy. The first experiments were carried out in 1931 by Keesom and van Dijk (7) who succeeded in obtaining a partial separation of the isotopes of neon in a distillation experiment. Very soon thereafter other separations using the VPIE were successful, and in the middle and late thirties a number of authors including Scott, Brickwedde, Urey and Wahl (8) and Topley, Bailey and Eyring (9) applied the concepts of statistical thermodynamics to the problem of the VPIE of structured molecules. They pointed out that there were a number of factors which could contribute to the effect. Herzfeld and Teller (10) in an important paper which appeared in 1938, showed that at low temperatures the VPIE is principally determined by the isotopic zero point energy differences associated with the external degrees of freedom. At high temperatures, on the other hand, a classical treatment is justified and there is no isotope effect. The authors nicely showed that at the intermediate temperatures commonly encountered care must be taken to properly account for excitation into higher quantum levels. We

have seen earlier (11) that this can be accounted by a number of different but equivalent approaches. The original authors developed the VPiE in terms of an expansion about the classical limit in powers of successively higher quantum corrections. The method is therefore limited to "almost classical" systems. In the case of the intermolecular part of the potential the quantum correction is larger in the condensed than in the vapor phase because the mean square force in the (ideal) vapor is zero. It follows that the lighter isotope exhibits the higher vapor pressure. The inverse effect often observed for molecules with structure was attributed to the changes in the intramolecular potential which occur on condensation. In spite of this rather clear and early statement of the theoretical basis for the VPiE, confusion persisted until a reformulation was given almost twenty-five years later by Bigeleisen (12). This author reexpressed matters in terms of reduced partition function ratios (RPFRs) (13) thereby giving a demonstration of the important connection between the VPiE and details of the molecular structure. A good deal of the present paper is concerned with this point. We will return to a quantitative formulation of the Bigeleisen approach after a brief consideration of the pictorial model described below.

### B. A Physical Picture

In examining the VPiE, we are concerned with the equilibrium between the condensed and vapor phases. The latter may be approximated as an ideal gas (if this is not adequate methodologies exist for correcting to the ideal gas reference state). In the gas the freely rotating and translating molecule may be regarded as a set of  $3n-6$  coupled oscillators ( $n$  is the number of atoms, if the molecules are linear there are  $3n-5$  oscillators, if they are monatomic there are no oscillators and rotation is not defined). Two gross effects must be considered on condensation. First intermolecular forces in the condensed phase cause perturbations of the energy levels characterizing the internal oscillator energies. A given energy level may either be raised or lowered with respect to its gas phase value (blue or red shifted). Details will depend on the specific natures of the intermolecular force and the type of oscillator (for example it is well established that stretching motions of non-polar molecules are red shifted on condensation by the dispersion interaction). The second effect arises because the six (five for linear, three for monatomic molecules) external motions of the molecule, originally free (zero frequency) in the attenuated vapor, become hindered (of real frequency) as the molecule condenses into the attractive well defined by the intermolecular potential. These six external condensed phase modes are necessarily blue shifted from the (zero) gas phase values. Notice that for both internal and external modes the reduced masses of the particular motions are such that the more lightly substituted molecule undergoes the larger shift.

Since the intramolecular motions can shift either to the blue or red the net isotopic difference of the shifts can be either positive or negative, and can therefore lead to positive (normal) or negative (inverse) VPIEs. In general, excitation into upper vibrational levels must be considered and these contributions can lead to complicated temperature dependencies (14). Some of the ideas outlined above are presented in a conventional schematic fashion in Figure 1. Diagrams are given for both internal and external modes.

### C. Functional Forms

The ideas that we have crudely expressed above and in Figure 1 have been quantified by Bigeleisen (12) who derived an expression for the VPIE. In this equation a prime stands for the

$$\ln \frac{P'}{P} = \ln \frac{s}{s'} f_c - \ln \frac{s}{s'} f_g + (RT)^{-1} (P'V' - PV) - (B_o P + \frac{1}{2} C_o P^2)' + (B_o P + \frac{1}{2} C_o P^2) - (RT)^{-1} \int_v^{v'} P' dv \quad (1)$$

lighter isotope,  $P'/P$  is the VPIE, and  $(s/s')f_c$  and  $(s/s')f_g$  are Reduced Partition Function Ratios (RPFs) for the condensed and gas phases as introduced by Bigeleisen and Mayer (13). The  $(s/s')f$  terms in the equation represent the differences in quantum effects between the condensed and gaseous states. The correction terms account for the effect due to the difference between the Gibbs and Helmholtz free energies and from gas imperfection. They are necessary because the (separated) samples are being compared at the same temperature but at different pressures. If a comparison at the same condensed phase molar volume is derived then the additional correction,  $(RT)^{-1} \int_v^{v'} P' dv$ , is required. The correction terms are usually small and may often be neglected. They have been evaluated for a number of different systems by various authors (15-18).

A simplification to equation (1) obtains if  $\ln(P'/P)$  is itself small. With  $B \approx B'$  and  $V \approx V'$  and neglecting  $(RT)^{-1} \int_v^{v'} P' dv$  and terms of order  $C_o P^2$  then

$$\ln \frac{f_c}{f_g} = \ln \frac{P'}{P} \left[ 1 + P(B_o - \frac{V}{RT}) \right] \quad (2)$$

Equations (1) and (2) refer to measurements on separated isotopes. It is also important to develop a relation between the reduced partition function ratio (RPFs) and measured separation factors,  $\alpha$ , referring to single stage isotopic enrichments (on distillation) for dilute nonideal solutions. In the case of infinite dilution the molar volumes of the two isomers are identical (they are determined by environment) and one obtains (19)

$$\ln \alpha = \ln \left( \frac{N'}{N} \right)_{\text{vapor}} / \left( \frac{N'}{N} \right)_{\text{liquid}} = \ln \frac{f_c}{f_g} - \frac{(v' - v)^2}{2\beta'v'RT} \quad (3)$$

Here  $\beta$  is the isothermal compressibility and  $V$  the molar volume of the condensed phase. The last term is usually very small and is often neglected. This accounts for the common and mistaken idea that RPFRRs are directly measured in distillation experiments.

Equations (1), (2) and (3) relate the RPFRRs to the measured VPIEs. The next step is to develop a methodology relating RPFRRs to the changes in the  $3nN$  dimensional potential function which occur on condensation. The alternative, to directly measure the isotope effects on each and every energy level that contributes to RPFRR, is not only tedious and impossible, but also inelegant. Therefore, a "standard manual" for calculating isotope effects would now plunge into a detailed exposition of the methodology of calculating partition functions and reduced partition functions for condensed and vapor phase molecules given the molecular structure and some information concerning the potential energy surface. The commonly employed procedures are most easily understood in terms of the isolated molecule gas phase approximation. Conventionally, electron-nuclear coupling effects are ignored (that is the Born-Oppenheimer approximation is assumed, we have earlier seen some indications of the inadequacy of this approximation (1)), and then the molecular RPFRRs are further approximated as a product of rotational, translational and internal vibrational parts. The rotation and translation contributions to RPFRR are zero in the ideal gas reference because the potential for these modes is zero. In the condensed phase they may be expressed in terms of the mean square forces exerted on the translational motions and the mean square torques on the rotational ones. Next the intramolecular degrees of freedom are often approximated with harmonic oscillator potentials. (This is normally reasonable because our interest lies in accurate assessments of isotopic differences in the changes the frequencies on condensation, not in the absolute value of the frequencies themselves. Therefore, we expect that many of the difficulties connected with small anharmonicities might cancel when we take ratios to determine the VPIE. Still, it is to be hoped that refinements will soon permit an accurate assessment of the anharmonic corrections. Wolfsberg (20) and Hulston (21) have cleared up apparent difficulties in the methodology commonly employed to evaluate anharmonic corrections for polyatomic systems.) The isotope effects on the intramolecular energy level distributions can now be calculated straightforwardly from the intramolecular potential. This potential is isotope independent within the frame of reference defined by the validity of the (usually very good) Born-Oppenheimer approximation. We note that the procedure has been subjected to many and varied experimental verifications, principally by spectroscopic techniques (22). It is well established.

The problem is more complicated for the condensed phase. Here it becomes necessary to include the mutual interactions between many molecules. We have already seen schematically (Figure 1) that the interaction may be thought of in first approximation

as consisting of two parts. First, the classical translations and rotations of the gas phase now become quantized as the molecules "fall into" the attractive well. Second, the same attractive intermolecular forces which account for that well perturb the intramolecular energy levels from the gas phase values. Factorization of these two effects, one from the other, is clearly not exact. Each is a manifestation of one and the same intermolecular force field and the two must be intimately coupled. In other terms the factorization of the canonical partition function per mole of material into  $n$  single particle microcanonical partition functions  $Q = q^n$ , which was exact (within the present context) in the attenuated gas reference state, is now conceptually inadequate. Even so, most calculations have proceeded by considering the motions of the "average condensed phase molecule (and its isotopic isomer)" in terms of their microcanonical partition functions. Such calculations are in fact strictly analogous with the gas phase calculations outlined above. As a first step factorization into internal, rotational and translational parts is assumed, and the three different kinds of motion are presumed to be describable with appropriate isotope independent potential functions. Stern, Van Hook and Wolfsberg (23) have described a model calculation based on the Bigeleisen theory. In the BSVHW approach, the harmonic approximation is applied to all  $3n$  modes of the "average molecule". In this approximation, equation (1) becomes after neglect of the correction terms

$$\frac{f_c}{f_g} = \prod_{\text{internal}}^{3n-6} \left[ \frac{(u_i/u_i')_c}{(u_i/u_i')_g} \right] \left[ \frac{\exp(u_i' - u_i)_c / 2}{\exp(u_i' - u_i)_g / 2} \right] \left[ \frac{(1 - \exp(-u_i')_c) / (1 - \exp(-u_i)_c)}{(1 - \exp(-u_i')_g) / (1 - \exp(-u_i)_g)} \right] \prod_{\text{external}}^6 \frac{u}{u'} \left[ \exp\left(\frac{u' - u}{2}\right) \right] \left[ \frac{1 - \exp(-u')}{1 - \exp(-u)} \right] \quad (4)$$

The result has been called the "complete" equation. The frequencies which enter may be calculated from mass and geometry considerations using standard techniques. The  $3n$  dimensional PE matrix is taken as isotope independent. Computer programs are available for this purpose. The potential and kinetic energy parameters describing the problem are expressed as matrix elements in the  $3n$  dimensional space. Off diagonal elements couple the different modes, and rotation-translation and internal-external interactions thereby enter in a natural way. These effects are important in VPIE considerations and the model has been used widely (4,5). At high temperatures, certain single modes, or ultimately all of the modes, may become excited and then can be treated in terms of series expansions in powers of quantum corrections. Such methodologies have been developed by Bigeleisen and co-workers (24) and by Jancso (25) in detail. Alternatively at low enough temperatures certain other modes may be treated in the zero-point energy approximation. In especially favorable cases the different motions

can be separated into a high lying set (generally the internal vibrations) which is treated in the zero point energy approximation, and a low lying one (the lattice modes) handled by the first order quantum correction. In this fashion one obtains the widely quoted approximate relation

$$\ln \frac{P'}{P} \approx \ln \frac{f_c}{f_g} = \frac{A}{T^2} - \frac{B}{T} \quad (5)$$

where the first term is interpreted as the first order quantum correction

$$A = \frac{1}{24} \left( \frac{hc}{k} \right)^2 \left[ \sum_{i}^{\text{ext}} (v_i'^2 - v_i^2) \right] \quad (6)$$

and the B term accounts for the shift in zero point energy of the high lying modes.

$$B = \frac{1}{2} \frac{hc}{k} \left[ \left( \sum_{i_g}^{\text{int}} v_{i_g}' - \sum_{i_c}^{\text{int}} v_{i_c}' \right) - \left( \sum_{i_g}^{\text{int}} v_{i_g} - \sum_{i_c}^{\text{int}} v_{i_c} \right) \right] \quad (7)$$

Some discussion of the BSVHW model is in order. Two important criticisms come rapidly to mind. First the model is severely limited by virtue of its adoption of the average molecule approximation. This is not physically reasonable. The motions of neighboring molecules must be intimately coupled through the intermolecular force field and this is only crudely recognized. The second criticism is concerned with the problem of anharmonicity. Clearly the harmonic approximation is more suitable for internal than it is for external modes. While it may be possible to introduce anharmonic corrections for these modes, it would appear that if this is to be done in a realistic fashion a number of higher order terms should be included (the motions are highly anharmonic). The concomitant higher order interactions introduced in such a treatment may well serve to destroy the chief appeal of the BSVHW approach which lies in its simplicity and in the straightforward method by which it handles internal-external interactions. Gordon (26) and others abandon this latter advantage by assuming separability of the internal and external motions. The external motions are then described in terms of the mean square forces and torques exerted on the average condensed phase molecule. This is certainly more realistic for these modes than is the introduction of the harmonic approximation, but it is achieved at the high cost of neglecting the consequences of internal-external coupling.

A different point of view has been taken by Fang and Van Hook in a qualitative discussion of the VPIE (27). These authors obtained data on the isotope effects on the vapor phase second virial coefficients of the deuterated methanes. The data were in good agreement with those of earlier workers (28). In the interpretation, separability of the internal vibrations from the external motions of the molecules was assumed. This approximation is commonly used in considering vapor phase intermolecular potentials.



The interaction is considered as equivalent to that between two nonvibrating but polarizable molecules. This amounts to separating out and averaging over the intramolecular contributions before introducing consideration of the intermolecular modes. In terms of this model it is readily demonstrated that the virial coefficient isotope effect can only be interpreted in terms of isotope dependent parameters for the Lennard-Jones force field. The values extracted from the VCIE are within experimental error of the measured isotope effects on the polarizabilities (29). These in turn were shown to be consistent with the IEs on molecular size as determined by electron diffraction (30) or molar volume measurements (31). The authors note that the IE on molecular size is well understood in terms of the vibrational properties of the isolated molecules. An isotope independent intramolecular potential function may be employed to calculate isotope effects on the mean square amplitudes of the internal modes and these in turn are found to be proportional to the molecular size and polarizability isotope effects. This correlation indicates that the isotope dependence of the effective intermolecular potential arises from the approximate procedure of separating the internal and external motions and the neglect of certain details of the vibrational properties of the interacting molecules. The authors emphasize this point. The isotope dependence in the intermolecular potential should not be regarded as an apparent contradiction to standard approaches based on the Born-Oppenheimer approximation. Rather it only underscores the crudeness of the standard method of separating out and averaging over the internal modes before considering the motions on the external potential surface(s). They (27) go on to indicate that an analogous approach may be useful in handling the external contribution to the VPIE. This would amount to substituting an isotope dependent external force field in the average molecule approximation in place of a detailed consideration of numerous higher order internal-external coupling and anharmonicity effects. Such isotope dependent force constants are to be regarded principally as a convenience in the sense that it is easier to approximate the real situation with an isotope dependent effective (perhaps harmonic) field than it is to attempt to solve the complicated many molecule problem exactly. The approach which is suggested has some similarities to earlier applications of DeBoer's modification of the law of corresponding states (32) to the VPIE of polyatomic systems following Steele (33). It is to be presumed that this suggestion will prove equally controversial. The magnitude of the expected isotope dependencies is small. For the translation modes of  $\text{CH}_4$  and  $\text{CD}_4$ , an extreme case, a ten percent difference in the translation force constant was estimated as an upper limit. This would correspond to about a 5% shift in the associated frequency, but this is not directly detectable because of the broad IR band associated with the lattice modes in the liquid. Normally corrections of this type are expected to be quite small. For practical purposes, they can be ignored when the

BSVHW model is employed to correlate isotope effects among a series of molecular isotopic isomers.

#### D. Specific Examples of VPIE Studies

While this paper is not intended to serve as a review, a few examples from the literature (including some work from our own laboratory) will serve to illustrate points of interest concerning the theory.

1. The Monatomic Gases. Extensive data on rare gas VPIEs is available, most recently from Bigeleisen and co-workers (34). Jancso and Van Hook have reviewed the situation as of 1973 (5). The results on monatomic liquids are of particular interest because realistic comparisons with fundamental theoretical calculations are possible. The interpretation is simplified because the only degrees of freedom are the translational ones. In the data analysis the mean value of the Laplacian of the positional energy in the condensed phase  $\langle \nabla^2 U \rangle$  (the mean square force) is obtained and can be compared with results from calculated or experimental radial distribution functions. Specific intermolecular potential functions can be tested in this fashion. In the context of the present paper it is worth noting that application of cell model calculations, in both the harmonic and various anharmonic approximations, demonstrate these to be inadequate. The vibrational coupling between atoms is completely ignored. However, good agreement was found with calculations based on the improved self consistent phonon theory of an anharmonic lattice using an LJ 13-6 potential. Such results reinforce the earlier criticism of the BSVHW model for the VPIE of structured molecules (Section C). In another calculation Weeks-Chandler-Anderson perturbation theory was used to calculate the mean Laplacian from the LJ 6-12 potential by Mandel (35). The calculated  $\langle \nabla^2 U \rangle$ 's were used to obtain isotope separation factors which were then compared with experiment. The comparison is given in Figure 2 and is really quite good

2. Diatomic and Linear Molecules: The Effect of Rotation and the Rotation-Translation Interaction. The possible importance of a rotational contribution to the VPIE is nicely demonstrated by the experimental results for NNO isotopic isomers. The results are old ones due to Bigeleisen and Ribnikar (36). Here the pertinent observation is that the VP difference between the isomers  $N^{15} N^{14} O^{16}$  ( $M = 45$ ), and  $N^{14} N^{15} O^{16}$  ( $M = 45$ ) is as large as that between  $N^{14} N^{15} O^{16}$  ( $M = 45$ ) and  $N^{14} N^{14} O^{16}$  ( $M = 44$ ). In the first pair the mass ratio is unity, but there is an isotope effect on the moments of inertia; in the second there is an isotope effect on mass but the moments of inertia are equal within 7 parts in  $10^5$ . Other evidence indicates that the change in intramolecular force constants on condensation is negligible. It was concluded that a sizable barrier to rotation exists in this condensed phase.

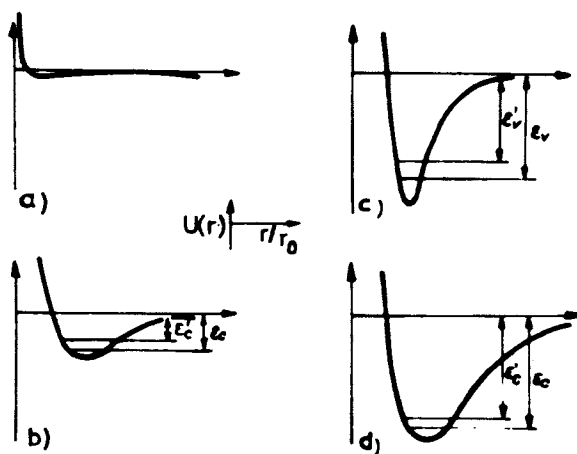
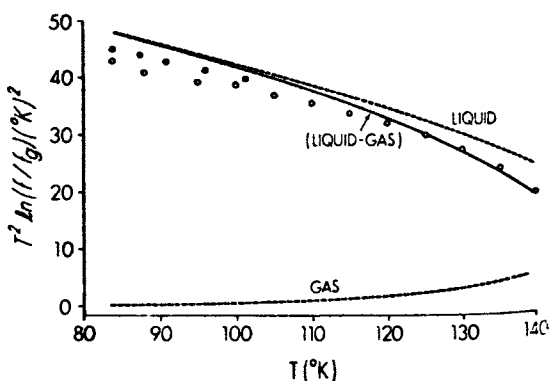


Figure 1. Potential energy diagrams. a. external translation (gas phase); b. external translation (condensed phase); c. internal vibration (gas phase); d. internal vibration (condensed phase). In a,  $r_0$  denotes the average intermolecular distance in the gas phase, in b,  $r_0$  denotes the value of the intermolecular distance evaluated at the minimum, and in c and d,  $r_0$  denotes the value of the coordinate describing the molecular distortion evaluated at the minimum. Notice for the external motions the zero point energy change on condensation,  $(E'_c - E_c) - E'_v - E_v > 0$ , because  $E'_v \cong E_v \cong 0$ , but for the internal motions it may be positive, negative, or zero depending on the effect of the intermolecular forces on the specific motion under consideration.



Journal of Chemical Physics

Figure 2.  $T^2 \ln(f/f_g)$  as a function of temperature for argon. The solid line is the difference between the liquid and the gas values represented by the dashed lines.  $\bullet$  experimental results on (34).  $\circ$  vapor pressure,  $\circ$  separation factor. The lines are calculated (35).

It is interesting that this prediction was confirmed by infrared measurements 11 years later.

Effects which couple rotational and translational motions sometimes occur when centers of mass and geometry in a molecule do not coincide. Friedman (37) developed an expression describing this situation in the limit of small quantum corrections. He considered relations between the center of electrical charge (or interaction) (CI), the center of mass (CM), and the geometric center (CG). The geometric relationships between the centers are expressed by Equation 8.

$$a = |CI - CM| = \frac{R(m_h - m_l)}{2(m_h + m_l)} - d \quad (8)$$

Here  $m_l$  and  $m_h$  are the light and heavy atom masses respectively and  $d = |CG - CI|$ . For a diatomic with both atoms isotopes of the same element,  $d = 0$ . Friedman obtained an expression for the first quantum correction to the configurational part of the partition function,

$$Q = Q_{CI} \left[ 1 - \frac{\beta^3 h^2 N}{24 M_{eff}} \langle \nabla^2 U \rangle \right],$$

in terms of an effective mass  $M_{eff}$  and the mean squared force,  $\langle \nabla^2 U \rangle$ , exerted on one molecule by all of the others. The effective mass takes the rotational contribution into account.

$$\frac{1}{M_{eff}} = \frac{1}{M} \left( 1 + \frac{2}{3} \frac{Ma^2}{I} \right)$$

The approach is tested by considering the relative vapor pressures of three isotopic molecules. One finds for the isotopic nitrogens  $N^{14} N^{14}$ ,  $N^{14} N^{15}$  and  $N^{15} N^{15}$ .

$$R = \ln \frac{P_{14-15}/P_{15-15}}{P_{14-14}/P_{15-15}} = 0.495$$

The measured value is  $0.494 \pm 0.002$ . In the absence of translation-rotation coupling  $R = 0.5$ . The theoretical ratio is independent of temperature and this, too, is in agreement with experiment.

Gordon (26) gave a somewhat similar approach in his discussion of the isotopic CO molecules. Rather than introduce an effective mass he considered the VPIE as arising from four terms; (i) the mean square force (translational contribution), (ii) the mean square torque (rotational contribution), (iii) the change in torque on isotopic substitution, and (iv) the intramolecular frequency shifts on condensation. Effects (ii) and (iv) can both be obtained from moment analysis of IR or Raman vibrational bands. Therefore by combining VPIE and spectroscopic data, values for both the mean square force and mean square torque can be obtained.

The method was illustrated by application to the isotopic COs (38) (Table 1). Friedman and Kimel (39) also evaluated mean square torques for CO in the liquid phase but their calculated values are much smaller than those derived by Gordon from measurements of the third and fourth moments of IR and Raman spectra. The most likely reason for the discrepancy is that Friedman's assumption of a spherically symmetric external force field for CO is not justified.

3. Polyatomic Molecules: Hydrogen-Deuterium Effects. A representative sampling of measured HD VPIE effects is shown in Figure 3. The information which it contains is far from exhaustive but does include a number of different kinds of effects. At the moment we are only concerned with gross features. These exhibit a wide difference, varying all the way from approximately 10% per D normal for HOH/DOD at the melting point, to about 1-1/2% per D inverse for substitution in nonpolar hydrocarbons. We note that the large normal effects are connected with molecules which strongly associate in the condensed phase, and associate through the position of isotopic substitution. The inverse effects often display minima in the VPIE temperature curves as expected from the earlier discussion of applicable theory (Equations 4 and 5).

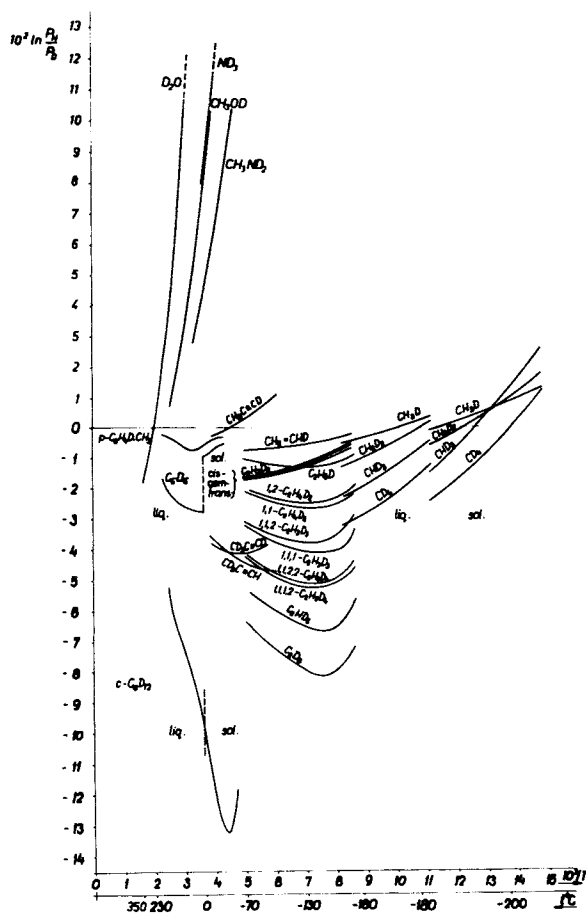
One interesting exception to the behavior (associated compounds=normal effects; nonassociated compounds=inverse effects) is that of the carboxylic acids. Some examples are shown in Figure 4 (40). The results indicate that deuteration at methyl or methylene, and also at carboxyl, increases the vapor pressure. The unexpected sign of the carboxyl effect is attributed to the fact that organic acids are highly associated, not only in the liquid, but also in the vapor, and this must be properly taken into account. More commonly, association in the vapor phase is not important and then normal effects are readily attributable to unusually large values for the intermolecular condensed phase frequencies, these can outweigh the normal red shifts in internal frequencies usually observed on condensation. For example, in the condensation of water vapor to the liquid at 313 K there is a net red shift of about  $283 \text{ cm}^{-1}$  in the internal frequencies but this is more than compensated by the appearance of three librational frequencies around  $500 \text{ cm}^{-1}$  and three hindered translations around  $160 \text{ cm}^{-1}$ . The VPIE is therefore normal and large. We shall discuss the water problem in more detail below. It is evident from Figure 3 that a similar situation obtains for deuteration on the  $\text{NH}_2$  group of methyl amine and to a lesser extent for substitution at acetylenic hydrogen positions which are also known to associate, but clearly the behavior of the compounds substituted at the non-polar methyl and methylene positions is different.

4. Applications of the BSVHW Model - i (methane). The principal successes of the BSVHW model have been in application to hydrocarbon VPIEs. As a first example we consider the calcula-

Table 1. Predicted VPTE and Changes in Mean-Squared Torques of the Isotopes of Liquid CO at 77 K. (26)

Isotope	$\frac{(P-P')V}{RT}$	$\frac{\langle(O'U)^2\rangle - \langle(OU)^2\rangle}{\langle(OU)^2\rangle}$ %
$^{12}\text{C}^{16}\text{O}$	0 <sup>a</sup>	0
$^{12}\text{C}^{17}\text{O}$	0.00285	3.7
$^{12}\text{C}^{18}\text{O}$	0.0056 <sup>a</sup>	7.5
$^{13}\text{C}^{16}\text{O}$	0.0076 <sup>a</sup>	-4.5
$^{13}\text{C}^{17}\text{O}$	0.0107	-1.1
$^{13}\text{C}^{18}\text{O}$	0.0132 <sub>s</sub>	2.3
$^{14}\text{C}^{16}\text{O}$	0.0147	-8.1
$^{14}\text{C}^{17}\text{O}$	0.0199	-5.1
$^{14}\text{C}^{18}\text{O}$	0.0202	-2.1

<sup>a</sup> Measured values. (38)



Chemical Reviews

Figure 3. Hydrogen-deuterium vapor pressure isotope effects for some compounds (5)

Table 2. F Matrix Elements for Isotopic Methanes

Gas		$F_{\text{gas}} - F_{\text{solid}}$	$F_{\text{gas}} - F_{\text{liquid}}$	$F_{\text{gas}} - F_{\text{ads}}$
5.495	$F_{\text{S}}, \text{CH Stretch (mdyn/\AA)}^{\circ}$	0.063	0.043	0.051
0.568	$F_{\text{B}}, \text{HCH bend (mdyn}\cdot\text{\AA)}^{\circ}$	0.000	0.003	0.002
0.165	$F_{\text{SB}}, \text{(mdyn)}$	0.000	-0.010	0.000
0.124	$f_{\text{SS}}, \text{(mdyn/\AA)}^{\circ}$	0.000	0.000	0.001
0.019	$f_{\text{BB}}, \text{mdyn}\cdot\text{\AA}^{\circ}$	0.000	0.000	0.000
0	$F_{\text{t}}, \text{CH}_4 \text{ Translation (mdyn/\AA)}$	-0.096	-0.057	-0.063
0	$F_{\text{r}}, \text{CH}_4 \text{ Rotation (mdyn}\cdot\text{\AA)}$	-0.008	-0.010	-0.021
	Reference	(41)BCJ	(41)BCJ	(42)VH
Calculated Frequency Differences of $\text{C}^{12}\text{H}_4$ ( $\text{cm}^{-1}$ ), [ $\nu_{\text{g}} - \nu_{\text{cond}}$ ]				
3143.7 <sub>1</sub> (A)	CH stretch	16.9	11.5	12.8
1574.2 <sub>2</sub> (E)	HCH bend	0.0	3.9	2.3
3154.1 <sub>3</sub> (F)	CH stretch	18.7	13.9	15.5
1357.4 <sub>4</sub> (F)	HCH bend	0.0	4.8	2.3
trans(F)		100.5	77.7	81.5
Rot(F)		63.5	72.3	106.0

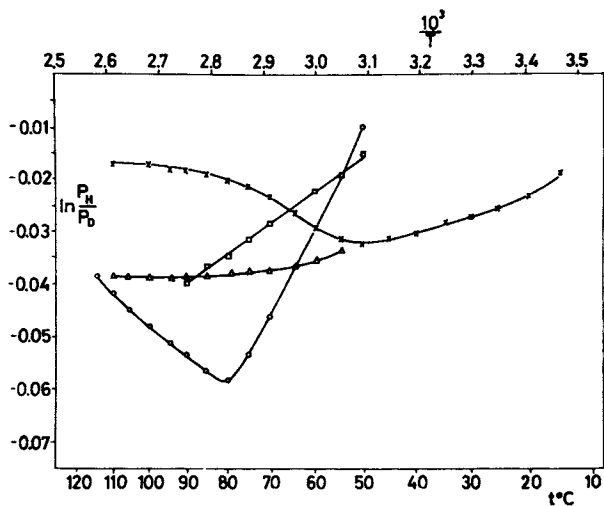


tions of Bigeleisen, Cragg and Jeevanandam (41) on methane. The authors successfully used a single isotope independent force field, Table 2, to rationalize the available VPIE data (from their own and another laboratory). A similar calculation on methane (vapor) = methane (adsorbed) effects was independently carried out by Van Hook (42). In either calculation the point of primary interest was the rotational contribution. The discussion is most conveniently made in terms of the approximate relation, Equation 5. The contribution of the internal modes is found primarily in the B term because these frequencies are large. The lattice contribution (A term) is from both translation and rotation. The effects may be sorted out, one from the other, by considering the behavior of molecules of the same total mass but different moments of inertia, e.g.,  $\text{CH}_3\text{D}/\text{C}^{13}\text{H}_4$ ,  $\text{CH}_2\text{D}_2/\text{C}^{14}\text{H}_4/\text{CH}_3\text{T}$ , etc. In other words data from a single isotopic pair, such as  $\text{CH}_4/\text{CH}_3\text{D}$ , only fixes the total lattice contribution, which in turn could be consistent with a large number of ratios of rotational to translational contributions. The experimental determination of A's (Table 3) for the different species unequivocally shows that rotation must contribute in the solid and liquid (41) and adsorbed (42) phases, and therefore must be hindered. It allows the ratio of librational to translational force constants to be fixed.

Table 3. Relative A Values for Isotopic Methanes

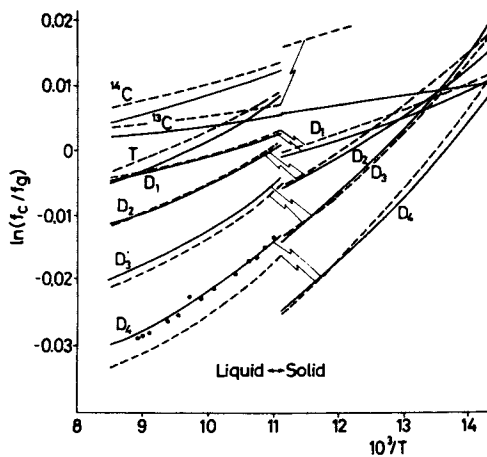
	Calculated for Free Rotor	Experimental		
		Solid (41) BCJ	Liquid (41) BCJ	Adsorbed (42) VH
$\text{CH}_3\text{D}/^{13}\text{CH}_4$	0.8	4.3	3.1	2.9
$\text{CH}_2\text{C}_2/^{14}\text{CH}_2$	0.9		2.3	
$\text{CH}_3\text{T}/^{14}\text{CH}_4$	0.7		2.2	

The detailed force fields used in the complete harmonic calculation are shown in Table 2 where the frequency shifts on phase change (which give rise to the isotope effects) are entered at the bottom. The agreement between the observed (spectroscopic) and calculated shifts is within the experimental precision with which the latter have been determined. The agreement between calculated and observed VPIEs is shown in Figure 5 where the calculated effects are plotted as the long dashes. The agreement is good in most details especially considering that one (isotope and temperature independent) approximate force field has been applied to calculate effects for seven different isotopic isomers. The agreement extends to the heats of fusion and vaporization as calculated from the slopes which are in reasonable agreement with the calorimetrically determined values; differences are on the order of a few calories per mole (5). Still, it is clear that the model is subject to refinement. It does not fit even all of the vapor pressure data simultaneously to within the experimental precision. This is particularly noticeable in the case of  $\text{C}^{13}$  substitution. The authors (41) suggest that a refined calculation in which due



Chemical Reviews

Figure 4. Vapor pressure isotope effects for organic acids deuterated at the carboxyl position (5, 40).  $\times$  =  $\text{CH}_3\text{COOH}$ ,  $\circ$  =  $\text{CH}_3\text{CH}_2\text{CH}_2\text{COOH}$ ,  $\square$  =  $(\text{CH}_3)_2\text{CHCOOH}$ ,  $\triangle$  =  $(\text{CH}_3)_2\text{CHCH}_2\text{COOH}$ .



Chemical Reviews

Figure 5. Vapor pressures of the isotopic methanes (41). — fit to data; ---- calculated from Table 2 (5).

account is taken of stretch-bend interactions and of the contribution of the anharmonicity in the external motions would improve the agreement. It is interesting, perhaps disturbing, to note that in the model the librational frequencies are found to be higher in the liquid than in the solid. We note here with respect to the intermolecular portion of the methane isotope effects that an alternative approach has been suggested by Steele (33) who advocates an application of the theory of corresponding states. A similar approach has been qualitatively discussed by Fang and Van Hook (27).

ii The deuterated ethylenes. The VPIEs of this series of compounds form an excellent example of the importance of coupling effects between the internal and external degrees of freedom. Extensive data are available (43,44) and detailed interpretive calculations have been performed by Stern, Van Hook and Wolfsberg (23) by Bigeleisen and Ishida (44). In these calculations the cell model was solved giving 18 harmonic oscillator frequencies for each isotopic isomer. Full account was taken of the contributions of the coupling terms in the F and G matrices, including coupling between the different external modes (44). The vapor pressure differences between the cis, trans, and gem didutero isomers is of particular interest. These are principally due to hindered rotation in the liquid (i.e., the principal moments of inertia are different for these three molecules), but in addition, superimposed on this effect, there is a ZPE effect due to coupling of the hindered rotation with certain internal vibrations. The specific internal frequencies which couple with the rotation are symmetry dependent. The same effect is manifested by the shifts in the internal frequencies themselves on condensation (i.e., in the B as well as the A term). In the absence of the effect the law of the geometric mean would be obeyed, and  $B(d-2)/B(d-1) = 2.00$ . The symmetry dependent perturbations may theoretically be shown to necessarily lower this value. The calculated and experimental values are compared below:

	$(B(d-2)/B(d-1))_{\text{theor}}$	$(B(d-2)/B(d-1))_{\text{expt}}$
trans	1.83	1.88
cis	1.89	1.93
gem	1.92	1.98

Agreement in the ordering trans-cis-gem is cited as particularly strong evidence in favor of the correctness of the approach. Note that the order is symmetry, not model, dependent. The magnitude of the shift does depend on the parameters inserted into the calculations. In the refined calculation (44) the authors indicate that anharmonicity in the rotational potential of the liquid must be taken into account to fit the data accurately. Later (45) the same force field was used to correlate the molecular volume iso-

tope effects for the deuterated ethylenes.

iii Other examples. Detailed model calculations have also been performed for a number of other systems. These include studies on the isotopic isomers of ethane (46), propylene (47), acetylene (48), methyl acetylene (49), alcohols (50), hydrogen sulfide (51), water (52,53), and numerous other compounds (5). Generally speaking, the theory has managed to successfully correlate the IEs of complete sets of isotopic isomers using isotope independent force fields consistent with the available spectroscopic data. It is to be emphasized, however, that the spectroscopic information is generally not complete enough to define a unique force field and it has proved necessary to appeal in part to the isotopic data itself in completing the parametrization. For example, in references (23), (46), and (49) data on one pair of isotopic isomers was used to fix the ratio of the internal to external contribution (within, of course, the bounds set by the spectroscopic information). The rest of the experimental data, including the information on the temperature coefficients, serve to test the theory. Similarly we have seen for the isotopic methanes that data on one pair of ratios comparing isomers of equivalent mass (i.e.,  $\text{CH}_4\text{-CH}_3\text{D}$  and  $\text{C}^{12}\text{H}_4\text{-C}^{13}\text{H}_4$ ) was used to fix the relative contributions of the translational and rotational modes. Again the approach is tested by the data for other sets of ratios ( $\text{CH}_4\text{-CH}_2\text{D}_2$  and  $\text{CH}_4\text{-CH}_3\text{T}$  and  $\text{C}^{12}\text{H}_4\text{-C}^{14}\text{H}_4$ , etc.). Within this context it seems fair to say that the Bigeleisen formulation of the VPIE, as parametrized through the BSVHW model, is reasonably successful in interpreting VPIEs of polyatomic molecules. It is particularly useful in correlating effects in series of isotopic isomers (i.e.  $\text{C}_2\text{H}_6\text{-C}_2\text{H}_5\text{D}$ ... $\text{C}_2\text{D}_6$ , or  $\text{HOH-HOD-DOD}$ ... $\text{TOT}$ , etc.). It is therefore reasonable to conclude that it is experimentally and theoretically established that the VPIE and related isotope effects can usefully serve as probes in investigations of intermolecular forces in condensed phases.

## E. Recent Work In Our Laboratory: Aqueous Solvent Effects

1. Introduction. Our recent work has been directed to studies on the equilibrium solvent isotope effects of aqueous solutions. The goal of this program is to contribute new and hopefully useful information to current discussions of the nature of the structure of water and of aqueous solutions. We have now accumulated a good deal of information about isotope effects on the properties of electrolyte solutions including vapor pressure, calorimetric, and freezing point studies. In addition, we have made and are continuing studies on nonelectrolyte aqueous solutions especially on systems expected to show hydrophobic bonding. However, the present report will be limited to a discussion of the work on electrolyte solutions. The experiments are designed to compare solvent isotope effects in the solutions with the isotope

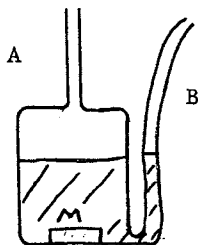
effects of the pure solvents. Calculations due to Van Hook (52) have demonstrated that the BSVHW model is applicable to the isotopic waters and to the mixed solvents. In the latter case the assumption of ideality of HOH-HOD-DOD mixtures has been shown to be consistent with the model calculations on the pure isotopic isomers. Since the calculated effects are dependent on the force constant inputs to the model, the rationale of our present experiments is that changes in the isotope effects with increasing salt concentration can be correlated with changes in the solvent model, in other words with structural considerations. The experiments are likely to prove useful even though it is recognized that present models for water itself may be naive, certainly this is so for the average molecule cell model. On the other hand, it is our hope that the trends which should become evident upon the gradual accumulation of data for a number of systems will help point the way to proper refinements in the model.

In any discussion of solution thermodynamics the choice of the standard is an important one and must be constantly kept in mind. Our standard state, the conventional one, is the hypothetical solution of unit aquamolal concentration, taken to the Henry's law infinite dilution limit. (A one aquamolal solution is one containing 1 mole of solute per 55.508 moles of solvent---for H<sub>2</sub>O this is 1000 grams. Our choice of the aquamolal concentration scale insures that all isotope effects are compared at equivalent mole fractions.) The properties of the solution are known in a thermodynamic sense when the standard and excess molal free energies,  $\bar{\mu}_1^0$  and  $\bar{\mu}_2^0$ ,  $\bar{\mu}_1^{\text{ex}}$  and  $\bar{\mu}_2^{\text{ex}}$  and their appropriate temperature and pressure derivatives,  $\bar{H}_1^0$  and  $\bar{H}_2^0$ ,  $\bar{H}_1^{\text{ex}}$  and  $\bar{H}_2^{\text{ex}}$ ,  $\bar{S}_1^0$  and  $\bar{S}_2^0$ ,  $\bar{S}_1^{\text{ex}}$  and  $\bar{S}_2^{\text{ex}}$ ,  $\bar{V}_1^0$  and  $\bar{V}_2^0$ ,  $\bar{V}_1^{\text{ex}}$  and  $\bar{V}_2^{\text{ex}}$ , and  $\bar{C}_p1^0$  and  $\bar{C}_p2^0$ ,  $\bar{C}_p1^{\text{ex}}$  and  $\bar{C}_p2^{\text{ex}}$ , etc., and the solvent isotope effects on all of these properties are known as functions of temperature and concentration. In the present paper we focus attention on the isotope effects. The standard state transfer properties of the solvent  $\Delta\mu_1^0 = \mu_1^0(\text{H}) - \mu_1^0(\text{D})$ ,  $\Delta H_1^0 = H_1^0(\text{H}) - H_1^0(\text{D})$ , etc. are defined in terms of the properties of the pure solvents because of our selection of the standard state. Thus  $\Delta\mu_1^0 = -RT \ln P_D^0/P_H^0$ , etc. These values are well established. The standard state transfer properties for the solute are not known. They correspond to the isotope effect per mole of salt on the process of transferring an infinitesimal quantity of salt from its standard state (crystal, 1 atm, the temperature of the experiment) to the pure solvents. The solution which is formed is at infinite dilution. The excess transfer isotope effects refer to the difference in the IE per mole of salt on the transfer between isotopic solutions (conc. M); and that for the standard state transfer (conc. 0). The experiments discussed in the present article are designed to measure the excess isotope effects on the partial molal free energies and enthalpies of the solvent and the electrolyte solute.

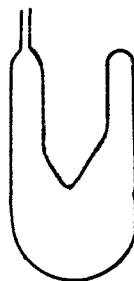
Three approaches will be described. In the first, precise measurements of the VPIEs over solutions at equal aquamolal con-

centrations give the isotope effects on the solvent activity (expressed in terms of the osmotic coefficients) and hence the solvent excess free energy of transfer as a function of temperature and concentration. The solute excess free energies can be obtained via a Gibbs-Duhem-Bjerrum integration if sufficient data are available to permit reliable extrapolation to infinite dilution. The excess partial molal enthalpies and entropies can then be obtained by differentiation with respect to the temperature. In the second series of experiments, we describe freezing point measurements on solutions of NaCl in HOH and DOD carried out as a function of concentration to low concentration. These measurements are designed to evaluate the assumptions earlier employed for the Gibbs-Duhem integrations of the VPIE data. In the third approach, we describe direct calorimetric measurements of isotope effects on the excess and standard heats of solution. The goal of this program is to ultimately employ the various IE data to test detailed model calculations of the solution structure. Unfortunately, we cannot yet report on this. Instead we will phenomenologically describe some of our experimental results and then discuss them in terms of current qualitative ideas of solution structure.

2. Experimental. The vapor pressure isotope effects were measured on either of two systems. Each was based on the same principle and we briefly describe the later and improved apparatus. The earlier equipment has been previously described (54). In our new apparatus two sets of two sample pyrex vessels are contained in an aluminum block mounted in a "Tronac" temperature bath which can be thermostated at any desired temperature between 0 and 80°C. The control is good to about  $\pm 3 \times 10^{-4}$ °C in the most favorable region (around room temperature), not that good at elevated temperatures. We estimate that the temperature differences within the block (and accordingly between the samples) as significantly better than  $\pm 1 \times 10^{-4}$ °. The vessels contain glass encased magnetic bars, M, and are stirred from below. The cells are of approximately 20ml volume and are constructed as diagrammed below.



Sample Cell



Degassing Cell

Connecting tube A is made from 6mm OD pyrex and after exiting through the bath lid is joined by means of a glass-metal seal,

through a valving manifold, to the differential capacitance transducer. The entire valving manifold, transducers, etc. is thermostated around 90°C to  $\pm 0.01$  degrees. Fill tube B is made from 3mm pyrex and is connected by means of a second valving manifold to our degassing facilities. The degassed solutions can be transferred under vacuum. All valves in both manifolds are high vacuum bellows type. The vacuum integrity of the system is such that the leak rate (system isolated from pumps) is less than 3 microns per normal working day. Proper degassing of the samples is critical. We employ numerous freeze-pump-thaw cycles and several sublimations in a specially designed pyrex vessel which is connected to the high vacuum manifold through a glass metal seal, a stainless steel bellows, and a high vacuum bellows valves. Both the degassing and the measurements are therefore carried out exclusively in pyrex. It is only momentarily (in the act of transfer) that the samples are exposed to metal.

In an experiment two of the sample vessels contain the two different isotopic solutions. The pressure difference between them is monitored to approximately  $\pm 0.03\%$  or  $\pm 0.001$  mm, whichever is larger. The other two vessels contain a solution of the normal isomer being compared against a standard solution, pure solvent, or vacuum. One run over the temperature range therefore furnishes us with a set of data on the total pressure and the isotopic pressure ratio as a function of temperature.

The calorimetric measurements were carried out either on an isoperibol solution calorimeter built by us following conventional (55) design and employing thermistor sensors and electrical heating and Peltier cooling, or (later) on a "Tronac 880" isothermal solution calorimeter.

The freezing point measurements employed a modification of an old technique (56) similar to the Beckman method. It was suggested from our experience in adiabatic calorimetry. In the experiments a thermistor forming one arm of a Wheatstone bridge is contained in a well stirred mixture of ice and water (or heavy ice and heavy water). Its resistance is monitored and defines a temperature (the scale is set in separate calibration experiments by resistance thermometry). After a stable base line is established (corresponding to  $\pm 2$  or  $3 \times 10^{-5}$  deg.) salt or concentrated solution is added, the temperature drops, and a new base line is established. A sample is taken and the temperature drop recorded. The chemical analysis for concentration is critical. We have developed a technique based on a suggestion of Richards (57) which is good to  $\pm 0.02\%$ . In this method, the chloride is precipitated with silver delivered from a weighing burette. The titration is followed potentiometrically and the end point deliberately exceeded by one or two drops. After curing and filtration, excess silver is determined by AA spectrophotometry. Our data in HOH as solvent is in quantitative agreement with Scatchard and Prentice (56) and defines the osmotic coefficients to  $\pm 0.0005$  unit in either solvent.

3. Discussion. First we consider the VPIE data. The changes in the isotopic pressure ratios are readily related to the isotope effects on the osmotic coefficients (58).

$$\Delta \ln R = \ln P_{\text{H}}^{\circ}/P_{\text{D}}^{\circ} - \ln P_{\text{H}}^{\text{m}}/P_{\text{D}}^{\text{m}} = \ln a_{\text{D}}/a_{\text{H}} = \frac{\nu_{\text{m}}}{55.51} (\phi_{\text{H}} - \phi_{\text{D}}) \quad (9)$$

In this equation  $m$  refers to the aquamolal concentration, the  $^{\circ}$ s to the pure solvent effects,  $a$  is the solvent activity and  $\phi$  the osmotic coefficient. Data for a number of different electrolyte solutions at one selected temperature are shown in Figure 6. The solutions all show a smaller VPIE than do the pure solvents. In the experiments  $\Delta \ln R$  is measured as a function of temperature and concentration, and we have phenomenologically fit the data (58,59) using the extended Debye-Hückel theory.

$$\phi = 1 - \frac{S}{a^3 I} [K(I) - 2 \ln K(I) - 1/K(I)] + b(T)I + c(T)I^2 + \dots$$

$$K = 1 + aI^{1/2} \quad (10)$$

In the equation  $I$  is the ionic strength,  $S$  is the DH limiting slope, and  $a$  is a parameter. We have presented arguments elsewhere (58) that the term in  $S/a^3 I$  is isotope independent. In that event

$$\Delta \phi = \frac{55.508}{\nu_{\text{m}}} \Delta \ln R = (B_{\text{H}} - B_{\text{D}}) I + (C_{\text{H}} - C_{\text{D}}) I^2 + \dots \quad (11)$$

The  $\Delta B(T)$ ,  $\Delta C(T)$ , etc. functions are derived from the data by least squares. They are tabulated for the different salts which have been investigated (58,59). The solvent excess free energies and excess enthalpies are readily obtained as functions of temperature and concentration. The data in Figure 6 shows the 25 degree isotherms. The effects are small for 1:1 electrolytes. Thus even at 10m, corresponding to a water/ion ratio of only 2.8, the VPIE of KF (for example) is depressed by only 4.4% (63 parts in 1420,  $\ln(P_{\text{H}}^{\circ}/P_{\text{D}}^{\circ}) = 0.142$  at 25°), that of NaBr by 14.6%, etc. The effects are about one order of magnitude larger for the  $\text{CaCl}_2$  solutions. This is just what is expected from the ionic strength relation given in the extended Debye-Hückel theory, equation (10). (Note  $\Delta \ln R = \Delta B \cdot I^2 + \dots$ ; for a 1:1 electrolyte  $I = m$ , but for a 2:1 salt  $I = 3M$  so  $\Delta \ln R \approx 9 \Delta B \cdot m^2$ ). The values of  $\Delta \ln R$  may be re-expressed in terms of the "structural temperature" concept originally introduced by Bernal and Fowler (60). This parameter is defined as that temperature increase for the pure solvent which gives a change in the VPIE equivalent to that observed upon addition of the salt. They are shown on the right hand side of the graphs. In this framework it is clear that the electrolytes are structure breakers. At high concentrations the effects are considerable, reaching 13° for 15m LiCl, and about 100° for 10m  $\text{CaCl}_2$ . It is interesting to note that the differences between NaCl, NaBr, NaI are not as marked as those between LiCl, NaCl, NaBr, NaI. This is



consistent with the trends observed in the values of the osmotic coefficients themselves (61).

The data on the temperature dependencies are important. At a given ionic strength, minima are indicated in all cases and there is a rough correlation between the temperature of the minimum and the structure breaking character. A Gibbs-Duhem extrapolation and integration followed by application of the Gibbs-Helmholtz equation allow the temperature coefficients to be compared with direct calorimetric measurements of the isotope effects on the excess solute enthalpies. The comparison at 25°C with the available data is shown in Table 4. A significantly large and negative excess heat capacity is indicated and this has been corroborated by Craft and Van Hook (62) with direct calorimetric measurements at 10, 25, 50 and 75°C. These results are reviewed in Figure 7. They are quantitatively consistent with the hypothesis that the aqueous structure is increasing at lower temperatures. This reassuring result is in accord with conventionally held ideas.

Table 4

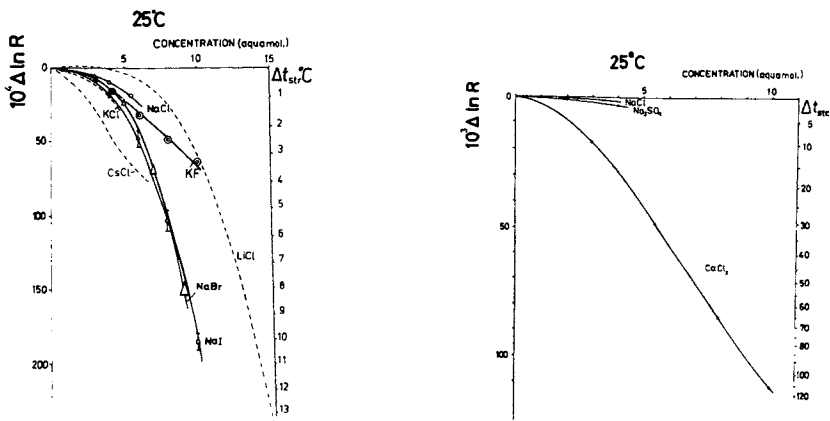
Comparison of Excess Enthalpies of Transfer  $\Delta H_{\text{salt}}^{\text{ex}}$ , in cal/mole. ( $\text{H}_2\text{O} \rightarrow \text{D}_2\text{O}$ ) at 25°C and Selected Concentrations

Salt	Concentration	Present Work	Calorimetric (and Ref.)
NaCl	2	34±6	39(67), 34(68), 32(62), 36(58)
KCl	2	15±24	39(67), 40(68), 33(62)
LiCl	4	-4±6	12(67), 47(68)
NaBr	2	37±7	36(67), 36(68)
NaI	2	43±7	31±6(68)
CaCl <sub>2</sub>	5.3	243±10	226±20(59)

In Figure 8, preliminary data of Craft and Van Hook (62) on freezing points on NaCl solutions in HOH and DOD are shown. This experimental program was instituted following a suggestion of H.S. Frank (63) that the earlier extrapolation procedures to infinite dilution (58,59) deserved critical examination. The fit to the data is given by

$$\frac{\Delta\theta}{\theta_H} = \frac{\Delta\lambda}{\lambda_H} + (K_1 + K_2m + \dots) \frac{2\lambda_D m^2}{\theta_D} = \frac{\Delta\theta}{\theta_H} = (0.0201 \pm 0.005) + (2.63 \pm 0.41 \times 10^{-2} \frac{m^2}{\theta}) - (1.08 \pm 0.20 \times 10^{-2}) \frac{m^3}{\theta} \quad (11)$$

The intercept corresponds to a predicted isotope effect on the heats of fusion of the pure solvent of  $71 \pm 2$  cal/m, in good agreement with the best calorimetric value  $65 \pm 4$  cal/m (64) taking  $T_f^{\circ}(\text{H}) - T_f^{\circ}(\text{D}) = -3.82$ . The present result is somewhat more precise than the old calorimetric data. The limiting slope is in good agreement with the value predicted from the extrapolated



Journal of Solution Chemistry

Figure 6. Vapor pressure isotope effects of some electrolyte solutions.  $\Delta \ln R = \ln R_o - \ln R_m$ ;  $R = P_H/P_D$  (59). a. 1:1 Electrolytes; b. 2:1 Electrolytes.

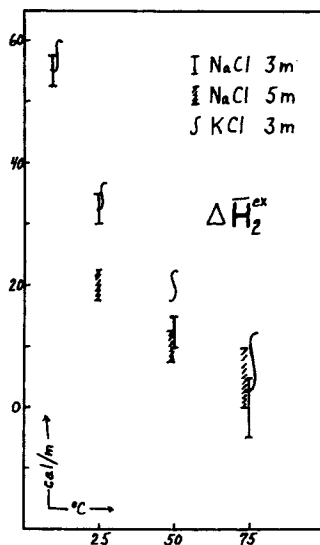


Figure 7. Solvent isotope effects on excess heats of solution at different temperatures

temperature coefficients of the VPiE studies (58) and substantiates the validity of our earlier Gibbs-Duhem extrapolation technique. The curvature in the isotopic freezing point vs. molality data is significantly more than was expected from the VPiE experiments (58,59). In these experiments the available data was fit over a broad temperature range to the simplest statistically significant form;

$$\phi_H - \phi_D = K_1^{VP}(T)m$$

The freezing point data require at least one higher-order term.

$$\phi_H - \phi_D = K_1^{fP}(T)m + K_2^{fP}(T)m^2$$

The observation above is essentially that when  $K_1^{VP}(T)$  is extrapolated to 0°C it is in reasonable agreement with  $K_1^{fP}(T)$ . Now since  $K_1^{VP}(T)$  is obtained from concentration data between 1.1 and 5m while  $K_1^{fP}$  is the limiting slope at much lower concentrations we must conclude that the temperature dependence of  $K_2^{fP}(T)$  is such that its contribution has essentially vanished by room temperature (or thereabouts). Thus we have qualitatively predicted the behavior of the isotope effect on the excess heat capacity in agreement with the observed behavior (Figure 7). This is equivalent to the statement that the longer range ordering terms in the extended theory are relatively more important at the lower temperatures and have larger temperature coefficients there.

5. Conclusions. We do not have any definite conclusions concerning the structure of water or aqueous solutions. These must wait for more complete interpretive calculations. However, it is clear that the effects which we have discussed above, although small, are self-consistent (that is from VPiE, to freezing point, to calorimetric data). Also they are sensitive to structural considerations. The general trends exhibited for all the salts are especially evident on examination of the  $\text{CaCl}_2$  data as shown in Figure 9. The effects for this salt are the largest of all those studied and for this reason the relative errors are smallest. The general trend to smaller excess isotope effects at either high concentrations or high temperatures is apparent and is consistent with the idea that aqueous structure is considerably decreased under these conditions. We conclude that systematic investigations of these aqueous solvent isotope effects will in the end make a significant contribution to the analysis and eventual understanding of the aqueous solvent structure problem. Quantitatively speaking this probably awaits further systematic accumulation of data. We are presently engaged in this enterprise and are currently examining a number of hydrophobic electrolyte and non-electrolyte molecules as solutes.

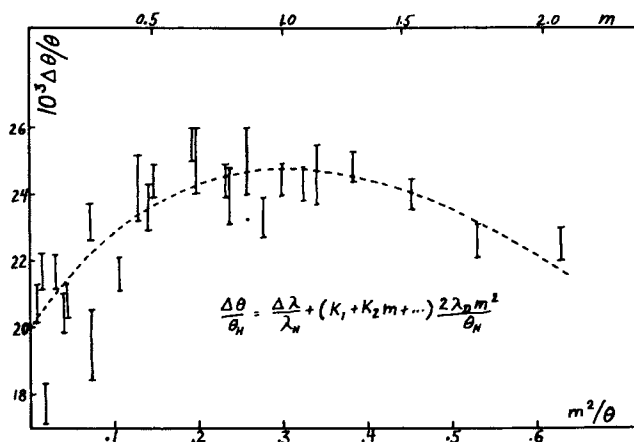
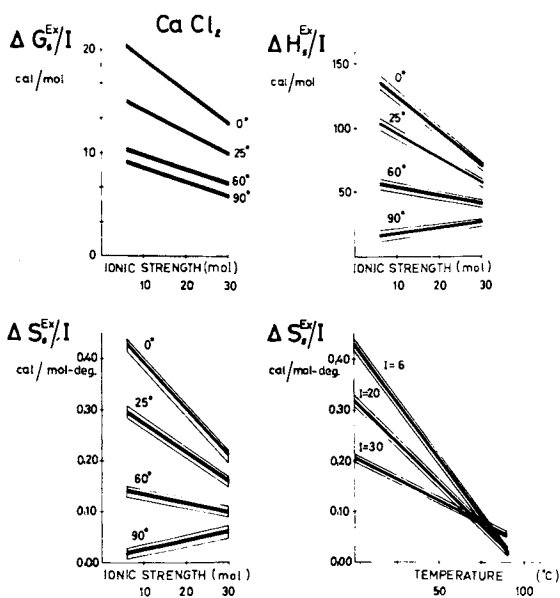


Figure 8. Solvent isotope effects on the freezing points of sodium chloride solutions



Journal of Solution Chemistry

Figure 9. Isotope effects on the solute excess thermodynamic properties of calcium chloride solutions (59).

### Acknowledgement

This research has been supported by the National Science Foundation under grant GP-25728 and by the National Institutes of Health, GMS-19991-02.

### Literature Cited.

1. Wolfsberg, M., This Symposium.
2. "Isotope Effects in Chemical Reactions", ACS Monograph 167, C. J. Collins and N. S. Bowman, Eds., Van Nostrand-Rheinhold, New York, 1971.
3. Lewis, G. N. and Randall, M., Revised by K. S. Pitzer and L. Brewer, "Thermodynamics", 2nd Ed., McGraw Hill, New York, 1961.
4. Bigeleisen, J., Lee, M. W. and Mandel, F., Ann. Rev. Phys. Chem., (1973), 24, 407 .
5. Jancso, G. and Van Hook, W. A., Chemical Reviews (in press).
6. Lindemann, F. A., Phil. Mag., (1919) 38, 17 ; Lindemann F. A., and Aston, F. W., Phil. Mag. (1919) 37, 523 .
7. Keesom, W. H. and van Dijk, H., Proc. Acad. Amsterdam, (1931) 34, 42.
8. Scott, R. B., Brickwedde, F. C., Urey, H. C. and Wahl, M. H., J. Chem. Phys., (1934) 2, 454 .
9. Topley, B. and Eyring, H., J. Chem. Phys., (1934) 2, 217; Bailey, C. R. and Topley, B., J. Chem. Soc., (1936), 921.
10. Herzfeld, K. F. and Teller, E., Phys. Rev., (1938) 54, 912 .
11. Bigeleisen, J., This Symposium.
12. Bigeleisen, J., J. Chem. Phys., (1961) 34, 1485 .
13. Bigeleisen, J. and Mayer, M. G., J. Chem. Phys., (1947) 15, 261 .
14. Stern, M. J., Spindel, W. and Monse, E. U., J. Chem. Phys., (1968) 48, 2908 ; Monse, E. U., Spindel, W. and Stern, M. J., Advances in Chemistry, (1969) 89, 148.
15. Van Hook, W. A., J. Chem. Phys., (1967) 46, 1907 .
16. Kiss, I., Jakli, G. and Illy, H., Acta Chim. Hung., (1972) 71, 59 .
17. Kiss, I., Jakli, G., Jancso, G. and Illy, H., Acta Chim. Hung., (1967) 51, 65 .
18. Gellai, B. and Jancso, G., Ber. Bunsenges. phys. Chem., (1971) 75, 156 .
19. Bigeleisen, J., J. Chem. Phys., (1963) 39, 769 .
20. Wolfsberg, M., J. Chem. Phys., (1969) 50, 1484 ; Advances in Chemistry, (1969) 89, 185 .
21. Hulston, J. R., J. Chem. Phys., (1969) 50, 1483 .
22. Nash, C. P., This Symposium.
23. Stern, M. J., Van Hook, W. A., and Wolfsberg, M., J. Chem. Phys., (1963) 39, 3179 .

24. Bigeleisen, J. and Ishida, T., *J. Chem. Phys.*, (1968) 48, 1311 ; Ishida, T., Spindel, W. and Bigeleisen, J., *Advances in Chemistry*, (1969) 89, 192; *J. Chem. Phys.*, (1971) 55, 5021 ; *Proc. Nat. Acad. Sci. U.S.*, (1970) 67, 113
25. Nemeth, G., Gellai, B. and Jancso, G., *J. Chem. Phys.*, (1971) 54, 1701 ; Report K.F.K.I.-15, Budapest, 1970.
26. Gordon, R. G., *J. Chem. Phys.*, (1966) 44, 576 .
27. Fang, A. and Van Hook, W. A., *J. Chem. Phys.*, (1974) 60, 3513.
28. Thomaes, G. and van Steenwinkel, R., *Mol. Phys.*, (1962) 5, 307 ; Gainar, I., Strein, K. and Schramm, B., *Ber. Buns. Ges.*, (1972) 76, 1242 .
29. Bell, R. P., *Trans. Far. Soc.*, (1942) 38, 422 ; Von Frivold, O. E., Hassel, D. and Hetland, E., *Z. Physik.*, (1939) 40, 29 .
30. Bartell, L. S., Kuchitsu, K. and DeNeui, R. T., *J. Chem. Phys.*, (1966) 44, 457 .
31. Grigor, A. F. and Steele, W. A., *J. Chem. Phys.*, (1968) 48, 1032 ; Fuks, S., Legros, J. C. and Bellemans, A. *Physica*, (1965) 31, 606.
32. de Boer, J. and Lunbeck, R. J., *Physica*, (1948) 14, 520 and 510.
33. Grigor, A. F. and Steele, W. A., *J. Chem. Phys.*, (1968) 48, 1038; Bigeleisen, J. and Wolfsberg, M., *J. Chem. Phys.*, (1969) 50, 561; Steele, W. A., *J. Chem. Phys.*, (1969) 59, 562.
34. Phillips, J. T., Linderstrom-Lang, C. U. and Bigeleisen, J., *J. Chem. Phys.*, (1972) 56, 5053; Lee, M. W., Fuks, S. and Bigeleisen, J., *J. Chem. Phys.*, (1970) 53, 4066; Lee, M. W., Eshelman, D. M. and Bigeleisen, J., *J. Chem. Phys.*, (1972) 56, 4585.
35. Mandel, F., *J. Chem. Phys.*, (1972) 57, 3929.
36. Bigeleisen, J. and Ribnikar, S. V., *J. Chem. Phys.*, (1961) 35, 1297.
37. Friedmann, H. "Advances in Chemical Physics", Prigogine, I., Ed., Interscience Publishers, New York (London) 1962, p. 225.
38. Johns, T. F., "Proceedings of the International Symposium on Isotope Separation", Kistemaker, J., Bigeleisen, J. and Nier, A. O. C., Eds., North-Holland Publishing Company, Amsterdam, 1958, p. 74; Ancona, E., Boato, G. and Casanova, G., *Nuovo Cimento*, (1963) 24, 111.
39. Friedman, H. and Kimel, S., *J. Chem. Phys.*, (1965) 42, 3327.
40. Rabinovich, I. B., Sokolov, N. N. and Artyukhin, P. I., *Dokl. Akad. Nauk SSSR*, (1955) 105, 762.
41. Bigeleisen, J., Cragg, C. B. and Jeevanandam, M., *J. Chem. Phys.*, (1967) 47, 4335.
42. Van Hook, W. A., *J. Phys. Chem.*, (1967) 71, 3270.
43. Bigeleisen, J., Ribnikar, S. V. and Van Hook, W. A., *J. Amer. Chem. Soc.*, (1961) 83, 2956; *J. Chem. Phys.*, (1963) 38, 489; Bigeleisen, J., Stern, M. J. and Van Hook, W. A., *J. Chem. Phys.*, (1963) 38, 497.

44. Ishida, T. and Bigeleisen, J., *J. Chem. Phys.*, (1968) 49, 5498.
45. Menes, F., Dorfmueller, T. and Bigeleisen, J., *J. Chem. Phys.*, (1970) 53, 2869.
46. Van Hook, W. A., *J. Chem. Phys.*, (1966) 44, 234.
47. McDaniel, R. L. and Van Hook, W. A., *J. Chem. Phys.*, (1970) 52, 4027.
48. Phillips, J. T. and Van Hook, W. A., *J. Chem. Phys.*, (1970) 52, 495.
49. Van Hook, W. A., *J. Chem. Phys.*, (1967) 46, 1907.
50. Borowitz, J. L. and Klein, F. S., *J. Phys. Chem.*, (1971) 75, 1815; Kiss, I., Jakli, G., Jancso, G. and Illy, H., *J. Chem. Phys.*, (1967) 47, 4851; Linderstrom-Lang, C. U. and Vaslow, F., *J. Phys. Chem.*, (1968) 72, 2645; Kiss, I., Jakli, G., Jancso, G. and Illy, H., *Acta Chim. Hung.*, (1968) 56, 271.
51. Gellai, B. and Jancso, G., *Ber. Bunsenges. phys. Chem.*, (1971) 75, 156.
52. Van Hook, W. A., *J. Phys. Chem.*, (1968) 72, 1234; (1972) 76, 3040.
53. Majoube, M., *J. chim. Phys.*, (1971) 68, 625; Wolff, H., "Phys. Ice, Proc. Int. Symp. 3rd.", 1968, p. 305.
54. Van Hook, W. A., *Isotopenpraxis*, (1968) 4, 161.
55. Arnett, E. M. and McKelvey, D. R., "Solute Solvent Interactions", Coetzee, J. F. and Ritchie, C. D., Eds., Interscience, New York, 1969.
56. Scatchard, G. and Prentice, S. S., *J. Amer. Chem. Soc.*, (1933) 55, 4355.
57. Richards, T. W., as quoted by J. R. Partington, "Textbook of Inorganic Chemistry", Macmillan, London, 1950, p. 91.
58. Pupezin, J., Jakli, G., Jancso, G. and Van Hook, W. A., *J. Phys. Chem.*, (1972) 76, 743.
59. Jakli, G. Chan. T. C. and Van Hook, W. A., *J. Soln. Chem.*, (in press).
60. Bernal, J. D. and Fowler, R., *J. Chem. Phys.*, (1933) 1, 515.
61. Robinson, R. A. and Stokes, R. H., "Electrolyte Solutions", 2nd Ed., Butterworths, 1962.
62. Craft, Q. C. and Van Hook, W. A., (in preparation).
63. Frank, H. S., Personal Communication.
64. Rossini, F. D., Knowlton, J. W. and Johnston, H. L., *J. Res. Natl. Bur. Stand.*, (1940) 24, 369.
65. Wood, R. H., Rooney, R. A. and Braddock, J. N., *J. Phys. Chem.*, (1969) 73, 1673.
66. Desnoyers, J. E., Francescon, R., Picker, P. and Jolicoeur, C., *Can. J. Chem.*, (1971) 49, 3460.
67. Wu, Y. C. and Friedman, H. L., *J. Phys. Chem.*, (1966) 70, 166.
68. Greyson, J. and Snell, H., *J. Phys. Chem.*, (1969) 73, 4423.

# The Electrochemical Determination of Equilibrium Constants for Isotope-Exchange Reactions

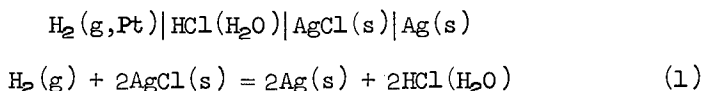
PETER A. ROCK

Department of Chemistry, University of California, Davis, Calif. 95616

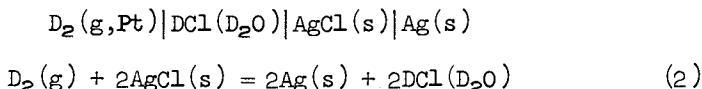
## I. Introduction

The basic idea involved in the use of electrochemical cells to study the thermodynamics of isotope-exchange reactions is to set up the appropriate electrochemical cells in duplicate, one with one isotope of the particular element of interest, and the other with the other isotope. The thermodynamic quantities for the isotope-exchange reaction are then obtained as a difference in the measured values for the two separate isotope cells. The difference method, which was first used by Abel, Bratu, and Redlich (1) (1935) and by Korman and La Mer (2) (1936) in their pioneering studies of hydrogen isotope effects, is outlined below for a particular hydrogen-isotope-exchange reaction:

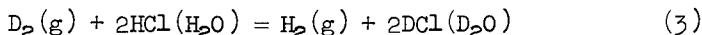
### hydrogen cell



### deuterium cell



The isotope-exchange reaction is

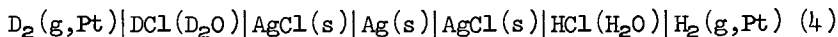


and the  $\mathcal{E}^\circ$  value for reaction (3) is given by  $\mathcal{E}_3^\circ = \mathcal{E}_2^\circ - \mathcal{E}_1^\circ$ . At 298.15 K the reported value (3,4,5) of  $\mathcal{E}_3^\circ$  is  $-4.34$  mV (mole-fraction composition scale), which yields an equilibrium constant of  $K_3 = 0.713$  (298.15 K).

The difference procedure outlined above is not useful, as such, for elements other than hydrogen, because the difference between the two  $\mathcal{E}^\circ$  values is then usually smaller than the sum of the absolute errors in the  $\mathcal{E}^\circ$  values for the two isotope cells. However, if we use electrochemical double cells without liquid



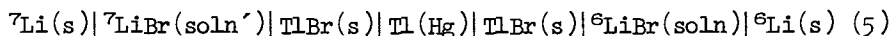
junction in which the two isotope cells are connected in series opposition to one another, then we can measure directly the  $\mathcal{E}^{\circ}$  value for the isotope-exchange reaction. For the reaction considered above, an appropriate double cell is



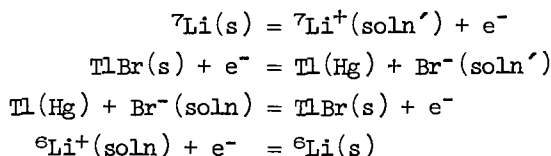
the overall cell reaction for which is reaction (3) above.

#### II.a. Experimental Results for Lithium-Isotope-Exchange Reactions.

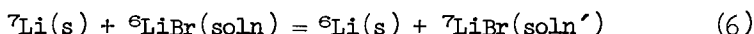
The cell diagram for a double-cell used for the study of lithium-isotope-exchange reactions is as follows



This double cell (Figure 1) involves four electrodes at which the following electrode reactions are postulated to occur consecutively (left-to-right) in the cell



The overall cell reaction is given by the sum of these four reactions, namely



Notice that  $Tl(Hg)$  and  $TlBr(s)$  do not appear in the net cell reaction because the  $Tl(Hg) | TlBr(s) | Br^-$  electrode functions as the cathode of one side and the anode of the other side of the double cell. The solvent need not be the same in the two halves of the double cell (see cell (4)), although in most cases of interest the solvent is the same (6).

Application to the Nernst equation to reaction (6) yields

$$\mathcal{E}^{\circ} = \mathcal{E} + \frac{RT}{\mathcal{F}} \ln \frac{a_{{}^7LiBr(soln')}}{a_{{}^6LiBr(soln)}} \quad (7)$$

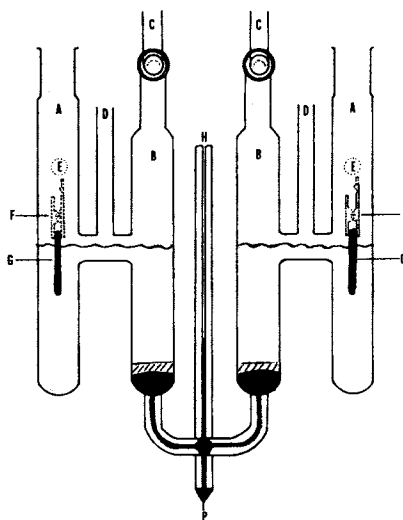
The application of equation (7) to a specific solvent case involves assumptions as to the nature of the dissolved  $LiBr$ . There are two limiting cases in the thermodynamic analysis:

(1) if the dissolved  $LiBr$  can be treated as a non-electrolyte, then

$$a_{LiBr} = m_{LiBr} \gamma_{LiBr} \quad (8)$$

for each isotopic species; whereas

(2) if the dissolved  $LiBr$  can be treated as a strong (i.e., com-



Journal of Chemical Physics

Figure 1. Schematic of the double cell.  ${}^7\text{Li}(s)$ - ${}^7\text{LiBr}(\text{soln})$ | $\text{TlBr}(s)$ | $\text{Tl}(\text{Hg})$ | $\text{TlBr}(s)$ | ${}^6\text{LiBr}(\text{soln})$ - ${}^6\text{Li}(s)$ . A,A are the outer cell compartments. The top is a standard taper 14/20 joint. B,B are the inner cell compartments containing  $\text{Tl}(\text{Hg})$ - $\text{TlBr}$ . C,C are droppers for sprinkling  $\text{TlBr}$  over  $\text{Tl}(\text{Hg})$  in vacuum. D,D are the tubes connecting the cell to the  ${}^7\text{LiBr}$  and  ${}^6\text{LiBr}$  solutions in PC. E,E are connections to the vacuum line. F,F are the alligator clamps, and G,G are the  ${}^7\text{Li}$  and  ${}^6\text{Li}$  metal electrodes. H is the capillary connecting the cell to the  $\text{Tl}(\text{Hg})$  reservoir. P is the platinum wire central electrode for measuring side potentials. The scale is 1:2.2 (8).

pletely dissociated) electrolyte then

$$a_{\text{LiCl}} = a_{\text{Li}^+} \times a_{\text{Br}^-} = m_{\text{Li}^+} \times m_{\text{Br}^-} \times \gamma_{\pm}^2(\text{LiBr}) \quad (9)$$

for each isotopic species. In equation (9)  $\gamma_{\pm}$  is the mean ionic activity coefficient. The isotope effect on  $\gamma_{\pm}$  the activity coefficient is negligible (i.e. at the same concentration  $\gamma_7 = \gamma_6$ ) for all isotopes except those of hydrogen where the effect is about (3) 2% in  $\log \gamma_{\pm}$  at 0.05 molal HCl(aq). The decision as to how to treat the dissolved electrolyte is based in part on independent studies of the LiBr solutions. For example, emf measurements on the separate side cells can be carried out in order to obtain the necessary activity coefficient data. In the case of weak electrolyte solutes, equation (7) becomes

$$\mathcal{E}^{\circ} = \mathcal{E} + \frac{RT}{\mathcal{F}} \ln \left\{ \frac{\gamma_6 m_7}{\gamma_6 m_6} \right\} \quad (10)$$

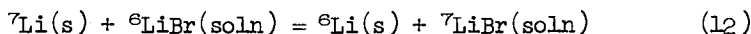
whereas for the strong electrolyte case we have

$$\mathcal{E}^{\circ} = \mathcal{E} + \frac{2RT}{\mathcal{F}} \ln \left\{ \frac{\gamma_{\pm 7} m_7}{\gamma_{\pm 6} m_6} \right\} \quad (11)$$

There are two critical tests of the cell data that must be carried out in order to establish the validity of the postulated cell reaction. The first of these is the voltage-current reversibility check which is based on the fact that around an equilibrium point the restoring force that acts to bring the system back into equilibrium is directly proportional to the displacement for small displacements. The reversibility check for an electrochemical cell consists of a plot of measured cell emf vs meter-scale deflection on the null-detector. If the resulting plot is linear and does not show any hysteresis loop, then that particular cell can be safely regarded as behaving reversibly. The second critical test of the cell reaction is provided by the constancy of the  $\mathcal{E}^{\circ}$  values calculated from several cells with different concentrations of the isotopic solute species. The variations in the concentration ratios should be such as to produce both positive and negative values of the measured cell voltages. The results (7,8) of measurements on double cells of type (5) for the solvents diglyme ( $\epsilon = 7.2$ ) and propylene carbonate  $\text{CH}_3\text{CHCH}_2$  ( $\epsilon = 65.5$ ) are given in Table I.



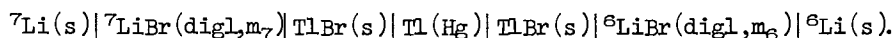
In both cases the cell reaction is



however, indiglyme LiBr is a weak electrolyte, whereas, in pro-

TABLE I.

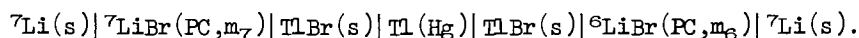
Results of measurements on the cell:



(T = 296.6 ± 1.0 K)			
$m_7$ (mol·kg <sup>-1</sup> )	$m_6$ (mol·kg <sup>-1</sup> )	$\mathcal{E}_{\text{obs}}$ (mV)	$\mathcal{E}^\circ$ <sup>a</sup> (mV)
0.03779	0.03099	-4.15 ± 0.20	0.92
0.03415	0.05923	14.82 ± 0.20	0.74
0.03524	0.03524	0.97 ± 0.10	0.97
0.05874	0.06037	1.55 ± 0.20	0.85
( $\mathcal{E}_{\text{avg}}^\circ = 0.87 \pm 0.18$ mV)			

<sup>a</sup>Calculated using Equation (10) with  $\gamma_7 = \gamma_6$ .

Results of measurements on the cell:



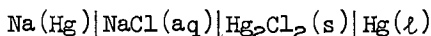
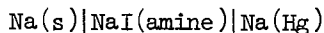
(T = 296.6 ± 1.0 K)			
$m_7$ (mol·kg <sup>-1</sup> )	$m_6$ (mol·kg <sup>-1</sup> )	$\mathcal{E}_{\text{obs}}$ (mV)	$\mathcal{E}^\circ$ <sup>a</sup> (mV)
0.05075	0.05080	0.86 ± 0.06	0.82
0.03372	0.04532	13.74 ± 0.05	0.66
0.04381	0.03775	-5.62 ± 0.09	0.95
0.04720	0.03903	-7.83 ± 0.04	0.53
0.03180	0.03374	3.49 ± 0.08	0.84
( $\mathcal{E}_{\text{avg}}^\circ = 0.76 \pm 0.13$ mV)			

<sup>a</sup>Calculated using Equation (11) with  $\ln \gamma_{\pm} = -1.6993 m^{\frac{1}{2}} / (1+m^{\frac{1}{2}}) - 0.451 m$ .

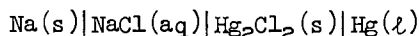
ylene carbonate LiBr can be treated as completely dissociated. The emf results confirm the postulated cell reaction in both cases.

The investigation of lithium-isotope-exchange reactions involving the isotopic metals and the isotopic ions in aqueous solution presents special problems because of the reaction of lithium metal with water. The clue to the resolution of this

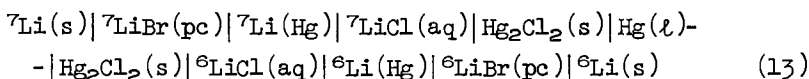
problem was provided by the method used by G. N. Lewis to determine the standard potentials of the alkali metals in aqueous media. Lewis and coworkers measured separately the voltages of the cells



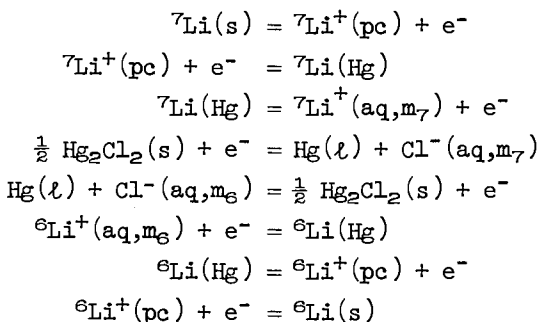
where the sodium amalgam is the same in both cells. The sum of the measured voltages for the two cells yields the voltage of the hypothetical cell



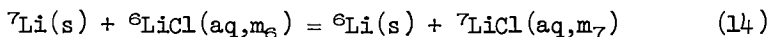
The cell that we have used (9) to study exchange between the isotopic lithium metals and the aqueous lithium ions is a quadruple cell, an eight-electrode cell. The cell diagram of the quadruple cell (Figure 2) is as follows (pc = propylene carbonate)



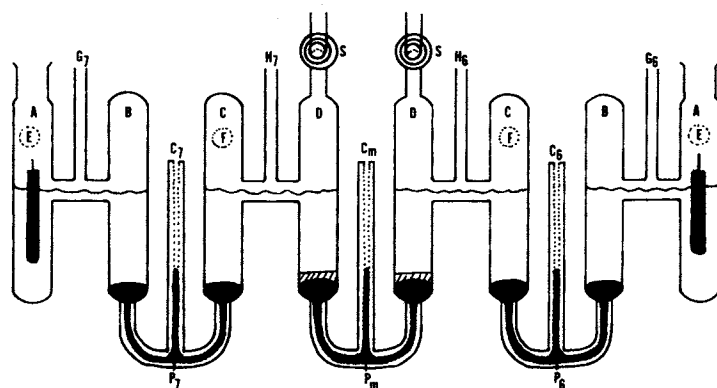
the postulated electrode reactions of the quadruple cell are



The sum of the above eight electrode reactions yields



Note that both lithium amalgams as well as the central  $\text{Hg}(\ell)$  and  $\text{Hg}_2\text{Cl}_2(\text{s})$  phases do not appear in the net cell reaction. Consequently we do not need to know the concentrations of  ${}^7\text{Li}$  and  ${}^6\text{Li}$  in the amalgams. The key to the success of the above quadruple cell is the combination of a high overvoltage for hydrogen evolution on a mercury surface (ca. 1V), together with a very low concentration of lithium in the amalgams ( $X_{\text{Li}} \sim 10^{-5}$ ). The results of emf measurements on the quadruple cell show that reaction (14) is indeed the cell reaction of the quadruple cell.

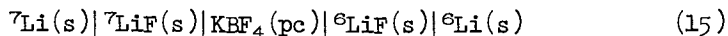


Journal of Chemical Physics

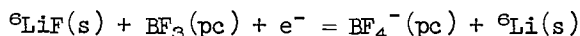
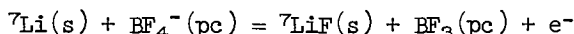
Figure 2. Schematic of the quadruple cell.  ${}^7\text{Li}(s)|{}^7\text{LiBr}(pc)|{}^7\text{Li}(\text{Hg})|{}^7\text{LiCl}(\text{aq})|\text{Hg}_2\text{Cl}_2(s)|\text{Hg}(l)|\text{Hg}_2\text{Cl}_2(s)|{}^6\text{LiCl}(\text{aq})|{}^6\text{Li}(\text{Hg})|{}^6\text{LiBr}(pc)|{}^6\text{Li}(s)$ . A,A are the outer cell compartments containing isotopic lithium electrodes in isotopic lithium bromides in PC; C<sub>7</sub>, C<sub>6</sub>, and C<sub>m</sub> are the capillary tubes connected to  ${}^7\text{Li}(\text{Hg})$ ,  ${}^6\text{Li}(\text{Hg})$ , and  $\text{Hg}(l)$  reservoirs, respectively; G<sub>7</sub>, G<sub>6</sub>, H<sub>7</sub> and H<sub>6</sub> are the delivery tubes connected to the  ${}^7\text{LiBr}(\text{PC})$ ,  ${}^6\text{LiBr}(\text{PC})$ ,  ${}^7\text{LiCl}(\text{aq})$ , and  ${}^6\text{LiCl}(\text{aq})$  solutions, respectively. E,E and F,F are connections to the vacuum line manifold; S,S are droppers for preparing the calomel electrodes. P<sub>7</sub>, P<sub>6</sub>, and P<sub>m</sub> are connection points for electrode leads that permit voltage readings of various sections of the complete cell (9).

The measured value  $\mathcal{E}^\circ$  is  $1.16 \pm 0.30$  mV, which corresponds to an equilibrium constant of  $1.046 \pm 0.013$  (296.6 K).

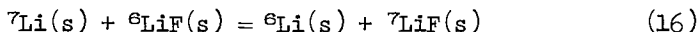
Lithium-isotope-exchange reactions involving the metals and pure solid salt phases can also be studied in electrochemical cells. Such reactions are particularly simple to analyze electrochemically because  $\mathcal{E} = \mathcal{E}^\circ$ . An example is the cell (10)



Lithium fluoride is insoluble in propylene carbonate, and the  $\text{KBF}_4$  acts as a source and sink for fluoride ions while keeping the fluoride ion concentration low and thereby preventing the attack by fluoride ion on the solvent. (Tetraalkylammonium fluorides decompose propylene carbonate, presumably by promoting ring opening followed by loss of carbon dioxide.) The electrode reactions for cell (15) are postulated to be



and the net cell reaction is



Measurements (10) on cell (15) have established reaction (16) as the cell reaction; the measured value of  $\mathcal{E}^\circ$  is  $2.49 \pm 0.15$  mV. Reaction (16) exhibits the largest lithium isotope effect that has been found experimentally. The measured equilibrium constants for the four different types of lithium-isotope-exchange reactions are summarized in Table II.

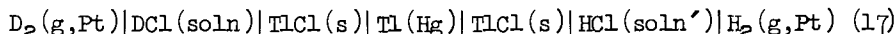
TABLE II. Lithium-Isotope-Exchange Reactions

<u>Reaction</u>	K (296.6 K) <u>(<math>\mathcal{E}^\circ</math> in mV)</u>
${}^7\text{Li(s)} + {}^6\text{LiBr}(\text{digl}) = {}^6\text{Li(s)} + {}^7\text{LiBr}(\text{digl})$	$1.035 \pm 0.007$ (8) ( $0.87 \pm 0.18$ )
${}^7\text{Li(s)} + {}^6\text{Li}^+\text{Br}^-(\text{pc}) = {}^6\text{Li(s)} + {}^7\text{Li}^+\text{Br}^-(\text{pc})$	$1.030 \pm 0.005$ (8) ( $0.76 \pm 0.13$ )
${}^7\text{Li(s)} + {}^6\text{Li}^+\text{Cl}^-(\text{aq}) = {}^6\text{Li(s)} + {}^7\text{Li}^+\text{Cl}^-(\text{aq})$	$1.046 \pm 0.013$ (9) ( $1.16 \pm 0.30$ )
${}^7\text{Li(s)} + {}^6\text{LiF(s)} = {}^6\text{Li(s)} + {}^7\text{LiF(s)}$	$1.10 \pm 0.01$ (10) ( $2.49 \pm 0.15$ )

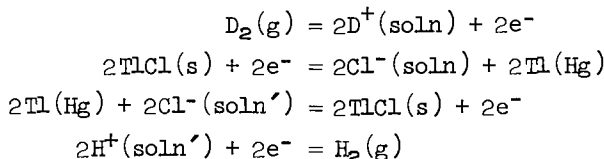
#### II.b. Experimental Results for Hydrogen-Isotope-Exchange Reactions.

Equilibrium constants for hydrogen-isotope-exchange reactions can be obtained either by the difference method or by the double-cell method. The difference method for hydrogen-isotope-exchange

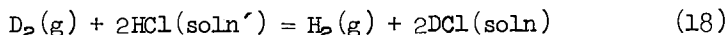
reactions is outlined in the introduction. The general cell diagram of a double cell that has been used (11) to study hydrogen isotope-exchange reaction is



The postulated electrode reactions for the double cell are as follows



The net cell reaction is given by the sum of the above four electrode reactions



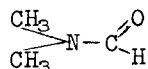
If the HCl(soln) can be treated as a strong electrolyte, then

$$\mathcal{E}^\circ = \mathcal{E} + \left(\frac{RT}{2\mathcal{F}}\right) \ln \left(\frac{P_{H_2}}{P_{D_2}}\right) + \left(\frac{2RT}{\mathcal{F}}\right) \ln \left\{ \frac{(mV_{\pm})_{DCl}}{(mV_{\pm})_{HCl}} \right\} \quad (19)$$

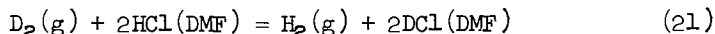
whereas, if HCl(soln) is a weak electrolyte, then

$$\mathcal{E}^\circ = \mathcal{E} + \left(\frac{RT}{2\mathcal{F}}\right) \ln \left(\frac{P_{H_2}}{P_{D_2}}\right) + \left(\frac{RT}{\mathcal{F}}\right) \ln \left\{ \frac{(mV)_{DCl}}{(mV)_{HCl}} \right\} \quad (20)$$

The dual requirements of non-exchangeable solvent hydrogen atoms and electrode reversibility severely limits the number of cases in which the solvent can be made the same on both halves of the double cell. One such case is provided by the solvent N,N-dimethylformamide (DMF)



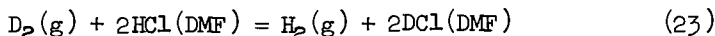
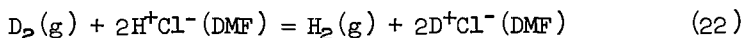
The hydrogen atoms of DMF ( $\epsilon = 37$ ) do not exchange at a measurable rate with DCl under anhydrous conditions (11), and both the hydrogen electrode and the Tl(Hg)|TlCl(s)|Cl<sup>-</sup>(DMF) electrodes are reversible in DMF. The overall cell reaction is



In this case it proved possible to obtain  $\mathcal{E}^\circ$  values for reaction (21) involving both the undissociated HCl(DMF) and the completely dissociated HCl(DMF) standard states. Even though HCl(DMF) is a weak electrolyte ( $K_a = 2.7 \times 10^{-4}$  at 25°C), Petrov and Umanskii (12) were able to establish a strong electrolyte standard state by



going to very low  $\text{HCl(DMF)}$  ( $< 10^{-5}$  molal) concentrations; consequently,  $\gamma_{\pm}$  values for  $\text{HCl(DMF)}$  were available. The calculated  $\mathcal{E}^{\circ}$  values based on strong and weak electrolyte standard states are  $7.64 \pm 0.38$  and  $8.12 \pm 0.54$  mV, respectively (296.6 K). The corresponding equilibrium constants for the reactions



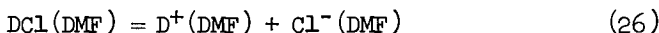
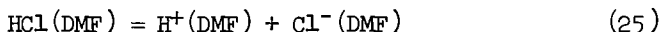
are  $K_{\text{ion}} = 1.82 \pm 0.05$  and  $K_{\text{neut}} = 1.89 \pm 0.08$ . These two K values yield a value of

$$K = (K_{\text{neut}}/K_{\text{ion}})^{\frac{1}{2}} = 1.02 \pm 0.04 \quad (296.6 \text{ K})$$

for the reaction



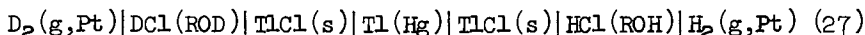
The value of K for reaction (24) was also determined independently by a conductometric method (13) in which K was determined as the ratio of K values for the reactions



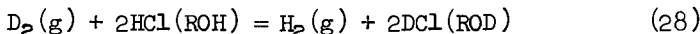
The value of K obtained was (25°C)

$$K = \frac{(2.68 \pm 0.03) \times 10^{-4}}{(2.64 \pm 0.02) \times 10^{-4}} = 1.02 \pm 0.04.$$

An example of a double-cell in which the solvents are not the same is the cell (14,18) ( $\text{ROH} \equiv \text{CH}_3(\text{CH}_2)_4\text{CH}_2\text{OH}$  and  $\text{ROD} \equiv \text{CH}_3(\text{CH}_2)_4\text{CH}_2\text{OD}$ )



for which the net cell reaction is



The results of measurements on cell (27) yield an  $\mathcal{E}^{\circ}$  value for reaction (28), calculated on the basis of strong electrolyte standard states for  $\text{HCl(ROH)}$  and  $\text{DCl(ROD)}$ , of  $3.53 \pm 0.95$  mV at 296.0 K; the value of the equilibrium constant is  $1.32 \pm 0.10$ .

The equilibrium constants for several hydrogen-isotope-exchange reactions involving elemental hydrogen are given in Table III.

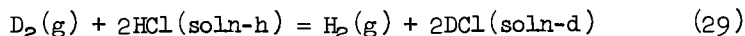
TABLE III. Hydrogen-Isotope-Exchange Reactions

Reaction	K (296.6 K) ( $\mathcal{E}^\circ$ in mV)
$D_2(g) + 2HCl(g) = H_2(g) + 2DCl(g)$	1.99* (8.87)*
$D_2(g) + 2HCl(DMF) = H_2(g) + 2DCl(DMF)$	$1.89 \pm 0.08$ ( $8.12 \pm 0.54$ )
$D_2(g) + 2H^+Cl^-(DMF) = H_2(g) + 2D^+Cl^-(DMF)$	$1.82 \pm 0.05$ ( $7.64 \pm 0.38$ )
$D_2(g) + 2H^+Cl^-(ROH) = H_2(g) + 2D^+Cl^-(ROD)$	$1.32 \pm 0.10$ ( $3.53 \pm 0.95$ )
$D_2(g) + 2H^+Cl^-(H_2O) = H_2(g) + 2D^+Cl^-(D_2O)$	$0.713^{\dagger}$ (-4.34 mV)

\*Calculated value, see H. C. Urey and D. Rittenberg, *J. Chem Phys.* **1**, 139 (1933) and reference (11).

$\dagger$ References (1), (3), (4), (5)

In an isotope-exchange reaction involving solvent asymmetry, for example, reactions (3) and (28), the numerical values of  $\mathcal{E}^\circ$  and of K depend on the concentration scale chosen for the solution-phase species. For example, application of the Nernst equation to the reaction



yields

$$\mathcal{E} = \mathcal{E}^\circ - \frac{RT}{2\mathcal{F}} \ln \left( \frac{P_{H_2}}{P_{D_2}} \right) - \frac{RT}{\mathcal{F}} \ln \left\{ \frac{(a_{D^+} a_{Cl^-})_h}{(a_{H^+} a_{Cl^-})_d} \right\} \quad (30)$$

where both  $\mathcal{E}^\circ$  and the activities depend on the choice of concentration scales. The cell voltage,  $\mathcal{E}$ , is a directly measureable quantity and consequently the value of  $\mathcal{E}$  must be independent of the concentration scale chosen, therefore we can write (using equation (30)) [ $c$  = molarity ( $a_i = c_i y_i$ );  $m$  = molality ( $a_i = m_i \nu_i$ ); and  $x$  = mole fraction ( $a_i = x_i f_i$ )]

$$\mathcal{E}_c^\circ - \frac{2RT}{\mathcal{F}} \ln \left\{ \frac{(cy^\pm)_{DCl}}{(cy^\pm)_{HCl}} \right\} = \mathcal{E}_m^\circ - \frac{2RT}{\mathcal{F}} \ln \left\{ \frac{(m\nu^\pm)_{DCl}}{(m\nu^\pm)_{HCl}} \right\} \quad (31)$$

and

$$\mathcal{E}_x^\circ - \frac{2RT}{\mathcal{F}} \ln \left\{ \frac{(xf^\pm)_{DCl}}{(xf^\pm)_{HCl}} \right\} = \mathcal{E}_m^\circ - \frac{2RT}{\mathcal{F}} \ln \left\{ \frac{(m\nu^\pm)_{DCl}}{(m\nu^\pm)_{HCl}} \right\} \quad (32)$$

If we take the limit of both sides of these equations as the concentrations go to zero, and we note that in the limit  $c/m = \rho$  and

$x/m = M_s/1000$  (where  $\rho_s$  is the density of the pure solvent and  $M_s$  is the molecular weight of the solvent), then we obtain

$$\mathcal{E}_c^\circ - \mathcal{E}_m^\circ = \frac{2RT}{\mathcal{F}} \ln \left( \frac{\rho_{sd}}{\rho_{sh}} \right) \quad (33)$$

$$\mathcal{E}_x^\circ - \mathcal{E}_m^\circ = \frac{2RT}{\mathcal{F}} \ln \left( \frac{M_{sd}}{M_{sh}} \right) \quad (34)$$

Combination of equations (33) and (34) with the relation

$\mathcal{E}^\circ = \frac{RT}{n\mathcal{F}} \ln K$ , yields the results

$$K_x = K_m \left( \frac{M_{sd}}{M_{sh}} \right)^4 \quad \text{and} \quad K_c = K_m \left( \frac{\rho_{sd}}{\rho_{sh}} \right)^4 \quad (35)$$

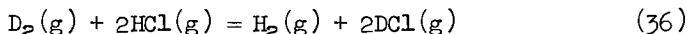
For reaction (3) we have 25°C

$$\mathcal{E}_m^\circ = -9.78 \text{ mV} \quad K_m = 0.467$$

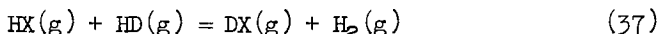
$$\mathcal{E}_c^\circ = -4.53 \text{ mV} \quad K_c = 0.703$$

$$\mathcal{E}_x^\circ = -4.34 \text{ mV} \quad K_x = 0.713$$

II.c. Gas-Phase Reactions. Gas-phase, hydrogen-isotope-exchange reactions, for example



can also be studied in electrochemical cells. The determination of accurate ( $\pm 1\%$  error) values of equilibrium constants for gas-phase isotope-exchange reactions can provide the necessary data for a critical test of the theory of isotope-exchange reactions. The need for such an experimental test was first brought to our attention by Professor Max Wolfsberg. Kleinman and Wolfsberg (15) have calculated that there is a Born-Oppenheimer-approximation failure in the range of 3 to 10% at 300 K in the equilibrium constants for hydrogen-isotope-exchange reactions of the type

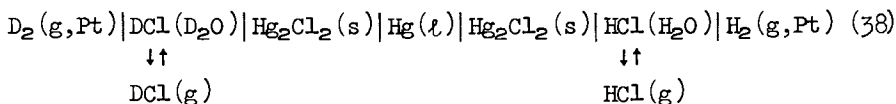


where X is Li (2.9%), B, N, or F (10.1%). Prior to the work of Kleinman and Wolfsberg (see paper in this volume) it was generally believed that the Born-Oppenheimer approximation contributed at

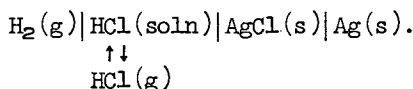
most an error of about 0.1% to the equilibrium constant of an isotope-exchange reaction.

Reactions of the type (37) are not suitable for study in electrochemical cells (16) because they involve the isotopically-mixed species HD. However, a reaction like (36) can be investigated directly in an electrochemical cell. The basic idea is to compare an experimental value of K for reaction (36) with two calculated (by Wolfsberg, et al.) values of K, one obtained invoking the Born-Oppenheimer approximation, and the other obtained without invoking the Born-Oppenheimer approximation. In this way the reliability of the Born-Oppenheimer approximation for hydrogen-isotope-exchange reaction can be tested experimentally.

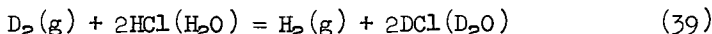
Reaction (36) is being studied in cells of the type



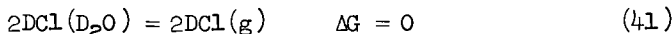
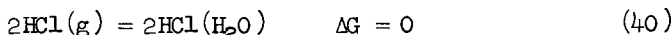
where the DCl(D<sub>2</sub>O) solution is in equilibrium with a gas phase containing DCl, D<sub>2</sub>, and D<sub>2</sub>O, and the HCl(H<sub>2</sub>O) solution is in equilibrium with a gas phase containing HCl, H<sub>2</sub>, and H<sub>2</sub>O. The basic idea for the design of the respective halves of the double cell (38) stems from the work of Aston and Gittler (17) on the cell



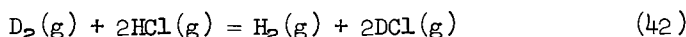
The net cell reaction for cell (38) is



Also, for the conditions prevailing in the cell



Addition of equations (39), (40), and (41) yields



and therefore

$$\Delta G_{42} = \Delta G_{39} = \Delta G_{42}^{\circ} + RT \ln \left\{ \frac{a_{\text{DCl}}^2(\text{g})}{a_{\text{HCl}}^2(\text{g})} \frac{a_{\text{H}_2}(\text{g})}{a_{\text{D}_2}(\text{g})} \right\}$$

Also

$$\Delta G_{39} = -2\mathcal{F}\mathcal{E}_{39}$$

where  $\mathcal{E}_{39}$  is the measured voltage of the cell. Thus (assuming ideal-gas behavior at pressures less than 100 Torr, for the purposes of discussion) we can write

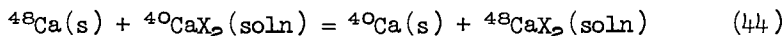
$$\mathcal{E}_{42}^{\circ} = \mathcal{E}_{39} + \frac{RT}{2\mathcal{F}} \ln \left\{ \left( \frac{P_{\text{DCl}}}{P_{\text{HCl}}} \right)^2 \frac{P_{\text{H}_2}}{P_{\text{D}_2}} \right\} \quad (43)$$

A measured value of  $\mathcal{E}_{39}$ , together with the corresponding measured values of the pressures  $P_{\text{DCl}}$ ,  $P_{\text{HCl}}$ ,  $P_{\text{H}_2}$ , and  $P_{\text{D}_2}$  (manometers), yields a value of  $\mathcal{E}_{42}^{\circ}$ , no extrapolations are necessary and measurements can be made with concentrated HCl solutions; for 14M HCl(aq),  $P_{\text{HCl}} \simeq 41$  Torr and  $P_{\text{H}_2\text{O}} = 4$  Torr, whereas for 16 M HCl(aq),  $P_{\text{HCl}} \simeq 120$  Torr and  $P_{\text{H}_2\text{O}} = 3$  Torr.

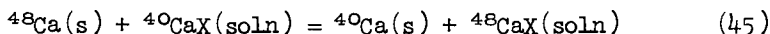
Our preliminary measurements (18) on cell (38) show that the cells are remarkably stable (emf fluctuation less than 12  $\mu\text{V}$  over 48 hours) and reversible. The major experimental problem concerns the determination of the composition of the gas phase in equilibrium with the cell electrolyte. Experimental pressure measurements give the sums  $P_{\text{HCl}} + P_{\text{H}_2\text{O}}$  and  $P_{\text{HCl}} + P_{\text{H}_2\text{O}} + P_{\text{H}_2}$ ; the gas phases in the two halves of the double cell must be analyzed in order to obtain  $P_{\text{HCl}}$  and  $P_{\text{DCl}}$ . If the measured pressure ratios are good to 0.3% (which corresponds to 0.1 Torr in the pressures for roughly equal pressures), then  $K$  can be obtained with an error of less than 0.5%. An example of some preliminary data for cell (38) is the following (20°C)  $\mathcal{E} = 4.596 \pm 0.011$  mV,  $P_{\text{HCl}} + P_{\text{H}_2\text{O}} = 60.72$  Torr,  $P_{\text{H}_2} = 706.30$  Torr,  $P_{\text{DCl}} + P_{\text{D}_2\text{O}} = 70.65$  Torr, and  $P_{\text{D}_2} = 697.60$  Torr. If we assume that  $(P_{\text{DCl}} + P_{\text{D}_2\text{O}}) / (P_{\text{HCl}} + P_{\text{H}_2\text{O}}) \simeq P_{\text{DCl}} / P_{\text{HCl}}$  (because at the time this cell was run we had not perfected our gas-phase analysis method), then we compute that  $K = 1.99$ . Further measurements on cell (38) are in progress.

#### II.d. Calcium-Isotope-Exchange Reactions.

There are several stable isotopes of calcium (40, 42, 44, 46, and 48). The 20% mass difference between  $^{40}\text{Ca}$  and  $^{48}\text{Ca}$  is larger than the 17% mass difference between  $^6\text{Li}$  and  $^7\text{Li}$ . The square root of the mass ratio is  $(48/40)^{\frac{1}{2}} = 1.095$  for calcium and  $(7/6)^{\frac{1}{2}} = 1.080$  for lithium. The electrochemical determination of equilibrium constants for isotope-exchange reactions of the type (19)



and

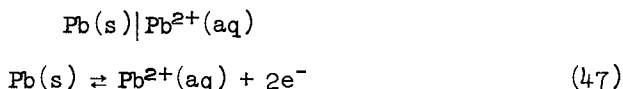


has not proved possible to date, because the conditions under which calcium metal electrodes behave reversibly have not been discovered. However, calcium-isotope-exchange reactions of the type

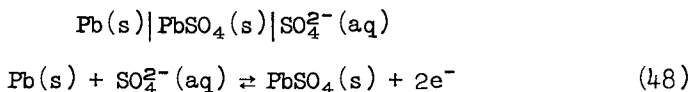


as well as analogous reactions involving hydroxyapatite, fluorapatite and other calcium salts of geological and biochemical interest, can be conveniently studied in electrochemical double cells involving electrodes of the third kind.

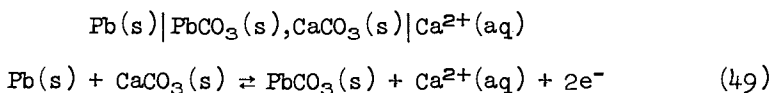
An electrode of the first kind involves a metallic phase in contact with an electrolyte phase containing the ions of the metal, for example



An electrode of the second kind involves a metallic phase in contact with an electrolyte solution in which the activity of the metal ions in equilibrium with the metallic phase is controlled by an anionic, solution-phase species that forms an insoluble salt with the metal ion, for example

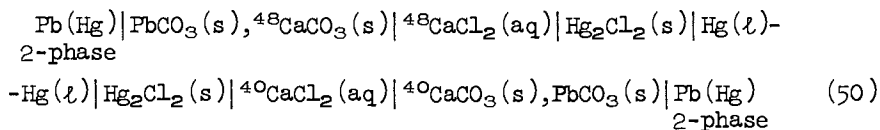


An electrode of the third kind involves a metallic phase in contact with an electrolyte solution in which the activity of the metal ions in equilibrium with the metallic phase is controlled by a different cationic, solution-phase species through the presence of two insoluble salts of the respective cations, for example



Electrodes of the third kind were first reported by Le blanc and Harnapp (20), and the particular type of third-kind electrode outlined above was used by Jakuszewski and Tanieuska-Osinka (21) to determine the Gibbs energies of formation of  $\text{Ca}^{2+}(\text{aq})$ .

The cell diagram for a double cell involving electrodes of the third kind, for which the net cell reaction is equation (46) is (22)



where we have employed a two-phase lead amalgam rather than  $\text{Pb}(\text{s})$  because the former can be prepared in a reproducible, strain-free state. We are presently using cells of the type (50) (both with aqueous and nonaqueous cell electrolytes) to investigate the thermodynamics of calcium-isotope-exchange reactions. The data from such cells should provide an independent test of other methods (such as mass-spectrometric analysis of equilibrium phases), which suggest that there is no isotopic fractionation in the precipitation of calcium salts from aqueous media (23,24) involving  $\text{Ca}^{2+}(\text{aq})$ . The results of Heumann (24) on isotope exchange between  $\text{Ca}^{2+}(\text{aq})$  and calcium ions chelated on Dowex Al resin suggest that if cell (50) is run with chelated calcium ion in solution (e.g.  $\text{CaEDTA}^{2+}$ , or calcium chelated by biologically-important ligands), then isotopic fractionation might be observed. Fractionation of calcium isotopes between inorganic salts and chelated calcium ion is a process of obvious potential interest as a probe into biological processes.

### III.a. Isotope-Exchange Reactions as a Probe for the Study of Ion Solvation.

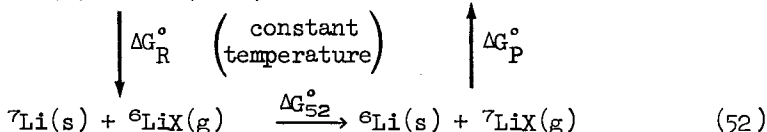
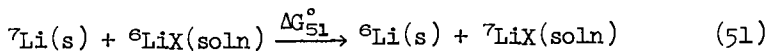
In thermodynamics we are no longer content to know the value of an equilibrium constant for a chemical reaction; we also want to know why the equilibrium constant has that particular value. In other words, we would like to be able to calculate the value of the equilibrium constant from microscopic properties (atomic masses, bond lengths, bond angles, force constants, dissociation energies, etc.) together with quantum-mechanical and statistical-thermodynamic theory.

Isotope-exchange reactions are the simplest class of chemical reactions, and consequently isotope-exchange reactions have played a central role in the development of theories of chemical reactions. The development of the theory of isotope-exchange reactions is outlined by Bigeleisen in the opening paper of this symposium. The Bigeleisen-Mayer theory of isotope-exchange reactions (25,26) has proved remarkably successful in predicting equilibrium constants for gas-phase reactions and for reactions involving gases and pure condensed phases. Although some major questions remain to be answered, especially in connection with the accuracy of the Born-Oppenheimer approximation for hydrogen-isotope-exchange reactions (see paper by Wolfsberg and Kleinman

in this volume), the overall status of the theory for such reactions appears to be excellent. The accuracy with which equilibrium constants can be calculated for reactions involving only gases and/or pure condensed phases rivals, and in some cases exceeds, the accuracy with which the equilibrium constants can be measured. The picture is not so clear for isotope-exchange reactions involving solution-phase species, because of major uncertainties associated with the nature and structure of solution-phase species; this problem is especially acute in the case of solvated ions.

The determination of equilibrium constants for heterogeneous, isotope-exchange reactions involving isotope-exchange between pure phases and solution phases yields partition-function ratios for the isotopic, solution-phase species. In favorable cases a comparison of calculated values for the solute partition-function ratio with the experimental value allows one to distinguish between possible solute models.

The statistical-thermodynamic expression for the equilibrium constant of reaction (51)



is

$$K = \left( \frac{q_{{}^6\text{Li}}(s)}{q_{{}^7\text{Li}}(s)} \right) \left( \frac{q_{{}^7\text{LiX}}(\text{soln})}{q_{{}^6\text{LiX}}(\text{soln})} \right) \exp(-\Delta V/RT) \quad (53)$$

where  $q_i$  terms are the partition functions (including the zero-point energy factors) of the various species evaluated in the respective standard states. The volume change,  $\Delta V$ , for a symmetric lithium-isotope-exchange reaction such as reaction (51) is essentially zero (27), because  $\bar{V}_{{}^7\text{Li}}(s) = \bar{V}_{{}^6\text{Li}}(s)$  and  $\bar{V}_{{}^7\text{LiX}} = \bar{V}_{{}^6\text{LiX}}$  to within  $\pm 0.2\%$ . Consequently, equation (53) can be written as

$$K = \left( \frac{q_{{}^6\text{Li}}(s)}{q_{{}^7\text{Li}}(s)} \right) \left( \frac{q_{{}^7\text{LiX}}(\text{soln})}{q_{{}^6\text{LiX}}(\text{soln})} \right) \quad (54)$$

We shall adopt the following standard states in which the various partition-function ratios will be evaluated: (a) solids and liquids - the pure, unstrained material at one standard atmosphere

American Chemical  
Society Library  
1155 16th St., N.W.  
Washington, D.C. 20036



pressure ( $1.013 \times 10^5 \text{N}\cdot\text{m}^{-2}$ ) and the temperature of interest; (b) gases - the hypothetical, ideal gas at one standard atmosphere and the temperature of interest; and (c) solutes - the hypothetical, ideal solution containing unit-mole-fraction of the solute.

For the thermodynamic cycle given above - equations (51) and (52) - we have

$$\Delta G_{51}^{\circ} = \Delta G_{52}^{\circ} + \Delta G_{\text{R}}^{\circ} + \Delta G_{\text{P}}^{\circ} \quad (55)$$

and therefore (using  $\Delta G^{\circ} = -RT \ln K$ )

$$K_{51} = K_{52} K_{\text{R}} K_{\text{P}} \quad (56)$$

but

$$K_{\text{R}} K_{\text{P}} = \frac{a_{6\text{LiX}}(\text{g})}{a_{6\text{LiX}}(\text{soln})} \cdot \frac{a_{7\text{LiX}}(\text{soln})}{a_{7\text{LiX}}(\text{g})} = \frac{a_{6\text{LiX}}^*(\text{g})}{a_{7\text{LiX}}^*(\text{g})} \simeq \frac{P_{6\text{LiX}}^*}{P_{7\text{LiX}}^*} \quad (57)$$

where  $a_i^*(\text{g})$  is the Henry's law constant for the solute  $i$  in the particular solvent. Combination of equations (56) and (57) yields

$$K_{51} = K_{52} (P_{6\text{LiX}}^*/P_{7\text{LiX}}^*) \quad (58)$$

In other words the treatment of solution-phase species (i.e. taking  $K_{51} = K_{52}$ ) as gas-phase species is equivalent to the assumption that there is no isotope effect on the Henry's law constant for the isotopic solutes.

An experimental determination of  $K$  for a reaction of the type (51) can be combined with a calculated value for the partition-function ratio of the isotopic solids,  $q_{6\text{Li}}(\text{s})/q_{7\text{Li}}(\text{s})$ , to obtain an "experimental" value for the partition-function ratio of the solute species,  $q_{7\text{LiX}}(\text{soln})/q_{6\text{LiX}}(\text{soln})$ .

### III.b. Evaluation of Partition-Function Ratios for Isotopic Solids.

The quantitative evaluation of the partition-function ratio

$$K_{\text{s}} = q_{6\text{Li}}(\text{s})/q_{7\text{Li}}(\text{s}) \quad (59)$$

for the isotopic lithium metals requires a choice of model for the solids. The choice of a particular model for the solid phase determines the form of the frequency distribution function for the lattice, which in turn determines the partition-function ratio. A mole of a monatomic solid has  $3N_0 - 6 \simeq 3N$ . (where  $N_0$  is Avogadro's number) vibrational frequencies (normal modes). The

partition function  $q_1$  for a one-dimensional, harmonic oscillator of frequency  $\nu$  is given by

$$q_1 = \exp\left(\frac{D_e - h\nu/2}{kT}\right) \left\{1 - \exp(-h\nu/kT)\right\}^{-1} \quad (60)$$

where  $D_e$  is the dissociation energy measured from the bottom of the potential well. For isotopic species the  $D_e$  values are equal (Born-Oppenheimer approximation). If we assume that the solid consists of  $3N_0$  harmonic oscillators, then  $K_s$  can be written

$$K_s = \left[ \prod_{i=1}^{3N_0} \left\{ \frac{1 - \exp(-h\nu_{i7}/kT)}{1 - \exp(-h\nu_{i6}/kT)} \right\} \exp\left\{-h(\nu_{i6} - \nu_{i7})/2kT\right\} \right]^{1/N_0} \quad (61)$$

An Einstein solid is one in which all of the atoms are treated as three-dimensional harmonic oscillators with frequency  $\nu_E$ . Thus for monatomic Einstein solids, equation (61) becomes

$$K_s = \left\{ \frac{1 - \exp(-h\nu_{E7}/kT)}{1 - \exp(-h\nu_{E6}/kT)} \right\}^3 \exp\left\{-3h(\nu_{E6} - \nu_{E7})/2kT\right\} \quad (62)$$

The Einstein characteristic temperature is defined by the relation

$$h\nu_E = k\theta_E \quad (63)$$

and thus equation (62) can also be written as

$$K_s = \left\{ \frac{1 - \exp(-\theta_{E7}/T)}{1 - \exp(-\theta_{E6}/T)} \right\}^3 \exp\left\{-3(\theta_{E6} - \theta_{E7})/2T\right\} \quad (64)$$

The Einstein frequency  $\nu_E$  is inversely proportional to the atomic mass of the lattice atoms and thus

$$\theta_{E6} = \theta_{E7} (m_7/m_6)^{1/2} \quad (65)$$

Thus the calculation of  $K_s$  requires an experimental value of  $\theta_{E7}$  or  $\theta_{E6}$ , which can be obtained from heat capacity measurements. It is usually  $\theta_D$  ( $=h\nu_D/k$ ), the Debye characteristic temperature which is reported, but  $\theta_E$  can be calculated from  $\theta_D$  using the relation (7,8)

$$\theta_E = 3\theta_D/4 \quad (66)$$

If we take  $\theta_{D7} = 353\text{K}$  (28), then we compute that  $K_s = 0.7811$  at  $25^\circ\text{C}$  for Einstein solids.

The atoms in a Debye solid are treated as a system of weakly coupled harmonic oscillators. Normal modes with wavelengths that are large compared to the atomic spacing do not depend on the discrete nature of the crystal lattice, and consequently these normal modes can be obtained by treating the crystal as an isotropic elastic continuum. In the Debye treatment of a solid all of the normal modes are treated as elastic waves. The partition function for a Debye solid cannot be obtained in closed form, but the thermodynamic functions for a Debye solid have been tabulated as a function of  $\theta_D/T$ . For the pair of isotopic metals  ${}^6\text{Li}(s)$  and  ${}^7\text{Li}(s)$  we have ( $\Delta V = 0$ )

$$\Delta G^\circ = \Delta A^\circ + P\Delta V^\circ = \Delta A^\circ$$

and

$$K = \exp(-\Delta A^\circ/RT) = \exp\left\{-\Delta(A^\circ - E_0^\circ)/RT\right\} \exp(-\Delta E_0^\circ/RT) \quad (67)$$

The function  $(A^\circ - E_0^\circ)/RT$  is tabulated (29,30) as a function of  $\theta_D/T$ , and the zero-point-energy term is given by

$$\Delta E_0^\circ/RT = 9(\theta_{D7} - \theta_{D6})/8T \quad (68)$$

where  $\theta_{D6} = \theta_{D7} (m_7/m_6)^{1/2}$ . Thus, for the isotopic Debye solids we have

$$K_s = \exp\left\{\left(\frac{A^\circ - E_0^\circ}{RT}\right)_7 - \left(\frac{A^\circ - E_0^\circ}{RT}\right)_6\right\} \exp\left\{\frac{9(\theta_{D7} - \theta_{D6})}{8T}\right\} \quad (69)$$

If we take  $\theta_{D7} = 353\text{K}$ , then we compute that  $K_s = 0.7809$  at  $25^\circ\text{C}$ .

The most sophisticated model for the solid phases is that developed by Born and von Kármán (32). We have carried out a Born-von Kármán (BVK) lattice calculation for the isotopic lithium metals. In our calculations we have followed closely the methods described by de Launay (33). In our model for the atomic interactions we chose to consider only central forces, and to take only the forces between nearest and next-nearest neighbors as significant. This choice was dictated mainly by the fact that the secular equation for a bcc (as is lithium) crystal with this type of force interaction has been treated (34). In our calculations we used the root-sampling method and solved the secular equation for 3311 values of the wave propagation vector,  $\vec{k}$ . These values of  $\vec{k}$  were obtained from the coordinates of a cubic grid of 3311 points in the irreducible element of the first Brillouin zone. The nearest- and next-nearest-neighbor force constants,  $\alpha_1$  and  $\alpha_2$ ,

were calculated from the macroscopic elastic constants  $C_{11}$ ,  $C_{12}$  and  $C_{44}$ , using the relations given by Bauer (35), viz.,  $\alpha_1 = \frac{3}{2}aC_{44}$ , and  $\alpha_2 = 2a(C_{11}-C_{12})$ , where  $a$  is the lithium bcc lattice parameter,  $2a = 3.50 \text{ \AA}$ . The values of the lattice constants used were those reported by Nash and Smith (36). In the harmonic approximation the lattice constants should be independent of temperature. This is not confirmed experimentally. We have therefore used the lattice constants reported for the lowest temperature that was investigated experimentally (77 K), because at this temperature the lattice vibrations will be more nearly harmonic.

The calculated lattice spectrum is approximated as a histogram of the number of oscillators vs frequency (Figure 3a). The partition function ratio,  $q_{6\text{Li}}(s)/q_{7\text{Li}}(s)$ , for the isotopic lithium metals can be calculated from our histogram of the lattice spectrum using the equation

$$K_s = \frac{\prod_i \{\exp(-3h\nu_{i6}/2kT)[1-\exp(-h\nu_{i6}/kT)]^{-3}\} g_{i6}}{\prod_i \{\exp(-3h\nu_{i7}/2kT)[1-\exp(-h\nu_{i7}/kT)]^{-3}\} g_{i7}} \quad (70)$$

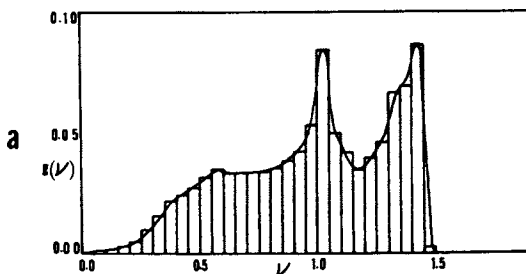
where  $g_i$  is the fraction of oscillators having the frequency  $\nu_i$ ;  $\sum_i g_i = 1$ . Substitution of the  $g_i$  values obtained from the BVK calculations into equation (70) yields  $K_s = 0.7866$  at 298.15 K.

The results obtained for  $K_s$  show that the value of  $K_s$  is not strongly dependent on the detailed nature of the model chosen for the isotopic solids; the total variation in  $K_s$  is less than 1%. However, when considered from the point of view of lithium-isotope-exchange reactions, a 1% variation of  $K_s$  may be as much as 30% of the total isotope effect.

BVK-lattice calculations can also be carried out for isotopic lithium salts, and we have carried such calculations for the isotopic pair of salts  ${}^7\text{LiF}(s)$  and  ${}^6\text{LiF}(s)$  (37). Within the harmonic-oscillator approximation the partition-function ratio for the isotopic lithium fluorides can be written as

$$\frac{q_{7\text{LiF}}(s)}{q_{6\text{LiF}}(s)} = \left\{ \prod_{i=1}^{6N} \left( \frac{1-\exp(-h\nu_{i6}/kT)}{1-\exp(-h\nu_{i7}/kT)} \right) \exp \left( \frac{-h(\nu_{i7}-\nu_{i6})}{2kT} \right) \right\}^{1/N} \quad (71)$$

where  $N$  is the number of  $\text{Li}^+$  or  $\text{F}^-$  ions in the crystal. The evaluation of equation (71) requires a knowledge of the frequency distribution function for the  $\text{LiF}(s)$  crystal lattice. Lithium fluoride is presumed to be an ionic crystal having a NaCl-type



Journal of Chemical Physics

Figure 3a. Born-von Kármán lattice spectrum of lithium metal calculated using elastic constants determined at 77°K. The vertical axis is the fraction of oscillators in a frequency range of 0.05. The horizontal axis is the frequency in reduced, dimensionless units,  $(3M\pi^2/2\alpha_1)^{1/2}$  (8).

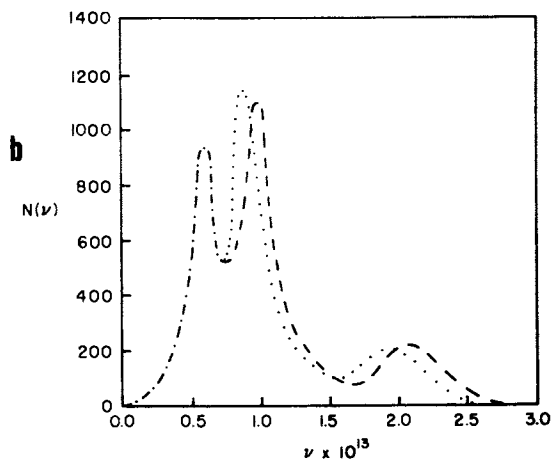


Figure 3b. Born-von Kármán vibrational frequency distribution for the  ${}^7\text{LiF}$  lattice ( $\cdots$ ) and for the  ${}^6\text{LiF}$  lattice ( $---$ ) calculated with 0°K input data. The line  $\cdots$  occurs in the region where the two distributions are indistinguishable (10).

structure. The vibrational spectrum for a NaCl-type of lattice was first calculated by Kellermann (38,39); the calculational methods developed by Kellermann were refined by Sayre and Beaver (40), and these methods have been applied to normal-isotopic-abundance LiF(s) by Karo (41). The Kellermann treatment involves the separation of the interionic forces into short-range repulsive forces between nearest neighbors only, and long-range Coulombic forces that extend over the entire crystal lattice.

The evaluation of the Coulombic force constants requires the summation of the Coulombic interactions over the whole of the crystal lattice for each wave vector considered. Kellermann, and Sayre and Beaver have carried out this summation for 48 evenly-spaced wave vectors in the irreducible element of the first Brillouin zone of NaCl(s). An exact evaluation of equation (71) would require the solution of the equations of motion for  $N/48$  evenly-spaced wave vectors in the first Brillouin zone. In the root-sampling method these  $N/48$  wave vectors are approximated by an evenly-distributed grid of points in the irreducible element. The 48 points in the irreducible element for which Coulombic force constants have been calculated correspond to 1000 wave vectors in the first Brillouin zone. For a given wave vector six equations of motion (assuming only central forces) are necessary to describe the three normal components of the displacement for the two types of atoms. In order for wave re-enforcement to occur these six equations must be simultaneously satisfied. Thus for a given wave vector six normal modes will be obtained; 1000 wave vectors yield 6000 of the  $6N$  normal modes of LiF(s). Because the frequencies are very densely packed it is assumed that the normalization to  $6N$  normal modes does not affect the form of the frequency distribution. The numerical evaluation of the frequency distribution of LiF requires the ionic masses, the equilibrium internuclear distances, and the compressibility as input parameters. The calculated frequency distribution functions for  ${}^7\text{LiF(s)}$  and  ${}^6\text{LiF(s)}$  are shown in figure 3b. As can be seen in the figure the isotopic shift in the frequency distribution becomes much more pronounced as the frequency increases.

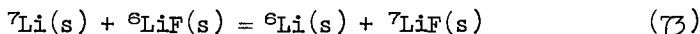
Equation (71) can be rewritten in the root-sampling approximation as

$$\frac{q_{7\text{LiF(s)}}}{q_{6\text{LiF(s)}}} = \prod_{i=1}^{288} \left[ \left( \frac{1 - \exp(-h\nu_{i6}/kT)}{1 - \exp(-h\nu_{i7}/kT)} \right) \exp\left(\frac{-h(\nu_{i7} - \nu_{i6})}{2kT}\right) \right]^{s_i/1000} \quad (72)$$

where  $s_i$  in equation (72) is the number of times that the  $i$ th wave vector is reproduced by the symmetry operations of the Brillouin zone ( $\sum_{i=1}^{288} s_i = 6000$ ). The repeat product in equation

(72) is over the 288 ( $= 6 \times 48$ ) eigenvalues which result from the solution of the equations of motion for the 48 points considered. The value of  $q_{7\text{LiF(s)}}/q_{6\text{LiF(s)}}$  calculated at 298.15 K (using 0 K values for the input parameters) is 1.376, whereas with room temperature values for the input parameters the calculated value is 1.367.

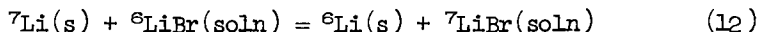
Combination of the BVK results for the solid fluorides with the BVK results for the isotopic lithium metals yields a calculated value (37) of  $K = 1.082$  for the reaction



compared to an experimental value of  $1.10 \pm 0.01$ .

### III.c. Evaluation of Partition-Function Ratios for Isotopic Solute Species. The Symmetric Solvent Case.

The simplest possible model for the partition-function ratio for isotopic species in a common solvent involves the assumption that the solute-phase species can be treated as gas-phase species. As noted earlier, as far as isotope-exchange reactions are concerned, this assumption is equivalent to the assumption that there is no vapor pressure isotope effect. For the reaction



the gas-phase model assumes that

$$\frac{q_{7\text{LiBr(soln)}}}{q_{6\text{LiBr(soln)}}} \sim \frac{q_{7\text{LiBr(g)}}}{q_{6\text{LiBr(g)}}} \quad (74)$$

The principal condition for the applicability of equation (74) is that the dissolved LiBr exists in solution as undissociated diatomic molecules and not as ions. There must, of course, be a significant amount of cancellation of terms in the partition-function ratio for the solute species. In particular all purely electrostatic interactions (e.g., ion-dipole, dipole-dipole, etc.) which are isotope independent, should cancel out. Dissolution of LiBr would be expected to lower the stretching frequency for the LiBr bond (42). The decrease in  $\omega_{\text{LiBr}}$  decreases the ratio of vibrational partition functions, primarily through the decrease in the vibrational zero-point energy. However, this effect would be partially offset by an increase in the zero-point energy arising from restricted rotation in the solution phase. Lastly, placing LiBr in a solvent cage will increase the ratio of translational partition functions. Presumably, these opposing effects for the most part cancel out, primarily because the frequency

shift on dissolution amounts at most to a few percent (43). The ratio of partition functions for the gaseous isotopic bromides is given in the harmonic-oscillator, rigid-rotor approximation by the expression (44)

$$\frac{q_{7\text{LiBr}}(g)}{q_{6\text{LiBr}}(g)} = \left( \frac{m_7 + m_{\text{Br}}}{m_6 + m_{\text{Br}}} \right)^{3/2} \frac{\mu_7}{\mu_6} \left\{ \frac{1 - \exp(-hc\omega_6/kT)}{1 - \exp(-hc\omega_7/kT)} \right\} \exp \left\{ \frac{-hc(\omega_7 - \omega_6)}{2kT} \right\} \quad (75)$$

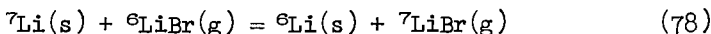
where the  $\mu_i$  values are the reduced masses,

$$\mu_i = m_i m_{\text{Br}} / (m_i + m_{\text{Br}}) \quad (76)$$

The (harmonic oscillator) vibrational frequencies are related by expression

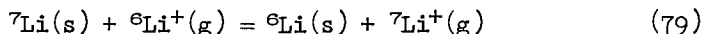
$$\omega_6 = \omega_7 (\mu_7 / \mu_6)^{1/2} \quad (77)$$

The use of equations (75), (76), and (77) together with the value of  $\omega_7 = 576.2 \text{ cm}^{-1}$  (42), and  $K_g = 0.7865$  yields a value of  $K = 1.035$  (at 296.15 K) for the reaction

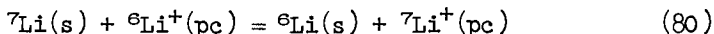


When anharmonic corrections are included (anharmonic oscillator, nonrigid rotor, vibration-rotation coupling, and the Wolfsberg  $G_0$  term), the calculated value of  $K$  remains unchanged. The experimental value of  $K$  for reaction (12) with diglyme as solvent is  $1.035 \pm 0.007$ ; the good agreement between the experimental and calculated values of  $K$  suggests that approximation (74) is a satisfactory approximation.

The approximation of the partition-function ratio for lithium ions in solution by the partition-function ratio for the unsolvated, gaseous lithium ions is not a good approximation. The calculated  $K$  value for the reaction

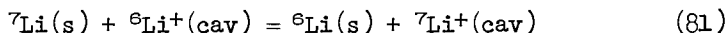


is 0.991, whereas the experimental value of  $K$  for the reaction



is  $1.030 \pm 0.005$ . Because propylene carbonate (pc) is usually only weakly coordinated to metal ions, a solute model involving a specific solvated-ion structure does not seem appropriate. We have treated the isotopic lithium ions in propylene carbonate as particles in cubical boxes (cavity model (8))



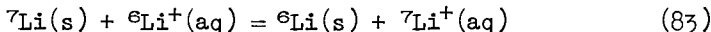


The partition-function ratio for the isotopic, caged ions is then

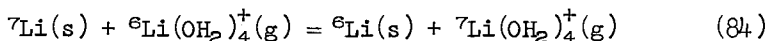
$$\frac{q_{{}^7\text{Li}^+(\text{cav})}}{q_{{}^6\text{Li}^+(\text{cav})}} = \frac{\sum_{n=1}^{\infty} \exp(-n^2 h^2 / 8m_7 b^2 kT)}{\sum_{n=1}^{\infty} \exp(-n^2 h^2 / 8m_6 b^2 kT)} \quad (82)$$

where  $b$  is the cavity dimension. The value of  $b = 1.377 \text{ \AA}$  makes the partition function ratio equal to 1.310 (note that  $1.030/0.7865 = 1.310$ ); this is the value of the partition-function ratio for the ions that yields the observed value of  $K$  for reaction (80). The diameter of  $\text{Li}^+$  is  $0.60 \text{ \AA}$ , and the cavity size is then about  $2.58 \text{ \AA}$  in this model. The predicted  $n = 1$  to  $n = 2$  translational transition energy is  $37.4 \text{ cm}^{-1}$ ; such translational transitions have been observed for neutral species in solution (45).

Isotope-exchange reactions involving strong, specific solvation of the solute apparently require the explicit incorporation of the solvated ions into the model. An example is provided by the reaction



The aquated lithium ion has a four-coordinate, tetrahedral structure (46); the model for reaction (83) then becomes (9)



The  $\text{Li}(\text{OH}_2)_4^+$  species is a 13-atom system with 33 normal vibrational modes. The number of normal vibrations can be decreased to 9 by treating the  $\text{H}_2\text{O}$  molecule as an  ${}^1\text{O}$  atom (pseudoatom approximation). Pseudoatom approximations have proved successful in the analysis of vibrational spectra for complex molecules (47). Of the nine normal modes of the  $\text{Li}{}^1\text{O}_4^+$  unit, there is only one triple-degenerate, genuine vibrational mode that involves movement of the lithium atom. Consequently, only this vibrational mode will change frequency on the substitution of  ${}^7\text{Li}$  for  ${}^6\text{Li}$ . The ratio of partition functions for the aquated ions is given by

$$\frac{q_{{}^7\text{Li}(\text{OH}_2)_4^+(\text{g})}}{q_{{}^6\text{Li}(\text{OH}_2)_4^+(\text{g})}} = \left\{ \frac{m_7 + 4m_{\text{H}_2\text{O}}}{m_6 + 4m_{\text{H}_2\text{O}}} \right\}^{3/2} \left\{ \frac{1 - \exp(-hc\omega_6/kT)}{1 - \exp(-hc\omega_7/kT)} \right\}^3 \exp \left\{ \frac{3hc(\omega_6 - \omega_7)}{2kT} \right\} \quad (85)$$

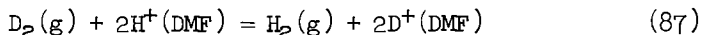
Because the isotopic substitution takes place at the center of mass, the ratio of rotational partition functions is unity. The

frequencies  $\omega_6$  and  $\omega_7$  are related through the Teller-Redlich product rule by the expression

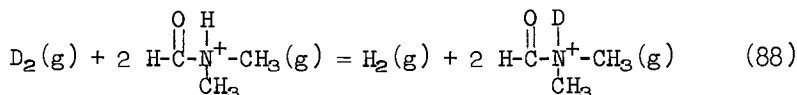
$$\omega_6 = \omega_7 \left\{ (m_7/m_6)(m_6+4m_{\text{H}_2\text{O}})/(m_7+4m_{\text{H}_2\text{O}}) \right\}^{1/2} \quad (86)$$

All that is needed to compute K for reaction (84) is a value for either  $\omega_6$  or  $\omega_7$ . The value of  $\omega_6$  that yields a value of  $K = 1.046$  (the experimental value of K for reaction (83)) is  $\omega_6 = 384 \text{ cm}^{-1}$ ; the corresponding calculated value of  $\omega_7$  is  $358 \text{ cm}^{-1}$ . Subsequent to the prediction of these values for  $\omega_6$  and  $\omega_7$ , laser Raman studies (56) of concentrated  $^6\text{LiCl}(\text{aq})$  and  $^7\text{LiCl}(\text{aq})$  solutions have led to the detection of  $\omega_6$  at  $380 \text{ cm}^{-1}$  and  $\omega_7$  at  $355 \text{ cm}^{-1}$ .

Another example of strong specific solvation of isotopic ions is found in the reaction



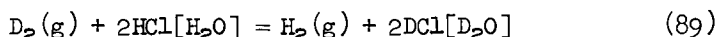
The availability of the amine nitrogen of DMF as a proton acceptor suggests that a reasonable model for reaction (87) is



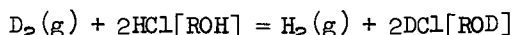
Unfortunately, the frequencies of the protonated DMF that are necessary to compute K for reaction (88) have not been obtained experimentally. However, an estimate of K for reaction (88) can be obtained if it is assumed that there are only two normal vibrational modes of protonated DMF that exhibit an appreciable H/D isotope effect. The two normal modes are: (a) the mode that is predominantly an N-H stretching frequency; and (b) the normal mode that is predominantly an N-H bending frequency. The reported values of the N-H stretching frequencies of amine salts lie in the range  $2700\text{--}2250 \text{ cm}^{-1}$ , and N-H bending frequencies from amides usually occur around  $1250 \text{ cm}^{-1}$ . If we assume that the N-H stretching frequency is  $2250 \text{ cm}^{-1}$ , then the value of the N-H bending frequency that is required to make the calculated value of K for reaction (88) equal to the experimental value of  $K = 1.82$  for reaction (87) is  $1180 \text{ cm}^{-1}$  (11). This model calculation is admittedly crude, but it is encouraging that the values of the frequencies required to give agreement with experiment are reasonably close to representative experimental values for these quantities.

#### III.d. Evaluation of Partition-Function Ratios for Isotopic Solute Species. The Asymmetric Solvent Case.

The calculation of equilibrium constants for isotope-exchange reactions involving solvent asymmetry, such as the reactions

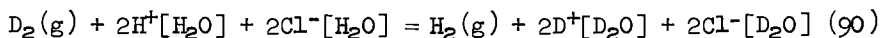


and

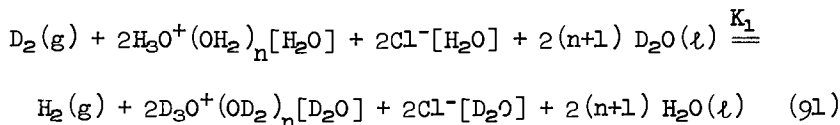


where R is n-hexyl and the species in square brackets is the solvent, requires a detailed consideration of transfer (or medium) effects as well as exchange effects (48, 49, 50, 52, 53, 54).

The equilibrium constant for reaction (89), based on mole-fraction-composition, strong-electrolyte standard states for  $HCl[H_2O]$  and  $DCl[D_2O]$ , is 0.713 at 298.15 K. Because this value of K for reaction (89) refers to strong electrolytes, we can re-write equation (89) as



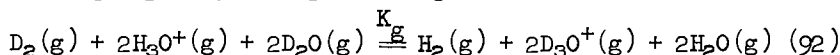
Reaction (90) can be written in even more detail in order to show explicitly the stripping of the solvent from the solvated hydronium ions that accompanies the exchange reaction



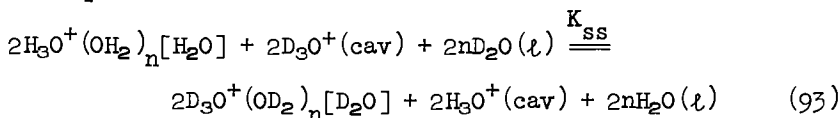
where n, the solvation number of the hydronium ion, is assumed to be the same in  $H_2O$  and  $D_2O$ .

Reaction (91) can be broken down into the following sequence of steps:

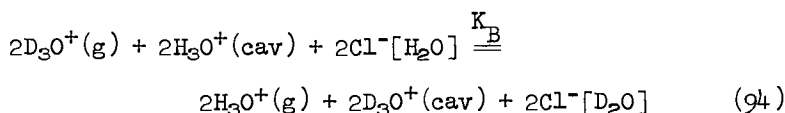
(i) the gas-phase, isotope-exchange reaction



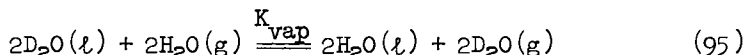
(ii) The solvent-stripping reaction, in which  $H_3O^+$  and  $D_3O^+$  are stripped of their solvation sheaths and are placed in hypothetical cavities in the respective liquids which have dielectric constants equal to the bulk values



(iii) The removal to the gas phase of the hydronium ions from their respective solvent cavities, and the transfer of  $Cl^-$  from  $H_2O$  to  $D_2O$



(iv) The vaporization of two moles of  $\text{D}_2\text{O}(\ell)$  and the condensation of two moles of  $\text{H}_2\text{O}(\text{g})$



Reaction (91) is equal to the sum of reactions (92), (93), (94), and (95), and therefore

$$K_1 = K_g K_{ss} K_B K_{\text{vap}} \quad (96)$$

where  $K_1 = 0.713$  at 298.15 K. The value of  $K_{\text{vap}}$  is given by the square of the ratio of vapor pressures of pure  $\text{D}_2\text{O}(\ell)$  and pure  $\text{H}_2\text{O}(\ell)$ ;  $K_{\text{vap}} = (P_{\text{D}_2\text{O}}^\circ/P_{\text{H}_2\text{O}}^\circ)^2 = 0.756$  at 298.15 K. The value of  $K_g$  can be calculated by standard statistical thermodynamic methods (25) to be  $K_g = 1.11 \pm 0.20$  (18), where the uncertainty in  $K_g$  arises from uncertainties in the vibrational frequencies for the hydronium ion. The value of  $K_B$  can be estimated from the Born equation as

$$K_B = \exp \left\{ - \frac{332 \text{ kcal} \cdot \text{\AA}}{RT} \left( \frac{1}{\epsilon_{\text{D}_2\text{O}}} - \frac{1}{\epsilon_{\text{H}_2\text{O}}} \right) \left( \frac{1}{r_{\text{H}_3\text{O}^+}} + \frac{1}{r_{\text{Cl}^-}} \right) \right\} \quad (97)$$

from which we compute ( $r_{\text{H}_3\text{O}^+} \simeq r_{\text{Cl}^-} = 1.82 \text{ \AA}$ ,  $\epsilon_{\text{D}_2\text{O}} = 77.936$ ,  $\epsilon_{\text{H}_2\text{O}} = 78.303$ ) that  $K_B = 0.964$ . Combination of these results yields a value of  $K_{ss} = 0.88 \pm 0.20$ . The closeness of  $K_{ss}$  to unity suggests that the water molecules bonded to the hydronium ion are not significantly more strongly bonded than the water molecules that are bonded to one another in bulk water, because otherwise there would be an appreciable isotope effect on  $K_{ss}$ . These results suggest, in agreement with the conclusions reached by Heinzinger and Weston (49), that the hydronium ion,  $\text{H}_3\text{O}^+$ , is an adequate representation of the proton in water, and that it is not necessary to invoke (55) the species  $\text{H}_9\text{O}_4^+$  to understand hydrogen-isotope-exchange reactions in water.

Acknowledgments: This work would not have been accomplished without the special efforts of my students: John C. Hall (lithium-isotope-exchange in diglyme and the BVK calculations);

Leonard F. Silvester (hydrogen-isotope-exchange in DMF, the preliminary work on the experimental test of the Born-Oppenheimer approximation, and the experiments on exchange between the isotopic metals and the isotopic fluorides); Gulzar Singh (lithium-isotope-exchange reactions in propylene carbonate and the quadruple cell for the exchange reaction between the isotopic lithium metals and the aqueous ions); Carlos H. Contreras-Ortega (hydrogen isotope exchange in n-hexanol); and Arnold Z. Gordon (calcium-isotope-exchange reactions). Numerous helpful and enjoyable discussions with C. P. Nash are also acknowledged.

This research was supported by the AEC under contract AT(04-3)-34 P.A. 169, by the NSF under Grant GP 33264, and in the early stages by the Committee on Research, UCD.

### Literature Cited

1. Abel, E., Bratu, E., and Redlich, O., Z. physik. Chem. (1934) A170, 153; (1935) A173, 353.
2. Korman, S. and La Mer, V.K., J. Amer. Chem. Soc. (1936) 58, 1396.
3. Gary, R., Bates, R.G., and Robinson, R.A., J. Phys. Chem. (1969) 68, 1186.
4. Goldblatt, M. and Jones, W.M., J. Chem. Phys. (1969) 51, 1881.
5. Noonan, E. and La Mer, V.K., J. Phys. Chem. (1939) 43, 247.
6. Electrochemical double cells are ideally suited for the study of Gibbs energies of transfer. For example, cell (5) could be set up with normal-isotopic-abundance lithium on both sides, but dissolved in different solvents. The cell reaction is then  $\text{LiCl(soln)} = \text{LiCl(soln}^*$ ).
7. Hall, J.C., Murray, Jr., R.C., and Rock, P.A., J. Chem. Phys. (1969) 51, 1145.
8. Singh, G., Hall, J.C. and Rock, P.A., J. Chem. Phys. (1972) 56, 1856.
9. Singh, G. and Rock, P.A., J. Chem. Phys. (1972) 57, 5556.
10. Hall, J.C., Silvester, L.F., Singh, G., and Rock, P.A., J. Chem. Phys. (1973) 59, 6358.
11. Silvester, L.F., Kim, J.J., and Rock, P.A., J. Chem. Phys. (1972) 56, 1863.
12. Petrov, S.M. and Umanskii, Yu. I., Russ. J. Phys. Chem. (1967) 41, 449.
13. Silvester, L.F. and Rock, P.A., J. Chem. Eng. Data (1974) 19, 98
14. Contreras-Ortega, C.H. and Rock, P.A., J. Electrochem. Soc. (1974) 121, 1048.
15. Kleinman, L.I., and Wolfsberg, M., J. Chem. Phys. (1973) 59, 2043.

16. The reason is that in the cell the isotopically-mixed species undergoes an isotopic disproportionation reaction, e.g.,  
 $2\text{HD} = \text{H}_2 + \text{D}_2$ .
17. Aston, J.G. and Gittler, F.L., *J. Amer. Chem. Soc.* (1955) 77, 3173.
18. Contreras-Ortega, C.H., Silvester, L.F. and Rock, P.A. unpublished results.
19. It is of interest to note that  $\text{Ca}^+(\text{g})$  is stable with respect to disproportionation into  $\text{Ca}(\text{s})$  and  $\text{Ca}^{2+}(\text{g})$ . Consequently, in weakly solvating media  $\text{Ca}^+(\text{soln})$  may be stable relative to disproportionation.
20. Le blanc, M. and Harnapp, O., *Z. physik. Chem.* (1933) A166, 321.
21. Jakuszewski, B. and Taniewska-Osinska, S. *Roczniki. Chem.* (1962) 36, 329.
22. Gordon, A.Z. and Rock, P.A. unpublished results.
23. Stahl, W. and Wendt, I., *Earth Plant. Sci. Letters* (1968) 5, 184.
24. Heumann, K.G. and Lieser, K.H., *Z. Naturforsch* (1972) 27b, 126. Heumann, K.G., *Z. Naturforsch* (1972) 27b, 492.
25. Bigeleisen, J. and Mayer, M.G., *J. Chem. Phys.* (1947) 15, 261.
26. Bigeleisen, J., "Proceedings of the International Symposium on Isotope Separation" (North-Holland Pub. Co., Amsterdam, 1958) pp. 121-157.
27. Snyder, D.D. and Montgomery, D.J., *J. Chem. Phys.* (1957) 27, 1033
28. Martin, D.L., *Physica* (1959) 25, 1193.
29. Gray, D.E., "American Institute of Physics Handbook" (McGraw-Hill Book Co., New York, N.Y., 1963) 2nd. ed. pp. 4/82.
30. Lewis, G.N. and Randall, M. "Thermodynamics" Second Revised Edition (McGraw-Hill Book Co. Inc., New York, N.Y. 1961) Revised by Pitzer, K.S. and Brewer, L. p. 659.
31. Hill, T.L., "Introduction to Statistical Thermodynamics" (Addison-Wesley, Pub. Co., Reading, MA., 1960) p. 100.
32. Born, M. and Huang, K. "Dynamical Theory of Crystal Lattices" (Oxford U.P., London, 1940)
33. de Launay, J., *Solid State Phys.* (1957) 2, 220.
34. Fine, P.C., *Phys. Rev.* (1939) 56, 355.
35. Bauer, E., *Phys. Rev.* (1953) 92, 58.
36. Nash, H.C. and Smith, C.S., *Phys. Chem. Solids* (1959) 9, 113.
37. Hall, J.D., Silvester, L.F., Singh, G., and Rock, P.A., *J. Chem. Phys.* (1973) 59, 6358.
38. Kellermann, E.W., *Philos. Trans. R. Soc. Lond.* (1940) A238, 513.
39. Kellermann, E.W., *Proc. R. Soc.* (1941) A178, 17.
40. Sayre, E.V. and Beaver, J.J., *J. Chem. Phys.* (1950) 18, 585.
41. Karo, A.M., *J. Chem. Phys.* (1959) 31, 1489.
42. Herzberg, G., "Molecular Spectra and Molecular Structure II. Infrared and Raman Spectra of Polyatomic Molecules", (Van Nostrand Co. New York, 1964) p. 534.

43. Jones, W.J. in "Infrared Spectroscopy and Molecular Structure," Davies, M. (Ed.) (Elsevier, New York, 1963) p. 160.
44. Bigeleisen, J., "Proceedings of the International Symposium on Isotope Separation" (North-Holland Pub. Co., Amsterdam, 1958) pp. 121-157.
45. Burgiel, J.C., Meyer, H., and Richards, P.L., J. Chem. Phys. (1965) 43, 4391.
46. Narten, A.H., Vaslow, F. and Levy, H.A., J. Chem. Phys. (1973) 58, 5017.
47. Herzberg, G., "Molecular Spectra and Molecular Structure II. Infrared and Raman Spectra of Polyatomic Molecules" (Van Nostrand, New York, 1964) p. 235.
48. Halevi, E.A., Israel J. Chem. (1971) 9, 385
49. Heinzinger, K. and Weston, R.E., J. Phys. Chem. (1964) 68, 744.
50. Heinzinger, K. and Weston, R.E., J. Phys. Chem. (1964) 68, 2179.
51. Kingerley, R.W. and La Mer, V.K., J. Amer. Chem. Soc. (1941) 63, 3256.
52. Swain, C.G. and Bader, R.F.W., Tetrahedron (1960) 10, 182.
53. O'Ferrall, R.A.M., Koeppl, G.W., and Kresge, A.J., J. Amer. Chem. Soc. (1971) 93, 1,9.
54. Van Hook, W.A., J. Phys. Chem. (1968) 72, 1234.
55. Eigen, M. and DeMaeyer, L., Proc. R. Soc. London (1958) Ser A, 247,505.
56. Nash, C.P., Donnelly, T. and Rock, P.A., unpublished results.

## Isotope Effects and Reaction Mechanisms

V. J. SHINER, JR.

Department of Chemistry, Indiana University, Bloomington, Ind. 47401

### Introduction

The subject of this contribution is so extensive, mature and well-developed that one can only hope in the space available here to give the non-specialist some general knowledge of the utility, the scope and the limitations of the use of isotope rate effects in the study of reaction mechanisms and an introduction to the more detailed literature for those who may wish to delve deeper. It is very much to be hoped that this technique will come into occasional, if not regular, use by all who undertake the investigation of reaction mechanisms and will not be considered to lie mainly in the province of those who make it a specialty. Probably the main barrier to more general use of this technique is the somewhat refined accuracy generally required in the measurement of reaction rates or in the measurement of isotope ratios if the competitive technique is used. These experimental requirements can be mastered reasonably readily with the more sophisticated commercial instruments which are now generally available. I do not intend here to discuss experimental techniques but rather the general framework for the interpretation of results which has been built up by many investigators over the course of the last twenty-five or so years. (1)

The earlier contributors to this symposium have outlined the basic theory of the interpretation of the effects of isotopic substitution on reaction rates originally developed independently by Bigeleisen and Mayer (2) and Melander. (3) They showed that it is the geometrical structure, nuclear masses and, most importantly, the vibrational force fields of initial and transition states that determine the magnitude of isotope effects on reaction rates.

Since these properties of the initial state reactants are subject to reasonably direct observation or derivation, the reaction mechanisms chemist uses experimentally measured isotope effects on reaction rates principally as a probe for features of the transition state vibrational force field. Primarily through



the efforts of Wolfsberg and Stern (4, 5, 6) computer programs are available which allow the calculation of expected isotope rate effects from completely specified structures and force fields of reactant and transition states containing up to 30 atoms. This kind of detailed modelling has been seriously investigated for only a relatively small number of real reactions. (7, 8, 9, 10) Such analyses are crucial to a greater understanding of the precise details of reactions but presently this aspect of the subject is still in its infancy and very much in the province of specialists. Rather than review these quantitative results I will here try to illustrate some of the general qualitative features of the theoretical analysis that can be used by reaction mechanisms chemists along with other elements of their traditional armamentarium to distinguish among a priori mechanistic possibilities.

The traditional reaction mechanisms chemist is at somewhat of a disadvantage thinking in terms of transition state force fields and/or vibration frequencies because most other techniques familiar to him do not relate directly to force fields but to such "electronic" properties as total energy, electron distribution, dipole moment or geometric structure. Of course all of these things are related through fundamental theory, but so far quantum mechanical calculations have not yielded very successful explanations of such things as the effects of substituents on reaction rates of organic compounds. Neither have they yet provided very accurate force constants for hypothetical transition states, but I think it is reasonable to hope for progress toward this goal and I would encourage theoreticians to give more thought and effort to the calculation of molecular force constants. Success in these efforts would greatly assist in the mechanistic interpretation of isotope effects.

### Primary Isotope Effects

If we consider the dissociation of a diatomic molecule, the energetics of the system can be qualitatively represented as in figure 1, wherein it is assumed for purposes of simplicity that the temperature is low enough so that all molecules are in their lowest vibrational state and therefore contain the zero point vibrational energy. Since, by the Born-Oppenheimer approximation the molecular energy and therefore the interatomic restoring forces depend only on nuclear and electronic charges and not on the nuclear masses, the vibrational force constants will be the same for both isotopic molecules. However, the heavier molecule,  $^2\text{A-B}$  will vibrate more slowly, as expected from Hook's Law, than the lighter molecule  $^1\text{A-B}$ . Since the zero point energy is proportional to the vibration frequency,  $^2\text{A-B}$  rests lower in the potential well than  $^1\text{A-B}$  and requires a higher "activation energy" to raise it to the dissociated state. It therefore should on the average attain that state at a slower rate than the lighter molecule and we expect a normal isotope rate effect, i. e., the lighter molecule reacts faster.

Of course, translational and rotational partition functions are usually different for molecules differing in isotopic substitution and, in general, will change on activation, leading to effects on reaction rates. Kinetic isotope effects from these sources are, however, generally dominated by the vibrational zero-point energy effects which are the main focus of all general, qualitative discussions.

This simply explains the occurrence of a primary isotope rate effect, "primary" referring to the fact that the rate determining step involves a bond to the isotopically substituted atom. However, many reactions which show large primary isotope effects do not involve dissociation into free particles but rather are displacement reactions wherein the isotopic atom is abstracted by an attacking agent. Since the isotopic atom is bound both in reactant and product and is bound also in the transition state, how can the occurrence of large isotope effects in such processes be explained?

This can be seen with the aid of figure 2 wherein the zero point energy levels are depicted qualitatively for diatomic initial and final states and for the triatomic "abstraction" transition state. (The inclusion of bending modes for the transition state is necessary, of course, in a rigorous treatment but will be ignored for simplicity in the qualitative argument.)

The stretching motions of the triatomic transition state can be visualized in the same way that one would visualize the stretching modes for a stable molecule, except that, from transition state theory, we expect one of these modes to have no restoring force but rather to be replaced by a translation in one direction to give products and in the other direction to give reactants. The arrows in the center of the figure represent the atomic movements expected for triatomic molecular stretching motions. The symmetrical stretch,  $\nu_S$ , has a restoring force and is a normal vibrational mode of the transition state. One intuitively knows this because if there were no restoring force for this motion it would continue indefinitely with the resulting dissociation of all three atoms giving a reaction which is not the abstraction process. The asymmetrical stretching mode expected for a normal molecule is, for the triatomic abstraction transition state, the reaction coordinate; in this motion in one direction,  $\nu_A$ , the CA bond contracts while the AB bond stretches, there is no restoring force and the continuation of this translation produces products; the reverse of this motion,  $\nu_B$ , produces reactants. It is important to note that if the transition state is symmetrical with the force of attraction between A and B equal to that between A and C and if the masses of B and C are equal, the frequency of the symmetric stretching mode will be the same for both isotopes of A, since A will not move in this vibration. Even if the transition state is not quite symmetrical the motion of A in the symmetrical stretching vibration will be relatively

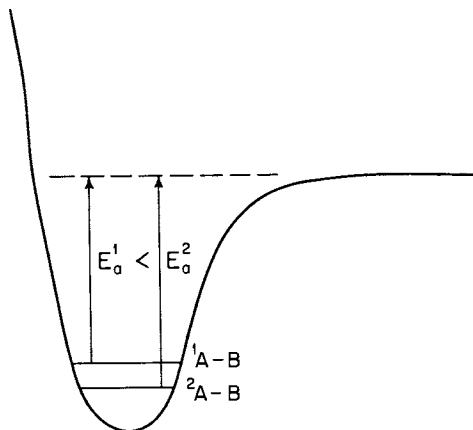


Figure 1. Dissociation of a diatomic molecule.  ${}^1\text{A} - \text{B} \rightarrow {}^1\text{A} + \text{B}$ .

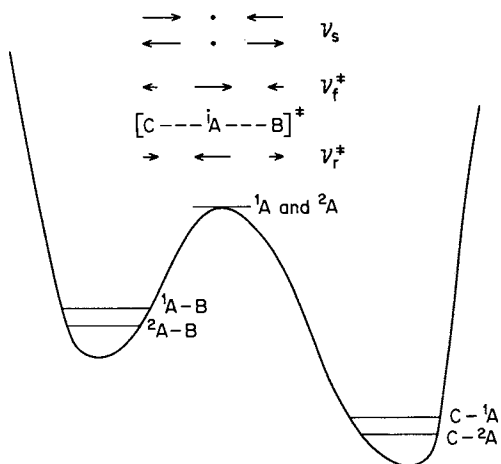


Figure 2. Abstraction reactions.  $\text{C} + {}^1\text{A} - \text{B} \rightarrow \text{C} - {}^1\text{A} + \text{B}$ .

unimportant and the zero point energy difference between the isotopic molecules will be small. Thus, for the symmetrical isotopic transition states in the abstraction reaction, there is no difference in zero point energies and one expects a large primary isotope effect because the difference in zero point energies in the initial state contributes to make the activation energy for the lighter isotope smaller than that for the heavier isotope. This analysis has always appealed to me as one of the nicest experimental demonstrations of the major hypothesis of transition state theory. The primary isotope effect shows that the transition state has a translational degree of freedom which replaces a vibrational one expected in a normal molecule.

Thus, whether the reaction involves a dissociation or a transfer, a simple diatomic molecular model can give useful semi-quantitative results indicative of the typical large primary isotope effects which might be observed for a simple bond cleavage. Some values calculated in this way are shown in Table 1. (11) In most cases primary isotope effects about this size have been observed, and results of this magnitude are taken as *prima facie* evidence that the isotopically substituted bond is being broken in the rate-determining step.

There is another obvious qualitative problem that immediately arises in examining any reasonably large collection of primary isotope effect data, particularly results on isotope effects in hydrogen transfer reactions. This is that many isotope effects in abstraction reactions are much smaller than the expected maxima. One explanation, due to Westheimer (12) and to Melander, (13) as to how this can arise is illustrated qualitatively in figure 3. In a very exergonic reaction, the reaction coordinate involves a stretching type motion in which A and B together move toward C. The stretching motion,  $v_a$ , is perpendicular to the reaction coordinate, has a restoring force, and involves the motion of the isotopic atom; hence there is a zero point energy difference in the stretching mode in the transition state between the two isotopic molecules and an activation energy difference that is less than the maximum. In the extreme, one could look at this as a diffusion controlled reaction with the approach of C to the A-B unit as the reaction coordinate and the internal vibration of A-B in the transition state being unaffected by C. This analysis suggests that primary isotope effects in a series of related reactions will vary with reactivity; the maximum effect being found for nearly thermoneutral reactions having transition states which are nearly symmetrical and increasingly smaller effects being exhibited by processes either increasingly endergonic or increasingly exergonic. Such behavior has apparently been found for both proton abstractions and for hydrogen atom abstractions. This would seemingly limit the utility of the primary isotope effect as a criterion of mechanism, but in practice one usually knows when to expect the occurrence of such asym-

Table I. Calculated Isotope Effects <sup>a, b</sup> for Diatomic Molecular Dissociation Model

Isotopic molecules		$\bar{\nu}_1$	$\bar{\nu}_2$	$\nu_{1L}/\nu_{2L}$	$k_1/k_2(25^\circ)$	$k_1/k_2(200^\circ)$
1	2					
C- <sup>1</sup> H	C- <sup>2</sup> H	3015	2212	1.36	6.93	3.39
C- <sup>12</sup> C	C- <sup>13</sup> C	1129	1107	1.020	1.055	1.036
C- <sup>12</sup> C	C- <sup>14</sup> C	1129	1088	1.038	1.109	1.069
C- <sup>14</sup> N	C- <sup>15</sup> N	1134	1116	1.016	1.044	1.029
C- <sup>16</sup> O	C- <sup>18</sup> O	1113	1086	1.025	1.068	1.045
C- <sup>32</sup> S	C- <sup>34</sup> S	915	908	1.008	1.018	1.013
C- <sup>35</sup> Cl	C- <sup>37</sup> Cl	804	798	1.007	1.014	1.010

<sup>a</sup>These results have been calculated using the equation (11)

$$k_1/k_2 = \sinh \frac{hC\nu_1}{2kT} \div \sinh \frac{hC\nu_2}{2kT} . \text{ For } \bar{\nu} \text{ measured in } \text{cms}^{-1} \text{ and } T \text{ in } ^\circ\text{A}; \frac{hC\bar{\nu}}{2kT} = \frac{0.71929\bar{\nu}}{T}$$

These calculations are especially easy to perform with one of the new "electronic slide rule" pocket calculators if it has a "hyperbolic sine" key. For such an approximation one only needs to know the isotopic masses and the approximate vibration frequency for one of the isotopic molecules; the frequency for the second isotopic molecule can be calculated from that for the first and the reduced mass relationship, e. g.:

$$\nu_{CD} = \nu_{CH} \left( \frac{(m_C + m_D) / m_C \cdot m_D}{(m_C + m_H) / m_C \cdot m_H} \right)^{1/2} = \nu_H \left( \frac{14 \cdot 12 \cdot 1}{12 \cdot 2 \cdot 13} \right)^{1/2} = \nu_H \cdot 0.73380$$

Since the reduced mass relationship assures that the ratio of frequencies for heavy and light molecules will be very nearly correct, any error in the estimated frequency will in general cause only an approximately proportional error in the logarithm of the calculated isotope effect so that the frequency does not have to be estimated with high precision to get reasonable answers.

<sup>b</sup>The examples cited assume that the atoms are held together by a single bond; calculations for examples with multiple bonds could be carried out using the appropriate frequencies.

metrical transition states as, for example, in the transfer of a proton between bases of strongly unequal basicity. In addition, this effect could be used, for example, to determine the effective basicity of a proton abstracting site in a reaction and to distinguish thereby between alternative transition state models. Bell (14) has pointed out that a plot of hydrogen kinetic isotope effects for a variety of proton transfer reactions vs. the difference in  $pK$  between the two bases shows a central maximum near  $\Delta pK = 0.0$  and decreasing limbs for  $\Delta pK < 0$  or  $> 0$ . An example of this is shown in figure 4 from Bell and Cox (14). Pryor and Kneiff (15) have shown that a similar relationship holds for a series of radicals reacting with thiols if the isotope effects are plotted vs. the heats of reactions.

Sims and coworkers (16) have recently pointed out that carbon transfer processes, such as  $S_N2$  reactions, should also show similar isotope effect behavior. Originally it was believed that carbon isotope effects in  $S_N2$  displacements on carbon might be small because bonding about carbon is qualitatively "preserved" in the transition state. The essence of this, as of any synchronous displacement process, is that the energy bill to be paid for breaking the "old" bond is partially reduced by the energy gained in forming the "new" bond. However, the analysis which we have made here suggests that, for nearly symmetrical transition states, carbon motion should be strongly involved along the reaction coordinate and carbon isotope rate effects should be large. The model calculations of Sims et al. (16) indicate how the effect should vary as the transition state bonding varies. This is shown in figure 5 for the incoming nucleophilic atoms oxygen, chlorine or sulfur displacing chloride ion from benzyl chloride. The upper curves display the  $^{12}C/^{14}C$  effect and the lower curve the  $^{35}Cl/^{37}Cl$  leaving group effects as a function of bond order ( $n_2$ ) of the forming bond, assuming that the breaking bond has bond order,  $n_1$ , equal to  $(1-n_2)$ . Although this general kind of behavior is certainly to be expected, no available experimental evidence supports the existence of a curve with a maximum. Many common  $S_N2$  reactions are probably not many kilocalories per mole away from thermoneutrality so the common observation of  $^{12}C/^{14}C$  effects in the range of 8-12% (17) seems to confirm the existence of near maximal isotope effects in the central region of the plot, but there is as yet no evidence supporting the systematic fall-off with  $n_2 > 0.5$  or  $< 0.5$ . One of the problems in interpreting a wide variety of data on this class of reactions is that big changes in nucleophilicity usually are accompanied by changes in attacking atom. This usually causes big changes both in bonding strength, as reflected in the force constants for normal single bonds, and in mass, which of course has its own effect on transition state symmetry independent of the force constant situation. Thus one needs a carefully designed set of experiments and a companion set of theoretical calculations to appropriately investigate the phenomenon. No doubt we will see results of efforts toward this end in the next few years.

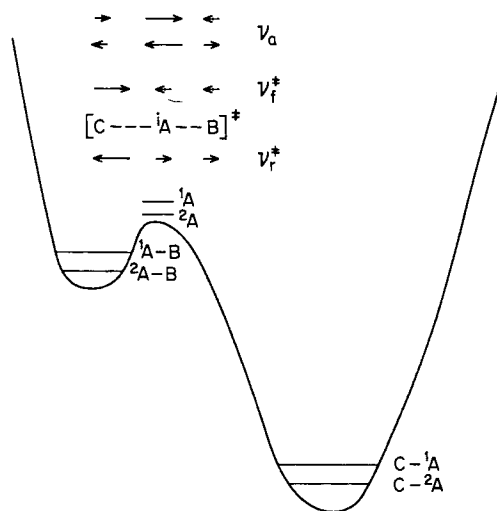
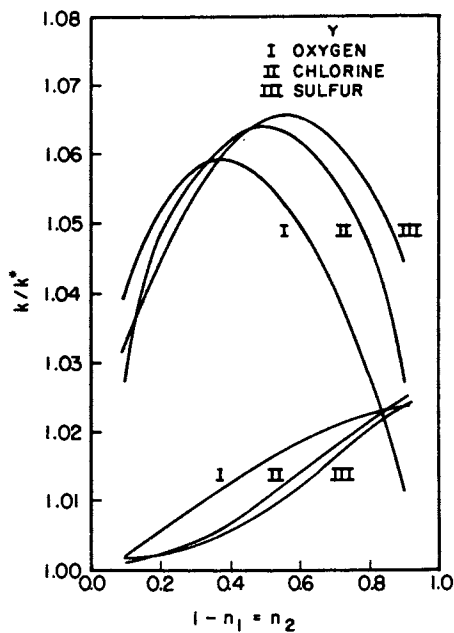
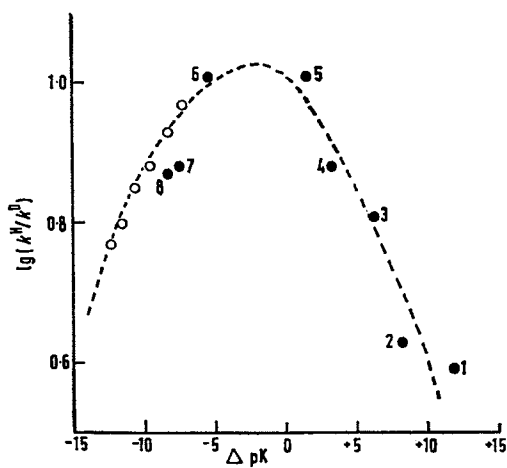


Figure 3. Very exergonic abstraction reaction.  
 $C + {}^1A - B \rightarrow C - {}^1A + B.$



Chemical Reviews

Figure 4. Relations between the primary isotope effect ( $k_H/k_D$ ) and the  $pK$  difference between the reacting bases in proton transfer



Journal of the Chemical Society, Part B

Figure 5. Calculated carbon-14 (upper curves) and chlorine-37 (lower curves) isotope effects for displacement on benzyl chloride by oxygen, chlorine, and sulfur as a function of bond order



### Secondary Isotope Effects

Having, thus far, given a very brief survey of the general shape of the theory and results on primary isotope effects in thermal reactions, I would like next to turn to secondary isotope effects. Here, for the sake of simplicity and brevity, I will confine my examples to the isotopes of hydrogen, since secondary isotope effects are usually so small that their reliable observation is difficult and they have been reported for isotopes other than those of hydrogen in only a few instances. It is convenient to divide secondary isotope effects into at least two kinds (one of which could be further subdivided):

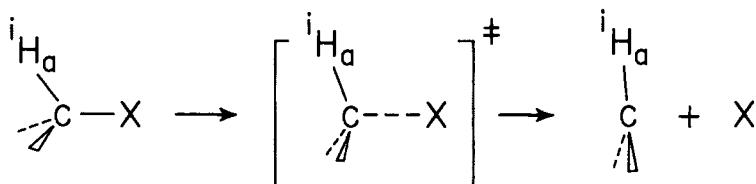
1.  $\alpha$ -effects. The isotopic atom is bound to an atom undergoing bond rupture and/or formation through its other valences. One can readily imagine several possible "sources" of an isotope rate effect in this situation:
  - a. The breaking bond causes a reduction in bending force constant to the  $\alpha$ -substituted isotopic atom.
  - b. A forming bond at the reaction center introduces a new bending force constant to the  $\alpha$ -substituted isotopic atom.
  - c. Rehybridization of the reaction center causes a change in bond strength and therefore a change in bond force constant to the  $\alpha$ -substituted isotopic atom.
  - d. Changes in electron density at the reaction center change the bond strength and bond force constant at the  $\alpha$ -substituted isotopic center.
  - e. A change in steric hindrance at the reaction center changes the force constants at the isotopic atom.
2. The second general kind of secondary isotope effects are those caused by isotopic substitution at positions in the molecule more remote from the reaction center. There are two general possible causes for such effects.
  - a. Electronic or steric intramolecular interactions between isotopic center and reaction center cause force constant differences between initial and transition states.
  - b. "No force constant change" effects could be caused by changes in moments of inertia, or masses or in mechanical coupling of vibrations. Wolfsberg and Stern (4) have shown that these effects generally are expected to amount to no more than a few percent per D atom (replacing H) for example.

Many isotope effects due to substitution of deuterium for hydrogen at positions  $\beta$ - or more remote from the reaction center have been observed. (18) There is only space here to refer the reader to more detailed summaries or to the original literature and to comment that each of the "big three" mechanisms of intramolecular interaction between reaction and isotopic centers has been shown in one case or another to cause isotope effects: 1) Hyperconjugative electron release from a C-H bond causes normal

deuterium isotope effects of the order of  $k_H/k_D = 1.30$  or less per D atom and the effect is qualitatively proportional to the expected change in hyperconjugative demand. 2) Inductive electron acceptance by a C-H bond causes small normal isotope effects (D compound reacting slower than H compound) of a few percent per D or less depending on demand. (19) 3) Increased crowding causes inverse isotope effects, the largest so far observed being around 10% per D. (20) Of course, effects in directions opposite to those enumerated above give the opposite kind of isotope effect i. e., inductive electron release by C-H causes an inverse isotope effect. The interaction effects referred to in each case are those in the transition states relative to the respective initial states.

I would like to take the rest of the space available to discuss some general qualitative theory about  $\alpha$ -d rate effects and some results obtained from the application of this technique to nucleophilic solvolytic substitution reactions.

We can represent the dissociation reaction of a bond having an  $\alpha$ -d substituent as follows:

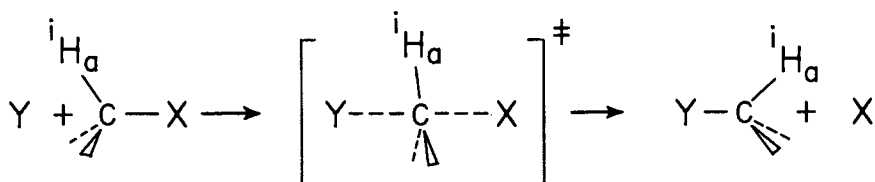


### $\alpha$ - Effect: Dissociation Reaction

The example involves a reacting carbon atom with the attachments to the two other valences unspecified; qualitatively this makes no difference in principle and the same general arguments should hold for other kinds of reacting atoms. As Wolfsberg and Stern (4) have argued, the partial breaking of the C-X bond in the reaction transition state should cause the bending force constant,  $f_{\text{HCX}}^\ddagger$ , in the transition state to be less than that of the initial state,  $f_{\text{HCX}}$ . Thus the zero point energy differences between H and D compounds should be smaller in the transition state (assuming no big changes in the other force constants constraining the H) and the activation energy for the reaction of the H compound should be smaller than that for the reaction of the D compound and a normal isotope effect should result. If we consider a series of related transition states having greater and greater degrees of C-X bond extension we would expect the isotope rate effect to increase with bond extension but to a smaller and smaller degree until a point is reached where the X group no longer has any influence on the transition state vibrations of the  $\alpha$ -H. Thus for reactions of this type the secondary isotope effect

should be a measure of the extent of C-X bond breaking in the transition state, asymptotically approaching some maximum value corresponding to complete bond cleavage. Of course, the maximum effect obtainable would depend on the nature of X and the strength of its bond to C, particularly as reflected in the initial state bending force constant.

For a concerted displacement the situation is similar except that a new bond to the entering group, Y, has been partially formed in the transition state,

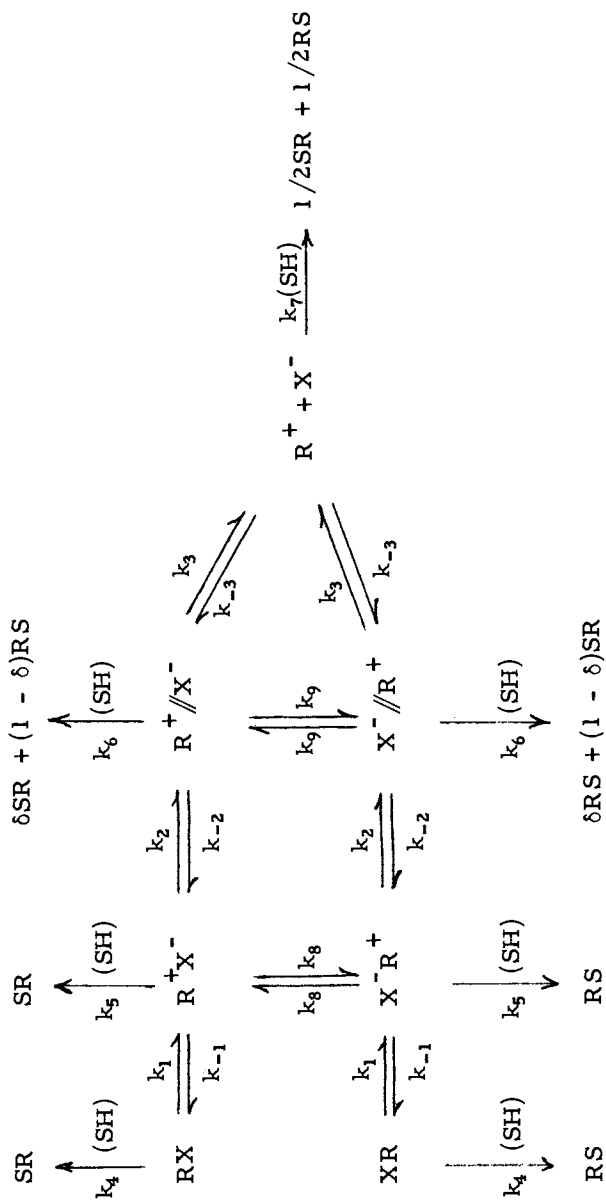


### $\alpha$ -Effect: Concerted Displacement Reaction

In the transition state the force constant,  $f_{\text{HCY}}^\ddagger$ , for the new bond partially, at least, compensates for the reduction in the initial state force constant,  $f_{\text{HCX}}$ , so that one expects the  $\alpha$ -D isotope effect to be significantly lower than that for a simple dissociation.

In the work from my own laboratory over the last ten years or so we have used a combination of experimental measurements on selected reactants and model calculations relating to  $\alpha$ -deuterium effects on the rates of solvolytic nucleophilic displacements on carbon to try to correlate all known results on such reactions in terms of Scheme I.

This is a generalized scheme incorporating the  $S_N1$  and  $S_N2$  mechanisms of Hughes and Ingold with the ideas of Winstein and coworkers and others on the existence of ion pair intermediates in reactions having carbonium ion character. The covalent substrate having a bond between the electronegative leaving group X and carbon is represented by RX; the compound having the opposite configuration at carbon is represented by XR. The  $S_N2$  reaction with a protic solvent nucleophile, SH, is represented by the arrow identified with rate constant  $k_4$ . The other products,  $\text{H}^+$  and  $\text{X}^-$ , are omitted for simplicity but are understood to be formed in this process as well as by the processes with rate constants  $k_5$ ,  $k_6$  and  $k_7$ . The solvolytic substitution product SR is represented as being formed in the  $S_N2$  reaction from react-



Scheme I

ant of the opposite configuration RX. RX can also ionize with a first order rate constant  $k_1$  to produce the tight ion pair,  $R^+X^-$ , visualized as two ions in direct contact. This intermediate can (1) "return" with a first order rate constant  $k_{-1}$  to covalent RX or (2) further separate with a rate constant  $k_2$  to the second carbonium ion type intermediate,  $R^+//X^-$ , the solvent separated ion pair, where  $//$  represents a solvent molecule between  $R^+$  and  $X^-$  or (3) by  $R^+$  rotating relative to  $X^-$  produce  $X^-R^+$ , the tight ion pair of configuration opposite the original tight ion pair or (4) undergo nucleophilic attack by solvent to produce substitution product expected to be of opposite configuration to  $R^+X^-$  because the front side is still "protected" from nucleophilic attack by the close proximity of  $X^-$ . The solvent separated ion pair,  $R^+//X^-$ , can (1) return to  $R^+X^-$ , (2) invert its configuration to  $X^-//R^+$ , (3) dissociate completely to kinetically independent  $R^+$  and  $X^-$  or (4) collapse by nucleophilic solvent attack at front or rear to give both SR and RS, probably in unequal amounts. The free carbonium ion  $R^+$  can (1) return to  $R^+//X^-$  or  $X^-//R^+$  with equal facility by associating with a kinetically free anion  $X^-$  or (2) form SR and RS in equal amounts by nucleophilic attack by solvent. In this scheme it is assumed that a solvent molecule is always reasonably closely positioned to R on front or back or both sides if  $X^-$  does not occupy one or the other of these sites. The effects of added salts, or added non solvent nucleophilies, the incursion of elimination or rearrangement are not included but could readily be so by obvious elaborations of the scheme.

In classifying a mechanism according to this general scheme it is first important to establish which of the several possible steps is the rate determining one and in which step the covalent bond to the incoming nucleophile is formed ("product forming step"). For example, if the reaction goes in the sequence of steps through the tight ion pair ( $R^+X^-$ ) to the solvent separated ion pair ( $R^+//X^-$ ) and then by nucleophilic attack on  $R^+$  to product, the rate determining step could be any of the three labeled with rate constant  $k_1$ ,  $k_2$  or  $k_6$ . The step with rate constant  $k_1$  will be rate-determining if  $k_2 \gg k_{-1}$ . The step with rate constant  $k_2$  will be rate determining if  $k_2 \ll k_{-1}$ , and  $k_6 \gg k_{-2}$ . The step with rate constant  $k_6$  will be rate determining if  $k_{-1} \gg k_2$  and  $k_{-2} \gg k_6$ .

From the point of view of the  $\alpha$ -isotope effect, one can identify three general classes into which all reactions of this mechanistic scheme will fall: (1) the one reaction in which the transition state has two partial covalent bonds to carbon, i. e., the  $S_N2$  reaction labeled with rate constant  $k_4$ . The  $\alpha$ -effect in this type of reaction should be low (see above). (2) Reactions in which the transition state has one partial covalent bond to carbon. These include those reactions with rate determining steps labeled with  $k_1$ ,  $k_5$ ,  $k_6$  and  $k_7$ . The  $\alpha$ -isotope effect in these types of reactions should be large but not at the maximum. (3) Reactions in which the transition state has no partial covalent bonds to car-

bon. These include the reactions with rate determining steps labeled  $k_2$ ,  $k_8$ , and  $k_9$ . The isotope effects in all of these type reactions should be at the maximum.

It is further important to realize that the maximum isotope effect will depend on the nature of the leaving group X and that the reactions in classes 1 and 2 above will show isotope effects that will, to some extent, depend on reactivity and (except for cases where the step labeled  $k_1$  is rate determining) on the nature of the incoming nucleophile. Of course, it is to be expected that many reactions will not clearly have one step as completely rate determining but might, for example, if  $k_{-1} \sim k_2$  have  $k_1$  and  $k_2$  both partly rate-determining.

In our efforts to classify a variety of reactions by the above scheme and to determine what range of  $\alpha$ -d effects apply for different mechanisms we have studied (18) examples including simple alkyl,  $\alpha$ -phenyl ethyl, benzyl and propargyl compounds having halide and sulfonate leaving groups in solvents ethanol-water, trifluoroethanol-water and more recently trifluoroacetic acid-water.

In Table 2 are shown the maximum values for the  $\alpha$ -d effects which we believe apply for the different leaving groups studied. For each of these leaving groups, effects of the size indicated have been observed in one or more reactions which show all of the characteristics of the Ingold  $S_N1$  or the Winstein Lim classification.

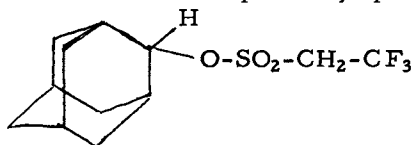
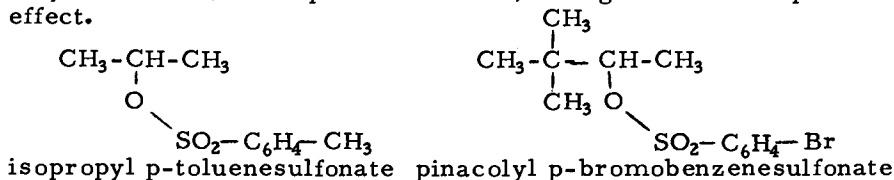
Table 2. Approximate Maximum  $\alpha$ -deuterium Rate Effects for Different Leaving Groups Attached to Saturated Carbon

Leaving Groups	-OSO <sub>2</sub> R	-Cl	-Br	-I
$k_H/k_{\alpha D}$	1.23	1.16	1.12	1.09

All of the reactions so far studied which show these maxima have been classified as involving rate determining formation of the solvent separated ion pair followed by nucleophilic attack. Reactions going via free carbonium ions are much rarer, and although they undoubtedly exist, we have not measured  $\alpha$ -d effects for any of them.

We have also studied reactions classified as having the step labeled with  $k_1$ , or the step labeled with  $k_5$ , rate determining. These reactions show  $\alpha$ -d effects about 2/3 rds or 3/4 ths of the listed maximum values. In addition, a number of reactions which we have examined seem to clearly involve  $S_N2$  attack by solvent,  $k_4$ , and to show isotope effects between 0.96 and 1.06 with reactions involving the iodide leaving group falling in the lower end of the range and those with a sulfonate group in the upper end.

Classically, one of the most interesting problems in solvolysis mechanisms relates to the reactions of secondary alkyl sulfonates. Therefore, I will choose three examples from this group of compounds to illustrate the kinds of conclusions which we derive from the study of  $\alpha$ -deuterium isotope rate effects. The esters are those of the isopropyl, pinacolyl (3,3-dimethyl-2-butyl) and 2-adamantyl groups; to obtain convenient reaction rates in the range of solvents involved we have used p-toluenesulfonate, p-bromobenzenesulfonate and 2,2,2-trifluoroethanesulfonate esters. We have shown, in at least one of the solvents involved, that a change among these three leaving groups causes only a few tenths of a percent of less, change in the isotope effect.



2-adamantyl trifluoroethanesulfonate

The rates of solvolysis of one or more of the three sulfonate esters of each of these three alkyl groups have been measured in ethanol-water, 2,2,2-trifluoroethanol-water and trifluoroacetic acid-water solvents. In addition, the corresponding  $\alpha$ -deuterio esters have been synthesized and their solvolysis rates measured under identical conditions. For ethanol-water and trifluoroethanol water mixtures the rates were measured conductimetrically and the first order rate constants obtained with an electronic computer using a doubly weighted non-linear least squares routine. (21) The reactions were followed for about two half-lives starting at about  $10^{-3}$  M initial concentration and taking a total of about 150 readings for each reaction. The standard errors in the rate constants and the reproducibility are both of the order of 0.1%. The rates of solvolysis in trifluoroacetic acid were measured using a Cary 118 ultraviolet spectrophotometer and following the reduction in the ester absorbance around 270 nm. from about 1.2 o. d. to about 0.7 o. d. at an initial concentration about  $3 \times 10^{-3}$  molar. (22) A computer program similar to that mentioned above was used to obtain the first order rate constants from around 200 readings per reaction. Standard errors and reproducibility in trifluoroacetic acid are only around 1%. apparently because the reactions are not precisely first order. In Table 3 are given the isotope effects expressed as the ratio of the first order rate constants for hydrogen and deuterium

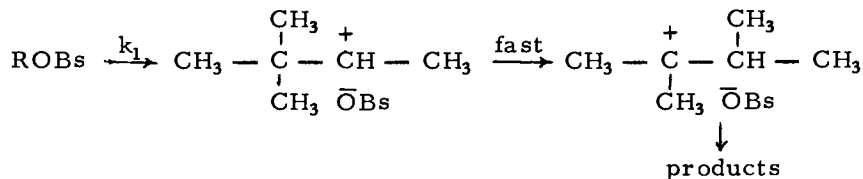
Table 3.  $\alpha$ -d Effects and Relative Rates of Solvolyses at 25°<sup>a</sup>

Solvent <sup>b</sup>	Isopropyl Sulfonates <sup>c</sup>		Pinacolyl Sulfonates <sup>c</sup> k/k <sub>ad</sub>	2-Adamantyl Sulfonates <sup>d</sup>	
	k <sub>H</sub> /k <sub>ad</sub>	k/k <sub>pin</sub> <sup>d</sup>		k <sub>H</sub> /k <sub>ad</sub>	k/k <sub>pin</sub> <sup>d</sup>
90E	1.08	3.35	-	-	-
50E	1.11	0.714	1.159	1.225	0.0315
97TFE	1.16	0.026	1.153	1.228	0.0595
99TFA	1.22	0.0041	1.16	1.22	0.207

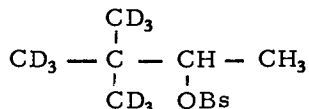
<sup>a</sup> From references 22, 23, and 24. <sup>b</sup> 90E is 90 vol. % ethanol, 10 vol. % water; 50E is 50 vol. % ethanol, 50 vol. % water; 97TFE is 97 wt. % 2,2,2-trifluoroethanol, 3 wt. % water; 99TFA is 99 vol. % trifluoroacetic acid, 1 vol. % water. <sup>c</sup> The sulfonate esters used were: in 90E the p-bromobenzenesulfonate; in 50E and 97TFE isopropyl-p-bromobenzenesulfonate and 2,2,2-trifluoroethanesulfonate, pinacolyl p-bromobenzenesulfonate and 2-adamantyl 2,2,2-trifluoroethanesulfonate; in 99TFA, isopropyl and p-bromobenzenesulfonate, pinacolyl p-toluenesulfonate and 2-adamantyl p-toluenesulfonate and p-bromobenzenesulfonate. <sup>d</sup> Rate relative to that of the corresponding pinacolyl ester.

compounds in four different solvents, and, for isopropyl and adamantyl esters, the ratio of their solvolysis rates to the corresponding faster solvolyzing pinacolyl esters. The results in the four solvents are interesting to compare because on progression through the series, 90 vol. % ethanol, 50 vol. % ethanol, 97 wt. % trifluoroethanol, 99 vol. % trifluoroacetic acid, the tendency towards slower nucleophilic reactions and more facile carbonium ion forming reactions becomes more and more pronounced. Adding water to ethanol affects the reaction primarily through increasing the solvent dielectric constant and its ability to ionize covalent bonds. Trifluoroethanol is about 1000 times less basic than ethanol or water (and therefore less nucleophilic) but it is nevertheless a good ionizing solvent because of its ability to stabilize anions by hydrogen bonding. (25) In trifluoroacetic acid these trends are extended considerably further. (26) Despite this wide range of nucleophilicity and ionizing ability we find that pinacolyl esters show almost the same  $\alpha$ -d effect on the solvolysis rate in each solvent! We have argued (23) that the esters of this alcohol all react by the same mechanism in each of these solvents and that this involves rate-determining formation of the tight ion pair; this tight ion pair does not return but rather rearranges rapidly by methyl migration to form the tertiary carbonium ion pair:





The tertiary carbonium ion is so much more stable than the secondary ion that it does not return but forms products. Essentially all of the products found are those of rearranged carbon skeletal structure. Return to the secondary structure seems highly improbable since all reactions which are expected to go through the pinacolyl cation structure never give significant yields of pinacolyl derivatives but always yield products of rearranged carbon skeletal structure. The only question which seems arguable about this mechanism is whether or not rearrangement is concerted with ionization; if so, it is expected to accelerate ionization but relative rate comparisons in several solvents (see below) do not suggest accelerated rates. Also, the  $\gamma$ - $d_9$  derivative does not show an appreciable isotope effect. (23) If a  $\text{CD}_3$  group were migrating in the rate-determining step



the HCC bending force constants should be lower in the transition state and an isotope effect should be observed. In any event, the extent of participation by methyl during ionization should be quite small, if not entirely absent. The  $\alpha$ - $d$  rate effect on pinacolyl sulfonate solvolyses are seen to be constant at 1.15 - 1.16 for all four solvents listed in Table 3. 2-Adamantyl sulfonates on the other hand, do not rearrange appreciably during solvolysis, apparently because to do so would introduce significant ring strain into the relatively strainless structure. They are also not readily subject to nucleophilic attack because the compact tricyclic structure hinders nucleophilic approach from the rear. Thus we believe that 2-adamantyl sulfonate esters undergo ionization to the tight ion pair and return, with rate determining formation of the solvent separated ion-pair which is nucleophilically attacked to form product. The  $\alpha$ - $d$  effects for 2-adamantyl sulfonates in the solvents shown in Table 3 are all in the range 1.22 - 1.23 (24) It is interesting to note that the 2-adamantyl sulfonates react from five to 32 times slower than corresponding pinacolyl esters. One would expect the adamantyl esters to ionize somewhat faster because the adamantyl structure has four carbon atoms in the gamma position relative to the reaction center (two on each side) while pinacolyl has only three. The corresponding difference in inductive effect on ionization should

contribute a factor of around two to the ionization rate ratio leading to estimated ratios of internal return to solvolysis for the 2-adamantyl derivatives of  $\sim 10$  in 99% trifluoroacetic acid,  $\sim 34$  in 97% trifluoroethanol and  $\sim 65$  in 50% ethanol. If pinacolyl solvolyses were accelerated by rearrangement these factors would be even smaller; the factor of  $\sim 10$  in TFA certainly could not be much smaller without causing  $k_1$  to be partly rate determining for 2-adamantyl and causing the  $\alpha$ -d effect to be lower than 1.22. Thus, the idea that rearrangement acceleration in pinacolyl ionization is small is reinforced. Return from 2-adamantyl tight ion pairs is probably less in TFA than in TFE and still less in ethanol because H-bonding of the more acidic solvent reduces the nucleophilicity of the leaving group and slows its recombination with  $R^+$  relative to the further separation to  $R^+//X^-$ . The situation with the isopropyl sulfonates is especially interesting: a very low  $\alpha$ -d effect, 1.08, is observed in 90% ethanol. This can only mean that an  $S_N2$  reaction is largely, but probably not completely, the reaction pathway. It is significant that in this solvent isopropyl sulfonates react about three times faster than the corresponding pinacolyl esters. Since the isopropyl ester must ionize slower than the pinacolyl ester due to the difference in inductive effects of the substituents, this faster observed rate can only be caused by an  $S_N2$  process. In 50% ethanol the isopropyl esters solvolyze at rates comparable to the corresponding pinacolyl esters and show increased  $\alpha$ -d effects. This must be due to the formation and reaction of tight ion pairs in addition to some fraction of  $S_N2$  reaction. In 97% trifluoroethanol the pinacolyl esters react about forty times faster than the corresponding isopropyl esters and the  $\alpha$ -d isotope effect for the isopropyl esters rises to 1.16. In this solvent the reaction must be going almost exclusively through tight ion pairs and the only way that the isopropyl compounds can be reacting so much slower is for the ion pairs to be undergoing return about four times more rapidly than they are nucleophilically attacked. In trifluoroacetic acid the very low nucleophilicity of the solvent reduces the rate of nucleophilic attack on the tight ion pairs of the isopropyl sulfonate esters so much that the rate of ester solvolysis is now 244 times slower than the rate of solvolysis of the corresponding pinacolyl esters, suggesting that internal return takes place about twenty times faster than solvolysis. In addition, in this solvent, attack on the tight ion pair is so slow that the rate determining step is now separation of the isopropyl sulfonate tight ion pair to the solvent separated ion-pair and the  $\alpha$ -d effect is 1.22, the same as observed for 2-adamantyl sulfonates in all three solvents! Thus isopropyl sulfonate solvolyses are truly "borderline" in character and can shift over a range of mechanisms with different solvents. There are many other observations which buttress these interpretations but no need or space to go into more detail here. It is hoped that these illustrations will show, in part at least, how secondary deuterium isotope

rate effects can be used in the intricate process of sorting out reaction mechanistic pathways. Because isotopic substitution involves a minimal perturbation of the reacting system and because of the solid basic theory underlying our understanding of these effects they allow us an unparalleled tool with which to attack mechanistic problems. I hope that this brief review has conveyed some flavor of the intellectual adventure and satisfaction which can be involved in such studies.

Acknowledgment The preparation of this paper and the new results reported here were supported in part by grant GP 32854 from the National Science Foundation. The author wishes to thank Dr. W. E. Buddenbaum and Mr. Richard Seib for reading the manuscript before publication and for valuable discussion and suggestions. Thanks are also due to The Chemical Society, London for permission to reproduce figure 4.

## Literature Cited

1. For a more detailed discussion of theory and the interpretation of results from a variety of reactions see: "Isotope Effects in Chemical Reactions", C. J. Collins and N. S. Bowman, eds., Van Nostrand Reinhold, New York, 1970 and references cited therein.
2. Bigeleisen, J. and Mayer, M. G., *J. Chem. Phys.*, (1947), 15, 261.
3. Melander, L. *Arkiv. Kemi.*, (1950), 2, 211.
4. Wolfsberg, M. and Stern, M. J., *Pure Appl. Chem.*, (1964), 8, 225.
5. Wolfsberg, M. and Stern, M. J., *Pure Appl. Chem.*, (1964), 8, 325.
6. Wolfsberg, M. and Stern, M. J., *J. Pharm. Sci.*, (1965), 54, 849.
7. Bigeleisen, J., *Can. J. Chem.*, (1952), 30, 443.
8. Willi, A. V., *Can. J. Chem.*, (1966), 44, 1889.
9. Katz, A. M. and Saunders, W. H., Jr., *J. Amer. Chem. Soc.*, (1969), 91, 4469.
10. Williams, R. C., and Taylor, J. W., *J. Amer. Chem. Soc.*, (1974), 96, 3721.
11. Melander, Lars, "Isotope Effects on Reaction Rates," pg. 12, Ronald Press, New York, 1960. The approximations involved are also discussed on pg 35. See also ref. 6, pg. 850, equation 6:  
$$k_1/k_2 = \frac{\nu_1 L}{\nu_2 L} \times (VP) \times (EXC) \times (ZPE)$$

For the diatomic model  $(VP) = (\nu_2 L / \nu_1 L)$   
Therefore,  
 $k_1/k_2 = (EXC) \times (ZPE) = \sinh 1/2 u_1 \div \sinh 1/2 u_2$ ,  
where  $u = h\nu / kT$ .
12. Westheimer, F. H., *Chem. Rev.*, (1961), 61, 265.
13. Melander, L. "Isotope Effects on Reaction Rates," pps. 24-32, Ronald Press, New York, 1960.
14. Bell, R. P. and Cox, B. G., *J. Chem. Soc., B*, (1971), 783.

# 9

## Isotope Chemistry and Biology

JOSEPH J. KATZ, ROBERT A. UPHAUS, and HENRY L. CRESPI  
Chemistry Division, Argonne National Laboratory, Argonne, Ill. 60439

MARTIN I. BLAKE

Department of Pharmacy, University of Illinois, College of Pharmacy, Chicago, Ill. 60612

### I. Introduction

The past decade has seen a keen and growing interest in the application of stable isotopes to chemical and biological problems (1,2). There have been three main driving forces for this interest: (a) The applications of magnetic resonance techniques to many complex chemical and biological problems are greatly facilitated by judicious use of stable isotopes; (b), the utility of gas chromatographic-mass spectrometric techniques in metabolic and environmental tracer studies is greatly enhanced by adjustment of the isotopic composition; and, (c), the availability of fully deuterated compounds and organelles from fully deuterated microorganisms (3) has made possible the investigation of many refractory problems of biological interest. These, together with an ever increasing availability of  $^{13}\text{C}$ ,  $^{15}\text{N}$ ,  $^{18}\text{O}$  and depleted  $^{12}\text{C}$  and  $^{14}\text{N}$  in high isotopic purity have triggered a wide response (4). Despite the many uses to which stable isotopes can be put, certain inherent limitations still prevail. Deuterium as heavy water is available in large quantities at a relatively low price, but incorporation of deuterium into living organisms can have severe toxic effects on higher plants and animals because of possible large kinetic isotope effects (5). The heavy isotopes of carbon, nitrogen and oxygen are far less toxic to living organisms than is deuterium, but the quantities available are limited and the price tends to be quite high.

Hydrogen of mass 2, deuterium, was discovered by Urey and his co-workers in 1932 (6). In the decade following this discovery there developed a large body of often confusing data (7,8) concerning the biology of heavy water. These early studies were interpreted to indicate that deuterium is toxic, and that high

concentrations are fundamentally incompatible with cellular growth and reproduction. However, in 1960, autotrophic fresh-water green and blue-green algae were successfully cultured in heavy water containing 99.7 atom percent  $^2\text{H}$ . This work was shortly followed by the cultivation of a wide variety of fully deuterated heterotrophic microorganisms (3,8). These successes led to a considerable effort to achieve full deuteration of higher plants and mammals, but to date these more complex systems have resisted full replacement of  $^1\text{H}$  by  $^2\text{H}$ . Toxic effects in mammals, for example, are apparent even at 10-15 atom percent  $^2\text{H}$  in tissue fluids.

The marked biological effects of deuterium are not observed when  $^{13}\text{C}$  is substituted for  $^{12}\text{C}$ , or  $^{15}\text{N}$  for  $^{14}\text{N}$ . The source of this differential effect is likely the much larger kinetic isotope effect associated with deuterium, as compared to the heavy, stable isotopes of carbon and nitrogen. The substitution of a heavy isotopic species in a chemical bond may change the rate of any reaction that involves scission of this bond. In simple terms, the effect on the reaction rate will depend on the mass ratio of the isotopic atoms in question. Thus, the mass ratio for the hydrogen isotopes,  $^2\text{H}/^1\text{H}$ , is 2, while the  $^{13}\text{C}/^{12}\text{C}$  ratio is only 1.08, and that of  $^{15}\text{N}/^{14}\text{N}$  is only 1.07. Consequently, kinetic isotope effects perhaps an order of magnitude less would be expected for heavy carbon and nitrogen than for heavy hydrogen.

The substitution of  $^2\text{H}$  for  $^1\text{H}$  also affects equilibrium constants, particularly the ionization constants of weak acids and bases dissolved in  $\text{D}_2\text{O}$  (10,11). The rates of acid-base catalyzed reactions may be greatly different in  $^1\text{H}_2\text{O}$  as compared to  $^2\text{H}_2\text{O}$  (2,12). Deuterium substitution will tend to increase slightly the strength of hydrogen bonds, and deuterium has a significantly smaller steric requirement than does  $^1\text{H}$ . Thus, rates of conformational interchange in deuterated biopolymers can be markedly different from those of normal isotopic composition. It is therefore not at all surprising that the overall biological effect of deuterium can be exceedingly complex. The isotopes of carbon and nitrogen may be expected to have qualitatively similar effects, but the magnitude of the effects of these isotopes are generally small enough to be within the range of the normal cellular control mechanisms.

## II. Deuterium

Through the past 45 years, since its discovery in 1930, the stable, rare hydrogen isotope of mass two

(deuterium) has been an increasingly useful tool in chemistry and biology. The history of deuterium has shown a progression from the simple to the complex, from tracer applications to massive substitution, from kinetic isotope effects in simple molecules to isotope effects in living organisms, and from its use to simplify the proton magnetic resonance ( $^1\text{Hmr}$ ) spectrum of ethyl alcohol to the simplification of the  $^1\text{Hmr}$  spectra of proteins. These most recent applications result from the ability to grow algae and other microorganisms in heavy water,  $^2\text{H}_2\text{O}$ , whose hydrogen content is 99.8 atom percent  $^2\text{H}$  and only 0.2 atom percent  $^1\text{H}$ .

Algae. After a succession of failures in other laboratories, Chorney and co-workers (13) succeeded in culturing two species of fresh-water green algae in heavy water. This work was quickly followed by the successful culture of a number of other algae in heavy water. The extraction of organic substrates (14) from these  $^2\text{H}$ -algae then made possible the cultivation of a number of heterotrophic bacteria and fungi in fully deuterated form. Many kinds of algae required a lengthy period of adaptation before routine culture in heavy water was possible. Often a small nutritional supplement (in the form of yeast extract) helped the algae to overcome the problems of total kinetic reorganization in the new culture medium. Near anaerobic conditions were also beneficial, as there were indications that respiration in adapting organisms was uncontrolled. After adaptation, however, the algae grew in a normal manner but at a slower than normal rate. A kinetic isotope effect ( $k_{\text{H}}/k_{\text{D}}$ ) of 3.5 was observed in the light saturated growth rate of several green and blue-green algae. However, because the large-scale production of isotopically-altered algae usually involves growth under light limiting conditions, this large isotope effect is not a major handicap in the production of large amounts of fully deuterated algae.

Deuterium Organisms in Esr. The availability of fully deuterated algae has permitted some significant biological problems to be attacked in new and effective ways. Deuterium had been used as a tool to aid in the simplification and interpretation of electron spin resonance (esr) and nuclear magnetic resonance (nmr) spectra of relatively simple organic molecules for many

years.\* In these cases  $^2\text{H}$  was introduced by chemical synthesis. A similar technique can now be applied to some extremely complex biological molecules. One of the more important results obtained by selective incorporation of  $^1\text{H}$  and  $^2\text{H}$  has been the elucidation of the chlorophyll free radical species that is involved in the light conversion act of photosynthesis (15). ESR studies on  $^2\text{H}$ -chlorophylls and  $^2\text{H}$ -organisms have shown that the free radical species formed by the exciting light is comprised of a pair of chlorophyll molecules arranged in a special configuration which permits them to act as an energy trap.

Deuterated Proteins in Nmr. Deuterated proteins can also serve as the basis for the simplification of the highly complex  $^1\text{Hmr}$  spectra of these molecules. Three basic experiments to this end have been described in the literature (16). (1) An autotrophic organism growing in  $^2\text{H}_2\text{O}$  can be induced to utilize an  $^1\text{H}$ -amino acid; the organism then biosynthesizes  $^2\text{H}$ -protein containing  $^1\text{H}$ -amino acid residues embedded in it; (2), an  $^1\text{H}$  prosthetic group can be bound to a fully deuterated apoprotein, making it possible to detect easily the prosthetic group by  $^1\text{Hmr}$ ; and (3), the slowly exchangeable amide protons can be observed in otherwise fully deuterated proteins by observing the time dependence of the  $^1\text{Hmr}$  spectrum when the protein is dissolved in  $^2\text{H}_2\text{O}$ . We describe here an example of a type (3) experiment, ie., the observation by  $^1\text{Hmr}$  of amide protons in a fully deuterated protein.

The protein resonance lines obtained in an  $^1\text{Hmr}$  experiment are generally quite broad. The large protein molecules tumble slowly in solution, and many dipole-dipole magnetic interactions and chemical shift anisotropies are not averaged out. In general, amide proton resonance peaks in molecules with molecular weights of 10-20,000 daltons have linewidths of the order of 30-35 Hz. However, in a deuterated protein, the dipole-dipole interaction is much decreased and most amide protons have linewidths in the range of 15-18 Hz. These amide protons appear 6 to 11 ppm downfield from tetramethylsilane, and the proton resonances

---

\* $^1\text{H}$  has a spin of  $1/2$  and a magnetic moment of 2.793 nuclear magnetons.  $^2\text{H}$  has a spin of 1 and a magnetic moment of 0.857 nuclear magnetons. Thus, when a deuterium atom is substituted for a protium atom, coupling constants are reduced by a factor of 6.5 and the frequency at which energy level transitions take place is also reduced by a factor of 6.5.



that originate from the aromatic amino acid side chains that are normally present in this region of the  $^1\text{Hmr}$  spectrum are of course absent in the fully deuterated protein. Thus, a clear, well-resolved view of the slowly exchangeable amide protons can be had. These protons are part of the hydrogen-bonded structure of the helix and pleated sheet portions of proteins and thus have considerable structural significance. Figure 1 shows an example of an  $^1\text{Hmr}$  study of amide protons in a deuterated algal ferredoxin.

Deuterated Nucleic Acids. Deuterated algae are a source of deuterated substrates for the growth of bacteria, yeast and molds (14). Deuterated bacteria have been found useful as a source of deuterated nucleic acids for use in ultracentrifugal density gradient analysis of the interactions of homologous DNA molecules. Fully deuterated DNA (all C- $^2\text{H}$  bonds) has a bouyant density  $0.04 \text{ g/cm}^3$  greater than normal (normal DNA's have bouyant densities in the range of  $1.70\text{--}1.71 \text{ g/cm}^3$ ). This technique has been exploited recently in the study of the interaction of bacterial and bacteriophage nucleic acids (17).

Deuterated Metabolites. A number of studies on the production of extracellular metabolites by deuterated organisms have been completed in recent years. These studies have involved the production and characterization of alkaloids (18), antibiotics (19), and the vitamin riboflavin produced by organisms grown in 99.8 atom percent  $^2\text{H}_2\text{O}$  (20). The use of various  $^1\text{H}$  (natural abundance) substrates in conjunction with  $^1\text{Hmr}$  analysis of the product has made it possible to obtain a quantitative assessment of the extent of solvent participation in the biosynthesis of these natural products. As might be expected, heavy water strongly inhibits the production of the extracellular material in all of the experiments. More recently, however, it has been observed that riboflavin production by the fungus Eremothecium ashbyii is stimulated by heavy water (Table 1). Evidently, there is an inverse isotope effect on this particular metabolic pathway.

Higher Plants. The effects of deuterium on higher plants have attracted particular attention. The early literature has been reviewed by Morowitz and Brown (7) and more recently by Flaumenhaft *et al.* (8). The first detailed study of the effects of extensive substitution of hydrogen by deuterium on the growth and development of higher plants was described by Blake *et al.* (21) who

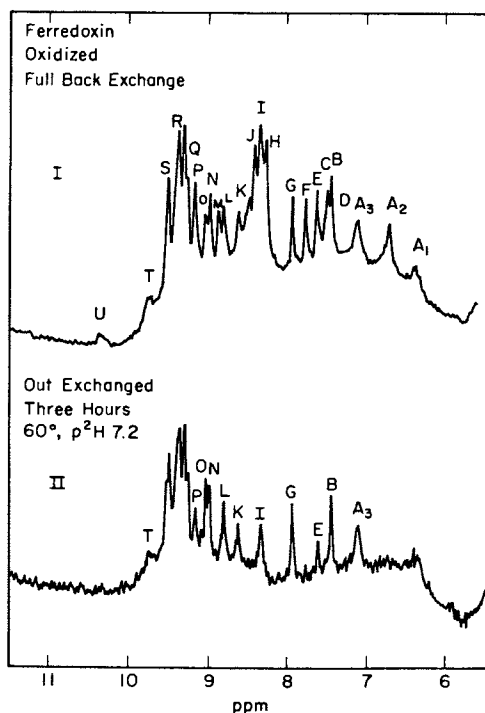


Figure 1. Proton magnetic resonance spectra at 220 MHz (Varian HR 220 spectrometer in the fast fourier transform pulse mode) of fully deuterated algal ferredoxin. About 26 slowly exchangeable protons (Spectrum I) are observable after back exchange in  $^1\text{H}_2\text{O}$  buffer at pH 9. After 3 hrs at  $60^\circ\text{C}$  in  $^2\text{H}_2\text{O}$  buffer, pH 7.2, 11 of these protons have completely out exchanged and 15 have been quite resistant to exchange (Spectrum II). These data indicate that this ferredoxin molecule contains two segments of helix (or pleated-sheet) secondary structure.

Table I

Stimulation of Riboflavin Production by *E. ashbyii*  
Subcultured from  $^1\text{H}_2\text{O}$  into Various Levels of  $^2\text{H}_2\text{O}$

Atom Percent Deuterium in Nutrient Water	Riboflavin Production (mg/liter)			
	Day	Day	Day	Day
	0	8	15	22
0	0	2.7	4.6	5.6
25	0	3.5	5.4	7.3
50	0	8.5	13.0	15.0
99	0	15.8	23.5	25.1

used peppermint (*Mentha piperita* L.) as the study plant. Above the 20 percent  $\text{D}_2\text{O}$  level there was a progressive inhibitory effect on growth with increase in the  $\text{D}_2\text{O}$  content of the nutrient as reflected in elongation growth of the axial shoot. Very pronounced repressive effects were observed at the 50 percent level, and growth essentially stopped in 70 percent  $\text{D}_2\text{O}$ . In a subsequent report the histologic effects of deuteration on peppermint were reported by Crane et al. (22). The major effect of deuterium on the growth of peppermint appeared to be inhibition of cell division. In the deuterated plants parenchyma cells were enlarged, while there appeared to be a reduction in the vascular tissue. In general, the effects of deuteration were more apparent in actively growing tissues than in tissue exposed to  $\text{D}_2\text{O}$  in the nutrient after differentiation had occurred. The effects of certain growth regulators on peppermint grown at different levels of  $\text{D}_2\text{O}$  in the nutrient solution were reported by Blake et al. (23). The inhibitory effects of deuterium on the cellular level were not reversed by gibberellic acid, naphthalene-acetic acid or indoleacetic acid. In some instances the inhibitory effects on growth were even greater than that attributable to the  $\text{D}_2\text{O}$  in the nutrient. It is interesting to note that maleic hydrazide, usually considered to be a plant growth inhibitor, actually stimulated the growth of peppermint cultured in deuterated media.

Perhaps the most intensively studied higher plant is *Lemna perpusilla* (duckweed), which was subjected to extensive deuterium replacement by Cope et al. (24). A large number of growth factors, individually and in combination, were included in the nutrient solution and their effect on the growth of duckweed at high levels of deuteration was observed. At deuterium levels in

the nutrient between 50 and 63 percent numerous abnormalities were produced, but these were largely eliminated by the addition of kinetin. None of the other additives produced a beneficial response. Even kinetin failed to evoke a protective effect when the  $D_2O$  level exceeded 63 percent. The inclusion of  $^2H$ -glucose in the nutrient solution (50 atom percent  $D_2O$ ) raised the fixed deuterium in the plant DNA to 75 percent.

In belladonna plants deuteration had a drastic effect on flower development (25). The number of calyx lobes, corolla lobes, and stamens, while invariably 5 in control flowers, increased to as many as 9 or 10 in plants grown in 70 percent  $D_2O$  medium. Abnormally shaped berries formed in plants grown in heavy water. The extent of malformation depended on the  $D_2O$  content of the medium and how late in the life cycle of the plant that the berry formed. The shapes ranged from pear-shaped to dumbbell-shaped to cylindrical. The misshapened berries resulted from the tenacity with which the corolla remained attached to the ripening berry in deuterated plants. As the berry enlarged, a constriction developed where the corolla was attached to the berry. The size and number of seeds were severely reduced in deuterated berries with only a few rudimentary seeds apparent in the 70 percent berries. A similar study with *Arabidopsis thaliana* gave much the same results (26).

A replacement culture technique was developed by Crane et al. (27) to study the effect of deuteration on alkaloid production in *Atropa belladonna*. Plants were grown to maturity in an aqueous ( $H_2O$ ) medium and were then transplanted to media containing 50, 60, 75 and 99.7 percent  $D_2O$ . The plants in 99.7 percent  $D_2O$  showed the drastic effects of deuteration almost immediately and all plants died in several days. Plants transplanted into 75 percent  $D_2O$  survived about 3 weeks, and the 50 and 60 percent  $D_2O$  plants withstood the stresses imposed by deuterium. These plants were harvested after a growth period of 7.5 months. Alkaloid production was reduced to from one-third to one-tenth that of the control plants. The absolute amount of alkaloid formed and the total amount of plant material produced were too small to permit isolation of alkaloid. It appeared from this study that alkaloid production was completely inhibited upon transfer of the plants from normal growth in  $H_2O$  to the deuterated medium.

Germination of seeds has been the object of study. Crumley and Meyer (28) observed a delay in the initiation of germination in four species of plants, the extent of which increased with the deuterium

concentration of the solvent. However, the number of seeds which finally germinated was only slightly lower for pure  $D_2O$  than for water. More recently, Siegel et al. (29) studied the germination of 11 species of seeds in high concentrations of  $D_2O$ , and observed only rye seeds were capable of germination at high  $D_2O$  concentrations. Blake et al. (30) found a simple relationship between the size of the seed and the germination capacity in high deuterium concentrations. Larger seeds are apparently more successful in germinating because they contain larger hydrogen-containing food reserves. Metabolic difficulties associated with deuterium incorporation are thus delayed until the hydrogen reserves of the seed are exhausted. If the basis for the observed effects is correct, then the species-specific deuterium effects should be separable from the effect of hydrogen-containing food reserves by growing the embryo in the absence of the hydrogen-containing endosperm. Removal of the seed structures from the embryos reduces to a minimum the availability of  $^1H$ . Crane et al. (31) studied the effect of deuterium replacement on the elongation of excised embryos of several species of seeds and noted that all embryos suffered growth inhibition in  $D_2O$ . Added sucrose mitigated the repressive effects of deuterium on growth. Siegel and Galston (32) demonstrated that biosynthesis does take place when winter rye seeds are germinated in 99.7 percent  $D_2O$ . Five isoperoxidases isolated from seeds germinated in  $D_2O$  were shown to be deuterated, and it was concluded that they were biosynthesized during the germination process.

In general, higher plants show more complex  $D_2O$  effects than do microorganisms. This is to be expected as their structure is more highly organized. The response to  $D_2O$  in higher plants is a graded one with 60 to 70 percent the maximum level tolerated in the nutrient medium. A primary response to deuteration appears to be suppression of the production of important metabolites including alkaloids, antibiotics, proteins, carbohydrates, etc. Some beneficial effects in helping higher plants adapt to deuterium have been noted with the plant growth stimulant kinetin and with the growth inhibitor maleic hydrazide. The complex nature of higher plants makes difficult a simple explanation of the observed effects of growth regulators in  $^2H_2O$ , and further systematic studies will have to be undertaken in order to better understand the phenomena taking place. The replacement technique used successfully for culturing certain fungi and molds was unfortunately not found to be applicable for higher plants.

### III. Biological Effects of Carbon-13

#### Culture Systems for the Growth of $^{13}\text{C}$ -Organisms.

The culture of microorganisms in systems requiring only the substitution of deuterium presents no complex problems in apparatus design. Usually, the isotope is presented in the form of  $^2\text{H}_2\text{O}$ , and only the prevention of exchange with isotopically normal water in the ambient atmosphere is required. Utilization of  $^{13}\text{C}$  presents somewhat more complex problems, because the isotope in its most economical form is available as  $^{13}\text{CO}_2$ . Of course, carbon dioxide is the optimum substrate for the production of photosynthetic organisms, but it does present problems in manipulation and conservation. The current price of this isotope makes mandatory a completely sealed growth system, not, in this case primarily to prevent isotopic attenuation with the external carbon dioxide, but to prevent loss of the rare, expensive material.

Equipment for the culture of photosynthetic microorganisms in the liquid phase on  $^{13}\text{CO}_2$  presents no large problem in design or construction. All that is required, in addition to a suitable, tight container for the algal culture, is a sufficiently large volume to contain the gas phase at a reasonable carbon dioxide level and a circulating pump to carry the gas mixture over the culture. Lighting and other arrangements may be arranged as in the culture of the same organisms in  $^2\text{H}_2\text{O}$ . A useful concentration of carbon dioxide is around 20%, with nitrogen as a carrier gas.

Culture of saprophytic microorganisms with  $^{13}\text{C}$  compositions is often facilitated by direct use of substrates derived from  $^{13}\text{C}$  algae. Alternatively, specific metabolites or precursors prepared by organic synthetic methods may be added to the substrates of whatever yeasts, fungi, bacteria, etc. are desired. The techniques useful in many such growth experiments have been described (33).

Growth of terrestrial higher plants from  $^{13}\text{CO}_2$  presents several complications in apparatus design. The system must be capable of sustaining normal plants growth for long periods in a completely sealed condition. Obviously, provision must be made to assure inorganic nutrient supplies, adequate carbon dioxide levels, control of temperature, humidity, soil moisture and light intensity. Such systems have been constructed and operated to produce tobacco and other higher plants at levels of over 90% enriched  $^{13}\text{C}$ , and are described in detail elsewhere (34). It is to be emphasized that these growth chambers differ in one important aspect

from most previously described "phytotrons" or "biotrons" (35).

Whereas most special growth chambers in use are by necessity not sealed and are closely linked to the outside environment to permit easy control of temperature and humidity, and in many cases for a continuous supply of carbon dioxide, the growth chambers discussed here were designed with the same philosophy used where manipulation of radioactive or other toxic materials must be employed. Our growth chambers thus are provided with glove ports for internal manipulations, hermetically sealed bulkheads, etc.

The principal structural features are as follows: ceiling and walls are 1/4" thick methacrylate plastic; floor and structural elements were aluminum. Approximate dimensions are: 1 x 2 x 3 M. A heat exchanger supplied by external chilled water provided temperature and humidity control. Sensors buried in the vermiculite or sand support medium allowed monitoring of soil moisture content. Carbon dioxide was provided from external cylinders, and nutrient was supplied to each plant through a sealed bulkhead. Alternatively, solid inorganic nutrient was provided from a pellet buried in the sand/vermiculite soil medium, and the condensed water of transpiration recycled and distributed to each plant by means of an automatic dispenser controlled by a preset timer. This system was probably most satisfactory from the viewpoint of eliminating periodic additions of external liquid nutrient and subsequent withdrawal of the condensed water of transpiration. Such an automated system is capable of smooth functioning for long periods of time without attendance. A view of these systems is shown in Figure 2; the crop is tobacco, enriched to a level of > 90%  $^{13}\text{C}$ .

Biological Effects of  $^{13}\text{C}$  Substitution in Living Organisms. The consequences of substitution of  $^{13}\text{C}$  for  $^{12}\text{C}$  in biological systems are of interest as a problem in isotope biology, as well as carrying entirely pragmatic implications. Numerous suggestions have been made (36) involving possible uses of  $^{13}\text{C}$  compounds in clinical diagnosis and other medical applications. It is therefore of paramount importance to determine the extent of any possible deleterious effects of  $^{13}\text{C}$  substitution in living organisms.

Given the small difference in the masses of  $^{12}\text{C}$  and  $^{13}\text{C}$ , relative to those of hydrogen and deuterium, it would be expected that the kinetic isotope effects and therefore the disruption of metabolic function when these isotopes are interchanged, would be much less

pronounced. This expectation tends to be born out by experimental findings. In the case of unicellular, photosynthesizing organisms, only relatively small differences are seen in growth rate, size distribution or gross morphology (37), when  $^{13}\text{C}$  is substituted for  $^{12}\text{C}$  at levels above 90% enrichment. Disturbance of normal biological function by  $^{13}\text{C}$  substitution is somewhat more easily demonstrated when this isotope is substituted in conjunction with deuterium and other stable isotopes.

The effect of a high level of  $^{13}\text{C}$  substitution on complex organisms, plants or animals, is ambiguous at present. Experiments aimed at growth of  $^{13}\text{C}$  tobacco and other flowering plants at levels of isotopic enrichment around 90% provide some evidence. Compared to controls, the isotopically substituted plants showed slightly retarded flowering, the production of fewer flowers, abscising more frequently, and seemingly abnormal pollen. Any abnormality in the reproductive cycle is particularly suggestive, in light of the experience with deuterium substitution and its marked effects on reproduction. Examination of  $^{13}\text{C}$  pollen by the technique of scanning electron microscopy revealed a high degree of morphological abnormality. Subsequent experiments with morning glory tended to support these observations. Investigations of various  $^{13}\text{C}$  pollens are still in progress and any conclusions at this time must be regarded as tentative.

The substitution of  $^{13}\text{C}$  at high levels in highly evolved animals evokes questions of great interest, of both practical and theoretical character. Conclusive answers are not, as yet, evident. The growth of  $^{13}\text{C}$  tobacco provided peripheral evidence. In the course of cultivation of  $^{13}\text{C}$  tobacco an adventitious infestation of white flies took place in one of the growth chambers, which had been isolated from the external environment for several weeks. Superficial examination by a time-of-flight mass spectrometer of the waxes elaborated by the wings of these insects indicated a high level of  $^{13}\text{C}$  substitution. The mass spectrum peaks are shown in Figure 3. It was estimated that the insect has somewhat more than 50%  $^{13}\text{C}$  in its isotopic carbon make-up. This unscheduled event probably produced the first highly enriched  $^{13}\text{C}$  insect. Whether the disparity with the substrate was due to complex metabolic fractionation patterns or whether performed embryonic tissue made a significant contribution cannot now be decided. An obvious lesson to be drawn would suggest the ease of producing  $^{13}\text{C}$  parasitic animals, given a suitable  $^{13}\text{C}$  plant substrate.





Figure 2. Automated culture of isotopically enriched plants in a closed growth system

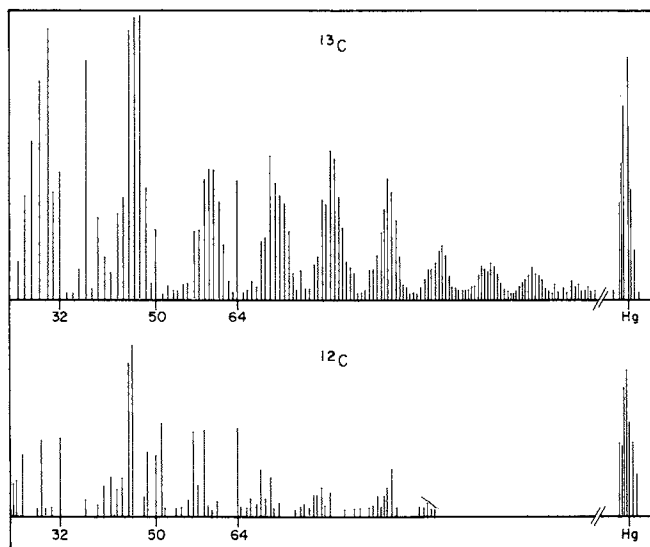


Figure 3. Mass fragment distribution of insect wax from normal abundance wax ( $^{12}\text{C}$ ) and  $^{13}\text{C}$  enriched wax

Long term experiments involving  $^{13}\text{C}$  substitution in mice have been attempted, with inconclusive results on the possible deleterious effects of the isotope (38). These animals were fed on a diet of performed  $^{13}\text{C}$  materials derived from laboratory synthesis, together with added vitamins, etc. of isotopically normal content. At present a long term study is under way to determine possible biological effects of  $^{13}\text{C}$  in fetal mice tissue (6).

Applications of  $^{13}\text{C}$  Substitution. The widespread use of highly enriched  $^{13}\text{C}$  for use in incorporation in compounds and organisms of special interest has only begun, but already it is evident that  $^{13}\text{C}$  will have extensive future uses. Limitations are imposed only by the investigator's specific interests and the ease of synthesizing the materials desired, whether by the biosynthesis in a specific organism or by laboratory organic synthesis. It is clear, from already reported applications in esr (39) and nmr (40), that the use of  $^{13}\text{C}$  may well become a routine technique in certain kinds of magnetic resonance studies. The significant property of  $^{13}\text{C}$  here is the non-zero nuclear spin, but other applications depend upon the isotopic mass difference itself. Separation of constituents by density gradient ultracentrifugation, as first used in the case of  $^{15}\text{N}$  (41) is an obvious possibility. Another application, already widely exploited is the use of  $^{13}\text{C}$  in mass spectrometry, either with highly enriched systems or at natural abundance levels. The proposed applications in clinical medicine, with mass spectrometry used in conjunction with chromatographic techniques, has already been mentioned (42).

#### IV. Nitrogen-15

Nitrogen-14 nuclei have a quadrupole moment, which means that nmr signals from  $^{14}\text{N}$  are broad and difficult to detect. An additional disadvantage is the fact that coupling between  $^{14}\text{N}$  and other nuclei is often unobservable due to the very short relaxation time of the  $^{14}\text{N}$  nucleus. Thus,  $^{14}\text{N}$ -H coupling is not observed in the peptide bond. It is therefore advantageous to perform magnetic resonance studies with biological materials substituted with  $^{15}\text{N}$ , which has a spin of 1/2 and no quadrupole moment. Deuterated protein containing  $^{15}\text{N}$  allows discrimination between hydrogen bonds involving amide groups or hydroxyl groups.

Recent work by Boxer et al. (43) has led to the assignment of four  $^{15}\text{N}$  nmr transitions in chlorophyll a and its magnesium-free derivative pheophytin. An analysis of the chemical shift changes induced by complexation with magnesium revealed that the magnesium atom selectively perturbs low lying  $n\pi^*$  states. The charge density in the four pyrrole rings becomes more nearly equivalent so that the energy differences among low-lying  $\pi\pi^*$  states are decreased.

#### V. Biological Effects of Multiple Isotope Substitution

Taken together, compounds of the elements hydrogen, oxygen, nitrogen and carbon constitute over 99% of the mass of living protoplasm. All of these elements possess stable, rare heavy isotopes. Although kinetic isotope effects in isotopes of elements other than hydrogen might be expected to have greatly lessened kinetic isotope effects, and therefore diminished biological effects, it is of interest to consider the results of substitution of more than one element by its heavy isotope. The overall present costs of  $^2\text{H}$ ,  $^{13}\text{C}$ ,  $^{15}\text{N}$  and  $^{18}\text{O}$  prohibit growth of organisms on any but the smallest scale, if all of these heavy isotopes are to be incorporated simultaneously. There have been only two extensive investigations to date of organisms incorporating deuterium plus other stable isotopes at high enrichment.

The basis for all such studies must be a totally deuterium-adapted organism, to which the other isotopes of interest may be added in the course of culture. An obvious combination is presented by deuterium and  $^{13}\text{C}$ ; this was carried out by Flaumenhaft et al. at enrichment levels of 99% + D and 95%  $^{13}\text{C}$  (44). C. vulgaris was grown in all combinations of  $^1\text{H}$ ,  $^2\text{H}$ ,  $^{12}\text{C}$  and  $^{13}\text{C}$ . The various isotopically altered cells were compared on the basis of size and shape, gross morphology, and structural changes in subcellular organelles, as indicated by cytological staining techniques.

The incorporation of  $^{13}\text{C}$  had no obvious effect on the growth cycle of the algae. The  $^{13}\text{C}$ - $^2\text{H}$  algae grew at about the same rate as  $^{12}\text{C}$ - $^2\text{H}$  cultures, as the  $^{13}\text{C}$ - $^1\text{H}$  grew at the rate seen in normal  $^{12}\text{C}$ - $^1\text{H}$  cultures. An examination of cell size distribution, however, revealed that in the change of isotopic composition from  $^2\text{H}$ - $^{12}\text{C}$  to  $^2\text{H}$ - $^{13}\text{C}$ , a marked change takes place, as seen in Figure 4. Evidently, the substitution of  $^{13}\text{C}$  in a deuterium adapted cell results in a tendency to undo some of the disruptive effects of deuterium, at least

as regards such a gross and statistical parameter as cell size distribution.

Studies on subcellular morphology and cytology tended to bear out the findings on size distribution. The partial reversal of effects attributable to deuterium substitution were bore out by investigation of the following features: (1) Nuclear size. Nuclei of  $^{13}\text{C}$ - $^2\text{H}$  cells were larger than those of  $^{13}\text{C}$ - $^1\text{H}$  cells, but smaller than those of the  $^{12}\text{C}$ - $^2\text{H}$  cells. (2) Nuclear shape. The nuclear size range seen in  $^{13}\text{C}$ - $^1\text{H}$  cells is about that seen in  $^{12}\text{C}$ - $^1\text{H}$  cells;  $^{12}\text{C}$ - $^2\text{H}$  cells have larger nuclei and are less spheroidal. (3) Nucleic acid content. DNA distribution was determined by cytochemical staining. The staining for DNA and RNA of  $^{13}\text{C}$ - $^2\text{H}$  cell nuclei was found to be intermediate between those of the  $^{12}\text{C}$ - $^1\text{H}$  cells and those of  $^{12}\text{C}$ - $^2\text{H}$ . As regards staining of cytoplasmic DNA, again, the character of  $^{13}\text{C}$ - $^2\text{H}$  cytoplasm was somewhere between that seen in  $^{13}\text{C}$ - $^1\text{H}$  cytoplasm and that of  $^{12}\text{C}$ - $^1\text{H}$ . The conclusions in regard to the RNA was somewhat at variance to the above pattern.  $^{13}\text{C}$ - $^2\text{H}$  cells produced RNA taking the form of thread-like accretions. These structures were never seen in cells made up of  $^{12}\text{C}$ , whether in combination with hydrogen or deuterium. (4) Protein and amino acid content. Staining of cellular protein material disclosed about the same patterns of intensity and occurrence as was seen for the nucleic acids. The staining for free amino acids indicated, again, that cells with the  $^{12}\text{C}$ - $^2\text{H}$  composition stained most heavily.

Other features revealed by cytological study included indications that the RNA content may be more nearly normal in  $^{13}\text{C}$ - $^2\text{H}$  cells than in the previously much studied  $^{12}\text{C}$ - $^2\text{H}$  cells. This observation must be qualified, as the distortion of cytoplasmic RNA was so great in  $^{13}\text{C}$  containing cells that comparisons were difficult. The most obvious changes brought about by  $^{13}\text{C}$  substitution, as seen by phase contrast microscopy, was in the thickness of cell walls. Cell walls of both types of  $^{13}\text{C}$ -grown cells were much thicker than ever seen in  $^{12}\text{C}$  cells, the  $^{13}\text{C}$ - $^2\text{H}$  showing up as being even thicker than those of  $^{13}\text{C}$ - $^1\text{H}$  cells.

All these observations indicate that prediction of likely changes when two heavy isotopes are substituted in an organism is not possible. Simple assumptions of linear additive kinetic isotope effects cannot account for the variations seen in this study. The second conclusion, that substitution of  $^{13}\text{C}$  for  $^{12}\text{C}$  in deuterated organisms tends to decrease the magnitude of the abnormality produced after adaptation to a

deuterated melieu is quite unexpected and cannot be explained at present.

The other study dealing with multiple isotopic substitution included all four heavy isotopes of hydrogen, carbon, oxygen and nitrogen. Uphaus et al. (45) grew cultures of deuterium-adapted *C. vulgaris* in volumes of 1-2 ml. The results of this study are of considerable interest, when taken as a preliminary effort, but the experiments suffered from two shortcomings. One of these arose from the use of only partially enriched  $^{13}\text{C}$  (55% mole-percent  $^{13}\text{C}$ ), which made any conclusions regarding the possible effects of  $^{13}\text{C}$  substitution ambiguous. The other weakness of the study was that the great expense of the isotopes made it impossible to follow patterns of change in the organism, if each isotope were added stepwise in sequence. The isotopic enrichments of the materials used were:  $^2\text{H}$ , 99%,  $^{13}\text{C}$ , 55%,  $^{15}\text{N}$ , 98%,  $^{18}\text{O}$ , 97%.

The results of extensive isotopic substitution of all four major elements in the biomass resulted in drastic changes, the processes or cellular metabolic disruption and growth abnormality progressing far beyond that seen during deuterium adaptation. The size distributions of the isotopic species studied are given in Figure 5. Visual observations by light microscopy gave the impression of even greater heterogeneity than that implied by the curves as determined with a cell counter. It is possible that the "monster" or giant cells seen after complete isotopic substitution may be part of the adaptive process and life cycle of these cells. Cell division may not always occur. A large quantity of cellular debris was present in mature cultures, much more in mass than could be accounted for by total disintegration of the original inoculum, which was about 1% of the final cell mass. Cells grown in  $^1\text{H}-^{18}\text{O}-^{13}\text{C}-^{15}\text{N}$  media appeared to resemble more closely isotopically normal cells than did those grown in  $^2\text{H}-^{16}\text{O}-^{12}\text{C}-^{14}\text{N}$  media, but many of their characteristics were intermediate between the extremes.

Cytological studies, using appropriate stains for various cellular components, produced the following observations:  $^2\text{H}-^{16}\text{O}-^{13}\text{C}-^{15}\text{N}$  cells: A greater amount of nucleic acid was produced by these cells than any other type studied. Large amounts of DNA appeared in both the nucleus and the periphery of chloroplasts. By contrast, the RNA content of these cells was the lowest found for any system. Nuclei of these cells were greatly enlarged and had a uniform distribution of DNA, suggesting either polyploidy or nuclear degeneration. The fast-green stain used to visualize proteins appears to

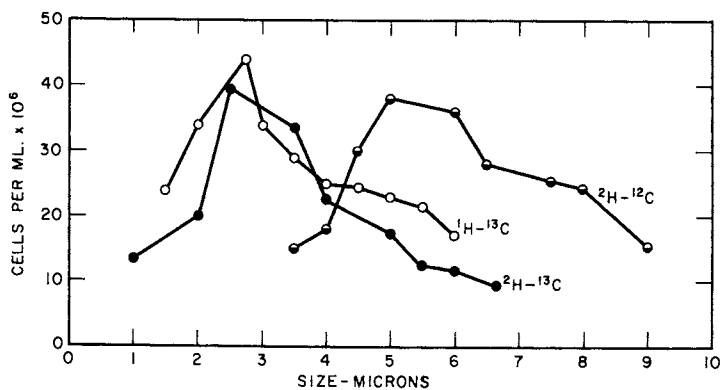


Figure 4. Size distribution of various isotopically substituted *Chlorella* cells

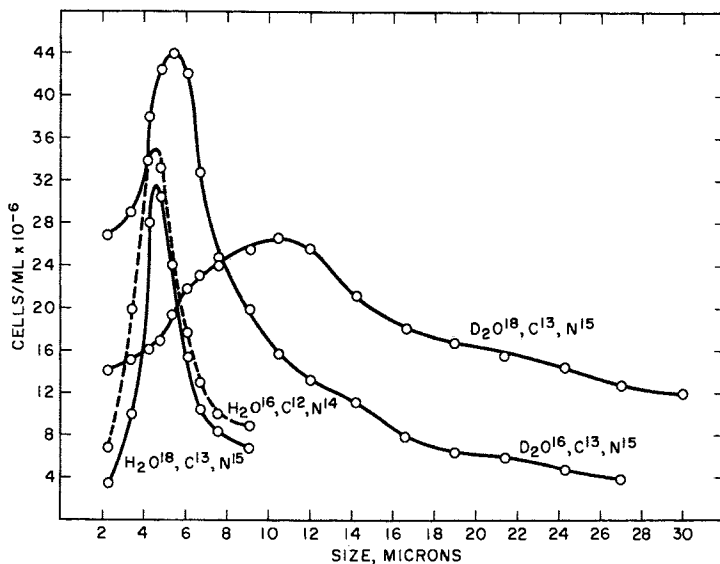


Figure 5. Size distributions of various *Chlorella* cells after multiple isotopic substitution

be deeply and uniformly distributed throughout the cell. Staining for carbohydrate distribution revealed that these cells contained much more such material than either of the  $^1\text{H}$  or  $^2\text{H}$  controls or the  $^2\text{H}$ - $^{18}\text{O}$  cells.

$^2\text{H}$ - $^{18}\text{O}$ - $^{13}\text{C}$ - $^{15}\text{N}$  Cells. These cell types showed the greatest variability in staining of components and the least localization of a particular component being stained. Young cells with this isotopic composition tended to resemble ordinary  $^1\text{H}$ - $^{16}\text{O}$ - $^{12}\text{C}$ - $^{14}\text{N}$  cells, with round and peripherally located nuclei which tended with aging to become multilobate; multiple nuclei were commonly found. Chloroplasts of these cells appeared to produce more DNA than those of other types. Protein staining indicated a large amount of this material, probably larger than in other isotopic types; this was also true of carbohydrate content. These cells had the most heavily stained and the thickest walls of any cell type.

$^1\text{H}$ - $^{18}\text{O}$ - $^{13}\text{C}$ - $^{15}\text{N}$  Cells. The trends in staining in this cell type indicated that it should be placed intermediate between cells of normal isotopic content and those of  $^2\text{H}$ - $^{16}\text{O}$ - $^{12}\text{C}$ - $^{14}\text{N}$ , tending to resemble the latter more than the former. Nuclei appeared to contain more RNA than did the  $^1\text{H}$ - $^{16}\text{O}$  control. The most significant difference between  $^{16}\text{O}$  and  $^{18}\text{O}$ -containing cells appeared in the nature of the carbohydrate distribution and content. Those containing the heavy oxygen isotope showed less clear staining of the cell walls.

Perhaps the most important generalization to appear from this study was that it is quite obvious that deviations from normalcy appear more and more as heavy isotopes are substituted into the organism. The tendency to form giant cells, some with a volume several orders of magnitude greater than normal cells, and a suggestion of increasing subcellular disorganization, is quite common. The exact contribution of each heavy isotope cannot be assessed at present and must await further studies on other organisms and large sized cultures.

The applications of multiply substituted organisms is at present limited by the high cost of the heavy isotopes, especially  $^{18}\text{O}$ . The even rarer  $^{17}\text{O}$  may have great future potential, because of its non-zero nuclear spin. Aside from areas of obvious application, such as mass spectrometry, there appears to be great potential for the study of biological problems by means of multiple resonance techniques as endor (electron-nuclear double resonance), with the use of multiply substituted organisms.

Literature Cited

1. Proceedings, First International Conference on Stable Isotopes in Chemistry, Biology and Medicine, P. D. Klein and S. V. Peterson, Eds., Argonne National Laboratory, Argonne, Illinois, 1973. National Technical Information Service, U.S. Department of Commerce, Springfield, Va., 22151. CONF-730525.
2. Katz, J. J. and Crespi, H. L., "Isotope Effects in Chemical Reactions," C. J. Collins and N. S. Bowman, Eds., 286-363, Van Nostrand Reinhold, New York, 1970, Chap. 5.
3. Katz, J. J. and Crespi, H. L., *Science* (1966) 151, 1187.
4. Matwiyoff, N. A. and Ott, D. G., *Science* (1973) 181, 1125.
5. Thomson, J. F., "Biological Effects of Deuterium," Pergamon, Oxford, 1963.
6. Urey, H. C., Brickwedde, F. G. and Murphy, G. M., *Phys. Rev.* (1932) 39, 164; *Ibid.*, (1932) 40, 464; Urey, H. C., *Science* (1933) 78, 566.
7. Morowitz, H. J. and Brown, L. M., U.S. National Bureau of Standards Reprint (1953) No. 2179.
8. Flaumenhaft, E., Bose, S., Crespi, H. L. and Katz, J. J., *Internat. Rev. Cytol.* (1965) 18, 313.
9. Wiberg, K. B., *Chem. Rev.* (1955) 55, 713.
10. Salomaa, P., Schaleger, L. L. and Long, F. A., *J. Amer. Chem. Soc.* (1964) 86, 1.
11. Salomaa, P., Schaleger, L. L. and Long, F. A., *J. Amer. Chem. Soc.* (1964) 86, 410.
12. Long, F. A., *Ann. N. Y. Acad. Sci.* (1960) 84, 596.
13. Chorney, W., Scully, N. J., Crespi, H. L. and Katz, J. J., *Biochim. Biophys. Acta* (1970) 37, 280; Crespi, H. L., Conrad, S. M., Uphaus, R. A. and Katz, J. J., *Ann. N. Y. Acad. Sci.* (1960) 84, 648.
14. Crespi, H. L. and Katz, J. J., in "Methods in Enzymology," C. H. W. Hirs and S. N. Timasheff, Eds., Academic, New York, 1972.
15. Norris, J. R., Uphaus, R. A., Crespi, H. L. and Katz, J. J., *Proc. Nat. Acad. Sci. U.S.A.* (1971) 68, 625.
16. Katz, J. J. and Crespi, H. L., *Pure and Appl. Chem.* (1972) 32, 221.
17. Crespi, H. L., Marmur, J. and Katz, J. J., *J. Amer. Chem. Soc.* (1962) 84, 3489; Stewart, C. R., Cater, M. and Click, B., *Virology* (1971) 46, 327; Smith, I., Dubnau, D., Morell, P. and Marmur, J., *J. Mol. Biol.* (1968) 33, 123.
18. Mrtek, R. G., Crespi, H. L., Blake, M. I. and Katz, J. J., *J. Pharm. Sci.* (1967) 56, 1234.



19. Nona, D. A., Blake, M. I. and Katz, J. J., *J. Pharm. Sci.* (1968) 57, 975.
20. Pluta, P., unpublished.
21. Blake, M. I., Crane, F. A., Uphaus, R. A. and Katz, J. J., *J. Pharm. Sci.* (1964) 53, 79.
22. Crane, F. A., Blake, M. I., Uphaus, R. A. and Katz, J. J., *J. Pharm. Sci.* (1964) 53, 612.
23. Blake, M. I., Crane, F. A., Uphaus, R. A. and Katz, J. J., *Lloydia* (1964) 27, 254.
24. Cope, B. T., Bose, S., Crespi, H. L. and Katz, J. J., *Botan. Gazz.* (1965) 126, 214.
25. Uphaus, R. A., Crane, F. A., Blake, M. I. and Katz, J. J., *J. Pharm. Sci.* (1965) 54, 202.
26. Bhatia, C. R. and Smith, H. H., *Planta* (1968) 80, 176.
27. Crane, F. A., Mohammed, K., Blake, M. I., Uphaus, R. A. and Katz, J. J., *Lloydia* (1970) 33, 11.
28. Crumley, H. A. and Meyer, S. L., *J. Tennessee Acad. Sci.* (1950) 25, 171.
29. Siegel, S. M., Halpern, L. A. and Giumarro, C., *Nature* (1964) 201, 1244.
30. Blake, M. I., Crane, F. A., Uphaus, R. A. and Katz, J. J., *Planta* (1968) 78, 35.
31. Crane, F. A., Blake, M. I., Uphaus, R. A. and Katz, J. J., *Can. J. Botany* (1969) 47, 1465.
32. Siegel, B. Z. and Galston, A. W., *Proc. Nat. Acad. Sci. U.S.A.* (1966) 56, 1040.
33. Kollman, V. H., Gregg, C. T., Hanners, J. L., Whaley, T. W. and Ott, D. G., *Proceedings of the First International Conf. on Stable Isotopes in Chemistry, Biology and Medicine, May 9-11, 1973, Argonne National Laboratory, Argonne, Illinois*, p. 30.
34. Uphaus, R. A., Blake, M. I., Kostka, A. G. and Katz, J. J., *J. Pharm. Sci.*, in press.
35. An extensive study of both commercial units and one-of-a-kind research systems is given in: "Lighting for Plant Growth," E. D. Bickford and S. Dunn, Eds., Kent State University Press, 1972.
36. Shreeve, W. W., *Proceedings of the First International Conf. on Stable Isotopes in Chemistry, Biology and Medicine, May 9-11, 1973, Argonne National Laboratory, Argonne, Illinois*, p. 390; Sweetman, L., *Ibid.*, p. 404.
37. Flaumenhaft, E., Uphaus, R. A. and Katz, J. J., *Biochim. Biophys. Acta* (1972) 215, 421.
38. Gregg, C. T., Los Alamos Scientific Laboratory, private communication.
39. Norris, J. R., Uphaus, R. A. and Katz, J. J., *Biochim. Biophys. Acta* (1972) 275, 161.

40. Katz, J. J. and Janson, T. R., *Annal. N. Y. Acad. Sci.* (1973) 106, 579.
41. Meselson, M. and Wergle, J. J., *Proc. Nat. Acad. Sci. U.S.A.* (1961) 47, 857.
42. Sweeley, C. C., Young, N. D., Bieber, M. A. and Holland, J. F., *Proceedings of the First International Conf. on Stable Isotopes in Chemistry, Biology and Medicine, May 9-11, 1973, Argonne National Laboratory, Argonne, Illinois*, p. 273.
43. Boxer, S., Closs, G. L. and Katz, J. J., *J. Amer. Chem. Soc.*, in press.
44. Flaumenhaft, E., Uphaus, R. A. and Katz, J. J., *Biochim. Biophys. Acta* (1970) 215, 421.
45. Uphaus, R. A., Flaumenhaft, E. and Katz, J. J., *Biochim. Biophys. Acta* (1967) 141, 625.

# INDEX

<b>A</b>	
A values, relative .....	116
Absorption band, infrared .....	35
Abstraction, hydrogen-atom .....	54
Abstraction reactions .....	167
Activated complex theory .....	49
Activity, optical .....	40
Activity, solvent .....	121
2-Adamantyl trifluoroethanesulfonate .....	178
Additivity, isotopic .....	20
Additivity, substituent .....	20
Adiabatic approximation .....	67
Adiabatic corrections .....	71, 73, 75
Aircraft fuel .....	91
Algae, $^2\text{H}$ .....	186
Algal ferredoxin .....	189
Alkyl sulfonates .....	178
Amide protons .....	187
Amino acid content .....	199
Ammonia-hydrogen exchange reaction .....	94
Anharmonic corrections .....	15, 105, 107
Animals, substitution of $^{13}\text{C}$ in .....	195
Aqueous concentration .....	120
Aqueous .....	
solutions .....	101
solvent effects .....	119
solvent structure .....	126
Argon .....	82, 110
Arrhenius plots .....	54
Arrhenius pre-exponential factors .....	50, 57, 59
Asymmetric solvent case .....	157
Atom abstraction, model hydrogen- .....	54
Atom exchange reactions, heavy .....	74
Atomic spectra .....	29
Automated culture .....	196
<b>B</b>	
Barrier .....	
double-minimum potential functions, .....	
low .....	38
Eckart .....	45
one-dimensional .....	47
permeability of .....	46
Bases in proton transfer, reacting .....	170
Belladonna plants .....	191
Bending forces .....	26, 173
Bending frequency .....	157
Beta calutron separator .....	80
Bigeleison and Mayer, isotope-exchange .....	
reaction theory of .....	146
Bigeleison and Mayer, reduced partition .....	
function ratio of .....	9
Biological effects of $^{13}\text{C}$ substitution .....	193, 194
Biological effects of multiple isotope .....	
substitution .....	199
Biology, isotope chemistry and .....	184
Bond extension .....	173
Bond order .....	171
Bonding studies, hydrogen .....	37
Bonding, transition state .....	169
Born-Oppenheimer .....	
approximation .....	2, 33, 39, 64, 105, 142
Born-Oppenheimer corrections .....	65, 69
Born-von Kármán (BVK) .....	
lattice calculations .....	151
lattice spectrum of lithium metal .....	152
solid .....	150
vibrational frequency distribution .....	152
BSVHW model .....	106, 112
<b>C</b>	
$^{12}\text{C}/^{14}\text{C}$ effect .....	171
$^{13}\text{C}$ .....	
biological effects of .....	193
$^{12}\text{C}$ reduced partition function ratio .....	22
culture of saprophytic microorganisms .....	
with .....	193
organisms .....	193
substitution .....	194, 195, 197
$^{35}\text{Cl}/^{37}\text{Cl}$ leaving group effects .....	171
$^{13}\text{CO}_2$ .....	193
C-X bond extension .....	173
Calcium chloride solutions .....	127
Calcium-isotope-exchange reactions .....	144
Calutron separator, beta .....	80
Carbon .....	
monoxide, liquid .....	113
saturated .....	177
solvolytic nucleophilic displacements .....	
on .....	174
Carbonium ions .....	176, 179
Cascade .....	
ideal separation .....	89
no-remixing separation .....	86
simple .....	85
thermal diffusion .....	82
Cation solvates .....	39
Cell(s) .....	
degassing .....	121
double .....	133
electrochemical .....	131
$^1\text{H}$ - $^{18}\text{O}$ - $^{13}\text{C}$ - $^{15}\text{N}$ .....	202
$^2\text{H}$ - $^{16}\text{O}$ - $^{13}\text{C}$ - $^{15}\text{N}$ .....	200
$^2\text{H}$ - $^{18}\text{O}$ - $^{13}\text{C}$ - $^{15}\text{N}$ .....	202
isotopically substituted <i>chlorella</i> .....	201
measurements on the .....	135
quadruple .....	137
sample .....	121
Chambers, growth .....	193, 194
Chemical .....	
exchange separation processes .....	9
exchange system, simple .....	92
isotope fractionation .....	7, 11

Chemical ( <i>continued</i> )		
isotope separation factors	10	
reactions, tunneling in	45	
Chemistry and biology, isotope	184	
<i>Chlorella</i> cells	201	
Chlorophyll free radical species	187	
Closed growth system	196	
Column, thermal diffusion	82	
Complete equation	106	
Complex(es)		
metal	37	
organisms	195	
theory, activated	49	
transition metal	37	
Compressors in a gaseous diffusion plant	92	
Concerted displacement reaction, $\alpha$ -effect	174	
Condensed phase isotope effects	101	
Condensed phase modes	103	
Configuration interaction	72	
Contour map	47	
Controlled thermonuclear reactors (CTR)	88	
Coriolis interaction	34	
Corresponding states, the law of	108	
Coulombic force constants	153	
Coupling		
constants	34	
effects	118	
$^{14}\text{N}$ -H	197	
Covalent substrate	174	
Cross over equilibrium	23	
Crowding	173	
CTR (controlled thermonuclear reactors)	88	
Culture		
of isotopically enriched plants	196	
of photosynthetic microorganisms	193	
of saprophytic microorganisms	193	
systems	193	
Current reversibility check, voltage	134	
<b>D</b>		
$\alpha$ -D rate effects	173, 179	
DeBoer's modification of the law of corresponding states	108	
Debye-Hückel theory	123	
Debye solid	150	
Degassing cell	171	
Degree of freedom, translational	167	
Deuterated		
algal ferredoxin	189	
belladonna plants	191	
ethylenes	118	
media	190	
metabolites	188	
nucleic acids	188	
organic acids	117	
proteins in NMR	187	
Deuterium	185	
compounds	5	
concentration	91, 95	
effects, hydrogen	112	
enrichment	88	
on higher plants, effects of	188	
kinetic isotope effects	55, 58	
organisms in ESR and NMR	186	
replacement of duckweed	190	
Deuterium ( <i>continued</i> )		
requirement projections	88	
on seed germination, effect of	191	
substitution	185	
vapor pressure isotope effects	114	
$\alpha$ -Deuterium rate effects	177	
Diagonal nuclear motion correction	67	
Diatomic		
initial and final states	166	
molecular dissociation model	168	
molecule spectra	30	
molecules	15, 64, 109, 166	
Difference method	131	
Diffusers in a gaseous diffusion plant	92	
Diffusion		
cascade, thermal	82	
column, thermal	82	
controlled reaction	167	
gaseous	83, 85, 89, 92	
plant, gaseous	85, 92	
stages, gaseous	89	
thermal	79, 81, 82	
Displacement reactions	165, 174	
Displacement, solvolytic nucleophilic	174	
Disproportionation reaction, isotopic	23	
Dissociation		
of diatomic molecule	166	
effect	173	
into free particles	165	
model, diatomic molecular	168	
photo-	97, 98	
Distillation		
deuterium enrichment by	88	
hydrogen	90	
process requirements	90	
water	90	
Distribution functions	4, 8	
Double cell	133	
Dual-temperature exchange	93, 95	
Duckweed	190	
<b>E</b>		
Eckart barrier	45	
Eckart function	47	
$\alpha$ -Effects	172, 173, 174	
Effects, isotope ( <i>see</i> Isotope effects)	131	
Electrochemical cells	131	
Electrochemical determination of equilibrium constants	131	
Electrolyte solutions, VPIEs of some	125	
Electron		
acceptance, inductive	173	
release, hyperconjugative	172	
spin resonance, deuterium organisms in	186	
Electronic isotope effect	65, 70, 74	
Electromagnetic separators	78	
Electronic wave-functions	66	
Elementary separation factor	84	
Energy		
diagrams, potential	110	
fusion	88	
level distributions	101, 105	
levels, zero point	166	
potential	2, 48	
reduced	46	
standard molar internal	5	
zero point	2, 15, 102, 106, 166	

- Enriched plants, isotopically ..... 196  
 Enrichment factor, single-stage ..... 93  
 Enthalpies, partial molal ..... 121  
 Enthalpies of transfer, excess ..... 124  
 Entropies, partial molal ..... 121  
 Equilibrium  
   constant(s)  
     electronic isotope effect on the ..... 70  
     exchange ..... 75, 93  
     isotope effects on ..... 64  
     isotope exchange ..... 5, 15  
     for an isotope exchange reaction ..... 6, 131  
     prediction ..... 146  
   cross over ..... 23  
   exchange of oxygen ..... 24  
   in ideal gases ..... 1  
   internuclear distances ..... 75  
   isotope exchange reaction ..... 17  
   orthogonal polynomial expansion  
     calculation of ..... 24  
   solvent isotope effects ..... 119  
 Esters, pinacolyl ..... 180  
 Ethylenes, deuterated ..... 118  
 Exchange  
   deuterium enrichment by ..... 88  
   effects ..... 158  
   equilibrium constant ..... 75, 93  
   isotope (*see* Isotope exchange)  
   reaction, ammonia-hydrogen ..... 94  
   reactions, gas phase heavy atom ..... 74  
   separation processes for uranium  
     isotopes ..... 9  
   system, dual-temperature ..... 95  
   system, simple chemical ..... 92  
   unit ..... 95  
 Exergonic reaction ..... 167  
 Expansion, orthogonal polynomial ..... 24  
 Expansion, Taylor series ..... 10  
 External condensed phase modes ..... 103  
 External interactions, internal- ..... 107
- F**
- F-sum rule ..... 36  
 Ferredoxin, deuterated algal ..... 189  
 Field, force (*see* Force field)  
 Final states, diatomic ..... 166  
 First order rules ..... 20  
 Flow, interstage ..... 86  
 Force(s)  
   constants ..... 34, 49  
     Coulombic ..... 153  
     vibrational ..... 32  
   fields ..... 34, 116  
     Lennard-Jones ..... 108  
     state vibrational ..... 163  
     mean square ..... 111  
     isotope chemistry and molecular ..... 16  
     stretching and bending ..... 26  
 Fractionation, chemical isotope ..... 7, 11, 21  
 Fragment distribution of insect wax, mass ..... 196  
 Free carbonium ion ..... 176  
 Free radical species, chlorophyll ..... 187  
 Freezing points ..... 122, 127  
 Frequency  
   distribution, Born-von Kármán  
     vibrational ..... 152
- Frequency (*continued*)  
   ratio ..... 38  
   vibration ..... 34  
 Fuel, aircraft ..... 91  
 Functional forms ..... 104  
 Fusion energy ..... 88
- G**
- Gas(es)  
   ideal ..... 1  
   monatomic ..... 109  
   phase  
     approximation, isolated molecule ..... 105  
     heavy atom exchange reactions ..... 74  
     isotopic exchange reactions ..... 65  
     reactions ..... 142  
 Gaseous diffusion  
   plant ..... 85, 92  
   stages ..... 89  
   uranium enrichment by ..... 83  
 Germination, seed ..... 191  
 GF-matrix method, Wilson ..... 32  
 Gibbs-Duhem-Bjerrum integration ..... 121  
 Graham's law ..... 84  
 Growth chambers ..... 193, 194  
 Growth system, closed ..... 196
- H**
- $^1\text{H}\text{-}^{18}\text{O}\text{-}^{13}\text{C}\text{-}^{15}\text{N}$  cells ..... 202  
 $^2\text{H}$ -algae ..... 186  
 $^2\text{H}\text{-}^{16}\text{O}\text{-}^{13}\text{C}\text{-}^{15}\text{N}$  cells ..... 200  
 $^2\text{H}\text{-}^{18}\text{O}\text{-}^{13}\text{C}\text{-}^{15}\text{N}$  cells ..... 202  
 Halide constants, methyl ..... 34  
 Harmonic calculation ..... 116  
 Harmonic solid lattice oscillations ..... 2  
 Hartree-Fock limit wavefunctions ..... 70  
 Heats of solution ..... 121, 125  
 Henry's law ..... 120  
 Hybridization tautomerism ..... 37  
 Hydrogen  
   atom abstraction model ..... 54  
   bonding studies ..... 37  
   chloride, isotopic variants of ..... 31  
   -deuterium VPIEs ..... 112, 114  
   distillation ..... 90  
   exchange reaction, ammonia ..... 94  
   isotope effects, primary ..... 49  
   -isotope-exchange reactions ..... 131, 138  
   kinetic isotope effects, primary ..... 50  
   liquid ..... 91  
   sulfide-water dual temperature  
     exchange ..... 93  
   transfer reactions ..... 167  
 Hyperconjugative electron release ..... 172
- I**
- Inductive electron acceptance ..... 173  
 Infrared absorption band ..... 35  
 Initial state reactants ..... 163  
 Initial states, diatomic ..... 166  
 Insect wax ..... 196  
 Integrated intensities ..... 38  
 Intermolecular potential ..... 108  
 Internal  
   energy, standard molar ..... 5  
   -external interactions ..... 107

Internal ( <i>continued</i> )	
partition function	5
Internuclear distances, equilibrium	75
Interstage flow	86
Intramolecular energy level distributions	105
Ion(s)	
free carbonium	176
isotopic	135
pair	176, 179
solvation	39, 146
Ionization, photo-	97, 98
Isolated molecule gas phase	
approximation	105
Isomers	20
Isopropyl sulfonate solvolyses	181
Isopropyl <i>p</i> -toluenesulfonate	178
Isotope(s)	
chemistry	
and biology	184
first order rules for	20
and molecular forces	16
quantum mechanical foundations of	1
effect(s)	20
condensed phase	101
for diatomic molecular dissociation	
model	168
electronic	65, 70, 74
on equilibrium constants	64
equilibrium solvent	119
kinetic	49, 50, 185
primary	164, 170
hydrogen	49, 50
and quantum-mechanical tunneling	44
and reaction mechanisms	163
relative tritium-deuterium kinetic	56, 59
secondary	172
on solute excess thermodynamic	
properties	127
solvent	125, 127
and spectroscopy	29
virial coefficient	107
vapor pressure ( <i>see</i> VPIE)	
exchange	
equilibria	5, 15
reaction(s)	
Bigeleisen-Mayer theory of	146
calcium	144
equilibrium	17
equilibrium constant for	6, 131
gas phase	65
hydrogen	131, 141
in ion solvation studies	146
lithium	132, 138
thermodynamics of	131
fractionation	7, 11, 21
light	8
of liquid carbon monoxide	113
neon	4
separation	
argon	82
factors	10
laser	96
methods of	77
at Oak Ridge through 1972	80
plutonium	79
process	7, 77, 94
scheme	96
Isotope separation ( <i>continued</i> )	
by thermal diffusion	81
uranium	79, 89
stable	184
substitution	198
uranium	9
Isotopic	
additivity	20
disproportionation reaction	23
exchange reactions, gas phase	65
ions	135
metals	135
methanes	115, 116, 117
paleotemperature scale	15
partition functions	6
rate constant ratio	58
solids	148
solute species	151
substitution	20, 29, 101, 172
on molecular properties	64
optical activity induced by	40
variants of hydrogen chloride	31
Isotopically	
enriched plants	196
substituted <i>Chlorella</i> cells	201
substituted plants	195
<b>K</b>	
Kinetic isotope effects	49, 50, 58, 185
<b>L</b>	
Laplacian, mean	109
Laser isotope separation	96
Lattice	
calculations, BVK	151
constants	151
oscillations, harmonic solid	2
spectrum of lithium metal, BVK	152
Leaving group effects	171, 177
Lennard-Jones force field	108
Limit wavefunctions, Hartree-Fock	70
Linear molecules	36, 109
Liquid hydrogen	91
Liquid phase	92, 193
Lithium-isotope-exchange reactions	132, 138
Lithium metal, BVK lattice spectrum of	152
Living organisms, <sup>13</sup> C substitution in	194
<b>M</b>	
Magnetic resonance spectra, proton	189
Mass fragment distribution of insect wax	196
Matrix elements for isotopic methanes, F-	115
Matrix method, Wilson GF	32
Mean	
Laplacian	109
square force	111
square torque	111, 113
Mechanisms, reaction	163
Media, deuterated	190
Metabolites, deuterated	188
Metal complexes	37
Metals, isotopic	135
Methane	112
isotopic	115, 116, 117
Methyl halides constant	34
Microcanonical partition functions	106

- Microorganisms, photosynthetic ..... 193  
 Microorganisms, saprophytic ..... 193  
 Minimum potential functions, low-barrier  
   double ..... 38  
 Modulating coefficients ..... 20  
 Molal enthalpies, partial ..... 121  
 Molecular  
   forces ..... 16  
   photo-predissociation process ..... 97  
   properties, effect of isotopic  
     substitution ..... 64  
   vibrations ..... 19  
 Molecule spectra, diatomic ..... 30  
 Molecule, standard molar internal energy  
   of the ..... 5  
 Monatomic gases ..... 109  
 Motion correction, diagonal nuclear ..... 67  
 Multiple isotope substitution ..... 198
- N**
- <sup>14</sup>N-H coupling ..... 197  
<sup>22</sup>Ne/<sup>20</sup>Ne, reduced partition function of ..... 17  
 Neon isotopes ..... 4  
 Nernst equation ..... 132, 141  
 Nitrogen-15 ..... 197  
 No-remixing separation cascade ..... 86  
 Nuclear  
   magnetic resonance, deuterium  
     organisms in ..... 186, 187  
   motion, diagonal ..... 67  
   shape ..... 199  
   size ..... 190  
 Nucleic acid ..... 188, 199  
 Nucleophilic displacements, solvolytic ..... 174
- O**
- Oak Ridge, isotope separation at ..... 80  
 One-dimensional barrier ..... 47  
 Optical activity ..... 40  
 Organic acids, deuterated ..... 117  
 Organisms, <sup>13</sup>C substitution on  
   complex ..... 194, 195  
 Orthogonal polynomial expansion  
   calculation ..... 24  
 Oscillations, harmonic solid lattice ..... 2  
 Osmotic coefficients ..... 122  
 Oxygen, equilibrium exchange of ..... 24
- P**
- Paleotemperature scale, isotopic ..... 15  
 Parametrization ..... 119  
 Parasitic operations ..... 91  
 Partial molal enthalpies and entropies ..... 121  
 Particle, permeability of a barrier to a ..... 46  
 Particles, free ..... 165  
 Partition function(s)  
   internal ..... 5  
   isotopic ..... 6  
   microcanonical ..... 106  
   <sup>22</sup>Ne/<sup>22</sup>Ne, reduced ..... 17  
   ratio(s) ..... 9, 147  
     of Bigeleison and Mayer, reduced ..... 9  
     <sup>13</sup>C/<sup>12</sup>C reduced ..... 22  
     for isotopic solids ..... 148  
     for isotopic solute species ..... 151  
     reduced ..... 104
- Partition function(s) (*continued*)  
   reduced ..... 11  
   translational and rotational ..... 165  
 Peppermint ..... 190  
 Permeability of a barrier to a particle ..... 46  
 Phase reactions, gas ..... 142  
 Photochemical isotope separation  
   processes ..... 94, 96  
 Photo-dissociation ..... 97, 98  
 Photo-ionization ..... 97, 98  
 Photo-predissociation process, molecular ..... 98  
 Photosynthetic microorganisms ..... 193  
 Pinacolyl *p*-bromobenzenesulfonate ..... 168  
 Pinacolyl esters ..... 180  
 pK difference in proton transfer ..... 170  
 Plant, gaseous diffusion ..... 85, 92  
 Plants  
   belladonna ..... 191  
   higher ..... 188  
   isotopically enriched ..... 196  
   isotopically substituted ..... 195  
   terrestrial higher ..... 193  
 Plutonium isotope separations ..... 79  
 Polyatomic molecules ..... 32, 112  
 Polynomial expansion calculation,  
   orthogonal ..... 24  
 Potential  
   energy ..... 2  
   diagrams ..... 110  
   surface, hypothetical ..... 48  
   function ..... 37, 38  
   intermolecular ..... 108  
 Predissociation, molecular ..... 98  
 Preexponential factors ..... 50, 57, 59  
 Pressure effects for deuterated organic  
   acids ..... 117  
 Primary isotope effect ..... 164, 170  
 Probability *vs.* reduced energy transition ..... 46  
 Product rule, Teller-Redlich ..... 33  
 Protein content ..... 199  
 Proteins, deuterated ..... 187  
 Protium compounds ..... 5  
 Proton(s)  
   amide ..... 187  
   magnetic resonance spectra ..... 189  
   transfer ..... 170
- Q**
- Quadruple cell ..... 137  
 Quantum-mechanical foundations of  
   isotope chemistry ..... 1  
 Quantum-mechanical tunneling ..... 44
- R**
- Radical species ..... 187  
 Rate  
   constant ratio ..... 50, 57  
   determining step ..... 176  
   rate effects,  $\alpha$ -deuterium ..... 177  
 Reactants, initial state ..... 163  
 Reaction mechanisms ..... 163  
 Reactors (CTR), controlled  
   thermonuclear ..... 88  
 Reduced partition function ..... 11, 17  
   ratio (RPPFR) ..... 9, 22, 104  
 Restoring force ..... 165

Reversibility check, voltage-current	134	Spectroscopy, isotope effects and	29
Riboflavin production	190	Stable isotopes	184
Rotation spectra, vibration	31	Standard molar internal energy of the	
Rotation-translation interaction	109	molecule	5
Rotational		Stern-Lindemann formulation of VPIE	2
partition functions	165	Stretching	
-vibrational interaction	68	forces	26
wave functions	30	frequencies	157
RPFs (reduced partition function		modes	165
ratios)	9, 22, 104	motion	167
		Substituent additivity	20
S		Substituted <i>chlorella</i> cells, isotopically	201
S <sub>N</sub> 2 reactions	169	Substituted plants, isotopically	195
Salt phases, solid	138	Substitution	
Sample cell	121	<sup>13</sup> C	195, 197
Saprophytic microorganisms	193	deuterium	185
Schroedinger equation	65	isotopic (see Isotopic substitution)	
Secondary alkyl sulfonates	178	multiple isotope	198
Secondary isotope effects	172	Substrate, covalent	174
Secular equation	19	Sulfonates, secondary alkyl	178
Seed germination	191	Surface, hypothetical potential energy	48
Separation		S.W.U. (separative work units)	87
cascade	85, 86, 89	Symmetric solvent case	151
factor, elementary	10, 84	Symmetry number ratio	11
isotope (see Isotope separation)		T	
Separative work units (S.W.U.)	87	Tautomerism, hybridization	37
Separator, Beta calutron	80	Taylor series expansion	10
Separators, electromagnetic	78	Teller-Redlich product rule	33
Single-stage enrichment factor	93	Temperature dependence of tunneling	50
Sodium chloride solutions	127	Temperature exchange, dual	93, 95
Solid		Terrestrial higher plants	193
Born-von Kármán (BVK)	150	Tertiary carbonium ion pair	179
Debye	150	Thermal diffusion	79, 81, 82
isotopic	148	Thermodynamic properties, solute excess	127
lattice oscillations, harmonic	2	Thermodynamics of isotope-exchange	
phase model	148	reactions	131
salt phases	138	Thermodynamics, solution	120
Solute excess thermodynamic properties	127	Thermonuclear reactors (CTR),	
Solute species, isotopic	151	controlled	88
Solution(s)		Tight ion pair	176
aqueous	101	Torque, mean square	111, 113
calcium chloride	127	Transfer	
electrolyte	125	effects	158
heats of	121, 125	excess enthalpies of	124
thermodynamics	120	proton	170
Solvates, cation	39	reactions, hydrogen	167
Solvation, ion	39, 146	Transition	
Solvent		metal complexes	37
activity	121	probability	46
case	154, 157	state	173
effects, aqueous	119	bonding	169
isotope effects	119, 125, 127	theory	167
-separated ion pair	176	triatomic	166
structure, aqueous	126	vibrational force field	163
Solvolytic		Translation interaction, rotation-	109
isopropyl sulfonate	181	Translational degree of freedom	167
mechanisms	178	Translational partition functions	165
relative rates of	179	Transmission probability	44
Solvolytic nucleophilic displacements	174	Triatomic molecule, linear	36
Spectra		Triatomic transition state	166
atomic	29	Tritium-deuterium kinetic isotope effects,	
diatomic molecule	30	relative	55, 58
lattice	152	Tunneling	
proton magnetic resonance	189	in chemical reactions	45
of small polyatomic molecules	32	and kinetic isotope effects	48
vibrational	31, 37, 153	quantum-mechanical	44



Tunneling ( <i>continued</i> )			
temperature dependence of	50		
Wigner	56		
<b>U</b>			
Uranium enrichment	83		
Uranium isotope separation	9, 79, 89		
Urey-Rittenberg formulation of isotope exchange equilibria	5		
<b>V</b>			
Vapor pressure(s)			
isotope effects (VPIE)	101		
and changes in mean-squared torques	113		
for deuterated organic acids	117		
hydrogen-deuterium	114		
of some electrolyte solutions	125		
Stern-Lindemann formulation	2		
studies	109		
theoretical basis for	103		
of isotopic methanes	117		
of the neon isotopes	4		
Vibration(s)			
frequencies	34		
molecular	19		
-rotation spectra	31		
Vibrational			
constants	32, 75		
force field, state	163		
frequency distribution, BVK	152		
Vibrational ( <i>continued</i> )			
interaction, rotational-	68		
modes of cation solvates	39		
spectra	37, 153		
Virial coefficient isotope effect	107		
Voltage-current reversibility check	134		
VPIE ( <i>see</i> Vapor pressure isotope effects)			
<b>W</b>			
Water distillation	90		
Water dual temperature exchange, hydrogen sulfide-	93		
Wave functions			
adiabatic corrections with	71		
electronic	66		
Hartree-Fock limit	70		
rotational	30		
Wave packet	44		
Wax, insect	196		
Wigner distribution function	4		
Wigner tunneling	56		
Wilson GF-matrix method	32		
<b>Z</b>			
Zero point energy (ZPE)	2, 102		
approximation	106		
difference	15		
effect	118		
levels	166		
Zeta constants	34		